U.PORTO
INSTITUTO DE CIÊNCIAS BIOMÉDICAS ABEL SALAZAR
UNIVERSIDADE DO PORTO

# ROLE OF NOGO-A IN THE INTACT CENTRAL NERVOUS SYSTEM: AN *IN VIVO* AND *IN VITRO* APPROACH

**LUíS CRAVEIRO**

Dissertation for the Ph.D degree in Biomedical Sciences, submitted to the Instituto de Ciências Biomédicas Abel Salazar, Universidade do Porto

**Porto**
**2008**

**LUíS CRAVEIRO**

# ROLE OF NOGO-A IN THE INTACT CENTRAL NERVOUS SYSTEM: AN *IN VIVO* AND *IN VITRO* APPROACH

Dissertation for the Ph.D degree in Biomedical Sciences, submitted to the Instituto de Ciências Biomédicas Abel Salazar, Universidade do Porto

Supervisor: Prof. Catedrático Martin E. Schwab
Affiliation: Brain Research Institute, Department of Neuromorphology of University of Zurich and Swiss Federal Technical Institute, Zurich, Switzerland.

Co-Supervisor: Prof. Catedrática Maria João Saraiva
Afiliation: Instituto de Ciências Biomédicas Abel Salazar, Universidade do Porto, Porto, Portugal.

Craveiro LM, Hakkoum D, Weinmann O, Stoppini L, Schwab ME. (2007). Neutralization of the membrane protein Nogo-A enhances growth and reactive sprouting in established organotypic hippocampal slice cultures. Submitted - under review.

Craveiro LM, Weinmann O, Roschitzki B, Gonzenbach R, Zoerner B, Willi R, Montani L, Yee BK, Feldon J, Schwab ME {}. Hippocampal circuitry rearrangements in the adult rat after Nogo-A neutralization. In preparation.

# Contents

# Acknowledgements:

I would like to thank Prof. Martin Schwab for the opportunity to perform my PhD thesis in his lab pursuing a question deviated from the more classical regenerative studies performed in his group. His knowledge and availability are both rare and admirable.

Agradeço à Prof. Maria João Saraiva o apoio, disponibilidade e eficiência durante estes anos de doutoramento.

I would like to thank Dr. Paul Hines for starting me into my research career and for always believing in me. His discussions in the late evenings always showed the care and dedication of an exceptional mentor and will always be inspirational.

Agradeço aos meus pais pela educação, apoio e orgulho que me deram e sentem. Sem eles esta viagem não existiria. Agradeço às minhas avós pelo apoio e fé em mim e aos meus avôs cujos espíritos olham por mim.

I thank Laura Montani for her patience, support, care, belief and her love. Without her this journey would have been much harder. She stayed by my side always, in the good times and specially the difficult ones making this journey easier. Our paths crossed and now remain as one.

Agradeço à Vânia Santos, por todo o apoio e motivação que me deu nos bons e principalmente nos maus momentos. Sempre acreditou e acredita em mim. Ensinou-me corajem e força de vontade. Ela é uma inspiração.

I also thank to all my friends, those of youth and still around, those with limited contact but that are always available and those who have been there throughout this journey of work and life.

I would like to give special thanks to Dr. RA McKinney for her friendship and care. Many lessons I took from her, which allowed me to proceed both in life and work. She has a great view of life and an outstanding sixth sense.

I would also like to thank Oliver Weinman for his dedication, guidance, help and support throughout my doctorate work.

I thank the GABBA PhD program and FCT for the allowing me to undertake this journey with educational and financial support.

# Summary:

The neurite outgrowth inhibitory myelin protein Nogo-A has been well studied in the context of central nervous system (CNS) injury and disease. We studied the effects of the application of neutralizing anti-Nogo-A antibodies in intact CNS tissue, both *in vitro* using organotypic hippocampal slice cultures, and *in vivo* using Long Evans rats. This study had the dual purpose of elucidating the role of Nogo-A in the adult intact CNS and determining the consequences of long-term treatment of adult rats with anti-Nogo-A antibodies, behaviorally and histologically.

*In vitro* cultures showed a growth response which was elicited with or without lesion. The results also gave indications that hippocampal circuitry might be altered. The vesicular GABA transporter mRNA was up-regulated after Nogo-A neutralization, together with other synapse related mRNAs. These results could mean changes of neurotransmission although no differences in the global network activity were detected.

*In vivo* data supported the results obtained with the culture system. Changes were detected at the growth and synaptic levels. Several cytoskeletal proteins were up-regulated and the subunit composition of the $GABA_A$ receptors was changed. An up-regulation of parvalbumin, a protein present in a subgroup on GABAergic interneurons, was also detected. Together, these results suggest a change in the inhibitory circuitry of the adult hippocampus. No differences were detected at the behavioral level. Memory did not seem to be affected and there were no signs of sensory-motor gating changes or increased anxiety.

Taken together we propose that Nogo-A has a structurally stabilizing role in the adult CNS as well as a regulatory role for plasticity at the synaptic level.

# Sumário:

A proteína da mielina Nogo-A inibitória do crescimento axonal tem sido bem estudada no contexto de lesões e das doenças do sistema nervoso central (SNC). Nós estudamos os efeitos da aplicação de anticorpos neutralizantes anti-Nogo-A em tecido intacto do SNC, tanto *in vitro* usando culturas organotipicas de hipocampo como *in vivo* usando ratos Long Evans. Este estudo teve a dupla finalidade de elucidar o papel de Nogo-A no SNC intacto adulto e de determinar as consequências do tratamento a longo prazo de ratos adultos com anticorpos anti-Nogo-A, tanto a nível comportamental como histológico.

As culturas *in vitro* mostraram a uma resposta de crescimento axonal que foi induzido com ou sem lesão do tecido nervoso. Dos resultados obtidos depreende-se que os circuitos do hipocampo poderão ter sido modificados. O mRNA do transportador vesicular de GABA sofreu um aumento após a neutralização de Nogo-A, assim como outros mRNAs relacionados com sinápses. Estes resultados poderão significar alterações da neurotransmissão embora nenhuma diferença na actividade global da rede fosse detectada.

Os resultados *in vivo* suportam as observações obtidas com o sistema de cultura. Foram detectadas mudanças a nível do crescimento axonal e sináptico. Diversas proteínas do citosqueleto sofreram um aumento de regulação e a composição das subunidades dos receptores de $GABA_A$ foi alterada. Um aumento de parvalbumima, uma proteína presente num subgrupo de interneurónios GABAergicos, também foi detectado. Colectivamente, estes resultados sugerem uma mudança nos circuitos inibitórios do hipocampo adulto. A nível comportamental, não foram detectadas diferenças. A memória não pareceu ser afectada e não foi detectado nenhum sinal de alterações do circuito sensorio-motor ou de aumento de ansiedade. Conjuntamente, nós propomos que a proteína Nogo-A tenha um papel de estabilização estrutural do SNC adulto assim como um papel regulador da plasticidade ao nível sináptico.

# Résumé:

La protéine de myéline Nogo-A inhibitrice de la pousse axonale a été bien étudiée dans le contexte de lésions et des maladies du système nerveux central (SNC). Nous avons étudié les effets de l'application des anticorps neutralisants d'anti-Nogo-A dans le tissu intact du SNC, employant aussi bien *in vitro* des cultures organotypiques de l'hippocampe, et utilisant *in vivo* des rats Long Evans. Cette étude a eu deux finalités, d'élucider le rôle de Nogo-A dans le SNC intact adulte et de déterminer les conséquences du traitement à long terme des rats adultes avec des anticorps d'anti-Nogo-A, tant au niveau comportemental qu'histologique. Les cultures *in vitro* ont montré une réponse de croissance axonale qui a été obtenue avec du tissu nerveux. Les résultats ont également indiqués que les circuits de l'hippocampe ont pu avoir été modifiés. Le mRNA du transporteur vésiculaire de GABA a subi une augmentation après neutralisation de Nogo-A, ainsi que d'autres mRNAs avec les  par synapses. Ces résultats pourraient signifier des altérations de la neurotransmission bien qu'aucune différence dans l'activité globale du réseau n'ait été détectée.  Les résultats obtenus *in vivo* ont soutenu les observations obtenues avec le système de culture. Des changements ont été détectés au niveau de la croissance  axonale et synaptique. Plusieurs protéines cytosquelette ont subi une augmentation de la régulation et la composition de sous-unités des récepteurs de $GABA_A$ a été altérée. Une augmentation de parvalbumine, une protéine présente dans un sous-groupe d'interneuronrs de GABA, a été détecté également. Collectivement, ces résultats suggèrent un changement dans les circuits inhibiteurs de l'hippocampe adulte. Uniquement des petites différences ont été détectées au niveau comportemental. La mémoire n'a pas semblé être affectée et il n'a été détecté aucun signe de altération du circuit sensori-motrice ou d'augmentation de l'anxiété. Conjointement, nous proposons que la protéine Nogo-A ait un rôle structurel de stabilisation du SNC adulte ainsi qu'un rôle de régulateur de la plasticité au niveau synaptique.

# Chapter 1: Introduction

# 1 Introduction

## 1.1 Normal Brain and plasticity

The central nervous system (CNS) capacity for plasticity and regeneration differ greatly between young and adult individuals. The young CNS is able to enter widespread remodeling processes while the adult CNS is much more restricted. With this notion, it was believed that neonatal lesions would have much less severe consequences than similar lesions at the adult stage. Modern fiber tracing techniques and sensitive neurophysiological methods coupled with careful behavioral assessments have demonstrated that new connections developing after lesions at early stages may not be so beneficial in functional terms. After removal of one cerebellar hemisphere, the deficits of locomotor behavior in young adult rats were distinctively less severe than the ones of young rats. The extensive and aberrant projections in the young rat underline the more severe outcome, while in the young adult remodeling is restricted and less aberrant projections form (Gramsbergen, 2001) therefore having less severe functional consequences. Similar observations were made after neonatal motor cortex removal, which produced more chronic abnormalities in movements of distal effectors and narrow beam performance (Kolb and Holmes, 1983). On the other hand, neonatal hemispherectomy in cats allowed for near normal behavior in complex locomotor, social and cognitive behavior when compared to hemispherectomized adult cats (Burgess et al., 1986). Increased sparing of performance in morris water maze task was also found after neonatal ablation of the frontal cortex when compared to the same lesion in the adult rat (Kolb et al., 1983) and normal development of language was observed after hemispherectomy of a human child as treatment for seizures (Smith and Sugar, 1975).

Adult brain plasticity can occur at three different levels: 1) Functional plasticity at the level of synapses regulated by activity; 2) Structural local plasticity at the level of synapse and spine numbers; 3) Structural plasticity at the level of dendritic and axonal arborizations. Changes at any of these levels eventually lead to behavioral changes, from everyday memory formation and storage to highly skillful piano playing.

The first level of plasticity, referred to as synaptic plasticity, is defined as the capacity of the brain to modify neural circuits, and therefore behavior, due to the neural activity generated by exposure to life experiences. More specifically, it refers to activity-dependent modification of the strength and efficacy of synaptic transmission at pre-existing synapses. This mechanism is thought to be the underlining mechanism of formation and maintenance of memory. It is also one of the key mechanisms for the

development of neural circuits and growing evidence suggests that disruption of these activity-dependent mechanisms contribute to neuropsychiatric disorders (Citri and Malenka, 2007). Synaptic transmission can be enhanced or depressed by activity and it requires local mRNA in order to have a fast response (Bramham and Wells, 2007).

Closely related to synaptic plasticity is structural plasticity at the synaptic level. Activity can not only can enhance or depress synaptic transmission but it can also induce the growth and formation of new spines and synapses. This second level of plasticity is a phenomenon that occurs throughout life. Increases in synapse number have been described when animals are placed in enriched environments. Also during the natural process of ageing there are decreases in the number of spines and synaptic density (Mora et al., 2007). The spine structure is therefore not static and it changes depending on neurotransmitter receptor activation or environmental and hormonal signals (Bonhoeffer and Yuste, 2002; Hering and Sheng, 2001; Nikonenko et al., 2002; Nimchinsky et al., 2002).

The third level of plasticity has direct influence on the other two. Axonal and dendritic arborization increases and decreases are also phenomena that occur throughout life. Again ageing and exposure to enriched environments can lead to such changes (Mora et al., 2007).

Experience alters the synaptic organization of the brain in several species, including humans, and despite the restrictions of the adult CNS, some changes occur in the adult and intact CNS. Increased or decreased dendritic arborization correlates with increased or decreased performance, respectively, in certain behavioral tasks as do factors that promote or inhibit growth. Changes in dendritic length, branching, spine density, synapse number and size, and metabolic activity are other ways by which behavioral performance is altered. Since the adult CNS lacks the ability of long distance axonal growth it is more likely that changes in axonal arborization of neighboring cells influence the dendritic growth or atrophy. Young animals housed in enriched environments consistently had an increase in overall brain weight with an estimated increase in cortical synapses in the order of 20%. Animals, which had one eye occluded before visual maze training, had the dendritic fields of that hemisphere increased (Kolb and Whishaw, 1998). These results indicate that local plasticity is possible in the adult intact brain and it can be influenced by experience and training. In addition, such changes are local and mechanisms exist to maintain stability of brain regions by a general growth inhibition within the CNS. Modulation of such mechanisms can translate into enormous benefits after lesions, but unsupervised growth might also be devastating to the adult CNS

# 1.2 Inhibition of neurite growth in the CNS

There is little to no capacity for regeneration of fiber tracts or neurons after lesions of the CNS. However, small lesions can have a surprisingly good functional recovery. The low ability of the CNS to regenerate is related to a multitude of factors, which can be divided in two broad classes: intrinsic factors of neurons and extrinsic factors of the tissue microenvironment. The growth state of a neuron and the factors it expresses, are intrinsic factors. Several molecules have been identified as intrinsic factors that regulate growth during development and regeneration after injury. Growth associated proteins such as Gap43 and CAP-23, transcription factors like CREB and the second messenger cAMP levels all have influence on the responses different neurons have after injury (Rossi et al., 2007). Their expression levels on different neurons shape their intrinsic potential to growth. Extrinsic factors relate to tissue repair, immune response, scar tissue formation and the properties of myelin. Thus, reduced regeneration capacity can be explained in part by the presence of molecules that do not allow lesioned axons to grow and reconnect in order to re-establish the normal circuitry. Several molecules have been identified to date, mainly via *in vitro* techniques. MAG, OMgp, ephrinB3, semaphorin-4D -5A, netrin-1 and Nogo-A (Benowitz and Yin, 2007; Benson et al., 2005; Filbin, 2003, 2006; Goldberg et al., 2004; Manitt et al., 2006; Moreau-Fauvarque et al., 2003; Schwab, 2004) are the most well known. Nogo-A, one of the most potent growth inhibitor of the adult CNS and the first one being discovered (Caroni and Schwab, 1988b) has been extensively studied in the past years.

## 1.2.1 Myelin

### 1.2.1.1 Nogo-A

Two decades ago, oligodendrocytes and myelin were identified as non-permissive substrate for axonal growth (Caroni et al., 1988; Schwab and Caroni, 1988) and two membrane fractions, termed NI-35/250, were identified as highly non-permissive to growth (Caroni and Schwab, 1988b). Antibodies raised against NI35/250, allowed for increased permissiveness *in vitro* in the presence of the myelin inhibitory milieu (Caroni and Schwab, 1988a). Later, using the mAb IN-1 antibody developed earlier it was demonstrated that the NI-35/250 epitope was present in myelinated areas of the CNS but not in PNS (Rubin et al., 1994) and shown that *in vivo* application of IN-1 was able to induce regeneration after spinal cord injury (Schnell and Schwab, 1990). More recently the NI-35/250 antigen for IN-1 was purified from bovine spinal cord (Spillmann et al., 1998) and its cDNA was later cloned and termed Nogo-A (Chen et al., 2000;

GrandPre et al., 2000; Prinjha et al., 2000). This field of research moved on to find strategies to neutralize or block Nogo-A function and induce growth responses attempting to overcome the devastating consequences of spinal cord injury (SCI) and other CNS injuries and disorders.

### 1.2.1.2 MAG

Myelin-associated glycoprotein (MAG) is present in myelinating cells of the CNS and of the PNS (Quarles et al., 1973; Quarles and Trapp, 1984; Trapp and Quarles, 1984) and it was implicated as a neurite growth inhibitor (McKerracher et al., 1994; Mukhopadhyay et al., 1994). Conflicting evidence between growth inhibition and growth promotion properties (Filbin, 1995) and with the inhibitory potential of MAG (Bartsch et al., 1995) have generated discussion amongst researchers, eventually leading to agreement with several reports corroborating the initial neurite growth inhibitory role (DeBellard et al., 1996; Li et al., 1996). Further proof was the identification that soluble MAG *in vivo* or MAG-Fc, have the ability to inhibit neurite growth *in vitro* (Tang et al., 2001; Tang et al., 1997) and even PNS MAG is inhibitory (Shen et al., 1998). As with Nogo-A, researches moved to find strategies to block MAG and induce axons to grow after injury. Antibodies directed against MAG were successful in blocking its inhibitory properties *in vitro* (Torigoe and Lundborg, 1998), the inactivation of MAG led to optic nerve regeneration (Wong et al., 2003) and pre-exposure of neurons to neurotrophins (Cai et al., 1999) or increased cAMP levels overcome MAG inhibitory properties (Cai et al., 2002; Gao et al., 2003; Qiu et al., 2002). MAG can signal via binding to the receptor complex NgR and p75 and therefore inhibits neurite outgrowth (Domeniconi et al., 2002; Liu et al., 2002; Wong et al., 2002). NgR2, a Nogo-66 receptor homolog, was recently identified has a selective receptor for MAG (Venkatesh et al., 2005). In addition to the NgR mediated MAG inhibition, gangliosides also function as MAG receptors to carry the inhibitory signals. Different types of neurons respond to MAG signaling via either NgR or gangliosides. Dorsal root ganglion cells inhibition due MAG signaling occurs via both NgR and gangliosides, while in cerebellar granular cells only gangliosides are responsible and in hippocampal neurons gangliosides are the main contributors with some involvement from NgR (Mehta et al., 2007).

### 1.2.1.3 OMgp

Another myelin protein involved in the neurite outgrowth inhibition is oligodendrocyte myelin glycoprotein (OMgp). It is a minor component of myelin (Mikol et al., 1990) expressed at the surface of oligodendrocytes (like Nogo-A) and more recently shown to

be expressed in the membrane surrounding the Nodes of Ranvier made by oligodendrocyte-like cells (Huang et al., 2005). It was found to be a neurite growth inhibitor, which also binds to the Nogo-66 receptor NgR (Kottis et al., 2002; Wang et al., 2002b) and is expected to converge to a common signaling cascade of MAG and Nogo-A (McKerracher and Winton, 2002). Its LRR domain, like that of Nogo-66, is the proposed sequence responsible for the growth inhibitory properties and NgR binding (Vourc'h et al., 2003; Wang et al., 2002b). Interestingly, OMgp-deficient mice exhibit elevated collateral sprouting from the CNS nodes of Ranvier, suggesting a more general role for OMgp in restricting axonal sprouting in development and physiology (Huang et al., 2005).

#### 1.2.1.4 Semaphorins

Semaphorins are a well know protein family involved in axon guidance during development. The mechanisms by which semaphorins are involved in guidance have been recently reviewed using class III semaphorins as an example (Mann and Rougon, 2007). In the past years, semaphorins started to be studied in the context of injury and their role in regeneration after lesion. The scar tissue is inhibitory for several reasons, one of them being the presence of leptomeningeal fibroblasts; cells with high expression of Sema3A. Protein extracts of these cells induced growth cone collapse, an phenomenon which could be eliminated by incubation with neuropilin-1, a semaphorin receptor (Niclou et al., 2003). Another family member, Sema4D has also been reported as an inhibitory protein both *in vitro* and *in vivo*. It was detected in mature oligodendrocytes and up-regulated at the surrounding of SCI lesion (Moreau-Fauvarque et al., 2003). These reports proposed a novel role for semaphorins as neurite growth inhibitors of the adult CNS. The growth cone collapse properties of semaphorins were not new and they use small family of Rho GTPases as signaling transducers (Vastrik et al., 1999). Further studies revealed another member of the semaphorin family, Sema5A, found to be expressed in mature oligodendrocytes and to inhibit neurite growth (Goldberg et al., 2004). After SCI, substantial regeneration was achieved by the application of a Sema3A specific inhibitor (Kaneko et al., 2006). These reports show that several members of the semaphorin family not only have a developmental role of axonal guidance but also seem to have a role in stabilizing the adult CNS by preventing neurite outgrowth.

#### 1.2.1.5 Ephrins

Ephrin family members, like semaphorins, are regulators of axon guidance during development. The small family of Rho GTPases is also involved in the signaling of this class of axon guidance molecules (Huot, 2004). During development, Ephrin-A2 can act as a promoter or inhibitor of neurite growth, at low or high concentrations, respectively (Hansen et al., 2004). In the adult CNS ephrins are still expressed and thus Ephrin-B3 was proposed to be another myelin based growth inhibitory molecule (Benson et al., 2005). Despite some evidence of ephrins as myelin based inhibitors, they are also involved in regulation of astrocytic gliosis and glial scar formation, indicating that ephrins may be inhibitory by several mechanisms (Goldshmit et al., 2006).

#### 1.2.1.6 Netrin-1

Recently another protein, Netrin-1, has been implicated in axonal growth inhibition (Manitt et al., 2006). Netrin-1 is a bifunctional guidance protein during development, attracting some axons and repelling others depending on the receptors expressed by the axons. Netrin-1 is expressed in the adult CNS (Manitt and Kennedy, 2002) in myelinating oligodendrocytes, at the peri-axonal myelin membrane and neurons (Manitt et al., 2001). By looking at netrin-1 expression after injury, the authors suggest that the proximity to the lesion and the oligodendrocyte expression resemble that of growth inhibitory myelin associated proteins such as Nogo-A (Manitt et al., 2006). Currently, there is no proof, neither *in vitro* nor *in vivo*, showing a direct role of Netrin-1 as a neurite outgrowth inhibitor.

### 1.2.2 Scar Tissue

After penetrating lesions of the CNS, an astroglial-mesenchymal scar is formed. This structure has traditionally been thought to be responsible for the axons' inability to regenerate through the lesion. Whether it is the physical scar or some molecular factors expressed at the scar which prevent axonal regeneration was an unanswered question. *In vitro* studies, using E18 hippocampal cells, proposed that factors expressed at the scar in the absence of myelin were responsible for the lack of regenerative responses (Rudge and Silver, 1990). The 3D-structure of the astroglial scar was also shown to be inhibitory, but only for adult neurons (Fawcett et al., 1989). These results indicate the several aspects of scar tissue were implicated in the regenerative response of neurons. Chondroitin Sulfate Proteoglycans (CSPGs) (Oohira

et al., 1991; Snow et al., 1990a) and Tenascin (Crossin et al., 1990; Faissner and Kruse, 1990), proven inhibitory *in vitro* and present in astrocytes (Crossin et al., 1989; Grumet et al., 1985; Hoffman et al., 1988; Kruse et al., 1985; Prieto et al., 1990; Snow et al., 1990b; Steindler et al., 1989) were also up-regulated in scar tissue (McKeon et al., 1991), providing *in vivo* evidence of some factors present in the scar tissue responsible for the lack of regenerative response. Efforts have been made to influence the scar tissue and promoting axonal injury spanning from reducing scaring (Davies et al., 1997; Logan et al., 1999a; Logan et al., 1999b), delaying scaring (Klapka et al., 2005) or transplantation strategies to generate a more growth permissive environment of the scar tissue (Bartolomei and Greer, 2000; Davies et al., 1997; Enzmann et al., 2006; Oudega and Xu, 2006; Pearse and Bunge, 2006). As discussed above, also semaphorins and ephrins play an inhibitory role through their presence in the scar tissue (Goldshmit et al., 2006; Niclou et al., 2003).

#### 1.2.2.1 CSPGs

Chondroitin Sulfate Proteoglycans are present in the scar tissue and up-regulated after lesion (Lemons et al., 1999; McKeon et al., 1991; Morgenstern et al., 2002). Since they were shown to be inhibitory *in vitro* (Oohira et al., 1991; Snow et al., 1990a), research was dedicated to devise ways to overcome their inhibitory role and promote axonal regeneration. The use of chondroitinase ABC, an enzyme that specifically cleaves the chrondroitin sulfated glycosaminoglycan side chains on the core of the CSPG molecule, showed promising results in reverting the inhibitory properties of CSPGs *in vitro*, whether by cells grown over CSPG substrates (Dou and Levine, 1994) or by culturing cells onto spinal cord tissue sections (Zuo et al., 1998). Chondroitinase ABC application *in vivo* was able to cleave CSPGs (Lemons et al., 1999) and to promote axonal growth responses after injury (Barritt et al., 2006; Bradbury et al., 2002; Massey et al., 2006; Moon et al., 2001; Yick et al., 2000; Zuo et al., 2002) along with functional recovery (Caggiano et al., 2005; Huang et al., 2006). More recent studies have been focused on combination strategies using chondroitinase ABC along with other methods to promote regeneration (Chau et al., 2004; Fouad et al., 2005; Massey et al., 2007) in an attempt to produce a more pronounced response than each individual treatment. The addition of chondroitinase ABC allowed for a better penetration of the axons into the grafts and bridges implanted at the site of injury.

### 1.2.2.2 Tenascin-R

Extra-cellular matrix (ECM) molecules have also been implicated in axonal growth inhibition. Tanascin-R is a ECM molecule that is exclusively expressed in CNS (Pesheva et al., 1989) in oligodendrocytes and some neuronal cell types. Tenascin-R growth inhibitory effects *in vitro* have been shown in several publications, ranging from optic nerve fibers to mesencephalic, hippocampal and cerebellar neurons (Becker et al., 2000; Faissner and Kruse, 1990; Probstmeier et al., 2000; Xiao et al., 1997) and tenascin-R was shown to be up-regulated after optic nerve lesion (Becker et al., 2000). Experiments using antibody treatment against tenascin-R should reveal the importance of its inhibitory role in axonal growth in the injured CNS.

## 1.2.3 Concluding Remarks

Due to their complexity and importance, the brain and spinal cord need to remain stable throughout life. With millions of neurons and even more synaptic connections, aberrant growth could lead to severe problems for CNS function, much like the ones observed after cerebellar hemisphere ablation (Gramsbergen, 2001). Several molecules present in the CNS have axonal growth inhibitory properties, many of them present in myelin. Such molecules in the intact CNS could physiologically function to restrict growth in order to stabilize the network after differentiation. When the CNS is lesioned, the expected response would be controlled growth to compensate and replace lost connections, as is the case in PNS. Instead, the CNS generally increases the expression of inhibitory molecules present at the scar tissue. Many efforts were made attempting to overcome this inhibition of growth after injury with varying degrees of success, from neutralizing antibodies, to competition peptides, enzymatic digestion and transplantation. What seems to be common to many of the different inhibitory molecules, whether from myelin or scar tissue, is the downstream involvement of the small family of Rho GTPases and their activators and effectors (Alabed et al., 2006; David and Lacroix, 2003; Filbin, 2003; Jain et al., 2004; Monnier et al., 2003). Although it is possible to consider one unique treatment to block the different inhibitory signals, a complete block of Rho GTPase function could have serious consequences to the cells, given their pivotal role in cytoskeletal organization, e.g. regulation of actin, cell polarity, microtubule dynamics and even transcription factor activity (Etienne-Manneville and Hall, 2002; Wittmann and Waterman-Storer, 2001). The signal specificity of Rho GTPases is largely due to the association with particular guanine nucleotide exchange factors, which may attach to scaffolding proteins linking GTPase and effectors in large complexes (Govek et al., 2005). The cell permeable application of C3 transferase, a

Rho-kinase blocker, is a good general tool for growth induction but might be limited the time course of long distance regeneration. The development of lentivirus for long term expression of C3 transferase or dominant negative proteins within the RhoA signaling cascade could provide a better tool after SCI (Gross et al., 2007).

# 1.3 Nogo-A molecular details

## 1.3.1 Reticulons

The reticulon family (RTNs) is constituted of membrane-bound proteins of which Nogo is a member. Historically RTNs were first known has NSPs, name arising from a neuroendocrine-specific protein anchored mainly on the membrane of smooth endoplasmatic reticulum (ER) (van de Velde et al., 1994). Other members have been identified as belonging to this family (Moreira et al., 1999; Roebroek et al., 1996) including Nogo-A (Chen et al., 2000; GrandPre et al., 2000; Prinjha et al., 2000). RTNs are present in plants, fungi and animals (Oertle et al., 2003b) with the exception of the RTN4A isoform, which is absent in fish (Diekmann et al., 2005). Although these proteins have received more attention in recent years, their functions are still elusive.

The RTNs (**Fig. 1.1**) have a great variety of the N-terminus resulting in many splice variants (Oertle et al., 2003b) but a well-conserved 188 amino acid long C-terminus, the reticulon homology domain (RHD) is responsible for the reticular localization of this family. Two transmembrane domains in the C-terminus region are responsible for the membrane localization and a 66 amino acid long loop in between may have a role in inter- and intra-cellular communication. This loop is known as Nogo-66 in RTN4 (Nogo) and binds to NgR (Nogo receptor) (Fournier et al., 2001) and possibly Caspr (Nie et al., 2003), to mediate neurite inhibition and $K^+$ channel localization at axonal paranodes, respectively. The variability of the N-terminus is proposed to be responsible for cell type specificity of the different isoforms (Di Scala et al., 2005; Oertle et al., 2003a). Mammalian RTNs are ubiquitously expressed in all tissues (Oertle and Schwab, 2003) but different members are preferentially expressed in certain tissues over others with the brain being rich in the expression of all four RTNs (Yan et al., 2006).

Aside from the well-known role in neurite growth inhibition of the RTN4A member, not much else is known about this family's function. Roles have been attributed in cellular trafficking, neurodegenerative diseases, and apoptosis (Yan et al., 2006) but much more remains to be discovered.

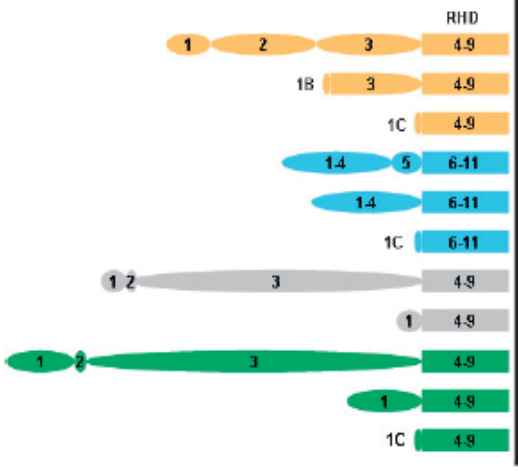


| RTN Family | Alternative symbols | Amino acids Human | Amino acids Mouse | Chromosome Human | Chromosome Mouse | Ref. |
|---|---|---|---|---|---|---|
| RTN1-A | Nsp-A | 776 | 780 | 14q23.1 | 12C3 | 2 |
| RTN1-B | Nsp-B | 356 | ND | | | |
| RTN1-C | Nsp-C | 208 | 208 | | | |
| RTN2-A | Nspl1-A | 545 | ND | 19q13.32 | 7A2 | 45,46 |
| RTN2-B | Nspl1-B | 472 | 471 | | | |
| RTN2-C | Nspl1-C | 205 | 204 | | | |
| RTN3-A | RTN3-A4b | 1032 | 964 | 11q13 | 19A | 7, 15 |
| RTN3-B | RTN3, RTN3-A1 | 236 | 237 | | | |
| RTN4-A | Nogo-A | 1192 | 1162 | 2p16.3 | 11A3.3 | 4-7, 31 |
| RTN4-B | Nogo-B, ASY | 373 | 356 | | | |
| RTN4-C | Nogo-C | 199 | 199 | | | |

**Figure 1.1. Schematic depictions of human and mouse RTNs.** RTNs are transcribed from four *rtn* genes and each has multiple transcripts. The N-terminal domain is depicted as ovals and the conserved reticulon homologous domains (RHD) as boxes. The number corresponds to each exon. The major alternative nomenclatures are also listed in the table. The numbers of amino acids are calculated based on the protein sequence database of the National Center for Biotechnology Information (NCBI). The chromosomal locations of the reticulon genes are provided through the NCBI Map Viewer. The amino acid information is adopted from either the NCBI protein database or publications. **(Yan et al., 2006)**

## 1.3.2 Nogo-A family

Nogo-A is a member of the reticulon family. It is also a member of the more restricted Nogo family. Three major members, two of which result of alternative splicing (Nogo-A and Nogo-B) and the third from the use of an alternate promoter (Nogo-C), constitute this smaller family. Seven other minor splice variants are part of this family (**Fig. 1.2**). Nogo-A is mainly expressed in oligodendrocytes but also in neurons, while Nogo-B seems to be ubiquitously expressed. The differential expression between Nogo-A and Nogo-B, which use the same promoter, is proposed to be due to tissue specific differential splicing (Oertle et al., 2003a)

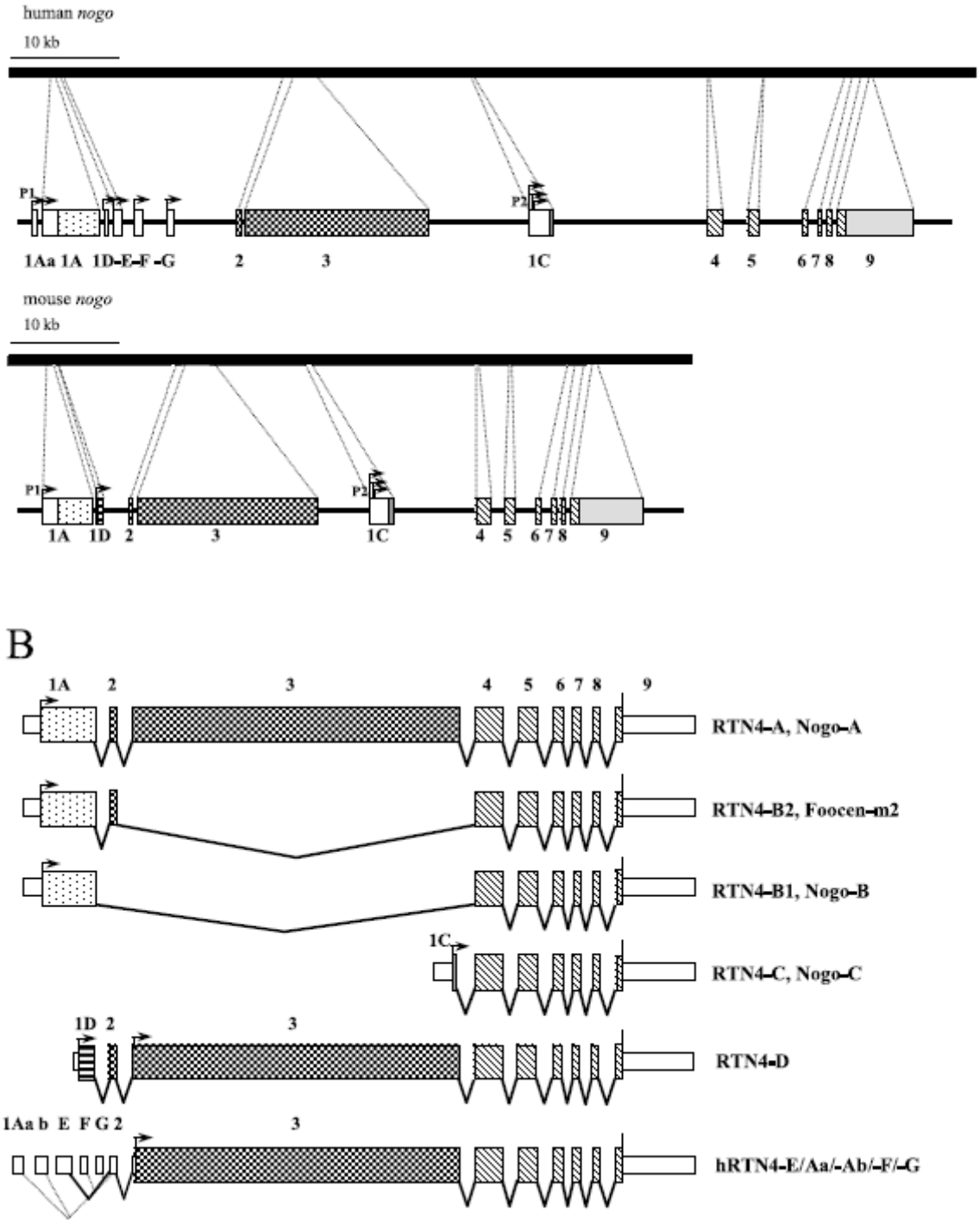


**Figure 1.2. Gene structure and splice-variants of human and mouse nogo**. (A) Schematised gene structure of human and mouse Nogo gene. There are 14 exons and eight separate start sites (1A, 1Aa, 1Ab, 1C, 1D, 1E, 1F and 1G; arrows) under different promoters (P1-P6). (B) The ten known nogo splice-variants. The RTN4-B2 isoform is a minor splicevariant, while RTN4-D, -E, -Aa, -Ab, -F and -G mRNAs are present in testis. Arrows are indicating the translation start sites. **(Oertle et al., 2003a)**

Nogo-A expression is mainly intracellular but a percentage of this protein is expressed at the surface of several cell types (Dodd et al., 2005). The membrane bound Nogo-A can have two possible topologies (**Fig. 1.3**). The extra-cellular topology of the N-terminal is responsible for the inhibitory role of Nogo-A.

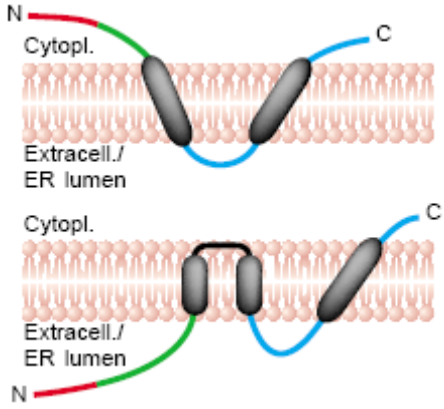


**Fig. 1.3**. Membrane topologies and subcellular localization of Nogo-A. Two proposed topologies for the C-terminal hydrophobic regions of Nogo-A. The lengths of the hydrophobic stretches (35 amino acids) could allow it to span the membrane once or twice. The N-terminal can be cytoplasmic or extracellular (proposed topology for the inhibitory effects). **Modified from (Oertle and Schwab, 2003)**

## 1.3.3 Nogo-A receptors and signaling

Nogo-A signals via the receptor complex NgR/p75/Lingo-1/Troy (Fournier et al., 2001; Mi et al., 2004; Park et al., 2005; Wang et al., 2002a) and an as yet unidentified Nogo-A specific receptor (Dodd *et al.*, 2005). Two active sites, Nogo-66 and a Nogo-A specific region, both lead to activation of RhoA and ROCK (Fournier et al., 2003; Hsieh et al., 2006; McKerracher and Higuchi, 2006; Niederost et al., 2002; Schweigreiter et al., 2004), therefore, affecting the neuronal growth machinery (**Fig 1.4**).

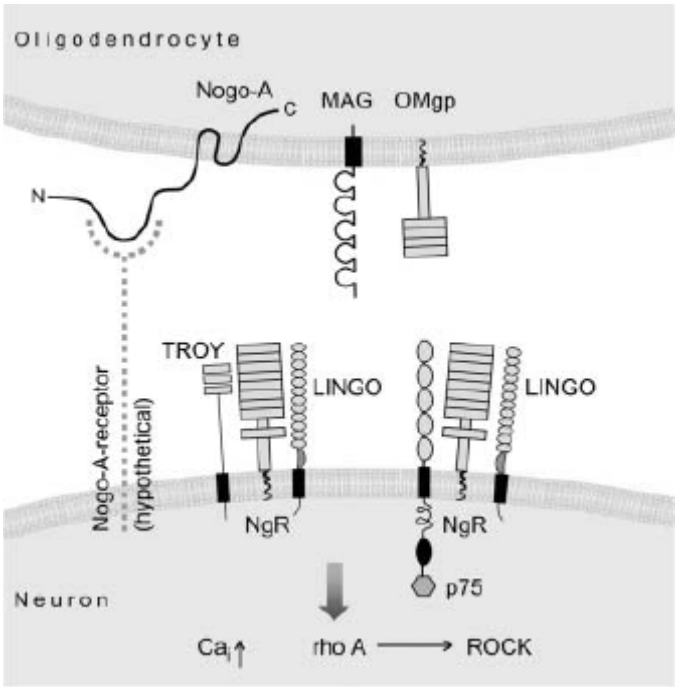


**Figure 1.4.** Scheme of Nogo receptor complexes interacting with myelin-associated inhibitory proteins Nogo-A, MAG and OMgp. Nogo-A, MAG and OMgp interact with receptor complexes comprising either NgR, p75 and Lingo or NgR, TROY and Lingo. An additional Nogo-A specific receptor remains to be identified. These interactions lead to an increase in intracellular calcium (Ca) levels and to activation of the rho pathway. **(Buchli and Schwab, 2005)**

The complexity of this small family of Rho GTPases is evident in the multitude of pathways and cellular processes they regulate (Etienne-Manneville and Hall, 2002) with many effects in cell motility, actin and tubulin (Wittmann and Waterman-Storer, 2001). A controversy arose with the publication of a report indicating that NgR KO animals showed only partial effects on regeneration *in vivo* (Zheng et al., 2005) and

that NgR function was related only to acute growth cone collapse but not to long term neurite growth inhibition (Chivatakarn et al., 2007). These results provide one possible explanation for why NgR KO animals show a partial increased regeneration both *in vitro* and *in vivo*. They also indicate different mechanisms for short and long-term inhibition by the different myelin associated inhibitors that signal through NgR, raising the possibility for the existence of other receptors, not yet identified. On the other hand, several other reports indicated partial regeneration *in vivo*, whether by inhibiting NgR transgenically with a soluble function-blocking NgR fragment, NgR(310)ecto, knocking-out NgR (Kim et al., 2004), or by knock-down via adeno-associated virus transfection of retinal ganglion cells (Fischer et al., 2004). The inhibitory effects of Nogo-A are still present through the Nogo-A specific region, which does not bind to NgR though it still converges to the small family of Rho GTPases (Niederost et al., 2002; Schweigreiter et al., 2004; Zhao et al., 2007).

## 1.4 Nogo-A and regeneration

The vast majority of the literature about Nogo-A and its signaling pathway is related to its involvement in axonal regeneration and sprouting after lesions of the CNS (both brain and spinal cord). Nogo-A and other molecules present in CNS myelin and scar tissue have growth inhibitory properties. Interfering with their signaling pathways has been successful in inducing a growth response after injury. Enhanced regeneration of injured fibers and improved functional recovery were observed in spinal cord lesioned rats and monkeys treated with anti-Nogo-A antibodies (Freund et al., 2006; Liebscher et al., 2005; Merkler et al., 2001; Schnell and Schwab, 1990; Schwab, 2004), in rats infused with NgR antagonist peptides (GrandPre *et al.*, 2002) or an activity-blocking receptor fragment (Li *et al.*, 2004), and in Nogo-A (Dimou et al., 2006; Kim et al., 2003; Simonen et al., 2003) or NgR (Kim *et al.*, 2004) knock-out mice. All these strategies have proved successful for Nogo-A block of function and allowing for *in vivo* regeneration of the corticospinal tract (CST), as well as other CNS tracts, and for enhanced recovery of sensory-motor functions lost by the injury (Schwab, 2004). Nogo-A effective neutralization come about the binding of the anti-Nogo-A antibodies to the Nogo-A protein and the consequent internalization of the complex (Weinmann et al., 2006) and removal of the inhibitory protein from the cell surface eliminating its usual signaling pathway.

## 1.4.1 Spinal Cord Injury

### 1.4.1.1 Rat

Nogo-A and its effects in Spinal Cord Injury (SCI) has historically been studied in rat models using function-blocking antibodies. The first report of *in vivo* regeneration after CST transection and mAb IN-1 secreting hybridoma cells implantation in the brain showed pronounced growth of the transected fibers up to 11mm caudal to the lesion in a short time of 2-3 weeks (Schnell and Schwab, 1990). Similar results were obtained by the infusion of a humanized recombinant Fab IN-1 into the lesion site (Brosamle et al., 2000). Nogo-A neutralizing antibody treatment (Liebscher et al., 2005; Merkler et al., 2001) or NgR blocking peptide application (GrandPre et al., 2002), not only led to the regrowth of injured fibers but also to functional locomotor recovery. Using another anti-Nogo-A antibody, raised against human Nogo 1-40 peptide (NEP1-40), it was demonstrated that after lesion there was a better preservation of injured axons and more normal histological appearance of the tissue (Atalay et al., 2007). Other methods of treatment, like vaccination with Nogo-A derived peptides (Hauben et al., 2001) or with recombinant DNA fragments encoding domains related to axonal inhibition (Xu et al., 2004), seem to be other possible strategies to induce regeneration after SCI.
Underlining the functional recovery after SCI and Nogo-A inhibition may be the reorganization of the motor tracts (Raineteau et al., 2002; Raineteau and Schwab, 2001) combined with the growth of the injured fibers.

### 1.4.1.2 Mouse KO

An increased regenerative response was expected from mice lacking Nogo-A. In 2003 three independent groups published the generation of Nogo-A KO mice (Kim et al., 2003; Simonen et al., 2003; Zheng et al., 2003) but unexpectedly with different regenerative responses ranging from none to profuse regeneration. These results were the basis for discussion in the Nogo-A field about the role of Nogo-A in growth inhibition after injury, when it is absent. Surprisingly, and despite all the results both *in vitro* and *in vivo* showing that blocking Nogo-A or its receptor leads to an increased growth response, the question of whether such results were true or unspecific responses from the treatments applied was raised by certain scientists in the field. It has been argued that one possibility for the difference observed between KO animals and acute treatment could be some additional effects of the treatments used beyond target inhibition or additional roles of Nogo-A beyond neuronal growth inhibition (Teng and Tang, 2005). Another explanation relates to the strategies used in the generation of the

KO. These strategies differed between the three groups and could underline the differences observed (Woolf, 2003). Another important factor, and more plausible explanation for the observed difference between the three KO animals, is the background strain of the animals. The three groups used mice with mixed backgrounds and so the contributions and compensations of their original backgrounds are not clear. The answer to different outcomes of Nogo-A KO's came from the analysis of the pure background animals' regenerative capacity; differences were found between the wild-type ability of C57/Bl6 or SV129 animals to regenerate. These differences also affected the outcome of the lack of Nogo-A in each of those backgrounds (Dimou et al., 2006). It is not yet clear exactly why the differences between the different KO exist but certainly the genetic background and the techniques used to generate the KO animals seem to be the most reasonable explanations without excluding other possible roles of Nogo-A signaling so far unknown and other mechanisms of compensation by differential regulation of other inhibitory proteins. The speculations still arise with the recent publication that the tracing techniques used to assess regeneration could be an artifact, thus explaining the differences in the regeneration of the different KO animals (Steward et al., 2007), although careful analysis dismissed such allegations (Cafferty et al., 2007) which fall short of reality.

#### 1.4.1.3 Monkey

Successful regeneration in mouse and rat models of SCI brought anti-Nogo-A treatment closer to clinical trials as a potential treatment of human patients suffering from SCI. In recent years, studies using Marmoset and Macaque Monkeys as models of SCI were performed using anti-Nogo-A antibodies. CST fibers were able to regenerate past the lesion site when treated with specific anti-Nogo-A antibodies (Fouad et al., 2004; Freund et al., 2006; Freund et al., 2007). These results were in line with the evidence from the rodent data. The monkeys treated with anti-Nogo-A antibodies and tested in several reaching tasks to assess manual dexterity after injury, recovered their performance levels almost completely: they were faster and more precise than monkeys receiving control antibody treatment (Freund et al., 2006). The primate data offer good expectations of success in the application of this treatment to human SCI patients.

### 1.4.2 Stroke/Ischemia/Hypoxia

Stroke ranks third in the leading cause of death in the United States (US). About 500000 people per year in the US have a first stroke, on average, every 45 seconds one American has a stroke. 88% of all strokes are ischemic (Thom et al., 2006). Most importantly, stroke has immense social repercussions since survivors many times are confined to a bed and receive care from family members or have permanent disabilities. In the context of plasticity and due to the high frequency of human strokes, several animal stroke models have been used to assess Nogo-A inhibition effects on recovery. The up-regulation of both Nogo-A and NgR in the core of ischemic cortex of rats (Wang et al., 2006a) and monkeys (Eslamboli et al., 2006) indicates an involvement of these two proteins in the pathology. The use of a NgR antagonist peptide reverted Nogo-A expression levels and increased regeneration (Wang et al., 2007a). Anti-Nogo-A treatment with monoclonal antibody 7B12 started 24h after photothrombotic cortical injury (PCI) lasting 2 weeks, resulted in animals which recovered to about 70% of pre-lesion performance on a forepaw task (6 to 9 weeks post PCI). Moreover, these animals showed sprouting at the spinal cord level from CST fibers of the intact side crossing the midline into the denervated side (Wiessner et al., 2003). Using a permanent model of stroke, middle cerebral artery occlusion (MCAO), and anti-Nogo-A treatment with the monoclonal antibody IN-1, both functional recovery and cortico-efferent projections from the opposite, unlesioned hemisphere were observed (Papadopoulos et al., 2002) as well as an increase in dendritic arborization and spine density in the contralateral cortex (Papadopoulos et al., 2006). More clinical intrathecal delivery, instead of the intracerebroventricular approach, of anti-Nogo-A antibodies as also been successful and showed behavioral recovery (Tsai et al., 2007). Stroke recovery after Nogo-A signaling blockade involves several CNS regions. Functional and anatomical recovery in the cortex, red nucleus and spinal cord occurred after blocking Nogo-A signaling whether by antibodies directed against it, by its or its receptor NgR complete absence in mice or blockade of its receptor in rats (Lee et al., 2004). Adult and aged animals also benefit from anti-Nogo-A treatment strategies with functional recovery and compensatory growth of fibers from unlesioned to deafferented regions of the brain (Markus et al., 2005). Delayed treatments with IN-1 one week after stroke was also demonstrated to be efficacious in both functional and structural recovery (Seymour et al., 2005). These results are important considering that human stroke patients often arrive in the hospitals too late to receive immediate treatment.

### 1.4.3 Traumatic Brain Injury

The hippocampus is a region that is particularly vulnerable to experimental and clinical traumatic brain injury (TBI) (Kotapka et al., 1994; Tate and Bigler, 2000). Cognitive impairment is one of the consequences of TBI (Hicks et al., 1993; Kline et al., 2002; Lyeth et al., 1990) and an increased expression of Nogo-A both in neurons and oligodendrocytes after TBI has been reported (Marklund et al., 2006). Despite the potential increase of the inhibitory environment with the up-regulation of Nogo-A expression, cognitive performance was enhanced following anti-Nogo-A treatment of a TBI animal model (Lenzlinger et al., 2005). Unlike the extensive reports showing sprouting of CST fibers after Nogo-A neutralization, TBI itself induced sprouting and no enhancement after treatment with anti-Nogo-A antibodies was observed so far; thus, the increased cognitive performance could be due to plastic events happening at the synaptic level. Although not analyzed in this study, it has been reported for stroke models that anti-Nogo-A antibody treatment induces changes in the dendritic arborization and spine density in the cortex (Papadopoulos et al., 2006). These plastic changes could underline the increased cognitive performance after TBI.

### 1.4.4 Concluding Remarks

In past years, several types of injuries to the CNS with drastic functional consequences have been studied in animal models in the context of promoting regeneration of lost axons, compensatory fiber growth, plasticity and functional recovery. With the discovery and identification of Nogo-A as a neurite outgrowth inhibitory molecule, antibody treatments against it have been devised and applied to several injury models. In all these models discussed above, the outcome has been that both structural and functional recoveries are greatly enhanced. This treatment is promising and clinicians as well as patients can be excited about the ongoing clinical trials with this treatment strategy.

## 1.5 Nogo-A and disease

Nogo-A appears not only to be involved in the inhibition of axonal growth after injury but more recently several studies have identified links between its expression and several pathological states of the CNS. A major concern common to the different neuropathologies where Nogo-A has been implicated is whether its role is of a simple bystander or its differential expression contributes or worsens the disease condition. In

one case, it becomes a good diagnostic or prognostic tool, in the other, it becomes a potential target, against which there already exist therapeutic tools.

### 1.5.1 ALS

About 4-8 per 1000,000 people suffer from amyotrophic lateral sclerosis (ALS) worldwide and an estimated 5,000 people per year are diagnosed with amyotrophic lateral sclerosis in the US (http://www.wrongdiagnosis.com/a/amyotrophic_lateral_sclerosis/stats.htm in July 2007). The search for markers and therapeutic agents for this deadly neurodegenerative disease has not generated a cure so far, and diagnosis can only be secure at more advanced stages of the disease. With no cure currently available, early diagnostics would enable the start of neuroprotective medication, the prevention of anxiety by disease progression, a rational planning of remaining life and avoid long and multiple investigations to rule out other diseases (Dengler et al., 2005). In the search for a potential diagnostic marker, an altered expression of Nogo-A in motor neurons of the lumbar spinal cord and in the gastrocnemius muscle of an ALS mouse transgenic model has been reported (Dupuis et al., 2002). It was discovered that Nogo-A increased expression occurred in the asymptomatic phase of the disease. These findings were confirmed in both post-mortem and biopsy samples of human patients suffering from ALS (Dupuis et al., 2002). In addition, a correlation between Nogo-A expression and disease severity has been drawn (Jokic et al., 2005). Initially, it was not clear if the increased expression levels of Nogo-A are a cause or a consequence of the disease progression. Then, Nogo-A KO mice crossed with an ALS transgenic mouse model had an increase in the live expectancy (Jokic et al., 2006). Furthermore, when they over-expressed Nogo-A in muscle fibers of wild type mice there was a denervation and consequent dye back of the motor neurons. These results suggest that a change in the regulation of Nogo-A in the skeletal muscle is involved in the cause for the progression ALS. Several other neuromuscular diseases also seem to have increased levels of Nogo-A in muscle biopsies, reinforcing the idea of Nogo-A as a marker for denervated muscle fibers, not exclusive to ALS, and its involvement in the muscle denervation and regeneration processes of these types of diseases (Wojcik et al., 2006).

The identification of the role of Nogo-A in ALS and its increased expression in muscle biopsies could be used has an early marker for the diagnosis of ALS in patients. Considering that, and knowing that a subset of the population of patients suffering from lower motor neuron syndrome (LMNS) progress to ALS, it would be important to

identify markers that would permit early treatment. Nogo-A levels have been found to predict this progression (Pradat et al., 2007). Although care should be taken and it may even be premature to state that Nogo-A is a therapeutic target for ALS (Tagerud et al., 2007), these findings have immense repercussions in a possible early treatment and can prove to be a great medical advancement.

### 1.5.2 Alzheimer's disease

There are now more than 5 million people in the United States (US) living with Alzheimer's disease (AD). Every 72 seconds, someone develops AD. The direct and indirect cost of Alzheimer's and other dementias amount to more than 148 billion dollars annually (http://www.alz.org/alzheimers_disease_alzheimer_statistics.asp in July 2007). An effective treatment would alleviate such a burden to the society. Recently, one study has revealed that in the human brain suffering from Alzheimer's disease Nogo-A expression is increased in hippocampal neurons of affected individuals when compared to the normal aged brain. Furthermore, Nogo-A was found in neuritic β-amyloid plaques, though no co-immunoprecipitation between Nogo-A and Aβ or APP was possible albeit different techniques used (Gil et al., 2006). Recently, RTN3 and RTN4B (Nogo-B) were found to interact with BACE1 (β-secretase), increasing Aβ production when over-expressed (He et al., 2006). These results indicate that members of the reticulon family may play a regulatory role Aβ production and therefore a role in plaque formation. If new therapies become available and successfully delay or halt neuronal death associated with AD, then a means of promoting growth and new synaptic connections would improve recovery of lost functions rather then solely halting the disease progression (Strittmatter, 2002). Several methods of blocking Nogo-A action are now available and antibodies exist against Nogo-B, although not tested in functional contexts, which could prove groundbreaking in AD therapy.

### 1.5.3 Psychiatric Disorders

Nogo expression and schizophrenia were linked in a study where Nogo was identified from a cDNA library used to search genes in the frontal cortex of schizophrenic patients (Novak et al., 2002). They found a homozygous CAA polymorphism in the 3´UTR region of the Nogo gene to have an increased prevalence in the affected individuals. This polymorphism of the Nogo 3´UTR region, known in eukaryotic cells to regulate gene expression, could contribute to its increased expression. One criticism to his study was the fact that there was no distinction between the different Nogo isoforms

and another was a study claiming that there was no link between the CAA insertion and schizophrenia (Xiong et al., 2005). The authors repeated their study, this time distinguishing the three Nogo isoforms and extending their analysis to include other psychiatric disorders studying tissue from schizophrenic, depressed and bipolar patients (Novak and Tallerico, 2006). They observed an increase for Nogo-A mRNA in the frontal cortex samples of schizophrenic patients and a decrease in depressed and bipolar patients but without statistical significance, having schizophrenia the highest average percent difference (12%) to controls. The levels of Nogo-B were decreased 17% in the cases of depression and Nogo-C had elevated expression (26%) in schizophrenia, in both cases with statistical significance. The presence of the CAA insert in the 3'UTR region of the Nogo gene was correlated with higher expression of Nogo-A and Nogo-C but not with Nogo-B. It remains unclear whether the altered Nogo expression is a cause or consequence of these diseases. Several reports indicated an association between chromosome regions which contain the Nogo and NgR genes to schizophrenia, thus suggesting a possible role of the Nogo signaling pathway in the disease (Novak and Tallerico, 2006). One has to consider that this relationship could be a consequence of another altered event near the Nogo and NgR loci. What seems to be relevant is the 13% or 27% increase in Nogo-A or Nogo-C expression, respectively, with the presence of the CAA insert when compared to another insert (TATC).

### 1.5.4 Multiple Sclerosis

There are no exact numbers of how many people have multiple sclerosis (MS). Currently about 250,000 to 350,000 people in the US have been diagnosed with MS. This estimate suggests that approximately 200 new cases are diagnosed each week. The life expectancy for people with multiple sclerosis is nearly the same as for those without MS. Because of this, multiple sclerosis statistics place the annual cost of MS in the US in the billions of dollars range (http://multiple-sclerosis.emedtv.com/multiple-sclerosis/multiple-sclerosis-statistics.html in July 2007). Being MS a demyelinating disease of the CNS and being Nogo-A a component of myelin (Chen et al., 2000; Huber et al., 2002) it is obvious to study the involvement of this protein in MS. To address this question different groups used both human patients and animal models. Serum IgM and cerebro-spinal fluid (CSF) IgG auto-antibodies against Nogo-A were elevated in some MS patients, particularly in younger patients (Reindl et al., 2003). The lack of serum IgG auto-antibodies against Nogo-A was confirmed later (Onoue et al., 2007), however, in this case NgR and Nogo-66 serum IgG were present in 60% and

30% of MS patients, respectively. The elevated amount of Nogo-A auto-antibodies could be inducing demyelination, as does MOG (Kerlero de Rosbo et al., 1990), or facilitate remyelination (Reindl et al., 2003). Different reports with rodents support the hypothesis that Nogo-A antibodies are not deleterious in MS but rather promote remyelination of the MS lesions (Karnezis et al., 2004; Merkler et al., 2003; Sicotte et al., 2003), being a means for repair (Bieber et al., 2001). These auto-antibodies against Nogo-A would be of particular interest considering the increase of Nogo-A expression surrounding chronic active demyelinating lesions (Satoh et al., 2005). Interestingly, there is not only an increase in anti-Nogo-A auto-antibodies in MS patients but a recent study found as well a 20 kDa band in western blot analysis reacting only with anti-Nogo-A antibodies and present only in patients clinically diagnosed with MS (Jurewicz et al., 2007). Furthermore, this Nogo-A fragment was shown to be part of the amino-terminal of Nogo, as antibodies directed to the C-terminus did not recognize such a band. This fragment could be a Nogo-A fragment or potentially one of the smaller Nogo isoforms containing exon 3. Based on the reports above-mentioned it seems feasible to conclude that Nogo-A or auto-antibodies against it present in the CSF or serum can be used as biomarkers for an easier diagnosis of MS, though auto-antibodies are also present in other neurological diseases (Reindl et al., 2003).

The presence of anti-Nogo-A auto-antibodies in MS patients (Onoue et al., 2007; Reindl et al., 2003) may be an indication of a response of the patients to improve their condition. The use of animal models for MS, called experimental autoimmune encephalomyelitis (EAE), supported such notion. Immunization with Nogo-A peptide and anti-Nogo-A IgG antibody intravenous application (Karnezis et al., 2004) or Nogo-66 fragment (Fontoura et al., 2004) resulted in the suppression of EAE, decreasing onset, progression and severity of EAE symptoms (Karnezis et al., 2004).

Overall, the interference with Nogo-A signaling by the innate immune response or antibody application can potentially prove an additional treatment for this debilitating disease, and its detection in the CSF can serve as an additional means of diagnosis for MS.

### 1.5.5 Epilepsy

Approximately 40 million people worldwide have epilepsy. It is more than three times as common as multiple sclerosis, Parkinson's disease and cerebral palsy. There are 1,000 epilepsy-related deaths a year, approx 600 of which are attributable to Sudden Unexpected Death from Epilepsy (SUDEP). Up to 70% of people with epilepsy could achieve full seizure control through medication

(http://www.epilepsynse.org.uk/PAGES/pdf/stats.pdf in July 2007). Only few reports have shown a link between increased expression of Nogo-A and epilepsy in animal models as well as human patients. An up-regulation of Nogo-A in the CA3-CA1 cells layers of the hippocampus was observed after kainic-acid induced seizures (Meier et al., 2003), suggesting that the Nogo-A increased expression was due to seizures. On the other hand, using a model of seizures induced by amygdala kindling it was suggested that the seizures could not be the reason for Nogo-A up-regulation since the contralateral hippocampus did not show increased Nogo-A expression (Takeda et al., 2007). Notwithstanding how Nogo-A is up-regulated, patients suffering from Temporal Lobe Epilepsy (TLE) that underwent surgery had a marked increase in both Nogo-A mRNA and protein levels in all neuronal types of the hippocampus, most pronouncedly in dendrites when compared to port-mortem control individuals (Bandtlow et al., 2004).

### 1.5.6 Cancer

Approximately 1500 Americans per day are expected to die from cancer. One in four deaths in the US is caused by cancer being the second highest cause of death. Between 1996 and 2002, the survival rate was 66% and in 2006 the US overall costs for cancer was estimated to be 206.3 billion dollars (http://www.cancer.org/downloads/STT/CAFF2007PWSecured.pdf in July 2007). Nogo-A increased expression has been linked to several CNS diseases indicating that it can be a potential therapeutic target in other conditions than its well-documented involvement in neurite growth inhibition. This isoform of the Nogo family may not be the only one with therapeutic potential. Nogo-B was investigated in the context of cell death and cancer research. Identified as ASY by (Li et al., 2001), Nogo-B seemed to have a new pro-apoptotic role particularly in cancer cells. Isolated from human diploid fibroblasts and localized to ER, ASY/Nogo-B induced apoptosis of tumorigenic cell-lines transfected with it. Furthermore, it was noted that its expression was reduced in human small cell lung cancer. Using a Yeast-two-hybrid method, ASY/Nogo-B was associated with ASYIP (identical to reticulon 3 – RTN3) in human cells and they are co-localized in the ER (Qi et al., 2003). Although these results would indicate a great advance in cancer research, such pro-apoptotic function was later refuted (Oertle et al., 2003c). In this study, it was observed that several tumors and tumor derived cell lines natively express Nogo-B including SaOS-2 cells used earlier. Over-expression of Nogo-B in SaOS-2 cells did not induce cell death and these cell lines do not differ in their proliferation rates, or in their sensitivity to pro-apoptotic stimuli (Oertle et al., 2003c). However, another study has given evidence that Nogo-B was able to reduce

the anti-apoptotic activity of Bcl-2 and Bcl-$x_L$ (Tagami et al., 2000). To date the role of Nogo-B remains unclear and the differences observed between the studies from (Tagami et al., 2000) and (Li et al., 2001) could be due to differences in transfection techniques (stable vs. transient) (Oertle et al., 2003c).

Nogo-B was not the only member of the Nogo family investigated in the context of cancer research. In oligodendroglial tumors the expression of Nogo-A was found to be negatively correlated with the malignancy of the tumor (Xiong et al., 2007) and glioma cells expressing NgR have their adhesion and migration capacities inhibited by the ligands Nogo-66 and MAG (Liao et al., 2004). Glioma tumors lack metastasis and are localized to the CNS (Maher et al., 2001). A localized therapy inducing Nogo-66 or MAG expression could result in containment of the tumor and a potential increase in NgR expression could inhibit its proliferation. The inhibitory properties of Nogo-A would be the responsible factor for the lack of migration and therefore the malignancy of the glioma. Primary and low-grade glioma cultures are sensitive to inhibitory proteins (Amberger et al., 1998; Xiong et al., 2007) while high-grade glioblastomas or the invasive CNS tumor line (C6 glioblastoma) were not inhibited by these myelin-associated inhibitory components (Paganetti et al., 1988; Xiong et al., 2007). The C6 glioblastoma cell line has high expression of a membrane-bound metalloendoprotease, which is able to neutralise the inhibitory effects of Nogo-A and other myelin-associated inhibitors (Hensel et al., 1998). Hence, the malignancy of these tumors resides on their migration ability (Xiong et al., 2007) and could be dependent on the expression of a membrane-bound metalloendoprotease. Nogo-A as a potent inhibitor protein would be a prime choice for tumor containment at early stages of the disease.

### 1.5.7 Concluding Remarks

There are immense costs of life, money and psychological effects of the diseases discussed above in the families and in the general population. Every new possible treatment can alleviate this burden and Nogo has been implicated in several diseases. Although in cancer, the role of Nogo-B in cell death remains unclear, the involvement of Nogo-A has been demonstrated in a series of reports of different neurological diseases. Different psychiatric disorders, Alzheimer's disease and epilepsy are associated with altered Nogo-A expression levels but it is unclear whether this is a cause or consequence of the diseases and whether a treatment against it would be beneficial. On the other hand, treatments against Nogo-A had positive outcomes in animal models of diseases like ALS and MS. A clinical use of antibodies against Nogo-A could be extremely important for the medical advancement in the treatment of some

debilitating neurological diseases. It would also be interesting to study the involvement of the small family of Rho GTPases, given their role in Nogo-A signal transduction.

## 1.6 Nogo-A and development

Nogo-A expression during development is different from the high oligodendrocyte expression of the adult CNS. In developing tissue, both humans and rats showed mRNA expression in neurons of the spinal cord, dorsal root ganglia, autonomic ganglia of the CNS and developing muscle tissue (Josephson et al., 2001). During chicken development, at E3, Nogo-A protein was detected in the spinal cord, a time at which motor neurons are generated and axonal outgrowth begins (O'Neill et al., 2004). In the rat brain, projection neurons expressed high amounts of both mRNA and Nogo-A protein during development as well as in post-mitotic cells of the developing cortex and cerebellum (Huber et al., 2002). Nogo-A message preceded myelination (O'Neill et al., 2004) and was highly present in pyramidal neurons of the hippocampus after birth (Meier et al., 2003; Mingorance et al., 2004). Differentiating neurons of the olfactory epithelium and bulb strongly expressed both mRNA and Nogo-A protein. Expression was present along the axon and growth cone as well as transiently in dendritic processes. Interestingly, Nogo-A was also expressed at branch points similar to the expression of microtubule-associated proteins (Richard et al., 2005) as well as axons and interneuron leading processes (Mingorance-Le Meur et al., 2007). Nogo-A induction is coincident with neural plate formation and up-regulation of FGF, which is involved in the transformation of non-neural ectoderm into neural precursors. Nogo-A diffuse expression in the neuroectoderm during the early proliferative phase of development and migration, along with its localization to large projection neurons of the optic tectum and tectal-associated nuclei during architectural differentiation, lamination and network, all lead to the proposition of a functional role of Nogo-A in the determination of neural identity and/or differentiation, as well as in network formation, neurite outgrowth, path-finding of large projection neurons and in synaptogenesis (Caltharp et al., 2007). Formation of neural circuits and target innervation occur at times where Nogo-A is expressed in the embryo and thus axon elongation and pathfinding can be part of the Nogo-A roles during development (O'Neill et al., 2004).
In the adult CNS there are also regions were Nogo-A expression is neuronal. Hippocampus, piriform cortex, red nucleus and oculomotor cortex (Josephson et al., 2001; Mingorance et al., 2004) are some of those regions. Some of which, like the hippocampus, are known for their plastic properties.

# 1.7 Nogo-A ablation in intact CNS: What is known.

Nogo-A function in the intact adult CNS tissue is not well known. Its neutralization *in vivo* produced a transitory growth response of Purkinje axons and of the corticospinal tract in intact adult rats (Bareyre et al., 2002; Buffo et al., 2000; Gianola et al., 2003). IN-1 antibody treatment induced the expression of growth related markers in adult intact Purkinje cells (Zagrebelsky et al., 1998), known for their poor intrinsic regenerative capacity. The increased expression of growth markers was followed by a robust but transient fiber growth that covered most of the granular layer (Buffo et al., 2000). A similar transient growth response induced cortico-spinal sprouting in the spinal cord of uninjured adult rats after Nogo-A neutralization (Bareyre et al., 2002). Cortical Layer V neurons had their mean dendritic length and number of branch points increased after Nogo-A inhibition after two weeks but no changes in spine density. All these changes were transient and were not seen six weeks after antibody administration (Buffo et al., 2000; Papadopoulos et al., 2005).

# Goal of the present thesis:

# 1.8 Effects of Nogo-A neutralization in the intact rat CNS

Since Nogo-A discovery and observation of its growth inhibitory capacity, research has mostly focused on the effects of its neutralization after CNS damage. We know very little about its role in the normal CNS with only few reports published. In order to circumvent the compensatory effects in the Nogo-A KO, acute administration of neutralizing antibodies against Nogo-A was the method of choice to study the lack of this molecule in the intact rat CNS tissue.

We aimed our study at extending the reports on growth response after Nogo-A neutralization in the intact adult CNS. Our testing hypothesis is whether Nogo-A neutralization induces a growth response in the intact adult CNS and whether such response induces any behavioral changes. We also want to understand which are the mechanisms involved in the growth and/or behavioral responses. We expect a mild growth response, as it has been reported earlier, with increased plasticity, which could induce cognitive behavioral changes in the adult rat. No gross cognitive behavioral changes are expected to occur since no adverse effects have been reported in the various injury and disease models, although they were not specifically assessed.

To answer our question we will start by using organotypic hippocampal slice cultures addressing the growth response question and the mechanisms underlining it. Then, adult Long Evans Rats will be used for cognitive behavior assessment. In both models, *in vitro* cultures and *in vivo* Nogo-A neutralization, a transcriptomic and a proteomic approach will be used to determine the mechanisms involved in Nogo-A neutralization. Immunofluorescence and immunohistochemical techniques will be employed for confirmation of the factors identified by the transcriptomics and proteomics approaches and to study anatomical changes after Nogo-A neutralization. Cognitive analysis will include classical memory behavior using the Morris Water Maze set-up, classical fear conditioning tests, anxiety and activity assessments.

The impact of this work is major. The potential of a better understanding of the molecular mode of action of Nogo-A and the potential for the identification of new areas where Nogo-A plays a role are clear with our transcriptomics and proteomics approaches. Clarification of cognitive effects after Nogo-A neutralization has great importance in consideration of clinical applications, e.g. for spinal cord injury. Current work in Prof. Schwab's group with Nogo-A knockout mice shows behavior changes in tasks related to schizophrenic symptomatology. Proof of lack of deleterious cognitive

effects would demonstrate the safety of this treatment and possible improvements would open new applications for debilitating diseases such as Alzheimer's disease.

# Chapter 2:

## Neutralization of the membrane protein Nogo-A enhances growth and reactive sprouting in established organotypic hippocampal slice cultures

# Neutralization of the membrane protein Nogo-A enhances growth and reactive sprouting in established organotypic hippocampal slice cultures

**Luis M. Craveiro[1], David Hakkoum[2], Oliver Weinmann[1], Luc Stoppini[3] and Martin E. Schwab[1]**

[1]Brain Research Institute, Department of Neuromorphology of University of Zurich and Swiss Federal Technical Institute, Zurich, Switzerland.
[2]Department of Basic Neurosciences, University of Geneva, Geneva, Switzerland.
[3]Capsant Neurotechnologies Limited Biomedical Sciences Building Bassett Crescent East Southampton United Kingdom

**Corresponding author:**
Luis M. Craveiro, Brain Research Institute, Winterhurerstrasse 190, 8057 Zurich, Switzerland.
Tel. +41 44 63 53213
Fax. +41 44 63 53303
E-mail: craveiro@hifo.unizh.ch

**Keywords:** Transcriptomics, MEAs, axonal growth, intact CNS, inhibition

# 2 Neutralization of the membrane protein Nogo-A enhances growth and reactive sprouting in established organotypic hippocampal slice cultures

## 2.1 Abstract

The reduced ability of central axons to regenerate after injury is significantly influenced by the presence of several molecules that inhibit axonal growth. Nogo-A is one of the most studied and most potent of these inhibitory molecules. Its neutralization or interference with its signaling allows for enhanced axonal sprouting and growth following injury. Using differentiated rat organotypic hippocampal slice cultures treated for 5 days with function blocking anti-Nogo-A antibodies we demonstrate an increase in CA3 fiber regeneration after lesion. In intact slices, five days of anti-Nogo-A treatment led to increased sprouting of intact CA3 fibers that are positive for neurofilament 68. A genomics approach not only confirmed these growth responses upon Nogo-A neutralization in intact cultures, but also showed changes at the synaptic and neurotransmission level. Our results demonstrate that Nogo-A neutralization for five days is sufficient for the induction of a growth response in mature CNS tissue without the pre-requisite of an injury. Nogo-A may therefore act as a tonic growth suppressor/stabilizer in the adult CNS.

## 2.2 Introduction

Adult Central Nervous System (CNS) lesions often have devastating consequences due to the low regeneration and structural repair capacity of the tissue. This phenomenon can partly be explained by the presence of neurite outgrowth inhibitory molecules, several of which have been identified (Benowitz and Yin, 2007; Filbin, 2006). Nogo-A, one of the most potent growth inhibitors of the adult CNS and the first one being discovered (Caroni and Schwab, 1988b; Chen et al., 2000), has been extensively studied *in vitro* and *in vivo*.

Nogo-A signals via the receptor complex NgR/p75/Lingo-1/Troy (Fournier et al., 2001; Mi et al., 2004; Park et al., 2005; Wang et al., 2002a) and an as yet unidentified Nogo-

A specific receptor (Dodd *et al.*, 2005). Two active sites, Nogo-66 and a Nogo-A specific region, both lead to activation of RhoA and ROCK (Fournier et al., 2003; Hsieh et al., 2006; McKerracher and Higuchi, 2006; Niederost et al., 2002; Schweigreiter et al., 2004), therefore, affecting the neuronal growth machinery.

In rats with stroke lesions, Nogo-A neutralization (Emerick et al., 2003; Papadopoulos et al., 2002; Papadopoulos et al., 2006), or NgR blocking peptides (Lee *et al.*, 2004), allowed compensatory fiber sprouting from the intact side across the midline and functional innervation of the denervated side. Enhanced regeneration of injured fibers and improved functional recovery were observed in spinal cord lesioned rats and monkeys treated with anti-Nogo-A antibodies (Freund et al., 2006; Liebscher et al., 2005; Merkler et al., 2001; Schnell and Schwab, 1990; Schwab, 2004), in rats infused with NgR antagonist peptides (GrandPre *et al.*, 2002) or an activity-blocking receptor fragment (Li *et al.*, 2004), and in Nogo-A (Dimou et al., 2006; Kim et al., 2003; Simonen et al., 2003) or NgR (Kim *et al.*, 2004) knockout mice.

Nogo-A function in the intact CNS tissue is not well known, but its neutralization *in vivo* produced a transitory growth response of Purkinje axons and of the corticospinal tract in intact adult rats (Bareyre et al., 2002; Buffo et al., 2000; Gianola et al., 2003). Nogo-A is relatively highly expressed in oligodendrocytes and some neurons of the hippocampus (Gil et al., 2006; Huber et al., 2002; Meier et al., 2003; Trifunovski et al., 2006). Organotypic hippocampal slice cultures are a good *in vitro* model to study hippocampal function and structure (Bahr, 1995; Gahwiler et al., 1997; Hakkoum et al., 2006; Stoppini et al., 1991, 1993). They mature *in vitro* and retain many *in vivo* features from a structural and functional perspective. We chose this model to study the effects of acute Nogo-A neutralization, using two function blocking monoclonal antibodies, 11C7 and 7B12 (Liebscher et al., 2005; Oertle et al., 2003d; Wiessner et al., 2003), exclusively targeted against the Nogo-A specific region. We observed induced growth responses morphologically and biochemically in differentiated cultures treated with antibodies only for 5 days. Also important, was the lack of observable undesirable effects like spontaneous epileptic activity after Nogo-A neutralization.

# 2.3 Material and methods

### Organotypic Hippocampal Slice Cultures and anti-Nogo-A antibody treatment:

Hippocampal slices were cultured as previously described (Stoppini *et al.*, 1991). Briefly, the hippocampus of P7 Wistar rats (bred in house) was dissected and immediately cut into 350 µm thick slices. Slices were separated in ice cold dissecting

medium and then 4 slices were placed into a Millicel-CM insert (Millipore, MA, USA) with 1 ml of culture medium and placed into 6 well plates (TPP, Switzerland). Cultures were kept for 21 days at 33ºC, in a 5% $CO_2$ atmosphere. Mouse monoclonal antibody 11C7, directed against rat aa 623–640 of Nogo-A, or 7B12, directed against rat aa 763–820 of Nogo-A (Oertle et al., 2003d), or control monoclonal antibody against wheat auxin, were applied as highly purified IgGs at a concentration of 3ug/ml in the culture medium for a period of 5 days (medium was changed every 2 days). Cultures undergoing lesions (mechanical transection at the level of CA3-CA1 junction performed at room temperature with a sterile razor blade after 21 days in vitro (DIV) had antibody treatment delivered immediately after transection.

The Nogo-A antibodies 11C7 and 7B12 were shown to enhance neurite outgrowth on Nogo-A containing substrate *in vitro* (Oertle et al., 2003d) and in the injured CNS *in vivo* (Liebscher et al., 2005; Wiessner et al., 2003). They recognize Nogo-A monospecifically on western blot (Dodd et al., 2005; Oertle et al., 2003d).

**Electrophysiology:**

Electrophysiological recordings were made using a multi-electrode array (MEA). Slices were cultured and recorded on sterilized and disposable cartridges that include a multi-electrode array consisting of 40 electrodes (30μm thick) made of pure gold by plasma evaporation (Biocell Interface, SA, La Chaux-de-Fond, Switzerland). The MEA is built on a porous and transparent membrane that is maintained in a sandwich between two chambers: the upper chamber, is the gas perfusion chamber that maintains the tissue at the gas-liquid interface, and the lower one is the perfusion chamber that contains sterile culture medium under perfusion. The chambers and the array are assembled and inserted into a console unit (Biocell Interface) where the temperature (33° C) and the perfusion parameters (10μl/minute) can be precisely monitored. The position of the slices on the electrodes can be visualized directly through the camera integrated within the connector. Each electrode can be assigned as stimulating or recording. Two recording sessions were usually performed: one before the lesion and a second at day 6 post-lesion. In both sessions, four electrodes located in the CA1 area were selected for recording of synaptic responses evoked by two stimulating electrodes located in the CA3 area. This stimulation paradigm yielded the activity across the lesion. In addition, we also monitored activity in the mossy fiber connection, using two stimulating electrodes located in the dentate hilus and four recording electrodes located in the intact part of the CA3 area, close to the site of lesion. This stimulation paradigm was used to assess the viability of the tissue. Stimulation parameters were maintained constant in all sessions (pulses of 4V, 0.5 ms, applied every 15 seconds). The

amplitude of responses recorded during a 10-minute period was averaged. Data are expressed as mean ± SEM of the number of slice cultures analyzed and statistical analyses were carried using the unpaired t test.

### Immunofluorescence:

Cultures were fixed with 4% PFA overnight and then kept overnight in permeabilization buffer containing 1.5% horse serum, 3% Triton-X and 0.2% Top-Block (Juro AG, Lucerne, Switzerland). Primary antibody incubation with rabbit polyclonal anti-neurofilament 68 (NF68) (AB1983, dilution 1:300, Chemicon International, Temecula, CA, USA), rabbit polyclonal anti-Gap43 (AB5220, dilution 1:1000, Chemicon International, Temecula, CA, USA), mouse monoclonal anti-NeuN (MAB377, dilution 1:300, Chemicon International, Temecula, CA, USA), mouse monoclonal anti-MAP2a/b (Abcam, Cambridge, UK, ab3096, dilution 1:300), or mouse monoclonal anti-CNPase (MAB326, dilution 1:1000, Chemicon International, Temecula, CA, USA) was performed in the permeabilization buffer for 5 days at 4° C. After washing, secondary antibody, Alexa 488 anti-mouse or Alexa 546 anti-rabbit (Invitrogen-Molecular Probes, Basel, Switzerland), was incubated for 2 hours. Cultures were then imaged with a Zeiss Axioskop2 mot plus for lower magnification images used in densitometry analysis. Confocal imaging was performed using a Zeiss LSM 410 confocal laser scanning microscope using lasers pre-tuned to 543 nm (Alexa 546) and 488 nm (Alexa 488), or a Spectral Confocal Microscope TCS SP2 AOBS (Leica) using a 63x oil immersion objective. Maximum Intensity Projections of the images were used to improve the signal-to-noise ratio.

### Quantification of axons and dendrites stained for NF68 or MAP2a/b:

Organotypic hippocampal cultures cultured for 21DIV were incubated with anti-Nogo-A antibodies (11C7 and 7B21) or control IgG for further 5 days. After fixation and immunohistochemical treatment described above, confocal images were taken with CA3 *stratum pyramidale* centered in the picture frame and partly containing *stratum oriens* and *stratum radiatum* (about 1/3 of the picture frame for each *stratum*). For NF68 quantification, a rectangle of fixed area (115 x 84$\mu$m) was placed in the area of the *stratum oriens* where most fibers were present. Using Imaris software (Bitplane AG, Zurich, Switzerland) each fiber in the field was manually traced. The software then calculated how many fibers were present. Imaging, coding and tracing were performed by blinded researchers. Due to the complexity of tracing of MAP2a/b positive fibers, we decided to use a densitometric analysis. Images were taken in the same regions

described above and ImageJ software (http://rsb.info.nih.gov/ij) was used to determine the overall signal intensity. As for NF68 quantification, all imaging, coding and tracing were performed by blinded researchers.

**Gene expression analysis:**

Upon the end of the treatment, groups of 24 cultures were pooled together and total RNA was extracted (RNeasy Lipid Tissue Mini Kit, Qiagen). Affymetrix Gene Chips (Rat Expression Array 230 2.0, Affymetrix Inc., Santa Clara, CA) were used for RNA hybridization, according to the manufacturer's protocol. Each condition (IgG vs. Medium only, 11C7 vs. Medium only, 7B12 vs. Medium only) was analyzed in triplicates. The dataset was flagged filtered for gene presence in at least two out of three chips, normalized first per chip and second for each gene to the median of the wild type replicates, and statistically restricted by a 1 way ANOVA $p<0.05$ (no multiple testing correction). The obtained list was then filtered for >1.2 fold changes. Gene analysis was then performed using Genespring 7.0, and the Rat Genome Database (http://rgd.mcw.edu) was used to obtain further information about the genes regulated.

**Western Blot Analysis:**

Hippocampal cultures were lysed in buffer containing 1% Nonidet P-40, 1% sodium cholate, 0.05% sodium dodecyl sulphate (SDS), 20 mM Tris pH = 7.5 and 100 mM NaCl, and then sonicated. Protein concentration was determined using the Bradford dye-binding assay (Bio-Rad, Hercules, CA, USA), according to the manufacturer's protocol, with bovine serum albumin as the standard. Fifteen micrograms of total protein were separated by SDS–polyacrylamide gel electrophoresis (10% gels) under reducing conditions and blotted onto pure nitrocellulose membranes (Bio-Rad). Membranes were incubated with antibodies against Gap43 (1 : 1000, polyclonal GAP-43; Chemicon, Temecula, CA, USA), and β-actin (1 : 5000; Chemicon, Temecula, CA, USA), followed by a horseradish peroxidase-conjugated secondary antibody (1 : 5000; Bio-Rad). The immunoreactive proteins were detected with an enhanced chemiluminescence kit (ECL; Amersham Pharmacia, Piscataway, NJ, USA) according to the manufacturer's protocol, by using ECL-Hyperfilm (Amersham Pharmacia). Quantification of signal intensities in western blots was performed with a densitometer using ImageJ software (http://rsb.info.nih.gov/ij). Densitometric values are expressed as means ± SEM in arbitrary units.

**Statistical Analysis:**

Statistical analysis was performed using the software GraphPad Prism. The Mann-Whitney test was used in all analyses except for electrophysiological data where the unpaired t-test was used. Results are expressed in means ± SEM.

# 2.4 Results

## Nogo-A expression in young and differentiated organotypic hippocampal slice cultures

Hippocampal slices dissected from P7 rats are known to develop into mature, differentiated and functional circuits within 3 weeks (Bahr, 1995; Gahwiler, 1981a, b, c; Noraberg et al., 2005; Stoppini et al., 1991, 1993). A morphological analysis of the 21 days *in vitro* (DIV) slice cultures using the neuronal nuclear marker NeuN, showed the typical cytoarchitecture of the hippocampus, which is highly similar to its *in vivo* morphology (**Fig 1**).

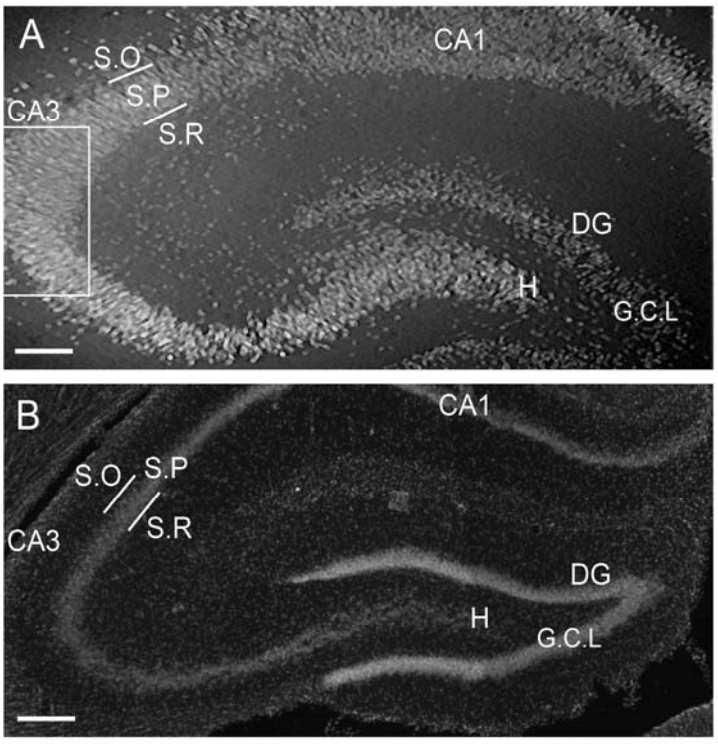


**Figure 1. Hippocampal organotypic slice culture morphology**
A) Typical architecture of pyramidal and granular cell layers in organotypic hippocampal cultures after 3 weeks *in vitro*. Box depicts the region where all subsequent imaging and analysis took place. B) Adult hippocampus *in vivo* (adult rat).. Both, *in vitro* culture and *in vivo* section are labelled with NeuN. Scale bar: A = 140 µm; B = 260 µm. S.O – *Stratum Oriens*, S.P – *Stratum Piramidale*, S.R – *Stratum Radiatum*, H – Hilus, G.C.L – Granular Cell Layer, DG – Dentate Gyrus

In both young (5 DIV) and differentiated (21 DIV) cultures, Gap43 was expressed in CA3 neuronal processes (**Fig 2A, A'**). NF68 expression changed from a high cell body expression in CA3 pyramidal cells in young cultures (**Fig 2B**) to a low cell body expression and more expanded axonal expression in differentiated cultures (**Fig 2B'**).

While NF68 was expressed both in axons and dendrites, MAP2a/b was expressed only in dendrites (**Fig 2C, C', D ,D'**) throughout culture development.

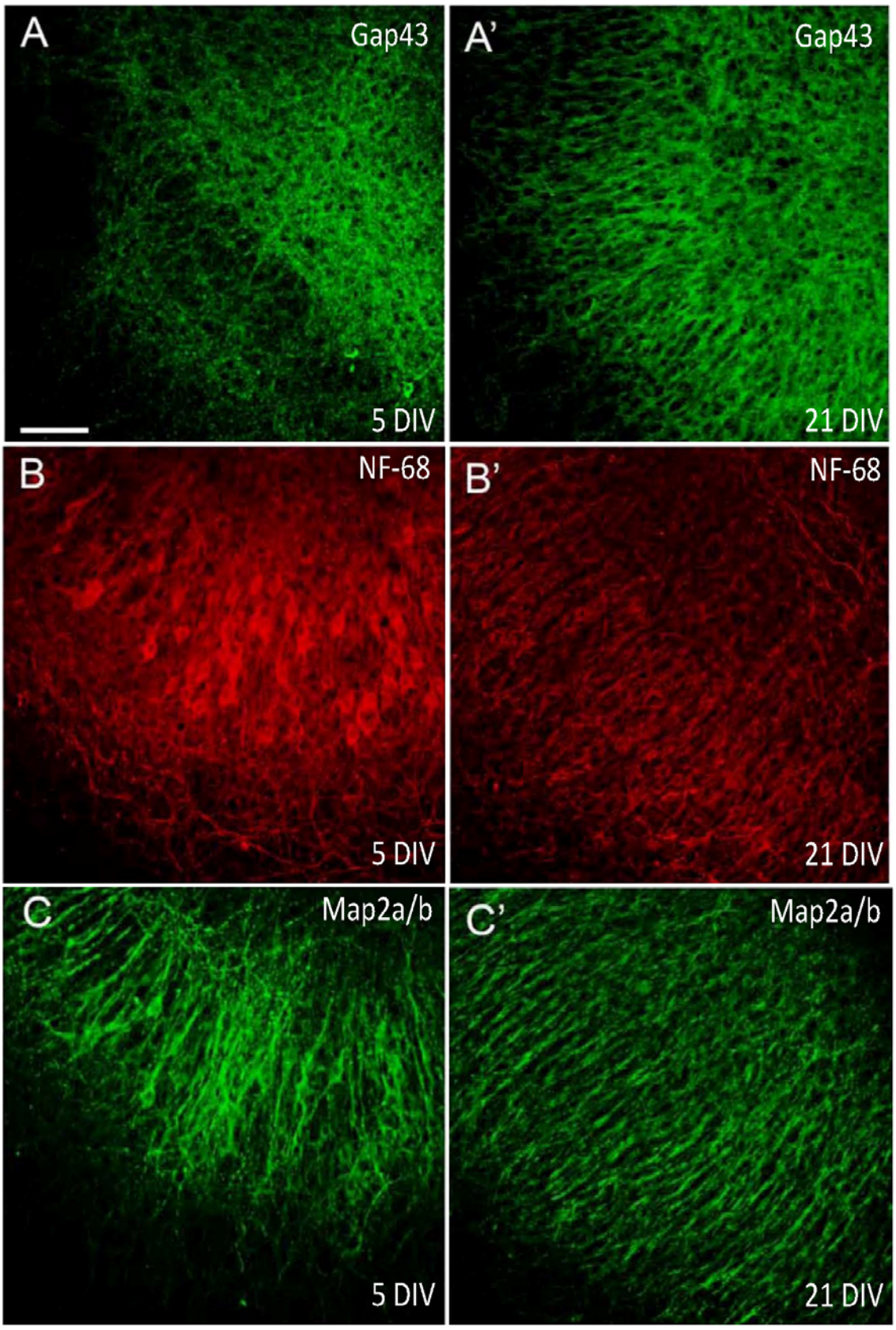

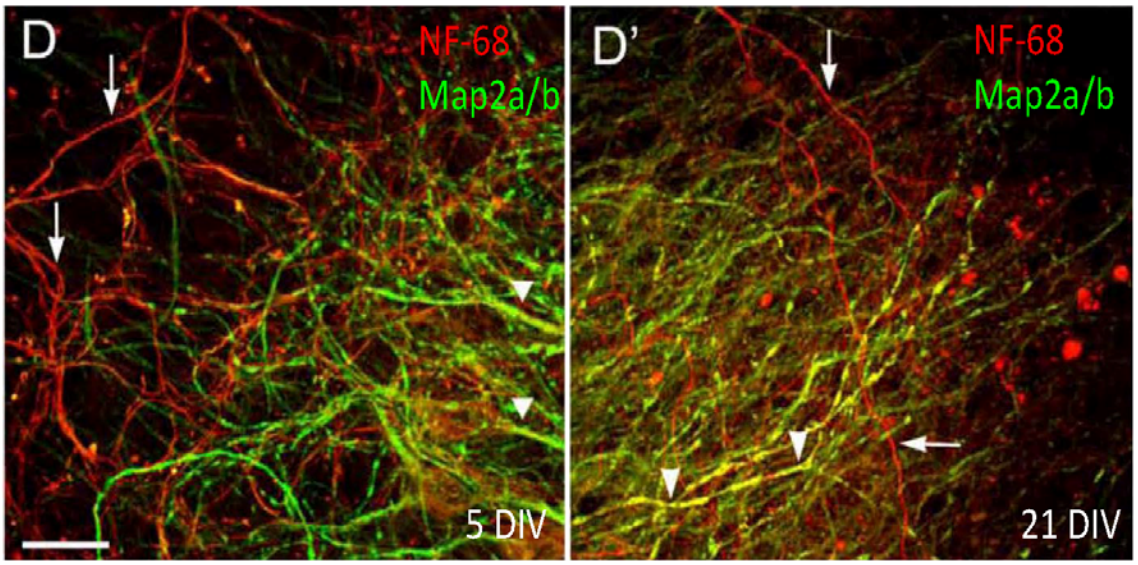


**Figure 2. Neuronal marker expression in young (5 DIV - A-D) and differentiated cultures (21 DIV - A'-D')**
CA3 pyramidal neurons in the *stratum pyramidale* (S.P.) and their axons is *stratum oriens* (S.O.) are positive for Gap43 (A, A'), NF68 (B, B'), and their dendrites, mainly in *stratum pyramidale*, are positive for MAP2a/b (C, C') in young cultures (A-D) and differentiated cultures (A'-D'). Note predominant cell body labelling of NF68 in young cultures (B). D, D': overlay from B and C, showing in red NF68 axonal labelling (arrows in D, D') and dendritic co-labelling of NF68 (red) and MAP2a/b (green) in yellow (arrowheads in D, D') on both young and differentiated cultures. Scale bar: A-C and A'-A' = 100 µm; D and D' = 40 µm

In line with *in vivo* development (Berger and Frotscher, 1994), hippocampal slice cultures showed an increase in the expression of CNPase, an oligodendrocyte marker, as the cultures matured (**Fig 3A, A'**). Nogo-A expression strikingly shifted from a primarily neuronal expression in young cultures (**Fig 3B, C**), to a primarily oligodendrocytic expression in the differentiated cultures (**asterix in Fig 3B'**) although pyramidal cells still expressed Nogo-A (**Fig 3B', C'**). This effect was gradual, however, as some oligodendrocytes expressing Nogo-A could already be observed in the young cultures (**arrow in Fig 3c**), and lower level Nogo-A expression persisted in pyramidal neurons of the CA3 region in the differentiated cultures (**Fig. 3C')**, similar to the adult *in vivo* situation (Trifunovski *et al.*, 2006). During the development of the cultures, it was always possible to detect cells positive for both CNPase and Nogo-A, although at early time points not all CNPase positive cells were also Nogo-A positive (**Fig 3E, E'**). The increased co-labelling of CNPase and Nogo-A with slice culture maturation is in line with the observed shift of Nogo-A expression from neuronal to oligodendrocytic as the culture matures.

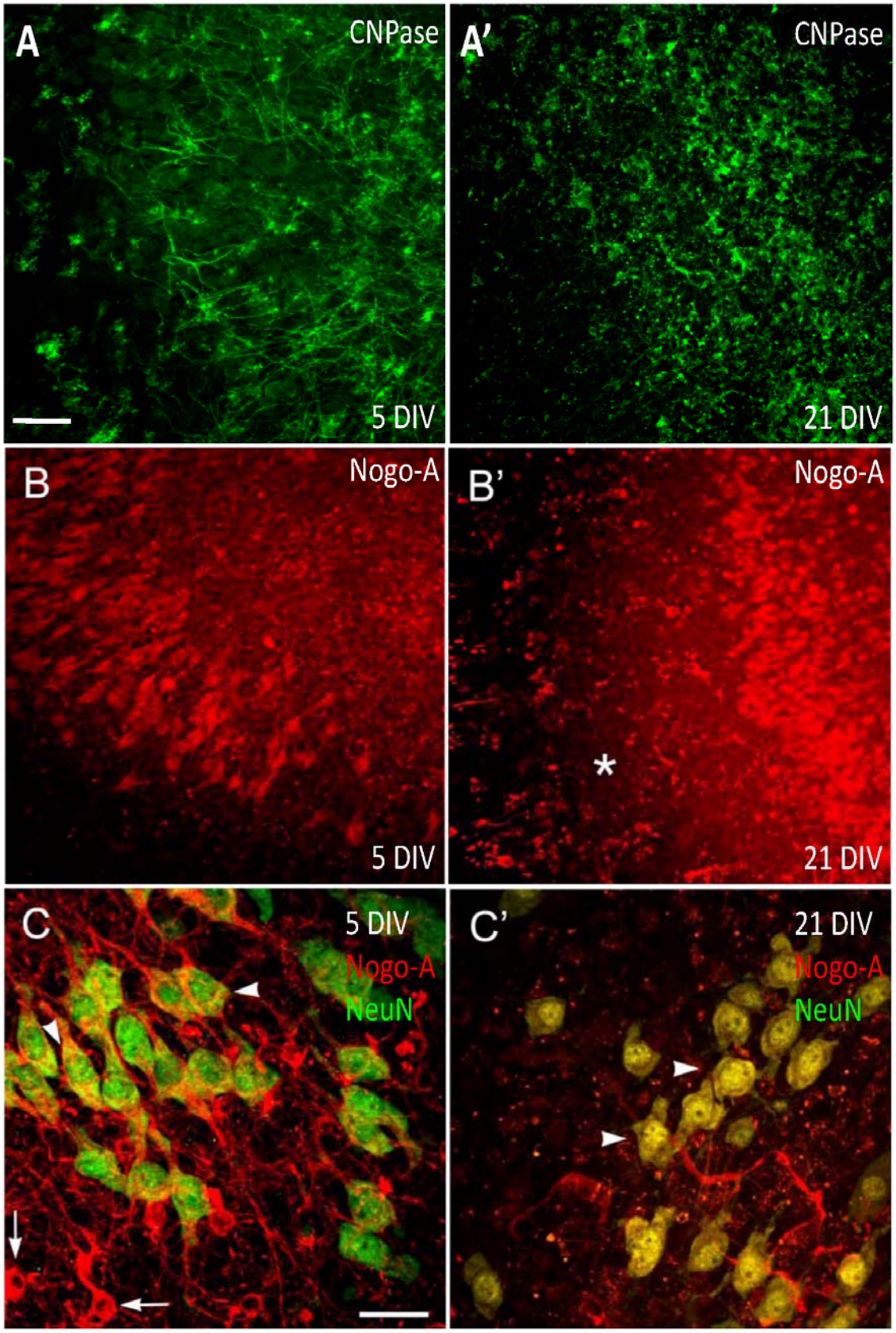
A
CNPase
5 DIV
A'
CNPase
21 DIV
B
Nogo-A
5 DIV
B'
Nogo-A
*
21 DIV
C
5 DIV
Nogo-A
NeuN
C'
21 DIV
Nogo-A
NeuN

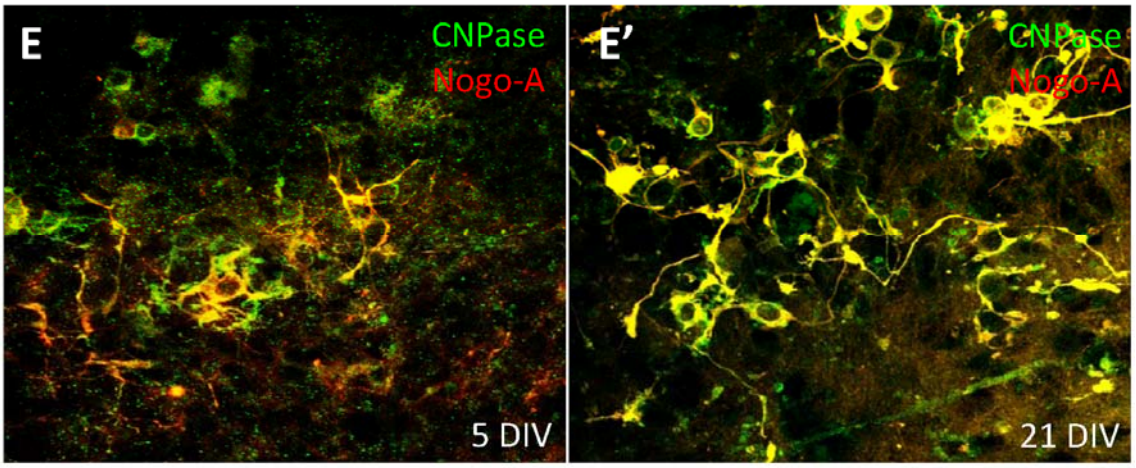


**Figure 3. Oligodendrocyte marker and Nogo-A expression in young (5 DIV – A-C) and differentiated cultures (21 DIV – A'-C')**
Oligodendrocytes labelled for CNPase are present in greater amounts in differentiated (21 DIV) cultures (A') compared to young (5 DIV) cultures (A). Co-labelling between Nogo-A and CNPase is almost complete in 21 DIV cultures, while in 5 DIV cultures some CNPase cells do not express detectable levels of Nogo-A. Nogo-A is most prominently expressed in pyramidal neurons (B, arrowheads in C) of young cultures. Some Nogo-A positive oligodendrocytes are present in young cultures (arrows in C; NeuN in green). In differentiated cultures Nogo-A is most prominently expressed in oligodendrocytes (asterix in B') but is still present in pyramidal cells (arrowheads in C'; NeuN in green). Scale bar: A, B,and A', B' = 100 µm; C and C' = 40 µm

## Nogo-A neutralization enhances regeneration of transected Schaffer collaterals

A sharp cut through the border between the regions CA3 and CA1 of 21 DIV organotypic hippocampal slice cultures was made with a sterile razor blade. The cultures were incubated with the neutralizing antibody against Nogo-A 11C7, with control antibodies or with culture medium alone for additional 5 days. Field potentials were evoked by stimulation of the CA3 region and recorded in CA1 before and 5 days after lesion and antibody treatment. The organotypic hippocampal slices were cultured on multi-electrode arrays (MEAs) for 21 days (**Fig 4A**). The lesion was complete since no activity could be elicited across the lesion site immediately after the cut, additionaly the trace of the razor blade is visible in the MEA-culture shown in **Fig 4A**. When the CA3 region was stimulated 5 days after lesion, the amplitude of the evoked potentials recorded in CA1 was 68.32% ± 4.583 SEM of the recorded values in intact slices for the anti-Nogo-A treated group, while the injured control antibody treated group showed only an average evoked potential amplitude 37.25% ± 3.443 SEM of that of the intact tissue (**Fig 4D; p=0.0005, Mann-Whitney**).

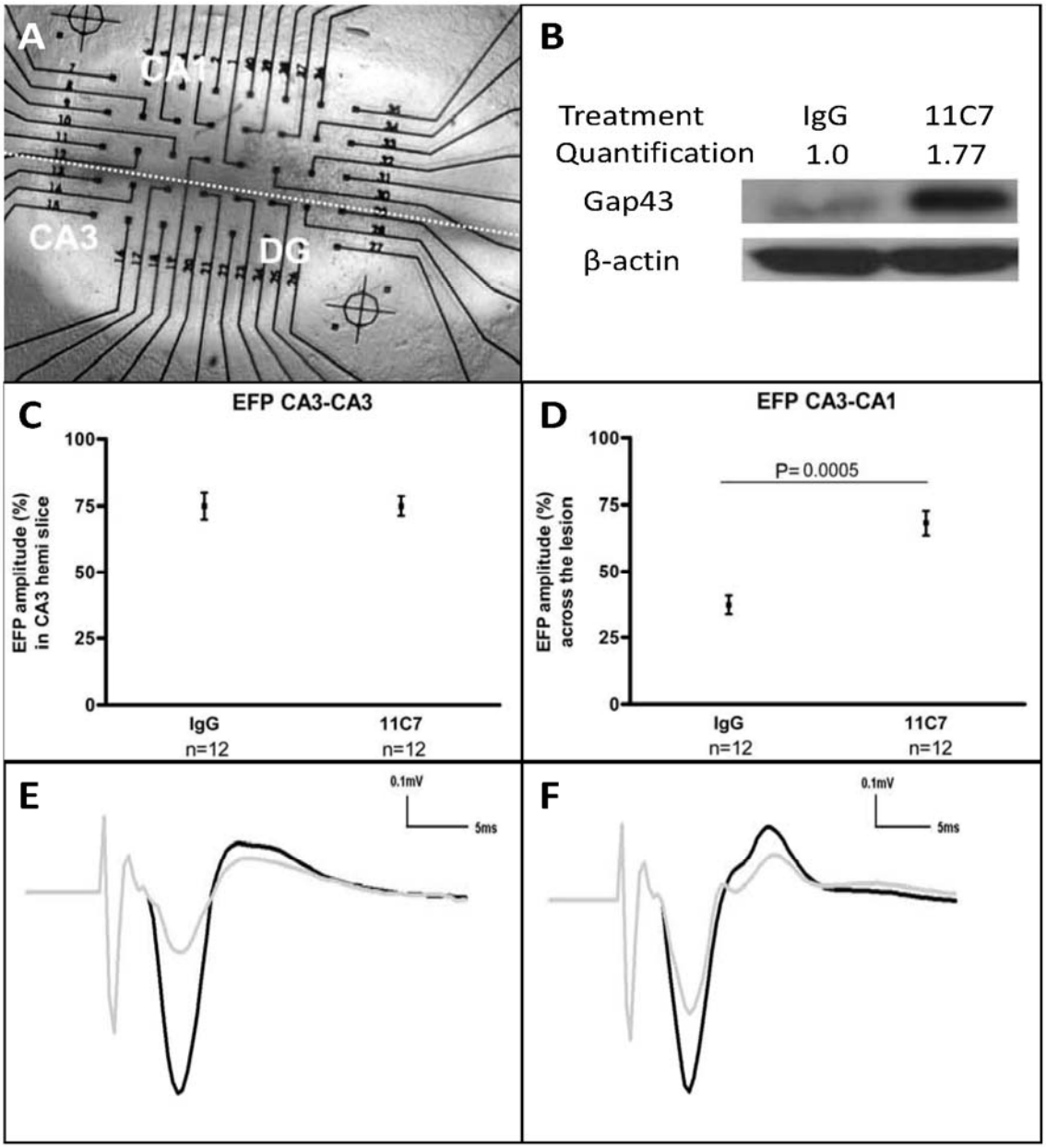


**Figure 4. Effect of Nogo-A neutralization on Schaffer collateral regeneration of 21 DIV organtotypic hippocampal slice cultures**

Organotypic hippocampal slice cultures were cultured for 21 days. The Schaffer collaterals were cut and function blocking antibodies against Nogo-A were added to the culture medium for additional 5 days. A) Micrograph of an organotypic hippocampal slice culture grown on the multi-electrode array. Dotted line indicates the razorblade lesion. B) Gap43 western blot from pooled cultures treated with IgG control or anti-Nogo-A antibody, showed an increase content of Gap43 after lesion and subsequent treatment anti-Nogo-A antibody (11C7) as compared to subsequent control IgG (IgG) treatment. Densitometric quantification, using ImageJ, of the intensity of the bands showed a 1.77 fold increase of Gap43 after anti-Nogo-A antibody treatment as compared to control IgG treatment. β-actin was used as loading control and the intensities of the bands were used to normalize Gap43 intensities in the corresponding treatments. C) No change in the mean amplitude of evoked field potentials in control CA3 stimulation -CA3 recording after lesion and 5 day treatment with control IgGs (IgG) or anti-Nogo-A antibody (11C7). N = 12 slice cultures. D) Increased evoked responses in CA1 after CA3 stimulation in injured, anti-Nogo-A antibody (11C7) treated cultures as compared to control antibody treatment (IgG). 11C7 = 68.32% ± 4.583 SEM; IgG = 37.25% ± 3.443 SEM; N = 12 slice cultures; P = 0.0005, Mann-Whitney Test. Averaged traces of the evoked potentials of control IgG (E) and anti-Nogo-A treated slice cultures (F), before (black lines) and after lesion and treatment (grey lines).

The averaged trace representation of the evoked potentials shows the increased amplitude of the response after Nogo-A neutralization (**Fig 4F**), while the control IgG treated cultures showed much lower evoked potentials (**Fig 4E**). An additional control for neuronal viability was the stimulation of CA3 and recording of CA3 potentials (**Fig 4C**); it showed no difference across the groups, therefore indicating that the observed effect with anti-Nogo-A treatment was not due to neuronal survival but rather to enhanced restoration of the connection of CA3 to CA1, i.e. the injured Schaffer collaterals. There was not a single culture with evidence of epileptic activity, neither in the control nor in the anti-Nogo-A antibody treated groups. We analyzed the expression of an important axonal growth marker, Gap43, by western blot. Within the 5 days of treatment after the lesion, Gap43 levels increased 1.77 fold in the lesioned anti-Nogo-A antibody treated cultures as compared to the lesioned control IgG treated ones (**Fig 4B**).

All these results show that suppression of Nogo-A for 5 days in this system enhanced functional regeneration of the CA3-CA1 Schaffer collaterals, in the absence of aberrant growth in the dentate gyrus and CA3 that would lead to epileptic activity.

### Nogo-A neutralization increases axonal sprouting in intact differentiated slice cultures

The regeneration results laid the ground for the question of axon growth in response to Nogo-A neutralization in 21 DIV intact cultures as a model of the intact brain. After 5 days of treatment with either one of two function-blocking specific anti-Nogo-A antibodies, 11C7 or 7B12, we observed a significant increase in the number of fibers labeled for NF68 (**Fig 5C, D; Fig 6A**) when compared to control antibody treatment or untreated cultures in the CA3 region (**Fig 5A, B; Fig 6A**). In contrast, MAP2a/b did not show detectable differences across the four different treatment groups (**Fig 5A'-D', Fig 6B**). NF68 is mainly expressed in axons, while MAP2a/b is a dendritic marker (**Fig 2D, D'**), thus the increase in NF68 positive fibers in the anti-Nogo-A treated cultures was most likely due to axonal sprouting, growth and arborization.

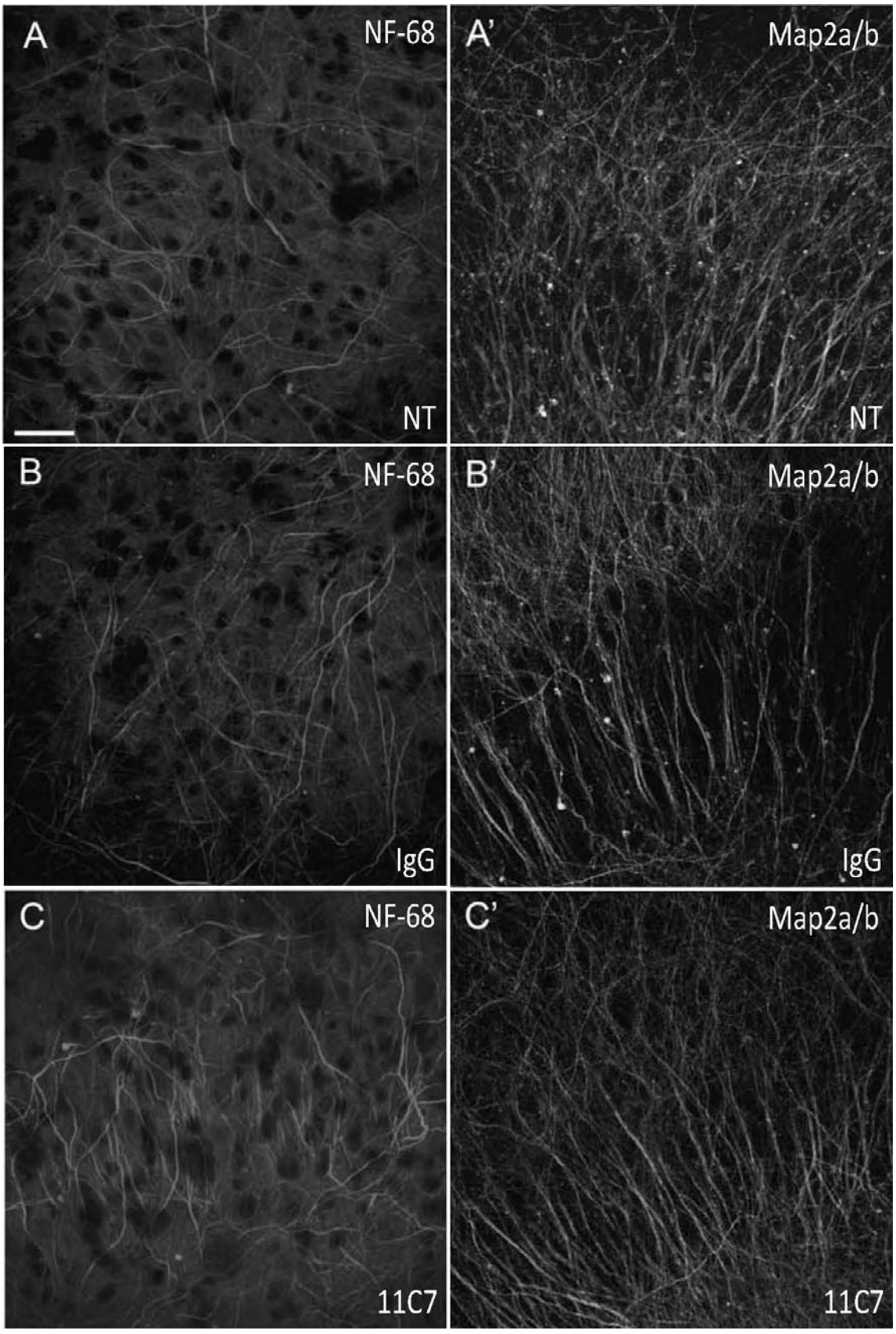
A
NF-68
NT
A'
Map2a/b
NT
B
NF-68
IgG
B'
Map2a/b
IgG
C
NF-68
11C7
C'
Map2a/b
11C7

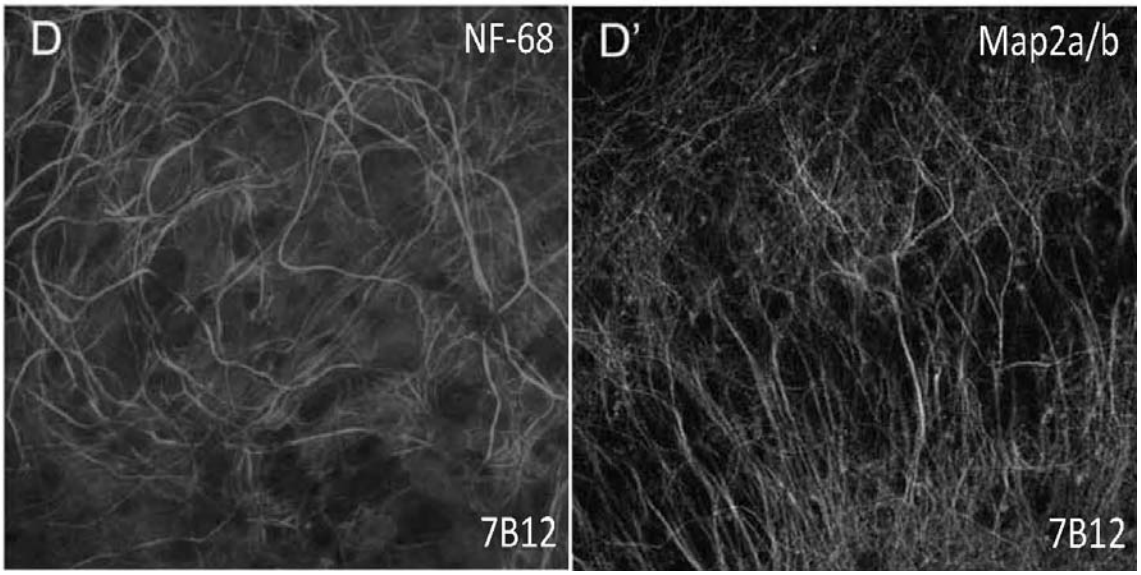


**Figure 5. Effect of Nogo-A neutralization in 21 DIV non-injured organotypic hippocampal cultures**
Organotypic hippocampal cultures were cultured for 21 days and subsequently received a five day treatment with medium alone (A, A'), control IgG (B,B'), or with anti-Nogo-A antibodies 11C7 (C,C') and 7B12 (D,D'). An increase in the number of fibres positive for NF68 in CA3 region after anti-Nogo-A antibody incubation 11C7 (C) and 7B12 (D) compared to medium alone (A) or control IgG treatment (B) indicates an increase of the growth properties of CA3 hippocampal neurons. MAP2a/b fibre density remained similar across treatments, medium alone (A'), IgG control (B'), 11C7 (C') and 7B12 (D') indicating the dendritic arborisation was not detectably influenced by Nogo-A neutralization. Scale bar = 40 µm.

Though potentially expected, stimulation/recording experiments showed that there were no detectable changes in the evoked activity of the unlesioned antibody treated cultures (**Fig 6C**) and most importantly, there was no evidence of epileptic activity, neither in control IgG treated nor in anti-Nogo-A treated cultures.

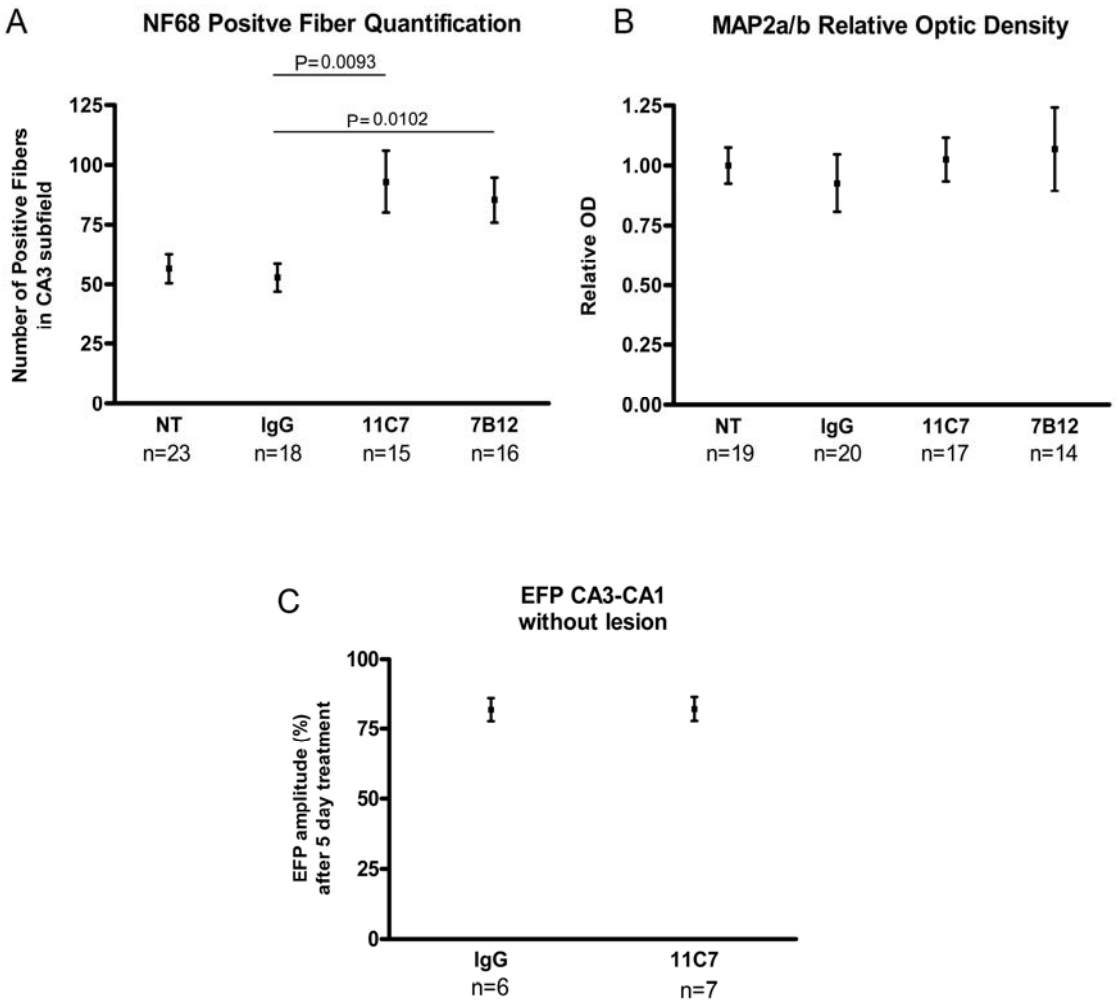


**Figure 6. Quantification of effect of Nogo-A neutralization in 21 DIV non-injured organotypic cultures**
A) Quantification of the number of NF68 positive fibres in the *stratum oriens* of CA3 area shown in **Fig 5** showed a significant increase in the number of fibres present after Nogo-A neutralization as compared to the control treatments. B) Densitometric analysis of MAP1a+2b immunoreactivity in CA3 region revealed no differences between the different treatment groups. C) Stimulation induced activity in 21 DIV non-lesioned cultures grown on MEAs after a 5 day antibody treatment did not detect differences in the CA3-CA1 evoked potentials between the anti-Nogo-A and the control IgG treated groups.

## Gene expression changes induced by Nogo-A neutralization

In order to better understand the mechanisms by which Nogo-A neutralization induces the above-mentioned morphological changes, a transcriptomic analysis was performed. Total RNA was extracted from 26 DIV slice cultures treated from day 21 to day 26 with anti-Nogo-A antibodies (11C7 or 7B12), control antibodies (IgG) or non-treated, medium alone (NT). After hybridization to the gene arrays and statistical analysis by GeneSpring 7.0, we compared 11C7 vs. NT, 7B12 vs. NT and IgG vs. NT and generated lists of genes up- or down-regulated by 1.2 fold. We combined these lists into one table of 11C7 and 7B12 common regulated genes and removed the genes that were also changed in the IgG vs. NT comparison (**Fig 7, Table 1**). Ninety-five genes

were differentially expressed at 26 DIV after 5 days of Nogo-A neutralization and common to both anti-Nogo-A antibodies (11C7 and 7B12). When assigned to functional categories (**Fig 7, Table 1**), 29.9% of the listed genes could be placed under a major category of growth related genes comprising Cell Adhesion, Extracellular Matrix (ECM), Growth Factor, GTPase Signal Transduction, Neurogenesis and Neuronal Survival categories. Interestingly, the third largest category with 8% of the genes was GTPase Signal Transduction and their regulators. This category includes genes that belong to the family of Rho GTPases, known to be crucially involved in Nogo-A signaling. RhoA and ROCK have been shown to be downstream effectors of the Nogo-A signaling pathway (Fournier et al., 2003; Hsieh et al., 2006; McKerracher and Higuchi, 2006; Niederost et al., 2002; Schweigreiter et al., 2004). Among the growth factors and axonal growth promoting genes, interleukin 1 beta (Il1b), transforming growth factor beta regulated gene 1 (tbrg1), tissue inhibitor of metaloproeinase-1 (TIMP-1) were up-regulated after Nogo-A neutralization, contrary to insulin-like growth factor 1 (Igf1), which was down-regulated. The second most up-regulated gene after Nogo-A neutralization was secretory leukocyte protease inhibitor (SLPI). This protein involved in immune processes has been shown to be involved in neuroprotective situations.

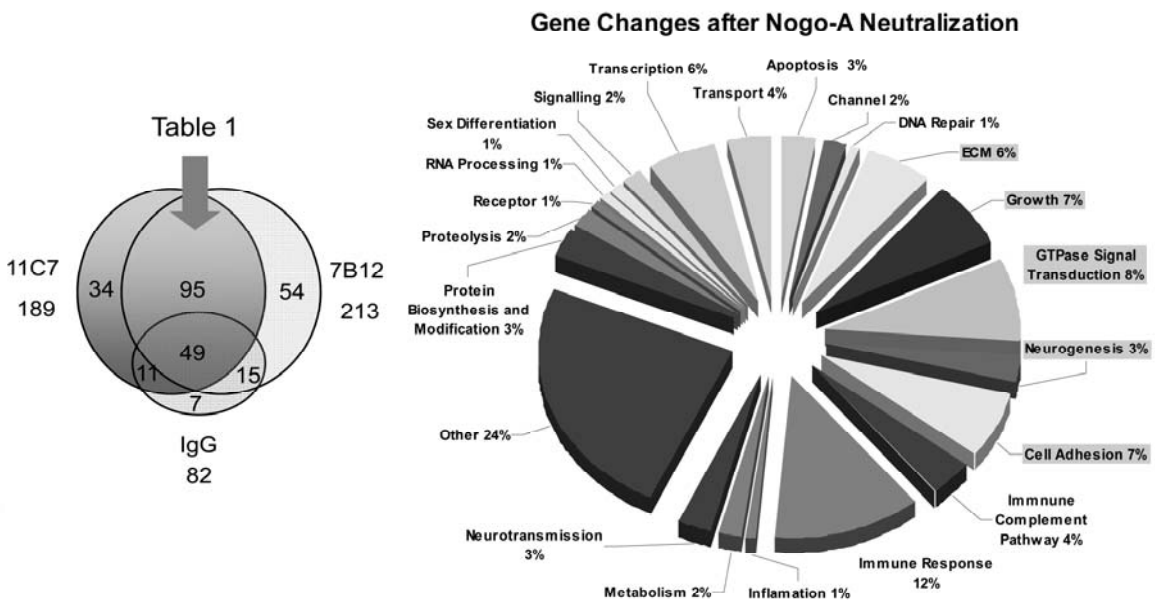


**Figure 7. Gene Expression changes induced by Nogo-A neutralization, category assignment and gene proportions**
Scheme depicting the gene distribution in the different treatment groups analyzed and schematic representation of the proportion of genes specifically regulated after anti-Nogo-A treatment in different functional categories. Highlighted in grey boxes are the categories containing genes with influence in growth responses.

## Table 1. Gene Expression changes induced by Nogo-A Neutralization

| Gene Symbol | Gene Name | Accession Number | 11C7 | | 7B12 | |
|---|---|---|---|---|---|---|
| | | | Fold Change | P value | Fold Change | P value |
| **Apoptosis** | | | | | | |
| Cipar1 | Castration induced prostatic apoptosis-related protein 1 | 1370962_at | 1.627 | 0.0348 | 2.028 | 0.0348 |
| Casp4 | Caspase 4 | 1387818_at | 1.403 | 0.0156 | 1.575 | 0.0156 |
| Lcn2 | lipocalin 2 | 1387011_at | 4.568 | 0.0361 | 11.5 | 0.0361 |
| **Cell Adhesion** | | | | | | |
| Asgr1 | asialoglycoprotein receptor 1 | 1370149_at | 1.522 | 0.038 | 5.801 | 0.038 |
| Lgals5 | Lectin galactose binding soluble 5 (Galectin-5) | 1369716_s_at | 1.623 | 0.00838 | 2.381 | 0.00838 |
| Alcam | Activated leukocyte cell adhesion molecule | 1370043_at | 0.812 | 0.0324 | 0.702 | 0.0324 |
| Stab1_predicted | Similar to stabilin-1 | 1374247_at | 1.587 | 0.00949 | 2.501 | 0.00949 |
| Ncam2 | Neural cell adhesion molecule 2 | 1384734_at | 1.236 | 0.0499 | 0.729 | 0.0499 |
| Lgals9 | Lectin galactose binding soluble 9 (Galectin-9) | 1387027_a_at | 1.713 | 0.0151 | 2.811 | 0.0151 |
| Chi3l1 | Chitinase 3-like 1 (cartilage glycoprotein-39) | 1392171_a | 1.314 | 0.0111 | 1.723 | 0.0111 |
| **Channel** | | | | | | |
| Cybb | Endothelial type gp91-phox gene | 1373932_at | 1.772 | 0.0231 | 3.712 | 0.0231 |
| Cybb | Endothelial type gp91-phox gene | 1379344_at | 2.045 | 0.0129 | 3.65 | 0.0129 |
| **DNA repair** | | | | | | |
| Rad52_predicted | Rad52 protein | 1377902_a_at | 0.754 | 0.0414 | 0.739 | 0.0414 |
| **ECM** | | | | | | |
| Agt | Angiotensinogen (serpin peptidase inhibitor, clade A, member 8) | 1387811_at | 0.776 | 0.0268 | 0.542 | 0.0268 |
| Serpine1 | Serine (or cysteine) proteinase inhibitor, member 1 | 1392264_s_at | 1.826 | 0.0457 | 3.244 | 0.0457 |
| Serping1 | Serine (or cysteine) proteinase inhibitor, clade G (C1 inhibitor), member 1, (angioedema, hereditary) | 1372254_at | 1.9 | 0.0207 | 2.274 | 0.0207 |
| Slpi | Secretory leukocyte protease inhibitor | 1367998_at | 10.61 | 0.00124 | 45.6 | 0.00124 |
| Slamf9_predicted | Similar to CD2 antigen family, member 10 | 1378443_at | 4.37 | 0.0129 | 9.72 | 0.0129 |
| Timp1 | Tissue inhibitor of | 1367712_at | 1.885 | 0.0392 | 3.231 | 0.0392 |

| | | | | | | |
|---|---|---|---|---|---|---|
| | metalloproteinase 1 | | | | | |
| **Growth Related** | | | | | | |
| Igf1 | Rat insulin-like growth factor I mRNA, 3' end of mRNA | 1388469_at | 0.654 | 0.0191 | 0.331 | 0.0191 |
| Igf1 | Rat insulin-like growth factor I mRNA, 3' end of mRNA | 1382599_at | 0.709 | 0.0088 7 | 0.279 | 0.0088 7 |
| Il1b | Interleukin 1 beta | 1398256_at | 1.321 | 0.0248 | 9.51 | 0.0248 |
| Nrp | Neuropilin | 1373577_at | 0.788 | 0.0287 | 0.594 | 0.0287 |
| Tbrg1 | Transforming growth factor beta regulated gene 1 (predicted) | 1371509_at | 1.249 | 0.0202 | 1.239 | 0.0202 |
| Tnfsf4 | Tumor necrosis factor (ligand) superfamily, member 4 | 1369481_at | 0.61 | 0.0088 1 | 0.296 | 0.0088 1 |
| Tnfrsf1b | Tumor necrosis factor receptor superfamily, member 1b | 1392731_at | 1.848 | 0.035 | 3.867 | 0.035 |
| **GTPase transduction** | | | | | | |
| Akt2 | RAC protein kinase beta | 1388765_at | 0.725 | 0.0255 | 0.69 | 0.0255 |
| Rapgef3 | Rap guanine nucleotide exchange factor (GEF) 3 | 1368660_at | 0.821 | 0.0305 | 0.564 | 0.0305 |
| Rac2 | Rac2_predicted | 1372404_at | 2.709 | 0.0348 | 4.414 | 0.0348 |
| Iqgap3_predicted | IQ motif containing GTPase activating protein 3 (predicted) | 1374902_at | 1.389 | 0.0407 | 1.865 | 0.0407 |
| Rheb | Ras homolog enriched in brain | 1375360_at | 0.707 | 0.0062 7 | 0.276 | 0.0062 7 |
| Myrip | Myosin VIIA and Rab interacting protein | 1384095_at | 0.807 | 0.0083 6 | 0.686 | 0.0083 6 |
| Rasgrp3_predicted | RAS, guanyl releasing protein 3 (predicted | 1390159_at | 0.504 | 0.0462 | 0.299 | 0.0462 |
| Arhgap21_predicted | Rho GTPase activating protein 21 (predicted) | 1378666_at | 0.686 | 0.0050 7 | 0.677 | 0.0050 7 |
| Ehd1_predicted | EH-domain containing 1 | 1372317_at | 1.858 | 0.0146 | 3.482 | 0.0146 |
| **Immune Complement Pathway** | | | | | | |
| Cfb | B-factor, properdin | 1389470_at | 7.564 | 0.0030 4 | 17.23 | 0.0030 4 |
| C2 | Complement component 2 | 1383391_a_at | 1.9 | 0.0186 | 2.713 | 0.0186 |
| Daf1 | Decay accelarating factor 1 | 1387951_at | 0.466 | 0.0463 | 0.519 | 0.0463 |
| C1r_predicted | complement component 1, r subcomponent (predicted) | 1383241_at | 1.284 | 0.0201 | 1.79 | 0.0201 |
| **Immune Response** | | | | | | |
| Saa3_predicted | Serum amyloid A 3 (predicted) | 1392647_at | 60.94 | 0.0137 | 149.4 | 0.0137 |
| Dcir1 / Clecsf6 | Dendritic cell inhibitory receptor 1 | 1382153_at | 2.162 | 0.0284 | 4.561 | 0.0284 |
| Lyz | Lysozyme | 1370154_at | 1.44 | 0.0447 | 2.844 | 0.0447 |
| Gbp2 | Guanylate binding protein 2, interferon-inducible | 1368332_at | 2.553 | 0.0206 | 7.9 | 0.0206 |
| Cxcl11 | Chemokine (C-X-C motif) ligand 11 | 1379365_at | 3.568 | 0.0215 | 7.644 | 0.0215 |
| Ltb | Lymphotoxin B | 1379499_at | 1.688 | 0.0206 | 2.77 | 0.0206 |
| Pdcd1lg1_predicted | Programmed cell death 1 ligand 1 (predicted) | 1382603_at | 1.691 | 0.02 | 3.327 | 0.02 |

| | | | | | | |
|---|---|---|---|---|---|---|
| Ltc4s | Leukotriene C4 synthase | 1387438_at | 0.477 | 0.0117 | 0.194 | 0.0117 |
| RT1-Aw2 | RT1 class Ib, locus Aw2 | 1388071_x_at | 1.348 | 0.0436 | 1.785 | 0.0436 |
| Dcir4 / Clec4a1 | Dendritic cell inhibitory receptor 4 | 1395003_at | 2.733 | 0.0168 | 5.161 | 0.0168 |
| Gp49b | Glycoprotein 49b | 1375917_at | 1.99 | 0.0396 | 3.749 | 0.0396 |
| Dcir3 | Dendritic cell inhibitory receptor 3 | 1389553_at | 2.875 | 0.00929 | 5.483 | 0.00929 |
| Lamp1 | Lysosomal membrane glycoprotein 1 | 1375629_at | 1.233 | 0.0458 | 1.807 | 0.0458 |
| **Inflammation** | | | | | | |
| Ncf1 | neutrophil cytosolic factor 1 | 1387413_at | 1.471 | 0.0328 | 4.482 | 0.0328 |
| **Metabolism** | | | | | | |
| Car8 | Carbonic anhydrase 8 | 1398431_at | 1.358 | 0.0303 | 0.781 | 0.0303 |
| Mell1_predicted | Similar to neprilysin (EC 3.4.24.11) II - rat (LOC313755), mRNA | 1384748_at | 0.361 | 0.0294 | 0.419 | 0.0294 |
| **Neurogenesis** | | | | | | |
| Dab2 | Disabled homolog 2 (Drosophila) | 1368202_a_at | 1.592 | 0.0214 | 2.629 | 0.0214 |
| Dab2 | Disabled homolog 2 (Drosophila) | 1372031_at | 1.702 | 0.0298 | 2.265 | 0.0298 |
| Kidins220 | Kinase D-interacting substance of 220 kDa | 1398311_a_at | 0.727 | 0.0387 | 0.815 | 0.0387 |
| **Neurotransmission** | | | | | | |
| Cnga2 | cyclic nucleotide gated channel 4 | 1387699_at | 4.605 | 0.0431 | 2.821 | 0.0431 |
| Egr1 | Early growth response 1 | 1368321_at | 0.758 | 0.0393 | 0.79 | 0.0393 |
| Slc6a12 | GABA transporter | 1387295_at | 1.278 | 0.0309 | 3.505 | 0.0309 |
| **Other** | | | | | | |
| MGC72612 | Similar to expressed sequence AI449175 | 1382113_at | 1.473 | 0.0277 | 0.728 | 0.0277 |
| RGD1562732_predicted | Similar to Glutathione S-transferase, theta 3 | 1371942_at | 0.832 | 0.0447 | 0.658 | 0.0447 |
| Lrrc46 | Leucine rich repeat containing 46 | 1375076_at | 0.781 | 0.0215 | 0.652 | 0.0215 |
| RGD1564982_predicted | Hypothetical LOC308556 | 1375464_at | 1.483 | 0.00019 | 1.742 | 0.000194 |
| RGD1565602_predicted | Similar to PLU1 (predicted) | 1376347_at | 0.831 | 0.0294 | 0.809 | 0.0294 |
| RGD1311517_predicted | Similar to RIKEN cDNA 9430015G10 | 1378750_at | 0.576 | 0.0225 | 1.384 | 0.0225 |
| RGD1559748_predicted | Similar to Palate lung and nasal carcinoma-like protein precursor (Tongue plunc-like protein) (predicted) | 1383203_at | 1.351 | 0.0338 | 0.661 | 0.0338 |
| RGD1565895_predicted | Similar to DRE1 protein (predicted) | 1385499_at | 0.572 | 0.0457 | 0.465 | 0.0457 |
| Ifitm3 | Interferon induced transmembrane protein 3 | 1387995_a_at | 1.534 | 0.0456 | 2.093 | 0.0456 |
| Adfp | Adipose differentiation-related protein | 1390383_at | 1.591 | 0.00215 | 1.558 | 0.00215 |

| | | | | | | |
|---|---|---|---|---|---|---|
| Best5 | Best5 protein | 1370913_at | 2.027 | 0.0001 7 | 6.885 | 0.0001 71 |
| RGD1310066 | Similar to mKIAA1002 protein (LOC362894 | 1373814_at | 0.777 | 0.0147 | 1.335 | 0.0147 |
| RGD1305820_predicted | Similar to KIAA1337 protein (LOC313705) | 1379955_at | 0.569 | 0.0497 | 0.688 | 0.0497 |
| RGD1305235_predicted | Similar to RIKEN cDNA 1700052N19 (LOC292267) | 1385741_at | 0.774 | 0.0115 | 0.797 | 0.0115 |
| Sertad1 | Similar to p34SEI-1 (LOC361526), mRNA | 1372417_at | 1.308 | 0.0041 4 | 1.237 | 0.0041 4 |
| Asahl_predicted | N-acylsphingosine amidohydrolase (acid ceramidase)-like (predicted | 1390472_at | 2.468 | 0.0116 | 4.772 | 0.0116 |
| Tmem106a | similar to hypothetical protein MGC37887 (predicted) | 1374948_at | 1.977 | 0.0295 | 3.422 | 0.0295 |
| RGD1304816_predicted | similar to mKIAA0674 protein (predicted) | 1384616_at | 2.177 | 0.0298 | 2.404 | 0.0298 |
| RGD1559588_predicted | similar to cell surface receptor FDFACT (predicted) | 1385047_x_at | 3.553 | 0.0174 | 6.655 | 0.0174 |
| RGD1561144_predicted | similar to N-acetylglucosamine 6-O-sulfotransferase (predicted) | 1392444_at | 1.248 | 0.0213 | 0.733 | 0.0213 |
| RGD1559588_predicted | similar to cell surface receptor FDFACT (predicted) | 1393688_at | 2.731 | 0.0163 | 5.974 | 0.0163 |
| --- | --- | 1396049_x_at | 0.792 | 0.0416 | 0.434 | 0.0416 |
| LOC288568 | similar to paired immunoglobin-like type 2 receptor alpha | 1398589_at | 9.641 | 0.0346 | 25.91 | 0.0346 |
| RGD1564403_predicted | similar to Leucine rich repeat and sterile alpha motif containing 1 | 1396668_at | 0.176 | 0.0028 1 | 0.107 | 0.0028 1 |
| --- | Similar to proline dehydrogenase; PRODH (LOC287950), mRNA | 1372920_at | 0.651 | 0.0244 | 0.656 | 0.0244 |
| Upk3b_predicted | similar to uroplakin IIIb (predicted) | 1383460_at | 1.435 | 0.0015 1 | 3.616 | 0.0015 1 |
| **Protein biosynthesis and modification** | | | | | | |
| Rpl39 | Ribosomal protein L39 | 1367934_at | 1.269 | 0.0135 | 1.84 | 0.0135 |
| RGD1310265_predicted | Similar to Alpha-1,4-N-acetylglucosaminyltransferase (Alpha4GnT) (predicted) | 1393701_at | 1.273 | 0.0302 | 1.269 | 0.0302 |
| Tufm_predicted | Tu translation elongation factor, mitochondrial (predicted) | 1395647_at | 0.595 | 0.0114 | 0.525 | 0.0114 |
| **Proteolysis** | | | | | | |
| Ubap2_predicted | Ubiquitin-associated protein 2 (predicted) | 1372127_at | 1.37 | 0.0158 | 1.255 | 0.0158 |
| Sod2 | Superoxide dismutase2 | 1370173_at | 2.051 | 0.0349 | 4.114 | 0.0349 |
| **Receptor** | | | | | | |
| Folr2_predicted | Similar to folate-binding protein 2 precursor - mouse | 1390348_at | 3.026 | 0.0089 6 | 5.643 | 0.0089 6 |

| | | | | | | |
|---|---|---|---|---|---|---|
| | (LOC293154), mRNA | | | | | |
| **RNA processing** | | | | | | |
| Exosc2_predicted | Exosome component 2 (predicted) | 1379348_at | 1.256 | 0.0386 | 1.298 | 0.0386 |
| **Sex Diff** | | | | | | |
| Spag9_predicted | Sperm associated antigen 9 (predicted) | 1394436_at | 0.816 | 0.0308 | 0.811 | 0.0308 |
| **Signaling** | | | | | | |
| Ms4a7_predicted | Similar to RIKEN cDNA A430103C15 (LOC293744), mRNA | 1378193_at | 4.955 | 0.0115 | 8.892 | 0.0115 |
| Ppp1r14c | Protein phosphatase 1, regulatory (inhibitor) subunit 14c | 1368716_at | 0.713 | 0.0486 | 0.629 | 0.0486 |
| **Transcription** | | | | | | |
| Cbx1_predicted | Chromobox homolog 1 (Drosophila HP1 beta) (predicted) | 1385157_at | 1.301 | 0.0408 | 1.257 | 0.0408 |
| Maf | V-maf musculoaponeurotic fibrosarcoma oncogene homolog (avian) | 1387165_at | 1.478 | 0.0494 | 2.648 | 0.0494 |
| Arid1a_predicted | AT rich interactive domain 1A (Swi1 like) (predicted) | 1389850_at | 1.329 | 0.0466 | 1.414 | 0.0466 |
| Catsper2_predicted | Cation channel, sperm associated 2 | 1391231_at | 0.607 | 0.0463 | 0.589 | 0.0463 |
| Whsc1l1_predicted | Wolf-Hirschhorn syndrome candidate 1-like 1 (predicted) | 1394868_at | 1.578 | 0.0439 | 1.494 | 0.0439 |
| Nfkbiz_predicted | Nuclear factor of kappa light polypeptide gene enhancer in B-cells inhibitor, zeta (predicted) | 1378032_at | 1.85 | 0.0332 | 3.57 | 0.0332 |
| **Transport** | | | | | | |
| Cp | Ceruloplasmin | 1368418_a_at | 1.378 | 0.032 | 0.679 | 0.032 |
| Fxyd2 | FXYD domain-containing ion transport regulator 2 | 1387799_at | 3.352 | 0.0416 | 10.99 | 0.0416 |
| Slc27a4_predicted | Solute carrier family 27 (fatty acid transporter), member 4 | 1381263_at | 1.6 | 0.0283 | 1.222 | 0.0283 |
| Slc25a15_predicted | Solute carrier family 25 (mitochondrial carrier; ornithine transporter) member 15 | 1393947_at | 1.23 | 0.00302 | 0.731 | 0.00302 |

The **Supplementary Tables 2 and 3** list the genes and categories that are unique to each of the anti-Nogo-A antibodies. The major categories of table 1 are represented in both supplementary tables. Changes of genes belonging to the same category were generally pointing in the same direction. One should note that 7B12 treatment induced both a greater fold of gene changes and usually a greater number of genes per category, when compared to 11C7 treatment. There were no genes unique to IgG

treatment that could be placed onto a growth related category **(Supplementary Table 6)** and many of the genes that were common to all three treatments (**Supplementary Table 7**) had opposite regulation to the Nogo-A specific antibodies or if in the same direction usually with lower fold changes. Such genes include Slc6a12, vesicular GABA transporter, from the Neurotransmission category, which is up-regulated after Nogo-A neutralization but is down-regulated after control IgG treatment. Genes common to 11C7 and IgG were changed in the same direction and to similar levels **(Supplementary Table 4)** indicating an unspecific effect of IgG type antibody treatment. While more differences existed between the common genes to 7B12 and IgG **(Supplementary Table 5)** they were not related to growth responses and would be related to unspecific effects, with the exception of distal-less homeobox 5 (Dlx5) a transcription factor involved in the development of the nervous system which was down-regulated after Nogo-A neutralization, while up-regulated after IgG control treatment.

# 2.5 Discussion

Using organotypic hippocampal slice cultures as a model, we show *in vitro* that neutralization of Nogo-A with function blocking antibodies enhanced axonal regeneration and reconnection after lesion. Interestingly, growth induction by antibodies against Nogo-A also occurred in intact differentiated cultures. mRNA profiling supported the observation of a growth enhancement effect of Nogo-A neutralization and indicated the involvement of small GTPases in Nogo-A signaling and growth regulation. Nogo-A therefore seems to tonically suppress the growth machinery of pyramidal neurons in both lesioned and intact differentiated hippocampal tissue.

### Organotypic hippocampal slice culture characterization

Organotypic slice cultures have been used frequently to study many aspects of brain function, development and regeneration (Bahr, 1995; Gahwiler, 1981a, b, c; Hakkoum et al., 2006; Mingorance et al., 2006; Stoppini et al., 1991, 1993). We characterized our culture system and determined the expression of several markers. Using the oligodendrocyte marker CNPase we saw an increase in the number of oligodendrocytes from cultures of 5DIV to cultures of 21DIV, indicating a normal maturation of these glial cells in the slice cultures system, as previously shown by (Berger and Frotscher, 1994). With culture maturation, CNPase positive oligodendrocytes were to a very high level Nogo-A positive as well, confirming the classical localization of Nogo-A in oligodendrocytes.

The neuronal growth marker Gap43 remained expressed after three weeks in our cultures in line with the characterization of (Mielke *et al.*, 2005). On the other hand, other reports (McKinney *et al.*, 1997; McKinney *et al.*, 1999)) observed a progressive decrease of Gap43 in roller-tube cultures after 3 to 5 weeks *in vitro*. The expression of NF68, a neurofilament protein localized in axons and dendrites (Kleiman et al., 1990; Shaw et al., 1985), was slightly increased during the maturation of the culture. This was expected considering that NF68 is a core part of the developing and mature neurofilament cytoskeleton (Reines et al., 2004; Shaw and Weber, 1981) and during culture maturation new axons and connections develop.

Nogo-A mRNA in the hippocampus was shown to be localized both in neuronal cells and in oligodendrocytes (Gil et al., 2006; Huber et al., 2002; Meier et al., 2003; Trifunovski et al., 2006). Our immunohistochemistry showed the same localization: Nogo-A protein was highly expressed in neuronal cells in the early stages of culturing, followed by oligodendrocyte expression and a decline to lower amounts in the cell bodies of pyramidal cells.

### Enhanced regenerative response after Nogo-A neutralization

Several groups have used organotypic hippocampal cultures as models to study regeneration after different types of lesions (Hakkoum et al., 2006; McKinney et al., 1997; McKinney et al., 1999; Mingorance et al., 2006; Stoppini et al., 1993; Stoppini et al., 1997). Lesions separating CA3 from CA1 can lead to regeneration of Schaffer collaterals across the lesion site (McKinney *et al.*, 1997). In our control cultures, stimulation of CA3 lead to responses in CA1 at the level of approximately 35% of intact CA1 evoked field potential amplitude. Nogo-A neutralization for a 5-day period following lesion induced a significant increase to approximately 65% of the response prior to injury, indicating functional regeneration and synaptogenesis. Reactive sprouting after Schaffer collateral lesion can induce increased excitability ultimately leading to epileptic activity (McKinney *et al.*, 1997). In the present study, neither the recording of normal activity nor stimulation of CA3 with recording of CA1 pyramidal cells gave any indication of epileptiform activity in the organotypic hippocampal cultures. We speculate that the absence of hyperexcitability in cultures treated with anti-Nogo-A may be related to enhanced GABAergic activity as reflected by the increase in mRNA levels for the vesicular GABA transporter **(Table 7)** in the anti-Nogo-A antibody treated cultures.

### Fiber growth induced in normal CNS tissue

We showed an increase of the number of fibers labeled for NF68 after Nogo-A neutralization, indicating axonal sprouting of uninjured cells in differentiated 21 DIV organotypic hippocampal slices treated with antibodies for 5 days. These results are in line with previous reports of up-regulation of genes related to axonal growth (Zagrebelsky *et al.*, 1998) and morphological signs of sprouting in Purkinje cells (Buffo *et al.*, 2000; Gianola *et al.*, 2003) after the application of 3 different anti-Nogo-A antibodies. The sprouting response was described as transient since about one month after the antibody interventions the aberrant sprouts disappeared. Similar results were obtained in the spinal cord for the cortico-spinal track fibers (Bareyre *et al.*, 2002). The increased number of fibers positive for NF68 without changes in MAP2a/b fiber density suggests that these fibers are axons.

Organotypic hippocampal cultures lack the afferent input but form intrinsic circuitry very similar to the *in vivo* situation (Holopainen, 2005). Aberrant sprouting has been described during culture maturation mainly in the dentate gyrus (DG) both from collaterals (Coltman *et al.*, 1995) and from CA3 pyramidal cells (Sakaguchi *et al.*, 1994). There have been reports of increased hyperexcitability of different types of hippocampal neurons (McBain et al., 1989; Muller et al., 1993; Streit et al., 1989). It is an important observation that, despite of axonal sprouting seen in the present experiments, we did not observe indications of epileptic activity neither spontaneous nor induced by repeated electrical stimulations. The observed elevation of vesicular Gaba transporter **(Table 7)** may indicate enhanced GABAergic inhibitory control in the anti-Nogo-A antibody treated cultures.

### Changes at the mRNA level induced by Nogo-A neutralization

Previous studies have shown that Nogo-A signaling activates the Rho family of small GTPases (Fournier et al., 2003; Hsieh et al., 2006; McKerracher and Higuchi, 2006; Niederost et al., 2002; Schweigreiter et al., 2004). Our transcriptomic results confirm the importance of that pathway. The members of the Rho family of small GTPases and their regulators were one of the most prominent categories of signaling molecules influenced by the neutralization of Nogo-A **(Table 1 and Fig. 8)**. Genes like Rac2, Arhgap21 or Iqgap3 are all involved in neuronal growth responses (Dubois and Chavrier, 2005; Menetrey et al., 2007; Wang et al., 2007b) and could be part of a signaling pathway influenced by Nogo-A. Though Nogo-A neutralization did not detectably alter RhoA gene expression level, it altered that of Rac2, which is a member of the Rac family suggested to be involved in Nogo-A downstream signaling (Niederost *et al.*, 2002). mRNA levels of Rho GTPase activating protein 21 (Arhgap21 also known

as Arhgap10 (Menetrey *et al.*, 2007)) were down-regulated after Nogo-A neutralization; Arhgap21 is a known Cdc42 activating protein involved in the regulation of the actin cytoskeleton (Dubois and Chavrier, 2005). This protein also interacts with RhoA to hydrolyze and inactivate the GTP bound, active form (Sousa *et al.*, 2005). Contrary to Arhgap21, the IQ motif containing GTPase activating protein 3 (Iqgap3) was up-regulated, and this Rac1 and Cdc42 effector plays a pivotal role in neurite outgrowth (Wang et al., 2007b). These changes indicate that complex regulatory mechanisms are activated by Nogo-A neutralization that are able to affect the cytoskeleton (mostly actin) and may be involved in the regulation of the axonal growth response observed.

Trophic factors and growth associated genes; several of them involved in growth processes were found to be influenced by Nogo-A neutralization. TIMP-1 is described to be continuously but weakly expressed in pyramidal and granular cells of the hippocampus after birth. It is also described to be involved in neuroprotection, inhibiting excitotoxic cell death of neurons. It also has growth factor activity and is positively regulated by IL1β (Gardner and Ghorpade, 2003). The mRNA levels of TIMP-1 and IL1β were up-regulated after 5 days of anti-Nogo-A antibody treatment. The effects of IL1 in the brain are controversial, ranging from *in vivo* evidence to worsen ischemic lesion outcome to *in vitro* neuroprotective, neurotrophic and neurite outgrowth properties at low concentrations (nM-μM) or neurotoxic effects at higher concentrations (mM) after long exposure (Rothwell and Strijbos, 1995). Naturally expressed in the hippocampus at low amounts, an increased expression within physiological levels could contribute to the outgrowth observed. IL1β could also contribute to the lack of epileptic activity due to its potentiation of GABA effects by enhancing conductance of $Cl^-$ and inhibition of $Ca^{2+}$ currents in hippocampal neurons (Rothwell and Hopkins, 1995).

Galectins are proteins involved in several aspects of immune responses. Galectin-5 and -9 are both up-regulated after Nogo-A neutralization. They are both expressed in brain tissue in low amounts and they are closely related to one another (Lensch *et al.*, 2006). The most well known member of this family is Galectin-1 with both anti- and pro-inflammatory properties (Toscano *et al.*, 2007). Interestingly, like cytokines and interleukins, Galectin-1 has been shown to promote peripheral nerve fiber growth when oxidized (Horie et al., 2005; Kadoya and Horie, 2005). Since Galectin-5 and -9 have not been so extensively studied, their involvement in CNS growth responses remains an interesting possibility.

A very interesting gene is the secretory leukocyte protease inhibitor (SLPI), the second highest up-regulated gene in our analysis. SLPI is involved in neuroprotective effects from stroke and ischemia (Feuerstein, 2006; Wang et al., 2003), it is a target of

epidermal growth factor (Velarde *et al.*, 2005) and a type 1 insulin growth factor like receptor-regulated protein (Wang et al., 2006b). Most recently, SLPI was shown to overcome MAG induced neurite outgrowth inhibition (Filbin, MT personal communication). SLPI was up-regulated 10.61 and 45.6 fold after 5 days treatment with anti-Nogo-A antibodies (11C7 and 7B12, respectively) and the possibility, therefore, exists that this pathway is also involved in the observed growth enhancement.

### Nogo-A localization

Whether the growth response induced by the function-blocking anti-Nogo-A antibodies is due to interference with oligodendrocyte, or neuronal Nogo-A or both remains unanswered. Several studies on spinal cord injury in rats and monkeys have shown that blockade of Nogo-A or its receptor complex allows axons to sprout and regenerate beyond the lesion site (He and Koprivica, 2004; Schwab, 2004; Yiu and He, 2003). The enhanced growth response in the hippocampal tissue could be due to the neutralization of an inhibitory signal from the oligodendrocytes to the neurons. Such a signal could physiologically function to restrict growth in order to stabilize the network after differentiation. We cannot exclude, however, that the effects observed are also due to neuronal Nogo-A neutralization, although the function of neuronal Nogo-A is not yet understood.

In conclusion, we show that Nogo-A neutralization induces axonal growth and sprouting in both lesioned and non-lesioned differentiated organotypic hippocampal slice cultures. This demonstrates the importance of Nogo-A as a negative regulator of growth and plasticity of the CNS. The lack of observable epileptic activity after treatment with Nogo-A specific antibodies suggests that fiber growth induced by Nogo-A neutralization may not be random or chaotic. Guidance and target recognition signals may still be present in the tissue, and activity-dependent mechanisms may control synapse stabilization and axon branch survival. The increased growth state of the neurons after Nogo-A neutralization and the decreased growth inhibitory properties of the CNS tissue are probably responsible for the enhanced sprouting and regeneration responses observed in many studies following spinal cord or brain injuries and subsequent Nogo-A neutralization.

### Acknowledgements:

We thank Andrea Patrignani from the Functional Genomics Center Zurich for expert assistance with the genomics experiments, Lotty Rietschin for patient training in the establishment of the slice culture system, Dr. R.A. McKinney for talented supervision and insight about confocal imaging and advice and Roland Schoeb for the elaborate

graphic work. This work has been supported by the Swiss National Foundation, the Swiss National Centre of Competence in Research, the Portuguese Fundação para a Ciência e Tecnologia and the GABBA PhD program in Porto, Portugal.

# 2.6 Supplemental Gene Tables

## Supplementary Table 1. Gene Expression changes induced by 11C7 anti-Nogo-A antibody only

| Gene Symbol | Gene Name | Accession Number | 11C7 | |
|---|---|---|---|---|
| | | | Fold Change | P value |
| **Apoptosis** | | | | |
| Apaf1 | apoptotic protease activating factor 1 | 1369198_at | 0.816 | 0.0416 |
| Pdcd6_predicted | programmed cell death 6 (predicted) | 1388767_at | 1.215 | 0.0457 |
| **Cytoskeletal** | | | | |
| Hook2_predicted | Similar to hook homolog 2 | 1386689_at | 0.672 | 0.014 |
| **ECM** | | | | |
| Cspg5 | chondroitin sulfate proteoglycan 5 | 1368704_a_at | 0.771 | 0.0183 |
| **Immune Response** | | | | |
| Neu1 | neuraminidase 1 | 1375684_at | 1.487 | 0.0135 |
| **Metabolism** | | | | |
| Ampd1 | adenosine monophosphate deaminase 1 (isoform M) | 1398306_at | 3.319 | 0.0459 |
| **Other** | | | | |
| Adar | adenosine deaminase, RNA-specific | 1368973_at | 0.811 | 0.00523 |
| Mospd3_predicted | Motile sperm domain containing 3 (predicted) | 1372210_at | 1.211 | 0.00682 |
| --- | --- | 1372920_at | 0.651 | 0.0244 |
| RGD1306157_predicted | similar to CG9882-PA (predicted) | 1374136_at | 1.263 | 0.0285 |
| Nyw1 | ischemia related factor NYW-1 | 1374923_at | 0.821 | 0.044 |
| Ccdc53_predicted | coiled-coil domain containing 53 (predicted) | 1375634_at | 1.389 | 0.0438 |
| Serpinb12_predicted | serine (or cysteine) peptidase inhibitor, clade B (ovalbumin), member 12 (predicted) | 1376243_at | 0.148 | 0.00958 |
| Pilra_predicted | paired immunoglobin-like type 2 receptor alpha (predicted) | 1376688_a_at | 12.04 | 0.0084 |
| --- | --- | 1379239_at | 2.248 | 0.00597 |
| RGD1309519_predicted | similar to hypothetical protein FLJ14007 (predicted) | 1380310_at | 1.258 | 0.0379 |
| RGD1310879_predicted | similar to methylenetetrahydrofolate dehydrogenase (NAD) (EC 1.5.1.15) / methenyltetrahydrofolate cyclohydrolase (EC 3.5.4.9) precursor - mouse (predicted) | 1381280_at | 1.26 | 0.0342 |
| Morc3_predicted | microrchidia 3 (predicted) | 1390142_at | 1.32 | 0.0394 |
| --- | --- | 1391453_at | 2.659 | 0.00241 |
| LOC362317 | Similar to KRIT1 | 1396078_at | 0.514 | 0.0283 |
| RGD1305158_predicted | Similar to RIKEN cDNA 1810030N24 (LOC297971), mRNA | 1399164_a_at | 1.227 | 0.0337 |
| **RNA processing** | | | | |
| Ssu72 | Ssu72 RNA polymerase II CTD phosphatase homolog (yeast) | 1377297_at | 1.313 | 0.00263 |

| | | | | |
|---|---|---|---|---|
| **Stress Response** | | | | |
| Tmem49 / Vmp1 | vacuole membrane protein 1 | 1370807_at | 1.245 | 0.00218 |
| **Synaptic** | | | | |
| Ctbp2 | C-terminal binding protein 2 | 1375963_at | 0.784 | 0.0145 |
| **Transcription** | | | | |
| Ahctf1_predicted | AT hook containing transcription factor 1 (predicted) | 1381611_at | 0.703 | 0.0227 |
| LOC361767 | similar to DNA polymerase lambda | 1389268_at | 1.395 | 0.0173 |
| RGD:708405 (LOC56081) | CTD-binding SR-like rA1 | 1367984_at | 0.806 | 0.036 |
| Ing3 | inhibitor of growth family, member 3 (predicted) | 1372945_at | 1.263 | 0.0458 |
| Elavl1_predicted | ELAV (embryonic lethal, abnormal vision, Drosophila)-like 1 (Hu antigen R) (predicted) | 1375892_at | 1.201 | 0.0185 |
| Prrx1 | paired related homeobox 1 | 1384234_at | 0.694 | 0.0366 |
| Polr2f | polymerase (RNA) II (DNA directed) polypeptide F | 1391699_at | 1.228 | 0.024 |
| Etv1_predicted | ets variant gene 1 (predicted) | 1392477_at | 1.496 | 0.0432 |
| **Transport** | | | | |
| Timm23 | translocase of inner mitochondrial membrane 23 homolog (yeast) | 1398763_at | 1.231 | 0.0493 |

## Supplementary Table 2. Gene Expression changes induced by 7B12 anti-Nogo-A antibody only

| Gene Symbol | Gene Name | Accession Number | 7B12 | |
|---|---|---|---|---|
| | | | Fold Change | P value |
| **Apoptosis** | | | | |
| Bnip3 | BCL2/adenovirus E1B 19 kDa-interacting protein 3 | 1387805_at | 0.74 | 0.0127 |
| **Cell Adhesion** | | | | |
| Tgm2 | transglutaminase 2, C polypeptide | 1369943_at | 2.584 | 0.0131 |
| **Cell Cycle** | | | | |
| Cdkn1b | cyclin-dependent kinase inhibitor 1B | 1373812_at | 0.816 | 0.0453 |
| **Channel** | | | | |
| Trpc2 | transient receptor potential cation channel, subfamily C, member 2 | 1389671_at | 0.732 | 0.00437 |
| **Cytoskeletal** | | | | |
| Tubb2 | tubulin, beta, 2 | 1371390_at | 0.823 | 0.0318 |
| Tmod2 | tropomodulin 2 | 1393418_at | 0.824 | 0.0153 |
| **Development** | | | | |
| Pitpnm_predicted | phosphatidylinositol membrane-associated (predicted) / Similar to Dres9 | 1389347_at | 1.29 | 0.0284 |
| **Growth factor** | | | | |
| Igf1 | insulin-like growth factor 1 | 1370333_a_at | 0.363 | 0.0104 |
| **GTPase transduction** | | | | |
| Mfn1 | mitofusin 1 | 1371717_at | 0.807 | 0.0365 |

| | | | | |
|---|---|---|---|---|
| Fnbp1 | rapostlin | 1372825_at | 0.785 | 0.0337 |
| Sh3md2 | Putative scaffolding protein POSH | 1383910_at | 0.765 | 0.0213 |
| **Metabolism** | | | | |
| Gclc | glutamate-cysteine ligase, catalytic subunit | 1370688_at | 0.748 | 0.0277 |
| Acaca | acetyl-coenzyme A carboxylase alpha | 1370893_at | 0.777 | 0.0246 |
| Akr1b8 | aldo-keto reductase family 1, member B8 | 1370902_at | 2.524 | 0.0366 |
| Ahcyl1_predicted | Similar to hypothetical protein (LOC362013), mRNA | 1383004_at | 0.726 | 0.0338 |
| **Neurogenesis** | | | | |
| Mdk | midkine | 1367682_at | 0.832 | 0.0374 |
| **Neuronal Growth** | | | | |
| Ptprz1 | protein tyrosine phosphatase, receptor-type, Z polypeptide 1 | 1388015_at | 0.733 | 0.00968 |
| **Neurotransmission** | | | | |
| PORF-2 | preoptic regulatory factor-2 | 1388165_at | 1.218 | 0.0493 |
| **Other** | | | | |
| Ahcy | S-adenosylhomocysteine hydrolase | 1367798_at | 1.243 | 0.0326 |
| Pxmp2 | peroxisomal membrane protein 2 | 1367885_at | 0.733 | 0.041 |
| Acbd5_predicted | acyl-Coenzyme A binding domain containing 5 (predicted) | 1373507_at | 0.8 | 0.0342 |
| RGD1561090_predicted | Similar to protein tyrosine phosphatase, receptor type, D | 1374591_at | 0.71 | 0.0318 |
| Gnptag_predicted | N-acetylglucosamine-1-phosphotransferase, gamma subunit (predicted) | 1374790_at | 0.814 | 0.0366 |
| RGD1311126_predicted | Similar to paired immunoglobin-like type 2 receptor alpha; cell surface receptor FDF03 (LOC288552), mRNA | 1376688_a_at | 33.12 | 0.0084 |
| --- | Similar to Rxrip110 protein (LOC361209), mRNA | 1379239_at | 0.505 | 0.00597 |
| Entpd5 | ectonucleoside triphosphate diphosphohydrolase 5 | 1382434_at | 0.825 | 0.0485 |
| RGD1306766_predicted | similar to hypothetical protein FLJ23514 (predicted) | 1383200_at | 0.725 | 0.0196 |
| Tm7sf1_predicted / Gpr137b_predicted | transmembrane 7 superfamily member 1 (predicted) | 1385025_a_at | 1.355 | 0.0323 |
| Aldh1a1 | aldehyde dehydrogenase family 1, member A1 | 1387022_at | 0.609 | 0.0388 |
| RGD1310602_predicted | similar to hypothetical protein MGC15396 (predicted) | 1389124_at | 0.8 | 0.0394 |
| LOC361990 | similar to DKFZP547E1010 protein | 1390058_at | 0.823 | 0.00113 |
| Morc3_predicted | Similar to HYPOTHETICAL PROTEIN KIAA0136 (LOC304074), mRNA | 1390142_at | 1.349 | 0.0394 |
| --- | Similar to cytokine receptor-like molecule (LOC367456), mRNA | 1391453_at | 4.191 | 0.00241 |
| --- | Similar to hypothetical protein FLJ23825 (LOC303750), mRNA | 1392062_a_at | 0.78 | 0.0259 |
| RGD1561855_predicted | similar to SH3-domain binding protein 3 | 1395532_at | 0.817 | 0.0133 |
| RGD1304977_predicted | similar to mKIAA0023 protein (predicted) | 1395982_at | 1.307 | 0.0321 |
| **Protein biosynthesis and modification** | | | | |

| | | | | |
|---|---|---|---|---|
| Lars2_predicted | Leucyl-tRNA synthetase, mitochondrial (predicted) | 1373602_at | 0.668 | 0.0305 |
| **Signaling** | | | | |
| Prkar1a | protein kinase, cAMP dependent regulatory, type I, alpha | 1386905_at | 0.812 | 0.00443 |
| **Stress Response** | | | | |
| Hrsp12 | heat-responsive protein 12 | 1368060_at | 0.748 | 0.0306 |
| Pink1_predicted | PTEN induced putative kinase 1 (predicted) | 1372199_at | 0.735 | 0.0435 |
| **Synaptic** | | | | |
| Adrbk1 | adrenergic receptor kinase, beta 1 | 1387429_at | 1.266 | 0.0263 |
| **Transcription** | | | | |
| Hit39 | zinc finger protein HIT-39 | 1370560_at | 0.622 | 0.00553 |
| Zfp46_predicted | Zinc finger protein 46 (predicted) | 1370984_at | 1.281 | 0.0448 |
| Ndn_predicted | necdin (predicted) | 1371947_at | 0.788 | 0.0482 |
| Crtc2 | CREB regulated transcription coactivator 2 | 1373828_at | 1.284 | 0.0148 |
| Lig4_predicted | Ligase IV, DNA, ATP-dependent (predicted) | 1383561_at | 0.811 | 0.036 |
| Prdm15_predicted | PR domain containing 15 (predicted) | 1390165_at | 1.317 | 0.0467 |
| Tmf1 | TATA element modulatory factor 1 | 1399066_at | 0.833 | 0.0363 |
| **Transport** | | | | |
| Slc25a10 | solute carrier family 25 (mitochondrial carrier; dicarboxylate transporter), member 10 | 1370020_at | 1.551 | 0.012 |
| Slc16a7 | solute carrier family 16 (monocarboxylic acid transporters), member 7 | 1370609_a_at | 0.775 | 0.00353 |
| Clcn4-2 | Putative chloride channel (similar to Mm Clcn4-2) | 1379932_at | 0.682 | 0.00373 |
| RGD1359380 | similar to hypothetical protein MGC7537 | 1388499_at | 0.742 | 0.00946 |
| Tcof1_predicted | Treacher Collins Franceschetti syndrome 1, homolog (predicted) | 1389537_at | 1.345 | 0.0478 |

## Supplementary Table 3. Gene Expression changes common to 11C7 and IgG treatment

| Gene Symbol | Gene Name | Accession Number | 11C7 | | IgG | |
|---|---|---|---|---|---|---|
| | | | Fold Change | P value | Fold Change | P value |
| **Apoptosis** | | | | | | |
| Cradd_predicted | CASP2 and RIPK1 domain containing adaptor with death domain (predicted) | 1382180_at | 1.362 | 0.0371 | 1.264 | 0.0371 |
| **Growth factor** | | | | | | |
| Cntfr | ciliary neurotrophic factor receptor | 1392749_at | 0.637 | 0.0383 | 0.659 | 0.0383 |
| **Metabolism** | | | | | | |
| Lisch7 | liver-specific bHLH-Zip transcription factor 7 | 1368368_a_at | 0.411 | 0.034 | 0.755 | 0.034 |
| **Neurotransmission** | | | | | | |
| Sstr3 | somatostatin receptor 3 | 1368598_at | 0.671 | 0.0132 | 0.616 | 0.0132 |
| **Other** | | | | | | |

| | | | | | | |
|---|---|---|---|---|---|---|
| Art3_predicted | ADP-ribosyltransferase 3 (predicted) | 1372065_at | 1.482 | 0.026 | 1.238 | 0.026 |
| RGD1309519_predicted | Similar to hypothetical protein FLJ14007 (predicted) | 1380310_at | 1.258 | 0.0379 | 1.227 | 0.0379 |
| Surf6_predicted | surfeit gene 6 (predicted) | 1390290_at | 1.31 | 0.00498 | 1.298 | 0.00498 |
| LOC298120 | similar to astrotactin 2 isoform b | 1395090_at | 0.626 | 0.00387 | 0.602 | 0.00387 |
| RGD1307235_predicted | similar to RIKEN cDNA 2310035C23 (predicted) | 1397730_at | 0.628 | 0.0327 | 0.695 | 0.0327 |
| **Transcription** | | | | | | |
| Idb4 | Inhibitor of DNA binding 4 | 1385923_at | 1.468 | 0.0225 | 1.419 | 0.0225 |
| Mll5_predicted | myeloid/lymphoid or mixed-lineage leukemia 5 (trithorax homolog, Drosophila) (predicted) | 1392564_at | 0.73 | 0.00848 | 0.798 | 0.00848 |

## Supplementary Table 4. Gene Expression changes common to 7B12 and IgG treatment

| Gene Symbol | Gene Name | Accession Number | 7B12 | | IgG | |
|---|---|---|---|---|---|---|
| | | | Fold Change | P value | Fold Change | P value |
| **Immune Response** | | | | | | |
| Vps52 | vacuolar protein sorting 52 (yeast) | 1369668_x_at | 1.903 | 0.0433 | 2.91 | 0.0433 |
| Spn | sialophorin | 1370987_at | 2.303 | 0.0106 | 1.451 | 0.0106 |
| **Metabolism** | | | | | | |
| Udpgtr2 | liver UDP-glucuronosyltransferase, phenobarbital-inducible form | 1370698_at | 0.226 | 0.0456 | 3.154 | 0.0456 |
| Cryl1 | crystallin, lamda 1 | 1376051_at | 0.705 | 0.0327 | 0.826 | 0.0327 |
| **Other** | | | | | | |
| Mawbp | MAWD binding protein | 1370320_at | 0.563 | 0.0143 | 1.279 | 0.0143 |
| LOC291940 | similar to hypothetical protein | 1397456_at | 1.657 | 0.0178 | 1.955 | 0.0178 |
| LOC366994 | Similar to oriLyt TD-element binding protein 7 | 1375467_at | 1.416 | 0.0453 | 1.558 | 0.0453 |
| MGC94755 | --- | 1377940_at | 0.761 | 0.0292 | 0.789 | 0.0292 |
| --- | --- | 1382693_a_at | 0.648 | 0.0404 | 0.684 | 0.0404 |
| **Signaling** | | | | | | |
| Mapk7 | mitogen-activated protein kinase 7 | 1370985_at | 1.377 | 0.0226 | 0.795 | 0.0226 |
| **Testis Development** | | | | | | |
| Fbln2 | fibulin 2 | 1389533_at | 1.521 | 0.0497 | 0.833 | 0.0497 |
| **Transcription** | | | | | | |
| Pax4 | paired box gene 4 | 1370140_a_at | 3.988 | 0.0105 | 0.52 | 0.0105 |
| Zfp503_predicted | zinc finger protein 503 (predicted) | 1377241_at | 1.545 | 0.0458 | 1.619 | 0.0458 |
| Dlx5 | distal-less homeobox 5 | 1387274_at | 0.717 | 0.0292 | 2.682 | 0.0292 |

| | | | | | | |
|---|---|---|---|---|---|---|
| LOC306464 | similar to myeloid leukemia factor 1 interacting protein | 1393844_at | 1.467 | 0.0122 | 1.64 | 0.0122 |

## Supplementary Table 5. Gene Expression changes induced by IgG control antibody only

| Gene Symbol | Gene Name | Accession Number | IgG | |
|---|---|---|---|---|
| | | | Fold Change | P value |
| **Apoptosis** | | | | |
| Zfp162 | zinc finger protein 162 | 1380106_at | 0.774 | 0.041 |
| **DNA repair** | | | | |
| Top1mt | DNA topoisomerase I, mitochondrial | 1380060_at | 0.553 | 0.0268 |
| **Other** | | | | |
| Cpxm1_predicted | carboxypeptidase X 1 (M14 family) (predicted) | 1390420_at | 0.785 | 0.0374 |
| Nudcd1_predicted | similar to chronic myelogenous leukemia tumor antigen 66 (predicted) | 1393753_at | 1.318 | 0.0233 |
| **Transcription** | | | | |
| Rxra | retinoid X receptor alpha | 1369101_at | 0.775 | 0.019 |
| MGC72584 | similar to postmeiotic segregation increased 1 | 1384523_at | 1.222 | 0.0106 |
| Baz1a_predicted | bromodomain adjacent to zinc finger domain, 1A (predicted) | 1385853_at | 1.333 | 0.0291 |

## Supplementary Table 6. Gene Expression common to all treatments

| Gene Symbol | Gene Name | Accession Number | 11C7 | | 7B12 | | IgG | |
|---|---|---|---|---|---|---|---|---|
| | | | Fold Change | P value | Fold Change | P value | Fold Change | P value |
| **Apoptosis** | | | | | | | | |
| Lcn2 | lipocalin 2 | 1387011_at | 4.568 | 0.0361 | 11.5 | 0.0361 | 0.753 | 0.0361 |
| **Cell Adhesion** | | | | | | | | |
| Asgr1 | asialoglycoprotein receptor 1 | 1370149_at | 1.522 | 0.038 | 5.801 | 0.038 | 0.652 | 0.038 |
| **Channel** | | | | | | | | |
| Kcna5 | potassium voltage-gated channel, shaker-related subfamily, member 5 | 1370268_at | 1.456 | 0.0226 | 1.455 | 0.0226 | 1.442 | 0.0226 |
| Tsga2 | Similar to testis specific gene A2; meichroacidin (LOC361818), mRNA | 1391228_at | 1.24 | 0.0212 | 1.315 | 0.0212 | 1.662 | 0.0212 |
| **Cytoskeletal** | | | | | | | | |
| Tubgcp6_predicted | Similar to tubulin, | 1374887_at | 0.821 | 0.0303 | 0.799 | 0.0303 | 0.795 | 0.0303 |

| | | | | | | | | |
|---|---|---|---|---|---|---|---|---|
| | gamma complex associated protein 6 | | | | | | | |
| Cap350 | centrosome-associated protein 350 | 1385824_at | 0.781 | 0.0431 | 0.768 | 0.0431 | 0.588 | 0.0431 |
| **DNA repair** | | | | | | | | |
| Asf1a_predicted | Similar to ASF1 anti-silencing function 1 homolog A | 1379192_at | 1.906 | 0.0178 | 1.406 | 0.0178 | 1.374 | 0.0178 |
| **ECM** | | | | | | | | |
| Car14_predicted | Similar to CA XIV (LOC361998), mRNA | 1374039_at | 2.103 | 0.0433 | 1.476 | 0.0433 | 1.985 | 0.0433 |
| Slamf9_predicted | Similar to CD2 antigen family, member 10 | 1378443_at | 4.37 | 0.0129 | 9.72 | 0.0129 | 1.243 | 0.0129 |
| **Immune Complement pathway** | | | | | | | | |
| Cfb | B-factor, properdin | 1389470_at | 7.564 | 0.00304 | 17.23 | 0.00304 | 0.804 | 0.00304 |
| **Immune Response** | | | | | | | | |
| --- | Similar to histocompatibility 28 (LOC310968), mRNA | 1379748_at | 2.063 | 0.00897 | 4.549 | 0.00897 | 1.84 | 0.00897 |
| Saa3_predicted | Similar to Bq135360 (LOC292922), mRNA | 1392647_at | 60.94 | 0.0137 | 149.4 | 0.0137 | 0.727 | 0.0137 |
| Lck | lymphocyte-specific protein tyrosine kinase | 1383320_at | 1.324 | 0.029 | 1.783 | 0.029 | 1.48 | 0.029 |
| Slfn3 | schlafen 4 | 1387134_at | 1.749 | 0.0465 | 23.71 | 0.0465 | 3.298 | 0.0465 |
| Gp49b | Similar to gp49B2 (LOC292594), mRNA | 1375917_at | 1.99 | 0.0396 | 3.749 | 0.0396 | 1.417 | 0.0396 |
| Lamp1 | lysosomal membrane glycoprotein 1 | 1375629_at | 1.233 | 0.0458 | 1.807 | 0.0458 | 0.632 | 0.0458 |
| **Inflammation** | | | | | | | | |
| Ncf1 | neutrophil cytosolic factor 1 | 1387413_at | 1.471 | 0.0328 | 4.482 | 0.0328 | 0.695 | 0.0328 |
| **Metabolism** | | | | | | | | |
| Mell1_predicted | Similar to neprilysin (EC 3.4.24.11) II - rat (LOC313755), mRNA | 1384748_at | 0.361 | 0.0294 | 0.419 | 0.0294 | 0.794 | 0.0294 |
| Pter | phosphotriesterase related | 1387851_at | 1.66 | 0.0279 | 1.249 | 0.0279 | 1.329 | 0.0279 |
| **Neurogenesis** | | | | | | | | |
| Dab2 | disabled homolog 2, mitogen-responsive | 1368202_a_at | 1.592 | 0.0214 | 2.629 | 0.0214 | 1.214 | 0.0214 |

| | | | | | | | | |
|---|---|---|---|---|---|---|---|---|
| | phosphoprotein (Drosophila) | | | | | | | |
| Efnb1 | ephrin B1 | 1369476_at | 0.828 | 0.0416 | 1.227 | 0.0416 | 0.755 | 0.0416 |
| **Neurotransmission** | | | | | | | | |
| Stx17 | syntaxin 17 | 1370597_at | 2.28 | 0.0387 | 7.024 | 0.0387 | 4.77 | 0.0387 |
| Cnga2 | cyclic nucleotide gated channel 4 | 1387699_at | 4.605 | 0.0431 | 2.821 | 0.0431 | 1.593 | 0.0431 |
| Nxph1 | neurexophilin 1 | 1393714_at | 0.762 | 0.0162 | 3.684 | 0.0162 | 0.333 | 0.0162 |
| Slc6a12 | GABA transporter | 1387295_at | 1.278 | 0.0309 | 3.505 | 0.0309 | 0.795 | 0.0309 |
| **Other** | | | | | | | | |
| Sertad1 | Similar to p34SEI-1 (LOC361526), mRNA | 1372417_at | 1.308 | 0.00414 | 1.237 | 0.00414 | 0.796 | 0.00414 |
| LOC497990 | Similar to tumor endothelial marker 7 precursor (LOC303505), mRNA | 1377110_at | 0.33 | 0.0386 | 4.84 | 0.0386 | 0.289 | 0.0386 |
| Dpf3_predicted | Similar to cer-d4 isoform XZ (LOC299186), mRNA | 1378300_at | 0.581 | 0.00263 | 0.563 | 0.00263 | 0.804 | 0.00263 |
| Gpatc1_predicted | Similar to evolutionarily conserved G-patch domain containing (LOC292810), mRNA | 1377436_at | 1.535 | 0.0365 | 1.208 | 0.0365 | 1.47 | 0.0365 |
| Bche | butyrylcholinesterase | 1387832_at | 1.572 | 0.00213 | 0.417 | 0.00213 | 0.804 | 0.00213 |
| LOC499991 | Ab1-219 | 1385397_at | 2.91 | 0.0125 | 3.909 | 0.0125 | 1.443 | 0.0125 |
| --- | Hypothetical LOC296591 (LOC296591), mRNA | 1389517_at | 1.398 | 0.0457 | 1.463 | 0.0457 | 1.551 | 0.0457 |
| --- | Similar to grp75 (LOC295778), mRNA | 1389930_at | 2.316 | 0.0411 | 1.528 | 0.0411 | 1.831 | 0.0411 |
| RGD1559882_predicted | Similar to hypothetical protein E130310N06 (LOC301709), mRNA | 1390938_at | 1.793 | 0.0204 | 0.765 | 0.0204 | 2.125 | 0.0204 |
| **Proteolysis** | | | | | | | | |
| Degs1 | degenerative spermatocyte homolog (Drosophila) | 1381384_at | 1.626 | 0.0383 | 0.364 | 0.0383 | 1.884 | 0.0383 |
| Fap | fibroblast activation protein | 1369422_at | 0.359 | 0.0275 | 1.653 | 0.0275 | 1.695 | 0.0275 |
| **Receptor** | | | | | | | | |

| | | | | | | | | |
|---|---|---|---|---|---|---|---|---|
| Trfr2_predicted | transferrin receptor 2 (predicted) | 1380066_at | 1.41 | 0.0247 | 2.18 | 0.0247 | 2.518 | 0.0247 |
| Folr2_predicted | Similar to folate-binding protein 2 precursor - mouse (LOC293154), mRNA | 1390348_at | 3.026 | 0.00896 | 5.643 | 0.00896 | 1.333 | 0.00896 |
| **Signaling** | | | | | | | | |
| Mapk4 | mitogen activated protein kinase 4 | 1378751_at | 0.47 | 0.00588 | 0.59 | 0.00588 | 0.715 | 0.00588 |
| Ms4a7_predicted | Similar to RIKEN cDNA A430103C15 (LOC293744), mRNA | 1378193_at | 4.955 | 0.0115 | 8.892 | 0.0115 | 1.289 | 0.0115 |
| **Transcription** | | | | | | | | |
| --- | Similar to Rxrip110 protein (LOC361209), mRNA | 1379239_at | 2.248 | 0.00597 | 0.505 | 0.00597 | 0.355 | 0.00597 |
| Phf11 | Similar to CLLL8 protein; chromosome 13 open reading frame 4 (LOC305931), mRNA | 1382546_at | 1.735 | 0.0498 | 2.213 | 0.0498 | 1.514 | 0.0498 |
| Jmjd2c_predicted | Similar to RIKEN cDNA 2410141F18 (LOC298144), mRNA | 1383911_at | 1.298 | 0.0084 | 1.24 | 0.0084 | 1.832 | 0.0084 |
| Znf408_predicted | Similar to zinc finger protein 408 (LOC311192), mRNA | 1397356_at | 1.645 | 0.0222 | 1.365 | 0.0222 | 1.56 | 0.0222 |
| Znf278 | zinc finger protein 278 | 1376870_at | 6.592 | 0.0139 | 1.819 | 0.0139 | 1.24 | 0.0139 |
| **Transport** | | | | | | | | |
| Slc16a1 | solute carrier family 16, member 1 | 1397803_at | 0.497 | 0.0336 | 1.292 | 0.0336 | 1.844 | 0.0336 |
| Slc7a2 | solute carrier family 7, member 3 | 1369460_at | 1.615 | 0.0436 | 7.326 | 0.0436 | 1.336 | 0.0436 |
| Fxyd2 | FXYD domain-containing ion transport regulator 2 | 1387799_at | 3.352 | 0.0416 | 10.99 | 0.0416 | 1.698 | 0.0416 |
| Nxn_predicted | Similar to red-1 (LOC360577), mRNA | 1392323_at | 1.917 | 0.0038 | 0.231 | 0.0038 | 1.793 | 0.0038 |

# Chapter 3:

## Hippocampal circuitry rearrangements in the adult rat after Nogo-A neutralization

# Hippocampal circuitry rearrangements in the adult rat after Nogo-A neutralization

**Luis M. Craveiro[1], Oliver Weinmann[1], Bernd Roschitzki[2], Roman Gonzenbach[1], Björn Zörner[1], Roman Willi[1], Laura Montani[1], Benjamin K. Yee[3], Joram Feldon[3] and Martin E. Schwab[1]**

[1]Brain Research Institute, Department of Neuromorphology of University of Zurich and Swiss Federal Technical Institute, Zurich, Switzerland

[2]Functional Genomics Center Zurich, University of Zurich and Swiss Federal Technical Institute, Zurich, Switzerland

[3]Laboratory of Behavioral Neurobiology, Swiss Federal Institute of Technology Zurich, Schwerzenbach, Switzerland

Corresponding author:

Luis M. Craveiro, Brain Research Institute, Winterthurerstrasse 190, 8057 Zurich, Switzerland.

Tel. +41 44 63 53213

Fax. +41 44 63 53303

E-mail: craveiro@hifo.uzh.ch

**Keywords:** Behavior, proteomics, transcriptomics, memory, GABA.

# 3 Hippocampal circuitry rearrangements in the adult rat after Nogo-A Neutralization

## 3.1 Abstract

The adult CNS contains proteins that inhibit the growth of nerve fibers. One such important protein is Nogo-A, which is mainly present in the insulating myelin sheath surrounding axons and in subpopulations of neurons. New therapeutical strategies in pre-clinical trials demonstrated that intrathecally infused antibodies reach their targets in the CNS. Function-blocking antibodies directed against the Nogo-A protein have been raised and were used in the present work.

Two to three months old male Long Evans rats were infused intrathecally for two weeks with antibodies against Nogo-A, control IgG or PBS, or for four weeks with anti-Nogo-A or control IgG antibodies. Hippocampi from rats which were infused for two weeks with anti-Nogo-A or control IgG antibodies were dissected, and total RNA as well as total protein were extracted and used for Affymetrix Gene Chip (Rat Expression Array 230 2.0) or quantitative proteomic Isotope-Coded Affinity Tag (ICAT) analysis, respectively. Gene analysis was performed using Genespring 7.0 and ICAT analysis was performed using Sequest software. Both approaches revealed modulation of several genes that were subdivided in categories, such as cytoskeleton, neurite growth, signaling, extracellular matrix and synapse related. Immunofluorescence data corroborated these findings. Together, the results are indicative of increased growth and/or plasticity as detected by the increased expression of Gap43, NF-68 and alpha-internexin triggered by the neutralization of Nogo-A. An increase in several synaptic markers was also observed including synaptophysin, the inhibitory vesicular GABA transporter (vGAT) and the vesicular Glutamate transporter 1 (vGlut1).

Rats that were infused for two or four weeks with anti-Nogo-A or control IgG antibodies were used for immunofluorescence and behavioral studies. The immunofluorescence data from the four-week time point showed a decrease in growth response, as suggested by the tendencies of increased expression of Gap43, NF-68 and alpha-internexin. On the other hand, there was an increase in inhibitory and excitatory pre-synaptic markers from the two-week to the four-week time-point. Furthermore, there was a differential regulation of the $GABA_A$ receptor subunits alpha-1, alpha-2 and alpha-5.

In our behavioral studies, rats did not show detectable alterations of hippocampal dependent behaviors such as elevated plus maze, reference or working memory.

In conclusion, Nogo-A neutralization in adult intact rats induces a transient growth response and a modulation of the synaptic circuitry without detectable cognitive behavioral consequences. The lack of behavioral abnormalities is of extreme importance in the context of on-going clinical trial and of unpublished observations of schizotypal behavior in Nogo-A knockout animals. This work demonstrates the function of Nogo-A as a regulator of neural connections stability as well as a growth suppressor and reveals a putative novel role in synaptic re-modeling.

# 3.2 Introduction

The low regeneration and structural repair capacity of the adult CNS accounts for the irreversible consequences after lesion. The identification of several growth inhibitory molecules present in the CNS (Benowitz and Yin, 2007; Filbin, 2006) account for the referred irreversible consquences. Nogo-A, one of the most potent growth inhibitors in the adult CNS and the first one to be discovered (Caroni and Schwab, 1988b; Chen et al., 2000), has been extensively studied both *in vitro* and *in vivo* experiments.

Nogo-A signals via the receptor complex NgR/p75/Lingo-1/Troy (Fournier et al., 2001; Mi et al., 2004; Park et al., 2005; Wang et al., 2002a) triggering a similar response to other inhibitory molecules which act via NgR. The existence of a Nogo-A specific receptor, as yet unidentified, has been suggested (Dodd et al., 2005). Two active sites, Nogo-66 and a Nogo-A specific region have been suggested and both lead to activation of RhoA and ROCK (Fournier et al., 2003; Hsieh et al., 2006; McKerracher and Higuchi, 2006; Niederost et al., 2002; Schweigreiter et al., 2004), thereby, affecting the neuronal growth machinery.

Rats which underwent stroke lesions exhibited compensatory fiber sprouting from the intact side across the midline and establish functional re-innervation of the denervated side after Nogo-A neutralization by antibody application (Emerick et al., 2003; Papadopoulos et al., 2002; Papadopoulos et al., 2006), or NgR blockade by peptides (Lee et al., 2004). Enhanced regeneration of injured fibers and improved functional recovery were also observed in spinal cord lesioned rats and monkeys treated with anti-Nogo-A antibodies (Freund et al., 2006; Liebscher et al., 2005; Merkler et al., 2001; Schnell and Schwab, 1990; Schwab, 2004), in rats infused with NgR antagonist peptides (GrandPre et al., 2002) or with an activity-blocking receptor fragment (Lindsay, 2004), as well as in some Nogo-A (Dimou et al., 2006; Kim et al., 2003; Simonen et al., 2003) or NgR (Kim et al., 2004) knockout mice.

Despite the importance of Nogo-A in regeneration, its function in the intact CNS tissue is not yet well understood. Its neutralization *in vivo* has been shown to produce a

transitory growth response of Purkinje axons and of the corticospinal tract in intact adult rats (Bareyre et al., 2002; Buffo et al., 2000; Gianola et al., 2003). Regarding its expression pattern in adults, Nogo-A is relatively highly expressed in oligodendrocytes and in some neurons of the hippocampus (Gil et al., 2006; Huber et al., 2002; Meier et al., 2003; Trifunovski et al., 2006). Neuronal Nogo-A expression is only observed in highly plastic regions of the adult brain such as the hippocampus, but during early development high Nogo-A expression is common to projection neurons (Huber et al., 2002). The function of neuronal Nogo-A during development and in plastic regions of the adult brain remains elusive although it could be related to the regulation of plastic events. Therefore, in our study, we addressed the question of which are the effects that acute Nogo-A neutralization could induce in the intact adult hippocampus.

This is the first comprehensive study of the effects of acute Nogo-A neutralization in adult intact rats. In adult rats treated with antibodies for two or four weeks, a transient growth response was elicited being highest at the two-week time point. At the synaptic level, an increase of expression was observed in the inhibitory and excitatory synaptic circuitry. Interestingly, there was a differential regulation of $GABA_A$ receptor subunits raising the possibility of a novel Nogo-A function in the regulation of synaptic function, especially of $GABA_A$ synapses and their receptor composition. The most significant effects were detected in the CA1 region of the hippocampus. Despite the observed changes in hippocampal circuitry, the behavioral studies performed did not detect major functional alterations. These results are in contrast to tour current ongoing work with Nogo-A knockout mice that show alterations in schizophrenia related behavioral tests. Our results showing the lack of major behavior modifications following acute neutralization of Nogo-A are of extreme importance in the context of the ongoing clinical trials for spinal cord injury with anti-Nogo-A antibodies providing first evidence that no major functional changes should be expected in the intact brain, especially concerning cognition and behavior.

# 3.3 Material and Methods

### Subjects

Male Long Evans rats, of 2-3 months of age (approximately 300g body weight) at the time of pump implantation surgery, were obtained from Janvier (Janvier, Le Genest-St-Isle, France). The animals were allocated randomly to six cohorts. Cohort 1 (n = 24) was used for a preliminary Morris Water Maze (MWM) test. From this cohort, three animals of each group were used for total RNA extraction for genomic analysis and another three animals of each group were used for total protein extraction for proteomic analysis. Cohort 2 (n = 24) was used for behavior analysis using the elevated plus maze (EPM), the open field (OF), and the MWM. From this cohort two animals from each group died during surgery recovery and one animal from the anti-Nogo-A antibody treatment group was removed due to infection around the pump. Cohort 3 (n = 24) was used for a second series of behavioral analysis with EPM, OF and MWM as well as prepulse inhibition (PPI) and histological analysis. From this cohort, five animals belonging to the anti-Nogo-A group were removed from the analysis. Two animals died during surgery recovery, one was euthanized due to the development of necrotic tissue around the area where the pump was implanted and two others were removed at the end of the study because the catheters were either twisted or removed during the course of the experimental procedures. Cohort 4 (n = 20) was used for histological analysis of four-week delivery without behavior testing. From this cohort, two animals were euthanized due to the development of necrotic tissue and infection around the pump implantation site. Cohort 5 (n = 10) was used exclusively for histological analysis of the two week time point. From this cohort, one animal from the anti-Nogo-A antibody treatment group died during surgery recovery. Cohort 6 (n = 20) was used for behavior analysis of working memory in the MWM and protein extraction for immunoblotting.

**Table 1. Animal numbers used in each behavior task**

| Cohort/ Experiment | Behavior Task | N per Treatment | |
|---|---|---|---|
| | | 11C7 | IgG |
| **2** | Elevated Plus Maze | 10 | 10 |
| | Open Field | 10 | 10 |
| | Morris Water Maze – Reference Memory | 9 | 10 |
| **3** | Elevated Plus Maze | 7 | 12 |
| | Open Field | 7 | 12 |
| | Prepulse Inhibition | 7 | 12 |
| | Morris Water Maze – Reference Memory | 7 | 12 |
| **6** | Morris Water Maze – Working Memory | 10 | 10 |

Cohorts 1-3 and 6 were housed under a 12:12 reversed light/dark cycle and were tested during the dark phase. Cohorts 4 and 5 were housed under a 12:12 normal light/dark cycle. The animals were housed in groups of four or five animals to a gage with food and water freely available. Room temperature was set at 21 ± 1°C and humidity at 55 ± 5%.

The Swiss Federal Veterinary Office approved all the procedures used in this study, which were conducted in accordance with the National Institutes of Health Guide for Care and Use of Laboratory Animals.

### Animals and Experimental Design

The present study consisted of six experiments. The first experiment aimed at studying the effects of Nogo-A neutralization in memory performance and at screening for effects at the molecular level. The mouse monoclonal IgG antibody 11C7, directed against the rat aa 623-640 of Nogo-A and the control monoclonal IgG antibody against cyclosporine were delivered intrathecally for two or four weeks. Anti-Nogo-A and control antibody delivery lasted two weeks but given the suboptimal behavior conditions in the first experiment with cohort 1, we decided to extend and optimize the testing conditions. Cohort 2 was added and a new experiment was performed repeating some behavior analysis as well as performing histological analysis based on the Gene Chip and ICAT screenings. Experiment 3 (cohort 3) was carried out to corroborate the results of experiment 2 and additionally to study PPI behavior, which is related with schizotypal disorders. Experiment 4 (cohort 4) aimed at confirmation of the histological results in animals that did not undergo behavior testing, i.e. to exclude a confound effects due to behavioral testing. Experiment 5 (cohort 5) was performed to analyze histologically the effects of Nogo-A neutralization for a two-week period. Experiment 6 (cohort 6) was done to analyze the effects of Nogo-A neutralization in working memory. Experiments 2-4 and 6 had anti-Nogo-A and control IgG antibody delivery for a period of four weeks. Experiments 1 and 7 had anti-Nogo-A and control IgG antibody delivery for a period of two weeks. The two time-points were chosen in order to evaluate possible time-dependent differences in protein expression due to Nogo-A neutralization.

### Surgical Procedures

Male Long-Evans rats 2-3 months old (approximately 300 grams of body weight) were deeply anesthetized with Hypnorm (120 µl / 200 grams body weight; VetaPharma Ltd, Leeds, United Kingdom) and Dormicum (0.75 mg in 150 µl per 200 grams of body weight; Roche Pharmaceuticals, Basel, Switzerland). To avoid eye desiccation, eye

ointment containing vitamin A (Vitamine A, Bausch & Lomb Swiss AG, Steinhausen, Switzerland) was applied.

A hole was drilled into the dorsal lamina of the second lumbar vertebra through which a fine catheter (32 gauge; Recathco, Allison Park, PA) was inserted into the intrathecal space and pushed up to T10. The catheter was connected to the outlet of an osmotic minipump (2.5 µl/h, 6 µg/µl antibody, Alzet 2ML4 for 4 week delivery or 5 µl/h, 3 µg/µl antibody, Alzet 2ML2 for 2 week delivery; Charles River Laboratories, Les Oncins, France), which was placed under the skin of the back of the animal and filled with monoclonal anti-Nogo-A (11C7) or control IgG antibody solution (6 mg or 12 mg dissolved in 2 ml PBS for two- or four-week delivery, respectively), to deliver antibodies at a constant rate into the CSF for 2 or 4 weeks.

Analgesics (Rimadyl, 5 mg/kg of body weight s.c., Pfizer AG, Zürich, Switzerland) and antibiotics (Baytril, 5mg/kg body weight s.c., Bayer AG, Leverkusen, Germany) were given post-operatively.

### Gene Analysis

Upon the end of the treatment, the right hippocampus of three animals per group was dissected and frozen over dry ice before tissue dissociation and total RNA extraction (RNeasy Lipid Tissue Kit, Qiagen). RNA was quantified by nanodrop (ND-100, NanoDrop Technologies, Welmington, DE, USA) quality was assessed using a bioanalyzer (2100 Bioanalyzer, Agilent Technologies, Santa Clara, CA, USA). Affymetrix Gene Chip (Rat Expression Array 230 2.0, Affymetrix Inc., Santa Clara, CA, USA) was used for cRNA hybridization, according to the manufacture's protocol. Each condition (IgG vs. PBS, 11C7 vs. PBS) was analyzed in triplicates. The dataset was flagged filtered for the presence of a gene in at least two out of three replicates, normalized first per chip and second per each gene to the median of the wild type replicates and statistically restricted by a 1-way ANOVA $p<0.05$ (no multiple testing correction). The obtained list was then filtered for $X \geq 1.2$ fold. Gene analysis was performed using Genespring 7.0 and the Rat Genome Database (http://rgd.mcw.edu) was used to obtain further information about the genes regulated.

### Protein Analysis

Upon the end of the treatment, the hippocampus of three rats per group was dissected and frozen over dry ice. The three hippocampi were pooled before the samples were dissociated in denaturing solvent (50 mM TRIS/HCl, pH 8.3; 5mM EDTA; 1% RapiGest, Waters, MA, USA) with an Ultra Thurax (T25 basic, IKA® Werke, Staufen, Germany). Once the solution became clear, the sample was left over ice for 30 minutes. The

mixture was then centrifuged (Biofuge 15R, Heraeus Sepatech, Germany) at 10'000 rpm at 4°C for 15 minutes. The supernatant was transferred to another eppendorf tube and the protein concentration was quantified in a Nanodrop spectrophotometer (ND-1000, NanoDrop Technologies, DE, USA). 600 μg of each protein sample was reduced by adding TCEP to give a final concentration of 2 mM for 10min at 60°C. One unit of the ICAT reagents was dissolved in 20 μl ACN and applied to the protein sample. The reaction mixture had a final volume of 93 μl and was incubated for 2 hours at 37°C in darkness. Afterwards the reaction was quenched by the addition of 1 μl 1M DTT. Both samples were pooled and trypsin was added (1:50 (w/w)). The samples were digested for 12 to 16 hours at 37°C. To reduce sample complexity the peptide mixture was fractionated by strong cation exchange chromatography on an Agilent 1100 System. The sample was diluted with 5.5 ml buffer A (10mM $KPO_4$, pH 3, 25% ACN) and the pH adjusted to pH 3 by addition of phosphoric acid. After centrifugation (15 min; 16000xg) the supernatant has been applied on a SCX column (PolySULFOETHYL A™, 2.1 x 200, 5 μm, 300 Å (PolyLC INC. Columbia, MD, USA)). Unbound material was flushed out for 5 minutes at a flow rate of 0.3 ml/min with 100% buffer A. Peptides were eluted by increasing the amount of buffer B (buffer A, 350mM KCl) with the following gradient: 5-25min, 0-30% B: 30-60min, 25-100% B; 50-60min, 100% B). 0.3 ml fractions were collected and based on the peptide content in the fractions were pooled to 10 final fractions. The combined fractions were concentrated to a final volume of 50 μl and diluted ten times in 2x PBS (20 mM $KPO_4$, pH 7.2, 300 mM NaCl).

The ICAT labeled cysteine containing peptides were affinity purified on an Avidin cartridge (Applied Biosystems, USA). The Avidin Cartridge was equilibrated with 2 ml of 2x PBS before samples were slowly loaded. After loading the sample, unbound material was washed out by addition of 500 μl 2x PBS. A second wash step was carried out with 1ml PBS. Unspecific binders were flushed out with 500 μl of 50 mM ammonium bicarbonate, pH 8.3, 20% methanol. ICAT labeled peptides were eluted with 800 μl of 0.4% TFA, 30% ACN. All fractions were dried completely and afterwards dissolved in 95 μl Cleaving Reagent A and 5 μl Cleaving Reagent B (Applied Biosystems, USA) to remove the avidin tag. After 2 hours at 37°C, the samples were evaporated to complete dryness in a centrifugal vacuum concentrator.

As additional cleaning step, samples were dissolved in 200 μl of 3% ACN, 0.1% TFA for 15 minutes at room temperature (~21ºC) and applied on $C_{18}$ SepPak® cartridges (Waters, USA). After washing with 2ml 3% ACN, 0.1% TFA the samples were eluted with 500 μl of 60% ACN, 0.1% TFA and dried again in a centrifugal vacuum concentrator.

For mass analysis the samples were dissolved in 10 µl 3% ACN, 0.2% formic acid and LC-MS/MS analysis was performed on an LTQ-FTICR hybrid mass spectrometer (Thermo Scientific, Germany) attached to an Eksigent nano HPLC System (Eksigent Technologies, USA). 4 µl of the ICAT labeled samples were applied to an in-house made tip-column (0.075 x 80 mm) packed with $C_{18}$ reverse phase material (ProntoSIL, $C_{18}$, 3 µm, 200 Å, AQ, Bischoff Chromatography, Germany) and equilibrated with 1% ACN, 0.2% formic acid. Peptides were eluted at a flow rate of 200 nl/min and with following gradient 0-5 minutes, 3-10% solvent B (80% ACN, 0.2% formic acid); 5-55 minutes, 10-40% B; 55-60 minutes 40-97% B; 60-65 minutes, 97% B. Precursor mass spectra were acquired at the ICR cell in a mass range of 300-2000 m/z. Based on intensity four data dependent MS/MS spectra were recorded with charge state 2+ or higher using collision induced dissociation. Target ions already selected for MS/MS were dynamically excluded for 60 seconds. Data were analyzed using the SEQUEST algorithm and quantification of the ratio of each protein (ICAT light versus ICAT heavy) was calculated using the ASAP Ratio program.

## Histological Procedures

### Tissue Processing

Once antibody delivered was over (2 or 4 weeks after pump implantation), animals were perfused through the ascending aorta with saline solution to remove the blood and then with a 4% PFA solution in 0.1M PB pH 7.4. The brains were carefully dissected and post-fixed overnight at 4°C and cryoprotected in 30% glucose solution for three days. For some antigens, one hemisphere was kept in order to optimize the protocol for detection of cytoskeletal growth related markers we compared different methods (**Table 3**). Brains were sectioned at 40 µm in a cryostat and sections of the dorsal hippocampus were used for the staining procedures and analysis. For all stainings, we used free floating sections mostly of the coronal plane, although some sagital sections were also analyzed.

For antigen retrieval, four conditions were tested for optimization of the detection of the cytoskeletal growth related markers.

Method I: Conventional tissue preparation with 4% PFA perfusion, overnight post-fixation and 30% glucose cry protection was performed with no additional antigen retrieval steps.

Method II: After animal perfusion, post-fixation and cryoprotection as described above, the sections were incubated in 20% methanol solution for 30 seconds at -20°C and then heated to 80°C for a 5-minute period in 0.1 M Tris buffer pH = 8.0.

Method III: After animal perfusion, post-fixation and cryoprotection as described above, we used a previously described protocol (Fritschy et al., 1998). In brief, brains were submerged in a 0.1 M citrate buffer pH = 6.2 and were microwaved for 3 minutes at 600 watt.

Method IV: After animal perfusion, post-fixation and cryoprotection as described above, we used a modified version of method III. After microwaving the brains, sections were cut and incubated for 10 minutes in a mixture of Methanol and Ethanol.

### Immunoperoxidase

The detection of the infused anti-Nogo-A and IgG control antibodies was performed by using rat-adsorbed anti-mouse antibodies coupled to biotin. The antisera were visualized using the ABC-DAB system (Vector Laboratories, Burlingame, CA, USA).

### Immunofluorescence

Prior to antigen retrieval, tissue was stabilized via a 10-minute incubation in 4% PFA, GA 0.1% containing picric acid 0.15% at 22°C step. An overnight incubation step at 4°C with primary antibodies (**Table 2**) was used for mouse monoclonal or rabbit polyclonal parvalbumin, rabbit polyclonal vGAT, and rabbit polyclonal vGlut1.

**Table 2. Primary Antibodies for Immunofluorescence and Immunoblot**

| Name / Source | Clone, Company, Location, Country | Dilution | |
|---|---|---|---|
| | | IF | WB |
| **PV / Mouse** | 235, Swant, Bellinzona, Switzerland | 1:500 | 1:500 |
| **PV / Rabbit** | PV28, Swant, Bellinzona, Switzerland | 1:500 | 1:500 |
| **vGAT / Rabbit** | 131 002, Synaptic Systems, Goettingen, Germany | 1:250 | 1:1000 |
| **vGlut1 / Rabbit** | 135 302, Synaptic Systems, Goettingen, Germany | 1:2000 | 1:1000 |
| **NF68 / Rabbit** | AB1983, Chemicon International, Temecula, CA, USA | 1:300 | 1:250 |
| **GAP-43 / Rabbit** | AB5220, Chemicon International, Temecula, CA, USA | 1:1000 | 1:1000 |
| **GAP-43 / Mouse** | G9264, Sigma-Aldriech Inc., USA | 1:250 | |
| **Cofilin / Rabbit** | Ab3842, Chemicon International, Temecula, CA, USA | 1:300 | 1:500 |
| **α-internexin / Rabbit** | AB7259, Abcam, Cambridge, UK | 1:500 | 1:5000 |
| **α-internexin / Mouse** | NB300-216, Novus Biologicals, Littleton, CO, USA | 1:500 | 1:10000 |
| **GAPDH / Mouse** | AB8245, Abcam, Cambridge, UK | | 1:15000 |

| | | | |
|---|---|---|---|
| **Synaptophysin / Rabbit** | Z66, Zymed Laboratories Inc., San Francisco, CA, USA | | 1:500 |

**Table 3. Method optimization for cytoskeletal markers**

| Cytoskeletal Markers | Method I | Method II | Method III | Method IV |
|---|---|---|---|---|
| Cofilin | no detection | low signal | low signal | low signal |
| alpha-internexin abcam | low signal | very good | good | good |
| Nf-68 abcam | no detection | low signal | no detection | no detection |
| Nf-68 chemicon | low signal | Good | very good | no detection |
| GAP-43 chemicon | no detection | no detection | low signal | no detection |
| GAP-43 sigma | good | Good | very good | no detection |
| PV | very good | very good | very good | low signal |

Method III yielded the best results and this was therefore the method of choice. Primary antibodies used were: rabbit polyclonal anti-NF68, mouse monoclonal anti-GAP-43, rabbit polyclonal and mouse monoclonal anti-α-internexin (**Table 3**).
Detection of the $GABA_A$ receptor subunits was performed according to a protocol published previously (Fritschy et al., 1998). The primary antibodies were kindly donated by Prof. J.M. Fritschy.

After three washing steps with PBS, secondary antibodies Alexa 488 anti-mouse or Alexa 546 anti-rabbit (Invitrogen-Molecular Probes, Basel, Switzerland) were used for antisera visualization and incubated for two hours at RT.

Sections were then imaged with a Zeiss Axioskop 2 mot plus for lower magnification images that were further analyzed by densitometry. Confocal imaging was performed using a Spectral Confocal Microscope TCS SP2 AOBS (Leica) using a 63x or 100x oil immersion objective. Maximum Intensity Projections of the images were used to improve the signal-to-noise ratio.

Background corrected optical density analysis was performed using ImageJ software (http://rsb.info.nih.gov/ij). Relative Optic Density values and cell counts are expressed as means ± SEM in arbitrary units.

Statistical analysis was performed using the software GraphPad Prism 4 for Windows (San Diego, CA, USA). The non-parametric Mann-Whitney test was used.

### Immunoblotting

The same samples used from the two-week treatment time-point for the ICAT were used for immunobloting. The samples from the four-week time-point followed the same procedure described in the proteomic protocol. Samples (30 µg) were resolved by 7-14% NuPAGE (Invitrogen), transferred onto polyvinylidenedifluoride membranes. After blocking (3% Topblock in 1X TBST), incubation with primary antibodies at room temperature for 3 hours followed. Primary antibodies used were mouse monoclonal and rabbit polyclonal anti-parvalbumin, rabbit polyclonal anti-Gap43, rabbit polyclonal anti-NF68, rabbit anti-α-internexin, mouse anti-α-internexin, rabbit polyclonal anti-vGAT, rabbit polyclonal anti-vGLUT1, rabbit polyclonal anti-Synaptophysin, rabbit polyclonal anti-Cofilin, and mouse monoclonal anti-GAPDH (**Table 2**). After washing, membranes were incubated with secondary antibodies. Proteins were detected by a chemiluminescent substrate (SuperSignal West Pico, Pierce Biotechnology)). Images were captured with Stella system (Agilent Technologies, Santa Clara, CA, USA).

Background corrected optical density analysis was performed with AIDA software (Raytest). Statistical analysis was performed using the software GraphPad Prism 4 for Windows (San Diego, CA, USA).

### Behavioral Analysis

Digital cameras were mounted above the Elevated Plus Maze, Open Field and Morris Water Maze and images were captured at a rate of 5 Hz and transmitted to a personal computer running the Ethovision (Noldus Technology, Wageningen, The Nederlands) tracking system.

### Elevated Plus Maze

The elevated plus maze (**Fig. 1**) was made of wood painted in black and elevated 67 cm above ground. The plus maze consisted of four equally spaced arms, 45 cm long and 10 cm wide, radiating from a square center measuring 10 x 10 cm. One pair of opposing arms, providing a secure environment, was enclosed in opaque walls except for the part at the center square. The remaining two arms were exposed with a 3mm high edge border. The maze was positioned in a testing room with diffuse lighting. A test session began by placing the subject in the central area facing one of the open arms. It was then allowed to explore freely for 6 minutes before being removed and placed back in the home cage. The maze was cleansed between each subject's test

sessions. Percent of time spent in the open arms and percent of open arm entry were used as measures of anxiety. Two independent experiments were performed.

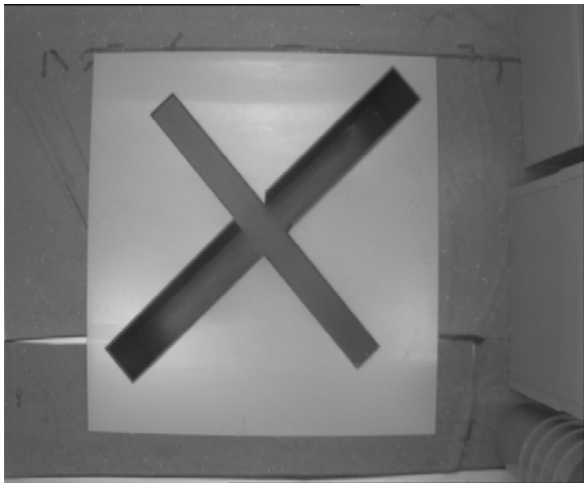

**Fig 1.** Elevated Plus Maze. The maze consisted of four equally spaced arms, 45 cm long and 10 cm wide, radiating from a square center measuring 10 x 10 cm. One pair of opposing arms, providing a secure environment, was enclosed in opaque walls except for the part at the center square. The remaining two arms were exposed and provided an aversive environment, propricious for anxiogenic behavior.

## Open Field

The open field (**Fig. 2**) was made of four grey plastic boxes of 78 x 78 x 45 cm and was positioned in a testing room with diffuse lighting. The session began by placing 4 subjects, one per box, at one of the corners of the box. The boxes were cleansed between each subject's test sessions. Locomotor activity (total distance travelled in cm) was recorded in the entire open field area as well as a center area defined as a square of 26 x 26 cm (26 cm from the walls) to measure risk assessment. The total duration of the task was one hour and locomotor activity was measured in 10-minute bins. Two independent experiments were performed.

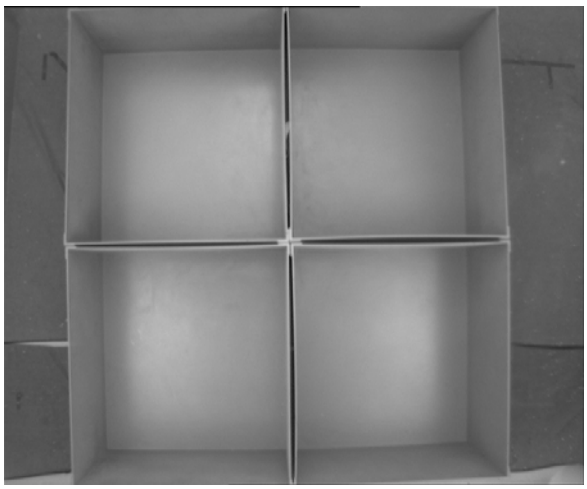

**Fig 2.** Open Field. made of four grey plastic boxes of 78 x 78 x 45 cm and was positioned in a testing room with diffuse lighting. Four subjects (one per box) can be tracket at the same time. General activity is recorded and measured in terms of distance travelled in the box.

### Prepulse Inhibition

The apparatus consisted of four acoustic startle chambers for mice (SR-LAB, San Diego Instruments, San Diego, CA, USA). Each startle chamber comprised a non-restrictive cylindrical enclosure (8.2 cm diameter, 20 cm length) made of clear Plexiglas attached horizontally on a mobile platform, which was in turn resting on a solid base inside a sound-attenuated isolation cubicle. A high-frequency loudspeaker mounted directly above (26 cm high) the animal enclosure inside each cubicle produced a continuous background noise of 68 dB and the various acoustic stimuli in the form of white noise. Vibrations of the Plexiglas enclosure caused by the whole-body startle response of the animal were converted into analogue signals by a piezoelectric unit attached to the platform that recorded and quantified movement in 1-ms intervals. These signals were digitized and stored by a computer. The reactivity score on a given trial was given by the amplitude of the whole body startle and defined as the average of one hundred 1-ms accelerometer readings collected from onset of the pulse stimulus (on pulse alone and prepulse plus pulse trials) or the prepulse stimulus (on prepulse alone and no stimulus trials). The sensitivity of the piezoelectric accelerometer was routinely calibrated to ensure consistency between chambers and across sessions.

Subjects were presented with a series of discrete trials comprising a mixture of four types of trials. These included pulse-alone trials, prepulse-plus-pulse trials, prepulse-alone trials, and trials in which no discrete stimulus (other than the constant background noise) was presented. A reduction of startle magnitude in prepulse-plus-pulse trials relative to those in pulse-alone trials constitutes the PPI effect.

Three pulse stimulus intensities of 100, 110 or 120 dB, of 30 ms in duration were employed as test conditions. Prepulses of three intensities were employed: defined as +6, +12 and +18 dB above background noise intensities. These allowed for nine possible prepulse-plus-pulse combinations. The duration of prepulse stimuli was 20 milliseconds. The lead interval (also referred to as SOA, stimulus onset asynchrony) of the prepulse and pulse stimuli on prepulse-plus-pulse trials was 100 milliseconds.

A session began with the animals being placed into the Plexiglas enclosure and consisted of 172 discrete trials presented. The interval between successive trials was variable with a mean of 15 s (ranging from 10 to 20 s). They were acclimatized to the apparatus for 2 min before the first trial began. The first and last six trials consisted of pulse-alone trials (two trials per each pulse intensity). These served to habituate and stabilize the animals' startle response. In the subsequent 160 trials, the animals were presented with 10 blocks of discrete test trials. Each block consisted of one trial of each of the following trial-types: three pulse-alone trials at 100, 110 or 120dB, three

prepulse-alone of each of the three levels of prepulse intensities, one no-stimulus trial and nine possible combinations of prepulse-plus-pulse trials in a pseudo-random order. All data were analyzed using analysis of variance (ANOVA) of the appropriate design. The experiment yielded four datasets that were separately analyzed: 1) comparison between the first and last six pulse alone trials, 2) average reactivity scores in pulse alone and no-stimulus trials across the 10 middle blocks of trials, 3) percentage of PPI scores, which were calculated on the basis of the individual rats' average scores in pulse alone and prepulse-plus-pulse trials across the middle 10 blocks of trials using the formula %PPI = (1 – reaction on pulse alone trials / reaction on prepulse-plus-pulse trials) x 100, for each of the nine prepulse-plus-pulse combinations and 4) individual animal average scores in pulse alone and prepulse-plus-pulse trial across the middle 10 blocks of trials without percentage normalization.

### Morris Water Maze

The water maze (**Fig. 3**) was a circular tank made of fiber glass painted black (2.10 m in diameter and 60 cm in depth). The tank was positioned in the middle of a testing room (3×4.9×2.9 m) with diffuse lighting and enriched with various posters and other distal visual stimuli around the room to provide the spatial cues. The bottom of the maze was raised 45 cm above the room floor. At the beginning of each day, the tank was filled with a mixture of cold and hot tap water to a depth of 32 cm, and the water temperature was maintained at 24±1 °C. A stable circular platform, measuring 22 cm in diameter and painted black, was submerged 2 cm below the surface of the water hidden from the rat's view. It had a rough surface, which allowed the rat to climb onto it easily once its presence was detected.

A separate white circular disk, measuring 11.5 cm in diameter, could be mounted on top of the hidden platform so that it was 22 cm above the water surface. When in place, the white disk served as a distinct visual cue for the location of the otherwise hidden platform. Four points, equally spaced along the circumference of the pool, were arbitrarily assigned as: N, E, S, W. These points served as the starting positions at which the animal was lowered gently into the water, with its head facing the wall of the water maze. The area of the pool was also conceptually divided into four quadrants (NE, SE, SW and NW) of equal size.

### Procedures

The reference memory procedure comprised 1 day of training using a visible escape platform (four trials per day), and four subsequent days of hidden platform training (four trials per day) with the platform fixed in the centre of the same quadrant (**Fig. 3**).

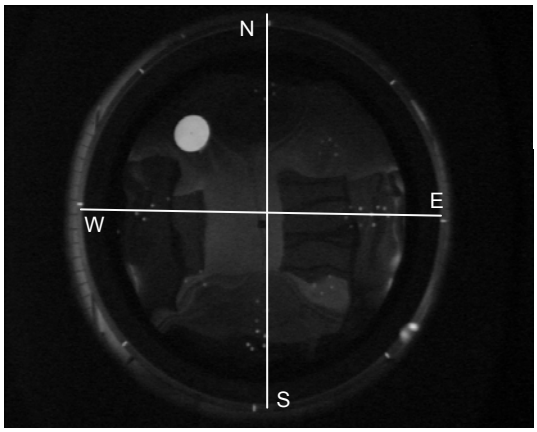


**Fig 3.** Platform location in the Morris Water Maze. Platform (in white for illustration purposes) is located in the middle of one of the four possible quadrants. The subject is placed in the water facing the wall at one of the four cardinal points.

### Visible platform training

This task served to familiarize the animals with the water maze testing procedure, and allowed the detection of possible between-groups difference in visual discrimination and motor control. On this day, the animals were trained to escape from the water by climbing onto the escape platform. The escape platform was made visible by attaching a visual cue directly above its location. There were four consecutive trials. The starting point was constant across trials (at position N), but the location of the escape platform varied among the four possible positions (NE, NW, SE, SW).

### Reference memory task

This spatial navigation task requires spatial learning and memory in rats. The subjects were tested in squads of four or five. The starting position varied across trials. At the beginning of a trial, the animal was placed into the water at the start location with the head facing the wall. A trial ended when the animal escaped onto the platform. Escape latency for each trial was recorded. If an animal failed to escape within 60 seconds, it was guided to the platform by the experimenter. In such trials, an escape latency of 60 seconds was assigned. The animals were allowed to spend 10 seconds on the escape platform and were then placed in a holding cage for 15 seconds before the next trial began. The animals were given four trials of acquisition training each day (for a 4 day period) with the escape platform fixed in the centre of the same quadrant. After this acquisition phase, the animals were then tested in a probe trial, as described below.

### Probe trial

The probe allowed an evaluation of the animals' spatial search pattern in the absence of the escape platform. One probe trial was performed 24h after the acquisition phase

of reference memory. In this task, the platform is removed from the pool. The subjects were released in one of the two distally located start positions relative to the original platform position, head facing the wall. The subjects were allowed to search for the platform for 60 seconds. A direct swim and longer time spent in the target quadrant where the platform was located represented more accurate search behavior.

### Working Memory

This spatial navigation task requires spatial learning and memory in rats. It differs from the reference memory task in that the platform location is changed every day, forcing the animals to learn that at any given day the platform will not be located at the same position where it was the previous day. More importantly, the animals need to learn to swim quickly to the platform location after its location is made known to the animals in trial one. Another difference refers to the location of the visual platform prior to the working memory testing. In order to have 12 non-repetitive available platforms, the visual platform was located at the center of the pool. The platform location varies from one day to the next in a non-repetitive manner and there are 12 different available positions for platform location (**Fig. 4**). The starting positions varied across trials (4 per day for the 15 second- and 45 minute-delay). Escape latency for each trial was recorded. If an animal failed to escape within 90 s, it was guided to the platform by the experimenter. In such trials, an escape latency of 90 s was assigned. The animals were allowed to spend 10 s on the escape platform and were then placed in a holding cage for 15 s before the next trial began. This was repeated for a 4 day period or when statistical significance between the first two trials was achieved. The procedure was repeated again in the next 2 days (days 5 and 6) but the delay between trials was extended to 45 minutes and the animals were returned to their home cage at the end of each trial. This procedure was again repeated for the delays of 90 and 180 minutes between trials (only two trials were performed). The increased inter-trial interval aims to increase the difficulty of the task forcing the animals to remember the platform location after one exposure for longer. The use of four trials per day aims at facilitating the learning of the task although the analysis only requires the first two trials.

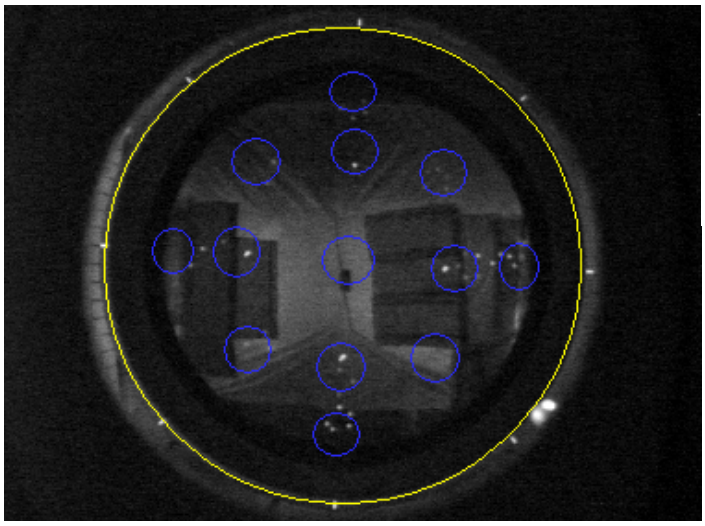

**Fig 4.** Platform locations in the Morris Water Maze. Platform locations are depicted in the blue circles. There are 13 available positions which can be used in a non-repetitive manner. The subject is placed in the water facing the wall.

### Data Analysis

The reference memory task was analyzed taking into account the time and distance, of the four daily trials, to reach the platform. A plot of the average across days indicates the learning curve. Probe trial results were analyzed by the percentage of time and distance spent in the quadrant that had contained the platform. The working memory task was analyzed taking into account the latency of the trials across days at each delay. The comparison between the first and second trials was used to index working memory performance of the animals. Statistical analyses were performed by analysis of variance (ANOVA) carried out using the SPSS software.

### Statistical Analysis

Statistical analysis of immunohistochemistry and western blots was performed using the software GraphPad Prism 4 for Windows (San Diego, CA, USA). Mann-Whitney test was used. Statistical behavioral analysis was done by ANOVA using SPSS 14.0 for Windows (Chicago, IL, USA). Results are expressed in mean ± SEM.

# 3.4 Results

### Molecular analysis of *in vivo* Nogo-A neutralization

Genomic and proteomic techniques were used to explore the effects of acute Nogo-A neutralization in adult rats. The “Cytoskeleton” category (18%) was one of the main affected categories in the proteome analysis and the sixth highest regulated category the family of small Rho GTPases (6%), is known to be involved in cytoskeletal regulation. This category is also highly represented in the genomic analysis (10%) (**Fig. 5**). Even if the represented affected categories were the same, the two techniques revealed very little overlap in terms of individual regulated molecules, a not surprising observation considering the growing evidence that relatively frequent discordance exists between mRNA expression and the expression and function of the encoded proteins (Robinson et al., 2003). A good example is given by the “Cytoskeletal” category (18% of protein changes versus 2% of mRNA changes).

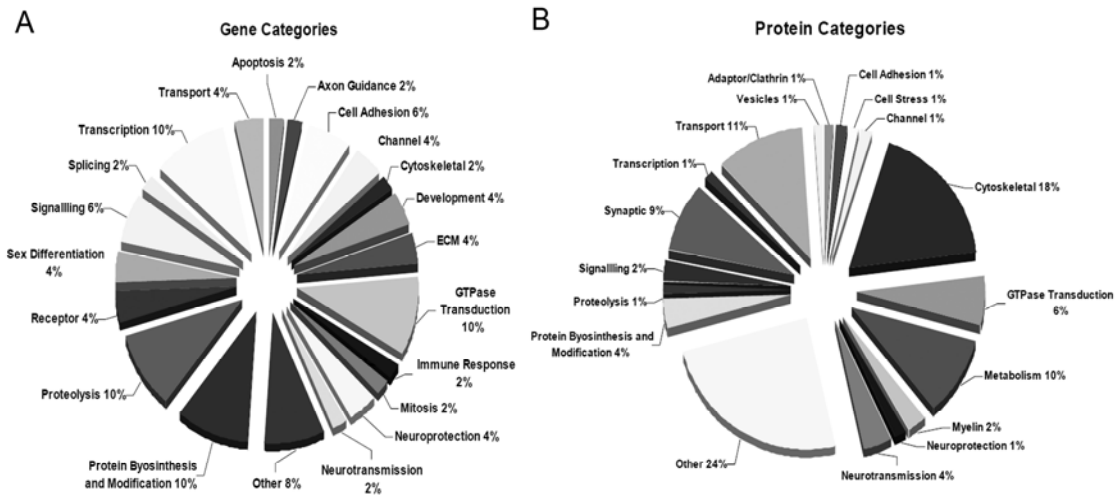


**Fig 5.** Graphical representation of the proportion of categories of gene and proteins altered after Nogo-A neutralization. A: Gene Categories. B: Protein Categories. Note the high proportion of cytoskeletal proteins regulated as well as the high proportion of proteins and genes belonging to the GTPase family of signal transducers.

The “Cytoskeletal” functional category included several proteins related to intermediate filaments as proteins well as involved in fiber growth such as α-internexin, tubulin, cofilin-1, CRMP-1 and -2, spectrin and neurofilament 68 (NF68). Particularly, NF68 and α-internexin are well known early neuronal growth markers, while cofilin has been shown to play a role in growth cone and actin dynamics. On the other hand, the genomic approach showed regulation in anti-Nogo-A antibody treated rats only in myosin polypeptide 8 and CRMP-5 as members of the “Cytoskeletal” and “Axon Guidance” functional categories, respectively. Common to both gene and protein

analyses was the down-regulation of Rab3, a member of the GTPase signal transducers, and Rho B, which was detected as down-regulated using the genomic approach even if the total protein level remained unchanged. GTPases are known to regulate many cellular events through their activation status including cytoskeletal rearrangements (Etienne-Manneville and Hall, 2002). Members of this family like Rho A, Rac 1 and possibly Cdc42 are part of the downstream signaling involved in growth inhibition (Niederost et al., 2002). We also detected different members of the same protein/gene family being regulated. CRMP-1 and -2 were found differentially regulated at the protein level but at the gene level, CRMP-5 was the only member of this family found to be differentially regulated. This protein family is involved in axonal guidance and is crucial for axonal growth. Other categories involved in neuronal network remodeling, via growth response or synaptic modulation, were also identified by both approaches. The “Cell Adhesion” category incorporates the chondroitin sulfate proteoglycan 3, which could function as a growth inhibitory protein, like Nogo-A. We found it down-regulated, which would speak for a non-compensatory role of this molecule following Nogo-A neutralization. On the gene level, Cadherin 13 is also down-regulated. Related to cell adhesion is also the “Extracellular Matrix (ECM)” category, where only the genomic approach detected differential regulation. The two genes identified were tissue inhibitor of metalloproteinase 2 (TIMP-2), which was down-regulated, while tenascin XA was up-regulated. Up to now, only tenascin-R, from the tenascin family of proteins, has been implicated in growth inhibition.

Other identified functional categories are related to synaptic events with “Neurotransmission” and “Synaptic” related proteins and genes. The “Neurotransmission” functional category incorporates the up-regulation of calcium calmodulin kinase-like vesicle-associated protein and glutamate dehydrogenase 1 precursor and the down-regulation of the solute carrier family 6 member 7 (neurotransmitter transporter, L-Proline) gene. The “Synaptic” functional category comprises the up-regulation of the vesicular GABA transporter (vGAT), synaptophysin and serine/threonine-protein phosphatase 1 (PP1) proteins. Interestingly, despite of the myelin localization of Nogo-A, no major changes were observed in other myelin protein expression levels (PLP 1.16 ± 0.1, MOG 1.18 ± 0.1).

A complete list of the significantly regulated genes (**Table 4**) and regulated proteins (**Table 5**) follows.

**Table 4. Gene Expression changes induced by Nogo-A Neutralization *in vivo***

| Gene Symbol | Gene Name | Accession Number | 11C7 | |
|---|---|---|---|---|
| | | | Fold Change | P value |
| **Apoptosis** | | | | |
| Ripk1_predicted | Receptor (TNFRSF)-interacting serine-threonine kinase 1 (predicted) | 1371529_at | 1.323 | 0.0498 |
| **Axon Guidance** | | | | |
| Dpysl5 | dihydropyrimidinase-related protein (CRMP5) | 1387141_at | 0.81 | 0.0497 |
| **Cell Adhesion** | | | | |
| Cdh13 | cadherin 13 | 1369425_at | 0.765 | 0.0359 |
| Aoc3 | amine oxidase, copper containing 3 | 1372615_at | 0.342 | 0.0315 |
| Scarf1_predicted | scavenger receptor class F, member 1 (predicted) | 1382722_at | 1.286 | 0.0347 |
| **Channel** | | | | |
| Cacna1g | calcium channel, voltage-dependent, T type, alpha 1G subunit | 1370508_a_at | 0.771 | 0.0224 |
| Slc8a3 | solute carrier family 8 (sodium/calcium exchanger), member 3 | 1387404_at | 0.741 | 0.0211 |
| **Cytoskeletal** | | | | |
| Myh8 | myosin, heavy polypeptide 8, skeletal muscle, perinatal | 1371053_at | 0.678 | 0.0463 |
| **Development** | | | | |
| Fzd1 | frizzled homolog 1 (Drosophila) | 1370256_at | 0.799 | 0.00561 |
| Dopey2_predicted | dopey family member 2 (predicted) | 1392458_at | 12.08 | 0.0485 |
| **ECM** | | | | |
| Timp2 | tissue inhibitor of metalloproteinase 2 | 1367823_at | 0.682 | 0.0111 |
| Tnxa | tenascin XA | 1388145_at | 1.241 | 0.041 |
| **GTPase transduction** | | | | |
| Gnb1 | guanine nucleotide binding protein, beta 1 | 1367731_at | 0.824 | 0.0376 |
| Rhob | rhoB gene | 1369958_at | 0.804 | 0.0132 |
| Reln | reelin | 1373957_at | 0.8 | 0.0233 |
| Rras_predicted | Harvey rat sarcoma oncogene, subgroup R (predicted) | 1388729_at | 1.243 | 0.0303 |
| Rab3b | Rab3B protein | 1370061_at | 0.799 | 0.0491 |
| **Immune Response** | | | | |
| Ccl19_predicted | chemokine (C-C motif) ligand 19 (predicted) | 1391925_at | 2.276 | 0.0393 |
| **Mitosis** | | | | |
| Mphosph1_predicted | M-phase phosphoprotein 1 (predicted) | 1380775_at | 1.553 | 0.0409 |
| **Neuroprotection** | | | | |
| Adnp | activity-dependent neuroprotective protein | 1369402_at | 0.831 | 0.0297 |
| Adnp | activity-dependent neuroprotective protein | 1389088_at | 0.83 | 0.0494 |
| **Neurotransmission** | | | | |
| Slc6a7 | solute carrier family 6 (neurotransmitter transporter, L-proline), member 7 | 1398457_at | 0.738 | 0.0497 |
| **Other** | | | | |
| Cbx7 | chromobox homolog 7 | 1371672_at | 0.824 | 0.0418 |

| | | | | |
|---|---|---|---|---|
| Emcn | endomucin | 1372587_at | 0.784 | 0.0472 |
| Gcnt2 | glucosaminyl (N-acetyl) transferase 2, I-branching enzyme | 1374903_at | 1.277 | 0.0437 |
| Exosc3_predicted | exosome component 3 (predicted) | 1392665_at | 0.824 | 0.0401 |
| **Protein biosynthesis and modification** | | | | |
| Ift88_predicted | intraflagellar transport 88 homolog (Chlamydomonas) (predicted) | 1375285_at | 0.587 | 0.0189 |
| Rpn2 | ribophorin 2 | 1385373_at | 0.56 | 0.0155 |
| Hsf2 | heat shock factor 2 | 1391423_at | 0.705 | 0.0335 |
| Mtrf1l_predicted | mitochondrial translational release factor 1-like (predicted) | 1392654_at | 0.832 | 0.0352 |
| RGD1311612_predicted | Similar to hypothetical protein FLJ12118 (LOC361184), mRNA | 1394500_at | 0.589 | 0.0443 |
| **Proteolysis** | | | | |
| Abhd7_predicted | abhydrolase domain containing 7 (predicted) | 1384869_at | 0.822 | 0.0153 |
| Abhd7_predicted | abhydrolase domain containing 7 (predicted) | 1394977_at | 0.609 | 0.0377 |
| Pcsk5 | proprotein convertase subtilisin/kexin type 5 | 1392773_at | 0.771 | 0.042 |
| Dpp10 | dipeptidylpeptidase 10 | 1393299_at | 0.778 | 0.0475 |
| Fts | fused toes | 1373837_at | 0.827 | 0.0469 |
| **Receptor** | | | | |
| Igsf1 | immunoglobulin superfamily, member 1 | 1370410_at | 0.77 | 0.0387 |
| Mamdc2 | MAM domain containing 2 | 1375983_at | 1.461 | 0.0183 |
| **Sex Diff** | | | | |
| Pabpn1 | poly(A) binding protein, nuclear 1 | 1382922_at | 1.779 | 0.0365 |
| Dzip1 | DAZ interacting protein 1 | 1391472_at | 0.82 | 0.00636 |
| **Signaling** | | | | |
| Camkk2 | Calcium/Calmodulin-dependent protein kinase kinase beta (CaM-kinase kinase beta) | 1368753_at | 1.371 | 0.00819 |
| Prkar2b | protein kinase, cAMP dependent regulatory, type II beta | 1371133_a_at | 0.774 | 0.024 |
| Map3k3_predicted | Mitogen activated protein kinase kinase kinase 3 (predicted) | 1382046_at | 1.206 | 0.033 |
| **Splicing** | | | | |
| RGD1308297 | Similar to CG10084-PA | 1393678_at | 0.809 | 0.0373 |
| **Transcription** | | | | |
| Mllt6_predicted | myeloid/lymphoid or mixed lineage-leukemia translocation to 6 homolog (Drosophila) | 1378971_at | 1.321 | 0.0445 |
| Rgpr | regucalcin gene promotor region related protein | 1387209_at | 1.344 | 0.0414 |
| Klf4 | Kruppel-like factor 4 (gut) | 1387260_at | 0.832 | 0.0324 |
| Phf12 | PHD finger protein 12 | 1394014_at | 0.83 | 0.043 |
| Gtf2f2 | General transcription factor IIF, polypeptide 2 | 1396388_at | 1.21 | 0.00823 |
| **Transport** | | | | |
| Xpo5_predicted | exportin 5 (predicted) | 1388956_at | 0.783 | 0.0209 |
| Slc31a2 | solute carrier family 31, member 2 | 1394954_at | 1.42 | 0.00889 |

**Table 5. Protein Expression changes induced by Nogo-A Neutralization *in vivo***

| Protein Symbol | Protein Name | 11C7 | |
|---|---|---|---|
| | | Fold Change | Protein Identification Probability |
| **Adaptor/Clathrin** | | | |
| Q66HM2_RAT | Adaptor protein complex AP-2, alpha 2 subunit | 3.05 ± 0.48 | 0.95 |
| **Cell Adhesion** | | | |
| CSPG3_RAT | Neurocan core protein precursor (Chondroitin sulfate proteoglycan 3) | 0.79 ± 0.01 | 0.98 |
| **Cell Growth** | | | |
| CD81_RAT | CD81 antigen | 0.78 ± 0.00 | 0.99 |
| **Cell Stress** | | | |
| HS105_RAT | Heat shock protein 105 kDa | 0.83 ± 0.00 | 1 |
| **Channel** | | | |
| VDAC1_RAT | Voltage-dependent anion-selective channel protein 1 | 1.45 ± 0.00 | 1 |
| **Cytoskeletal** | | | |
| Q6P9T8_RAT | Tubulin beta-2C chain | 1.16 ± 0.10 | 1 |
| ARP2_RAT | Actin-like protein 2 | 1.37 ± 0.00 | 0.93 |
| AINX_RAT | Alpha-internexin | 2.25 ± 1.07 | 1 |
| O70511_RAT | Ankyrin 3 | 0.81 | 0.81 |
| Q4V7C7_RAT | ARP3 actin-related protein 3 homolog | 1.14 ± 0.07 | 1 |
| COF1_RAT | Cofilin-1 | 1.28 ± 0.08 | 1 |
| DPYL1_RAT | Dihydropyrimidinase-related protein 1 (CRMP-1) | 1.38 | 0.88 |
| DPYL2_RAT | Dihydropyrimidinase-related protein 2 (CRMP-2) | 1.36 ± 0.09 | 1 |
| MAP1A_RAT | Microtubule-associated protein 1A | 1.14 ± 0.07 | 1 |
| NFL_RAT | Neurofilament light polypeptide | 1.21 ± 0.00 | 0.93 |
| SPTA2_RAT | Spectrin alpha chain, brain | 0.90 ± 0.00 | 1 |
| SPTN2_RAT | Spectrin beta chain, brain 2 | 1.49 ± 0.07 | 0.99 |
| TCPE_RAT | T-complex protein 1 subunit epsilon | 1.32 ± 0.00 | 0.99 |
| TBA6_RAT, TBA1_RAT | Tubulin alpha-1C chain / Tubulin alpha-1A chain | 1.22 ± 0.03 | 1 |
| Q9JMB3_RAT | Type II brain 4.1 | 0.76 ± 0.00 | 0.91 |
| **GTPase transduction** | | | |
| CDC42_RAT | Cell division control protein 42 homolog [Precursor] | 1.19 ± 0.00 | 0.99 |
| RAB3D_RAT, RAB3C_RAT | GTP-binding protein Rab-3D / Ras-related protein Rab-3C | 0.68 ± 0.00 | 0.96 |
| GNAO2_RAT, GNAO1_RAT | Guanine nucleotide-binding protein G(o) subunit alpha 1 / Guanine nucleotide-binding protein G(o) subunit alpha 2 | 0.66 ± 0.00 | 0.9 |
| RAB3A_RAT | Ras-related protein Rab-3A | 0.66 ± 0.00 | 0.98 |
| RHOB_RAT | Rho-related GTP-binding protein RhoB [Precursor] | 1.05 ± 0.02 | 1 |
| **Metabolism** | | | |
| AATC_RAT | Aspartate aminotransferase, cytoplasmic | 1.33 ± 0.01 | 0.94 |
| KCRS_RAT, | Creatine kinase, sarcomeric mitochondrial [Precursor] / | 1.58 ± 0.00 | 0.98 |

| | | | |
|---|---|---|---|
| KCRU_RAT | Creatine kinase, ubiquitous mitochondrial [Precursor] | | |
| PI52A_RAT | Phosphatidylinositol-4-phosphate 5-kinase type-2 alpha | 1.18 ± 0.00 | 0.94 |
| ODPA_RAT | Pyruvate dehydrogenase E1 component alpha subunit, somatic form, mitochondrial [Precursor] | 1.34 ± 0.03 | 0.99 |
| ODPB_RAT | Pyruvate dehydrogenase E1 component subunit beta, mitochondrial [Precursor] | 2.66 | 0.86 |
| AT2A2_RAT | Sarcoplasmic/endoplasmic reticulum calcium ATPase 2 | 1.22 | 0.86 |
| TALDO_RAT | Transaldolase | 4.26 ± 0.08 | 0.99 |
| UQCR2_RAT | Ubiquinol-cytochrome-c reductase complex core protein 2, mitochondrial [Precursor] | 1.19 ± 0.01 | 1 |
| **Myelin** | | | |
| MYPR_RAT | Myelin proteolipid protein | 1.16 ± 0.10 | 1 |
| MOG_RAT | Myelin-oligodendrocyte glycoprotein [Precursor] | 1.18 ± 0.10 | 1 |
| **Neuroprotection** | | | |
| ENOG_RAT | Gamma-enolase | 1.08 ± 0.06 | 1 |
| HPCL1_RAT, HPCA_RAT | Hippocalcin-like protein 1, Neuron-specific calcium-binding protein hippocalcin | 1.21 ± 0.03 | 0.99 |
| **Neurotransmission** | | | |
| CAMKV_RAT | CaM kinase-like vesicle-associated protein | 1.28 ± 0.05 | 0.99 |
| GLNA_RAT | Glutamine synthetase | 1.19 ± 0.04 | 1 |
| DHE3_RAT | Glutamate dehydrogenase 1, mitochondrial [Precursor] | 1.69 ± 0.33 | 1 |
| **Other** | | | |
| HCD2_RAT | 3-hydroxyacyl-CoA dehydrogenase type-2 | 3.03 | 0.95 |
| CAH2_RAT | Carbonic anhydrase 2 | 1.27 ± 0.00 | 0.94 |
| DNM1L_RAT | Dynamin-1-like protein | 1.30 ± 0.00 | 1 |
| GSTM1_RAT | Glutathione S-transferase Mu 1 | 0.82 ± 0.00 | 0.9 |
| GSTM4_RAT | Glutathione S-transferase Yb-3 | 1.36 ± 0.10 | 0.99 |
| GPDM_RAT | Glycerol-3-phosphate dehydrogenase, mitochondrial [Precursor] | 2.57 ± 0.42 | 1 |
| Q3KR86_RAT | Inner membrane protein, mitochondrial | 1.34 ± 0.00 | 1 |
| MDHC_RAT | Malate dehydrogenase, cytoplasmic | 1.40 ± 0.12 | 1 |
| MDHM_RAT | Malate dehydrogenase, mitochondrial [Precursor] | 1.43 ± 0.20 | 1 |
| NDUAA_RAT | NADH dehydrogenase [ubiquinone] 1 alpha subcomplex subunit 10, mitochondrial [Precursor] | 1.34 ± 0.00 | 0.99 |
| Q5BJZ3_RAT | Nicotinamide nucleotide transhydrogenase | 1.30 ± 0.00 | 0.91 |
| PARK7_RAT | Protein DJ-1 | 1.20 ± 0.00 | 0.91 |
| RINI_RAT | Ribonuclease inhibitor | 0.83 ± 0.00 | 1 |
| ALBU_RAT | Serum albumin [Precursor] | 0.58 ± 0.00 | 1 |
| Q5PPJ9_RAT | SH3-domain GRB2-like endophilin B2 | 3.11 | 0.8 |
| DHSA_RAT | Succinate dehydrogenase [ubiquinone] flavoprotein subunit, mitochondrial [Precursor] | 0.83 ± 0.06 | 0.98 |
| UQCR1_RAT | Ubiquinol-cytochrome-c reductase complex core protein 1, mitochondrial [Precursor] | 1.20 ± 0.00 | 1 |
| CB032_RAT | Uncharacterized protein C2orf32 homolog | 1.25 | 0.88 |
| **Protein biosynthesis and modification** | | | |
| RS16_RAT | 40S ribosomal protein S16 | 1.42 ± 0.00 | 0.99 |
| AMPL_RAT | Cytosol aminopeptidase | 2.97 | 0.85 |
| PPIA_RAT | Peptidyl-prolyl cis-trans isomerase A | 1.02 ± 0.02 | 1 |

| | | | |
|---|---|---|---|
| **Proteolysis** | | | |
| UE1D1_RAT | Ubiquitin-activating enzyme E1 domain-containing protein 1 | 0.83 ± 0.00 | 0.95 |
| **Signaling** | | | |
| GBB1_RAT | Guanine nucleotide-binding protein G(I)/G(S)/G(T) subunit beta 1 | 1.26 ± 0.25 | 1 |
| KPCG_RAT | Protein kinase C gamma type | 1.31 ± 0.24 | 1 |
| **Synaptic** | | | |
| VIAAT_RAT | Vesicular GABA transporter | 2.06 ± 0.00* | 0.92 |
| EAA2_RAT | Excitatory amino acid transporter 2 | 0.94 ± 0.02 | 1 |
| SSDH_RAT | Succinate semialdehyde dehydrogenase | 0.90 ± 0.04 | 1 |
| SYPH_RAT | Synaptophysin | 1.25 ± 0.15 | 1 |
| VAPB_RAT | Vesicle-associated membrane protein-associated protein B (VAMO-B) | 0.83 ± 0.00 | 1 |
| O35095_RAT | NORBIN | 0.83 ± 0.00 | 0.98 |
| PP1B_RAT, PP1G_RAT, PP1A_RAT | Serine/threonine-protein phosphatase PP1 | 2.21 ± 0.11 | 0.99 |
| **Transcription** | | | |
| SIRT2_RAT | NAD-dependent deacetylase sirtuin-2 | 1.29 ± 0.03 | 1 |
| MK03_RAT, MK01_RAT | Mitogen-activated protein kinase 3 (ERK-1), Mitogen-activated protein kinase 1 (ERK-2) | 0.81 ± 0.00 | 0.98 |
| **Transport** | | | |
| DLDH_RAT | Dihydrolipoyl dehydrogenase, mitochondrial [Precursor] | 1.51 ± 0.41 | 1 |
| NDUS6_RAT | NADH dehydrogenase [ubiquinone] iron-sulfur protein 6, mitochondrial [Precursor] | 1.25 ± 0.00 | 0.91 |
| MPCP_RAT | Phosphate carrier protein, mitochondrial [Precursor] | 1.24 ± 0.00 | 0.93 |
| AT2B1_RAT | Plasma membrane calcium-transporting ATPase 1 | 1.51 ± 0.07 | 1 |
| TRFE_RAT | Serotransferrin [Precursor] | 0.69 ± 0.03 | 1 |
| S38A3_RAT | System N amino acid transporter 1 | 0.65 | 0.97 |
| UCRH_RAT | Ubiquinol-cytochrome c reductase complex 11 kDa protein, mitochondrial [Precursor] | 0.83 ± 0.00 | 1 |
| NSF_RAT | Vesicle-fusing ATPase | 1.23 ± 0.00 | 1 |
| **Vesicles** | | | |
| VPP1_RAT | Vacuolar proton translocating ATPase 116 kDa subunit a isoform 1 | 0.73 ± 0.04 | 1 |

* Value obtained from database from (2005). In the current list (2007), based on an updated database, the software was not able to calculate the expression ratio. We decided to include this value because immunohistochemical data corroborates its up-regulation.

## Immunofluorescence and Immunoblotting

Based on the indications from the genomic and proteomic experiments of a possible growth and synaptic regulation in the adult rat hippocampus after acute Nogo-A neutralization, studies were done to confirm protein changes by immunoblotting and to analyze the tissue localization of the most relevant changes by immunofluorescence.

We first analyzed if it was possible to detect the internalization of anti-Nogo-A antibodies in the CNS tissue as demonstrated previously (Weinmann et al., 2006). Anti-

Nogo-A antibodies were detected using an antibody against IgG. In the animals that received the anti-Nogo-A treatment, a signal was detected in the white matter, where the myelin sheath (**arrows in Fig. 6C**) and oligodendrocytes were visible (**arrowheads in Fig. 6C**). Cerebellar purkinje cells in particular (**Fig. 6D**) as well as the hilar region of the dentate gyrus and CA1 pyramidal cells of the hippocampus (**Fig. 6E, F**) were positive for anti-Nogo-A antibodies around the soma. These results not only indicate that the antibodies against Nogo-A reached the hippocampus, but that they bound to Nogo-A and were internalized, therefore disabling Nogo-A signaling.

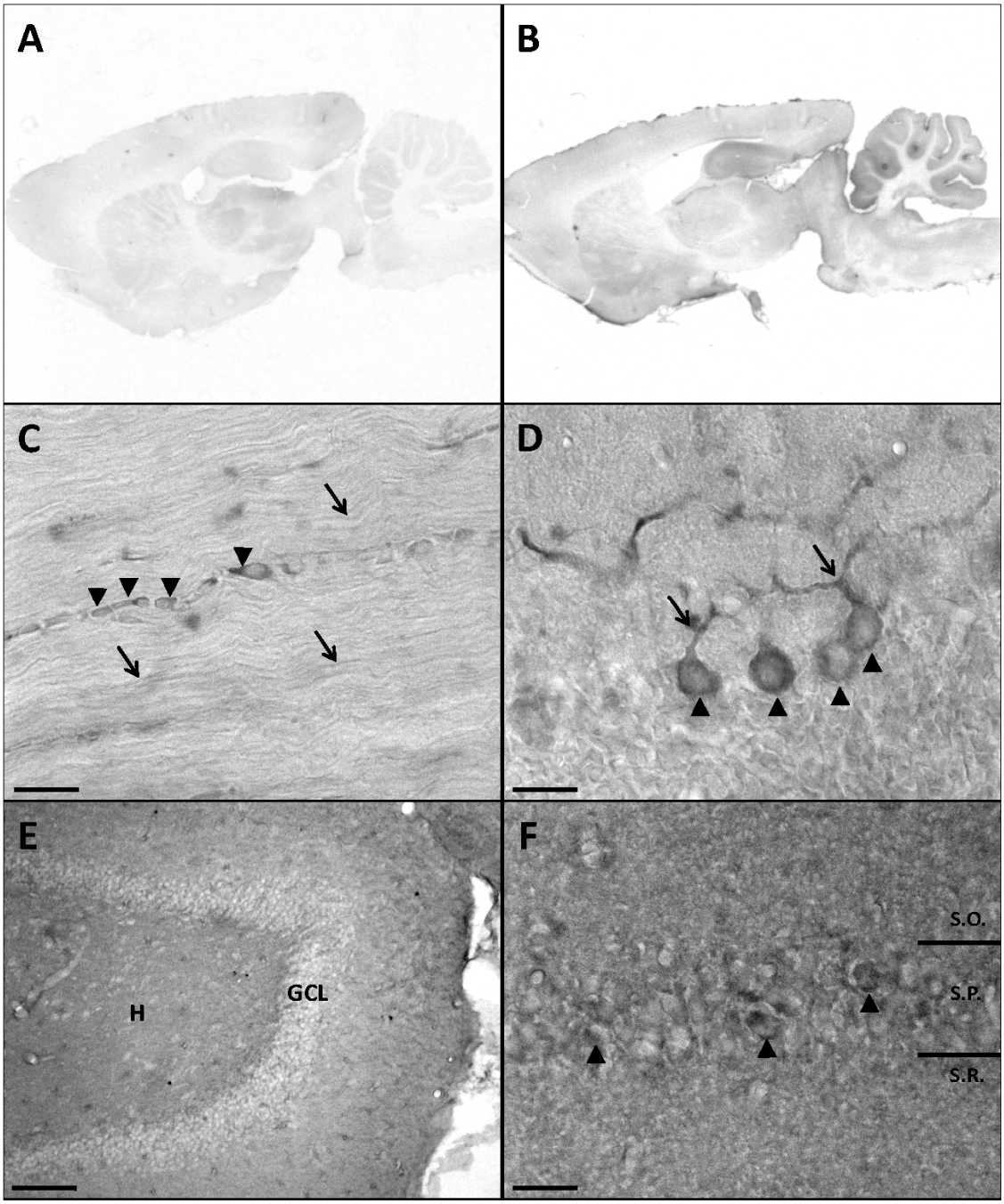


**Fig 6. Anti-Nogo-A antibody distribution in CNS detected in section processed for immunoperoxidase staining.** Antibodies anti-IgG were used to detect the presence in the tissue of anti-Nogo-A antibodies or control antibodies after intrathecal delivery via osmotic minipumps. A: Brain section from a control IgG treated animal. B: Brain section from an anti-Nogo-A treated animal. C: White matter close-up from an anti-Nogo-A antibody treated animal. Note the labelling of myelin (arrows) and the pearl neckless like string of oligodendrocytes (arrowheads). D: Cerebelum close-up depicting Purkinje cells (arrowheads) and their dendrites (arrows). E: Overview of the dentate gyrus showing the binding of anti-Nogo-A antibodies to Nogo-A present in the neuropil of the hilar and molecular layers. F: Close-up from the CA1 region of the hippocampus where it is possible to see positive labelling around cell from the *stratum pyramidale.* Scale bar C-D = 20 μm. Scale bar E = 200 μm. Scale bar F = 50 μm

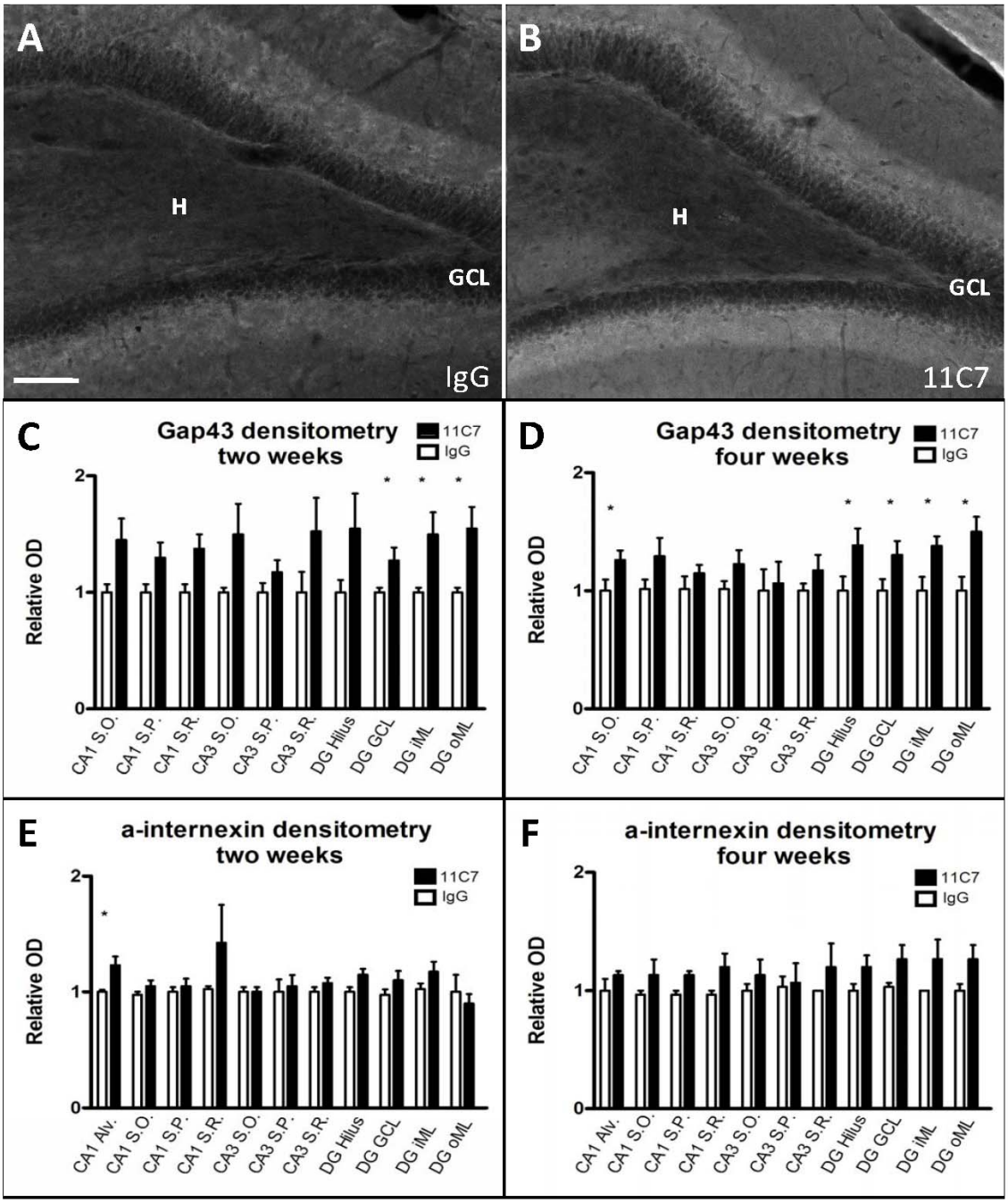


**Fig 7. Growth response analyzed two- or four-weeks after start of antibody delivery.** Expression levels of two markers related to axonal growth were quantified. A, B: Gap43 levels at the two week time point after Nogo-A neutralization (B) compared to IgG control (A) in the dentate gyrus region. Note the increased imunnolabelling of the inner and outer molecular layer as well as of the hilar region. Scale bar = 100 μm.. C, D: Graphical representation of the relative optic densities of Gap43 in several regions of the hippocampus at the two-week time-point (C) and at the four-week time-point (D). Note the higher expression (≈ 1.5 fold) of Gap43 after Nogo-A neutralization at the two-week time-point when compared to the expression (≈ 1.2 fold) at the four-week time-point, indicating a clear initial growth response which is reduced at later time-points. N = 4 for 11C7 and control IgG treatment groups at the two-week time-point and N = 7 at the four-week time-point. E, F: Graphical representation of the relative optic densities of alpha-internexin in several regions of the hippocampus at the two-week time-point (E) and at the four-week time-point (F). Only the alveus region of CA1 at the two-week time-point shows significant increased expression of alpha-internexin. N = 4 for 11C7 and control IgG treatment groups at the two-week time-point and N = 3 at the four-week time-point 0.1 ≥ P-value ≥ 0.05 = * analyzed using the Mann-Whitney test. S.O – *Stratum Oriens*; S.P – *Stratum Pyramidale*; S.R – *Stratum Radiatum*; DG – Dentate Gyrus; GCL – Granular Cell Layer; iML – Inner Molecular Layer; oML – Outer Molecular Layer.

We then analyzed the expression and localization of several growth markers at two different time points, two and four weeks of acute Nogo-A neutralization. At the two-week time-point the growth marker Gap43 (**Fig. 7C**) was up-regulated approximately 1.5 fold throughout the entire hippocampus with statistical significance in the dentate gyrus. On the other hand, α-internexin was only significantly up-regulated in the alveus of CA1 region (**Fig. 7E**). This growth response seems to be only transient since at the four-week time-point the levels of Gap43 were reduced to about 1.2 fold but still statistical significant for the dentate gyrus (**Fig. 7D**). α-internexin appears to be up-regulated at this later time-point, particularly in the dentate gyrus region, although without statistical significance (**Fig. 7F**). These results indicate that there is a transient growth response after acute Nogo-A neutralization in the intact adult rat hippocampus. Immunoblots for these markers confirmed the densitometric analysis at both time points (**Table 6**). No difference was detected in cofilin levels of expression, which was one of the cytoskeletal protein candidates from the ICAT with differential regulation.

We then addressed the changes at the synaptic level, concentrating in the excitatory glutamatergic and on the inhibitory GABAergic systems. The vesicular glutamate transporter 1 (vGlut1), involved in excitatory neurotransmission, showed a consistent increased expression after two weeks of Nogo-A neutralization (**Fig. 8C**) which became statistically significant at the four-week time-point (**Fig. 8D**). The CA1 region was the region of the hippocampus with the highest up-regulation of vGlut1. It was clear the increased vGlut1 puncta in CA1 *stratum pyramidale* after Nogo-A neutralization (**arrows in Fig. 6A, B**). An interesting observation, as well, was the close apposition between vGlut1 puncta and parvalbumin positive structures, which was increased at the four-week time-point (**Fig. 8E, F**). The increased puncta juxtaposed to parvalbumin positive structures could be indicative of an increased activation of parvalbumin positive cells, which in turn could lead to an increase in parvalbumin expression.

Interestingly, the GABAergic system was activated at the two-week time point and remained activated up to the four-week time point. As with vGlut1, parvalbumin immunoreactivity increased to statistical significant values from the two-week (**Fig. 9C**) to the four-week time-point (**Fig. 9D**). The CA1 region was again the hippocampal region with highest changes in parvalbumin expression but the CA3 region also had a statistically significantly higher expression of parvalbumin (**Fig. 9D**). Regional immunofluorescence densitometric analysis of the hippocampus revealed approximately a twofold significant increase of parvalbumin in all CA1 sub-regions and in the *stratum oriens* of CA3 region at the four-week time point (**Fig 9D**).

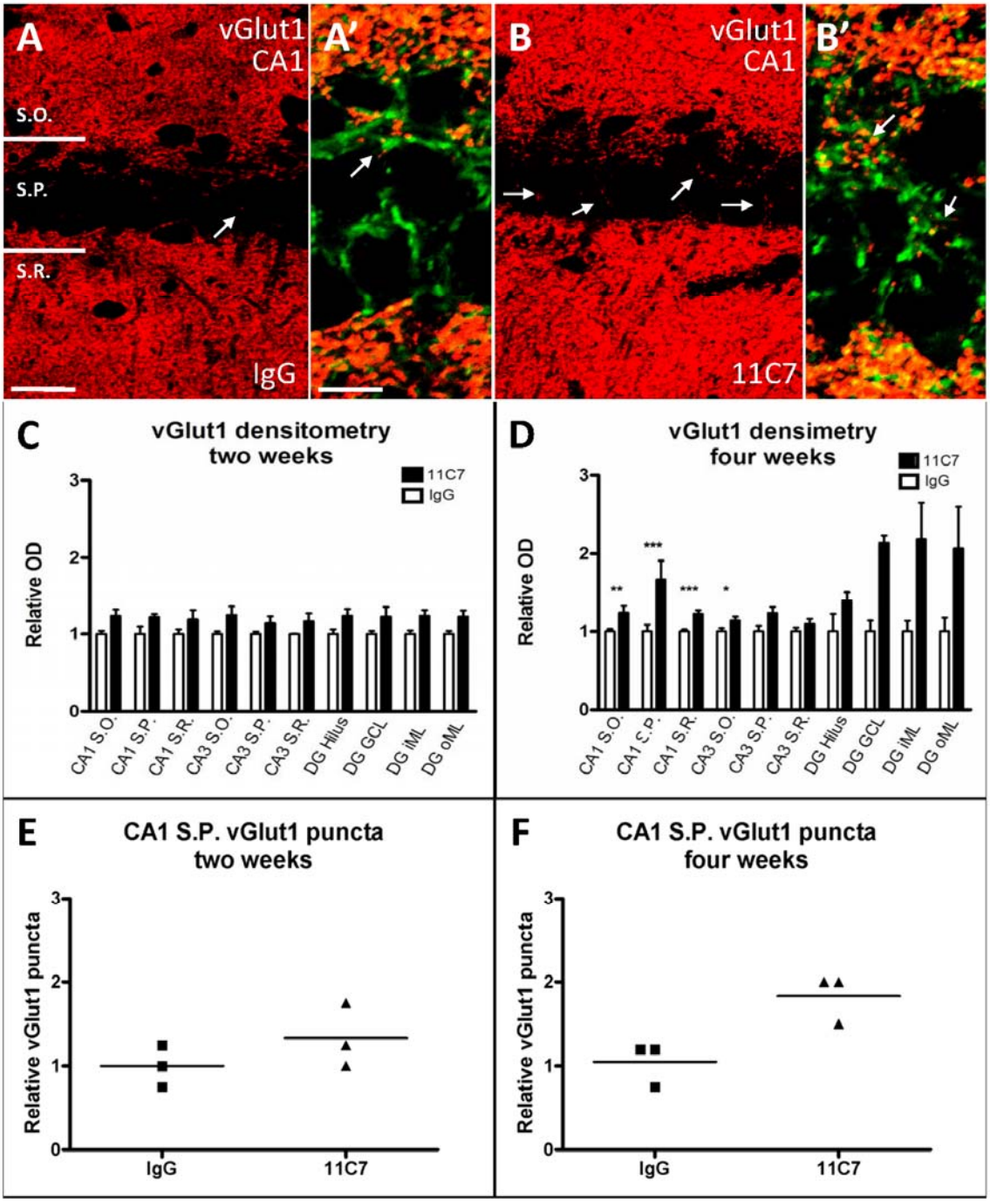


**Fig 8. Excitatory pre-synaptic marker vGlut1 analysis.** A: vGlut1 immunoreactivity in CA1 region of a representative control IgG antibody treated animal. A' indicates vGlut1 puncta (red) in puxtaposition to parvalbumin positive structures (green). B: vGlut1 immunoreactivity in CA1 region of a representative anti-Nogo-A antibody treated animal. B' indicates vGlut1 puncta (red) in puxtaposition to parvalbumin positive structures (green).Note the increased puncta of vGlut1 in CA1 *stratum pyramidale* and the increased number of vGlut1puncta juxtaposed to parvalbumin positive structures after Nogo-A neutralization. Scale bar A,B = 50 μm. Scale bar A', B' = 20 μm. C: Graphical representation of signal optic density from different regions of the hippocampus at the two-week time-point. D: Graphical representation of signal optic density from different regions of the hippocampus at the four-week time-point. N = 4 for 11C7 and control IgG treatment groups at the two-week time-point and N = 9 at the four-week time-point. Error bars are standard error of means and the p-values are depicted over the corresponding bars. White bars correspond to control IgG treatment and black bars correspond to 11C7 treatment. E, F: Quantification of the relative number of puncta in the *stratum pyramidale* of the CA1 region of the hippocampus for the two-week time-point (E) and four-week time-point. 0.1 ≥ P-value ≥ 0.05 = *; 0.05 > P-value ≥ 0.01 = **; P-value > 0.01 = *** analyzed using the Mann-Whitney test. S.O – *Stratum Oriens*; S.P – *Stratum Pyramidale*; S.R – *Stratum Radiatum*; DG – Dentate Gyrus; GCL – Granular Cell Layer; iML – Inner Molecular Layer; oML – Outer Molecular Layer.

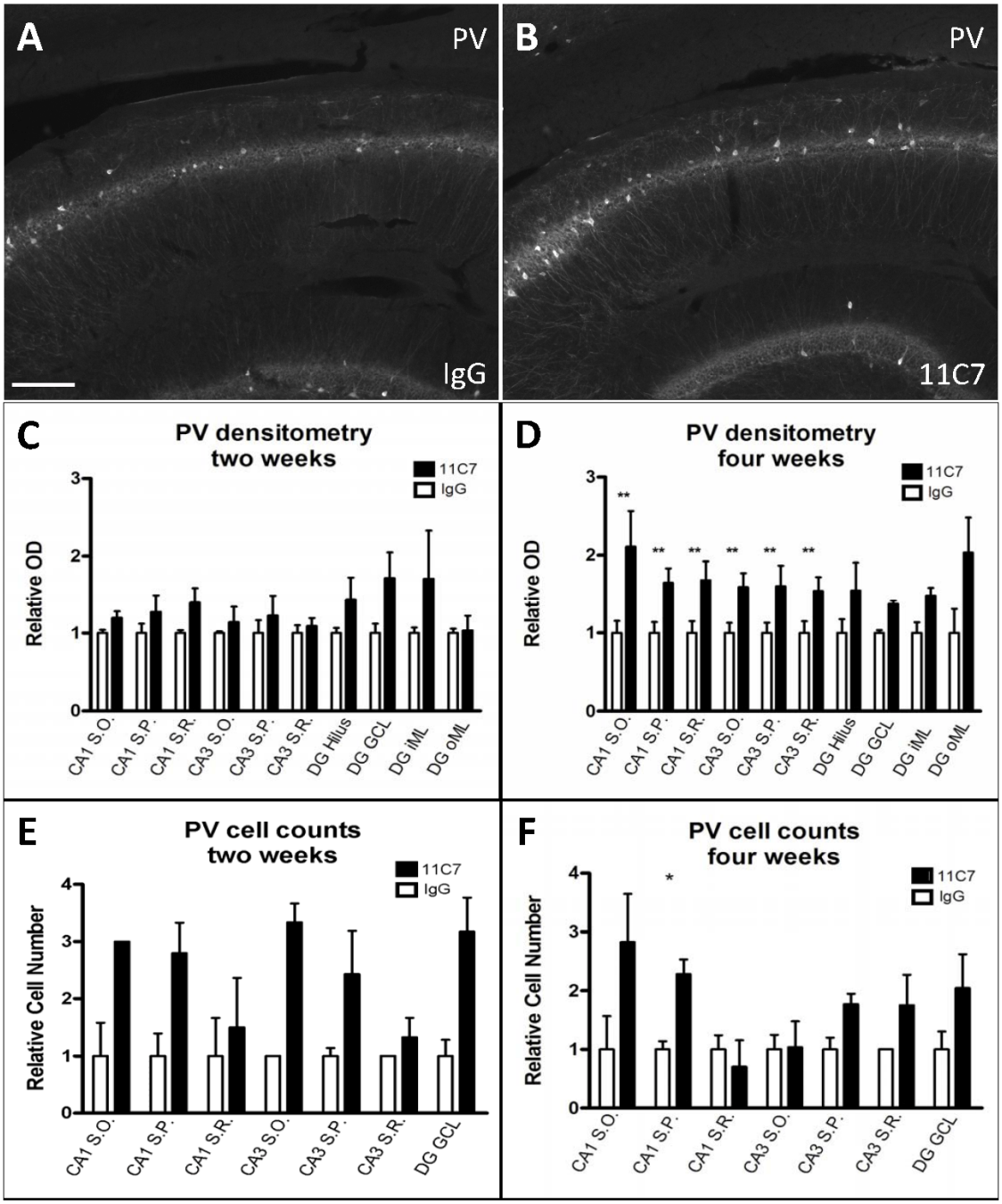
A
PV
IgG
B
PV
11C7
C
PV densitometry
two weeks
11C7
IgG
Relative OD
CA1 S.O.
CA1 S.P.
CA1 S.R.
CA3 S.O.
CA3 S.P.
CA3 S.R.
DG Hilus
DG GCL
DG iML
DG oML
D
PV densitometry
four weeks
11C7
IgG
Relative OD
**
E
PV cell counts
two weeks
11C7
IgG
Relative Cell Number
F
PV cell counts
four weeks
11C7
IgG
Relative Cell Number
*

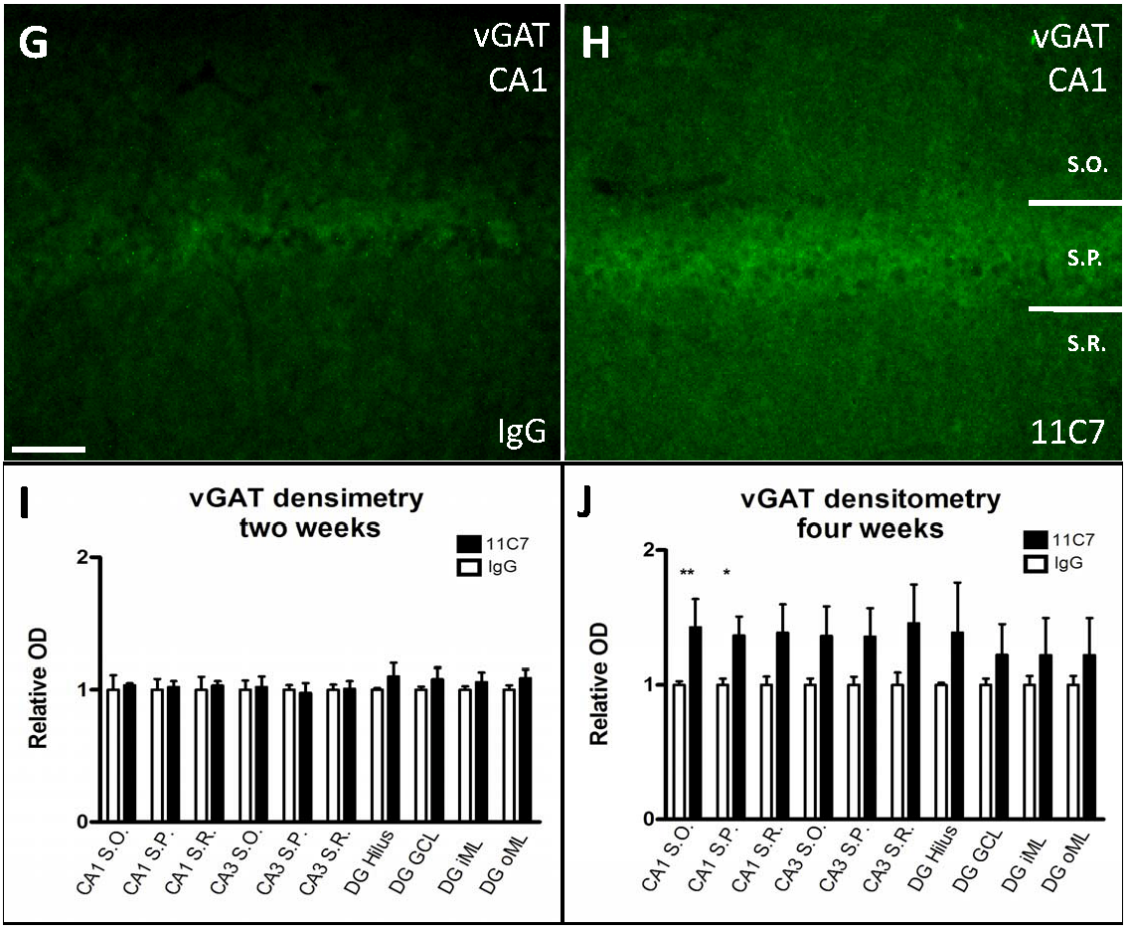


**Fig 9. Inhibitory pre-synaptic marker analysis of PV and vGAT.** A: Parvalbumin labelling in CA1 region of the hippocampus of a representative control animal treated with IgG. B: Parvalbumin labelling in CA1 region of the hippocampus of a representative anti-Nogo-A antibody (11C7) treated animal. Note the increased intensity of labelling after Nogo-A neutralization and the higher number of parvalbumin positive interneurons. C: Graphical representation of signal optic density from different regions of the hippocampus at the two-week time-point. D: Graphical representation of signal optic density from different regions of the hippocampus at the four-week time-point. N = 4 for 11C7 and control IgG treatment groups at the two-week time-point and N = 3 at the four-week time-point. Error bars are standard error of means and the p-values are depicted over the corresponding bars. White bars correspond to control IgG treatment and black bars correspond to 11C7 treatment. E: Graphical representation of the cell counts of the hippocampus. Error bars are standard error of means and the p-values are depicted over the corresponding bars. F: Graphical representation of the relative optic densities of parvalbumin. G: vGATlabelling in CA1 region of the hippocampus of a representative control animal treated with IgG. H: vGAT labelling in CA1 region of the hippocampus of a representative anti-Nogo-A antibody (11C7) treated animal. Note the increased intensity of labelling after Nogo-A neutralization. I: Graphical representation of the relative densities of vGAT in several regions of the hippocampus at the two-week time-point. No diferential expression was detected between the anti-Nogo-A antibody and IgG control treated groups. N = 4 for 11C7 and control IgG treatment groups at the two-week time-point and N = 5 at the four-week time-point. J: Graphical representation of the relative densities of vGAT in several regions of the hippocampus at the four-week time-point. Note the increased expression throughout the entire hippocampus, which reached statistical significance in the CA1 region. N = for 11C7 and control IgG treatment groups. Error bars represent the standard error of means (SEM). 0.1 ≥ P-value ≥ 0.05 = *; 0.05 > P-value ≥ 0.01 = **, analysed using the Mann-Whitney test. White bars refer to IgG treatment and black bars to 11C7 treatment. S.O – *Stratum Oriens*; S.P – *Stratum Pyramidale*; S.R – *Stratum Radiatum*; DG – Dentate Gyrus;. GCL – Granular Cell Layer; iML – Inner Molecular Layer; oML – Outer Molecular Layer. Scale bar A-B = 200μm. Scale bar G-H = 50 μm.

Cell counts also revealed an increased number of cells positive for parvalbumin at both time-points (**Fig. 9E, F**). These cells are consistent with parvalbumin positive basket cells that are the main inhibitory input into this region of the hippocampus. The increase in parvalbumin expression could be indicative of an increased activation of these cells and could be a response to the increased expression of vGlut1 at the four-week time-point. A significant increase in vGAT, another marker of the inhibitory circuitry, was detected in the *stratum pyramidale* of the CA1 region of the hippocampus, although all regions show an up-regulation without statistical significance (**Fig. 9J**) at the four-week time-point. This marker did not show an early response to Nogo-A neutralization (**Fig. 9I**), since regulation of its expression was only detectable at the four-week time-point (**Fig. 9J**). This observation could be suggestive of a compensatory response to the increased excitatory input or a consequence of an increased activation of parvalbumin positive cells. These results were consistent with our ICAT results showing an up-regulation of vGAT in the hippocampus after two weeks (**Table 5**) and with the immunoblotting data (**Table 6**).

The increased expression of parvalbumin and other molecules involved in the inhibitory circuitry of the hippocampus throughout the two time-points analyzed indicates that parallel to the growth response there is an increased activation of the GABAergic system may be present.

In order to understand better the inhibitory cell communication circuitry after Nogo-A neutralization, several $GABA_A$ receptor subunits were analyzed at the four-week time point. In order to assess proper $GABA_A$ receptor subunit localization, a sub-cellular analysis was performed. Again, the results show the differential regulation of these subunits. Proper co-localization of alpha-1 subunit with gephyrin, a post-synaptic scaffold protein of inhibitory synapses, was observed (**Fig. 10A-C**). In addition, the proper localization of the alpha-2 subunit in the axon initial segment of hippocampal CA3 pyramidal cells, described in the literature, proves the specificity of our detection system (**arrow in Fig. 10D**). Regional immunofluorescence densitometric analysis of the hippocampus revealed that the different components of $GABA_A$ receptors underwent differential regulation after Nogo-A neutralization. There was a clear loss of alpha-2 labeling of the axon initial segment of hippocampal CA3 pyramidal cells after Nogo-A neutralization (**arrows in Fig. 10E, F**). There is also a clear increase of diffuse labeling of the alpha-5 subunit in the CA3 *stratum pyramidale* (**Fig. 10G, H**). Alpha-1 (**Fig. 10M**) and alpha-5 (**Fig. 10L**) subunits were both up-regulated throughout the entire hippocampus, although, only alpha-1 had a statistically significant effect in CA1 *stratum pyramidale*. Interneurons of the CA1 hippocampal region, which express the alpha-1 subunit, have a clear increase in labeling in the cell soma (**Fig. 10I, J**). A

consistent general down-regulation of the alpha-2 subunit (**Fig. 10K**) was observed throughout the entire hippocampus, but without statistical significance, after anti-Nogo-A antibody treatment when compared to IgG control treatment.

A possible explanation for the observed changes refers to the removal of the growth inhibitory signal of Nogo-A, allowing for a growth response, as observed by the increased expression of growth marker Gap43. This growth response could lead to the increased excitation observed by the increased expression of vGlut1, which in turn would lead to the increased activation of parvalbumin positive cells, inducing its up-regulation. These over-activated parvalbumin positive cells could increase their expression of vGAT in order to compensate the increased excitation of the network. Other inhibitory cells could also up-regulate vGAT in order to achieve the inhibitory compensation and return stability to the network. The post-synaptic changes observed in the $GABA_A$ subunit composition could be a response to the increased GABA transmission. On the other hand, Nogo-A is expressed in interneuronal subpopulations as well as in granule and pyramidal cell of the hippocampus. Therefore, a more direct role of Nogo-A in the expression levels of vGlut1, parvalbumin and the GABAergic system cannot be excluded.

**Table 6. Immunoblot Quantification**

| Name / Source | Fold change 11C7 versus IgG | |
|---|---|---|
| | Two weeks | Four weeks |
| **PV / Rabbit** | | 1.08 ± 0.03 |
| **vGAT / Rabbit** | 1.42 ± 0.50 | 0.92 ± 0.04 |
| **vGlut1 / Rabbit** | 0.86 ± 0.07 | 0.83 ± 0.17 |
| **GAP-43 / Rabbit** | 1.04 ± 0.92 | 1.28 ± 0.18 |
| **Cofilin / Rabbit** | 0.96 ± 0.04 | 0.98 ± 0.23 |
| **α-internexin / Mouse** | 1.15 ± 0.21 | 1.11 ± 0.09 |
| **Synaptophysin / Rabbit** | 1.18 ± 0.27 | 1.03 ± 0.14 |

The immonublot data of the two-week time-point is consistent with the ICAT results but the high variability observed does not allow solid conclusions to be taken. Differences were observed between the immunoblots and the immunolabellings. These could be explained by the fact that the differences observed using the immulabellings are small and very localized, while the immunoblots were made from complete hippocampi, hence diluting any localized differences.

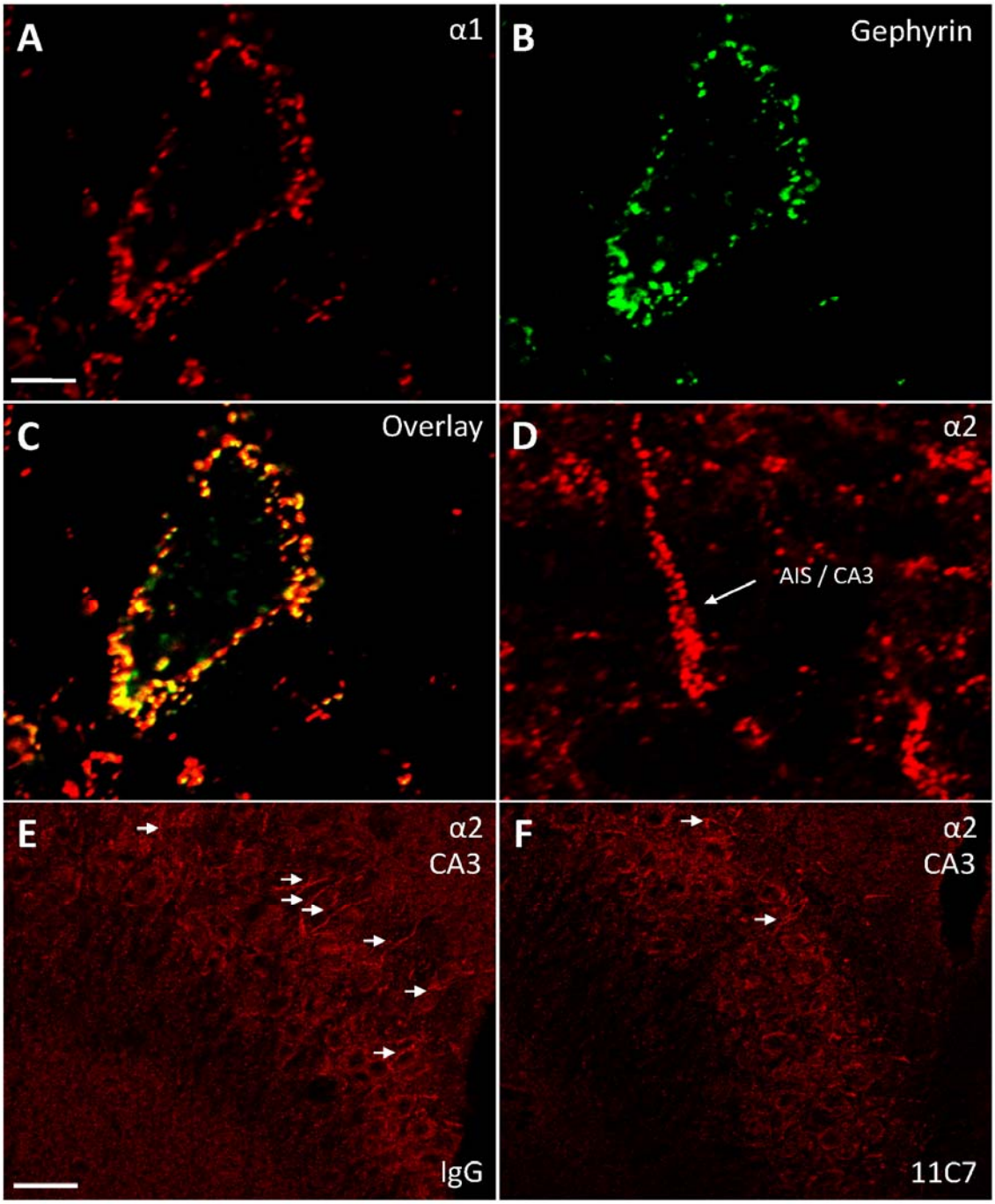
A
α1
B
Gephyrin
C
Overlay
D
α2
AIS / CA3
E
α2
CA3
IgG
F
α2
CA3
11C7

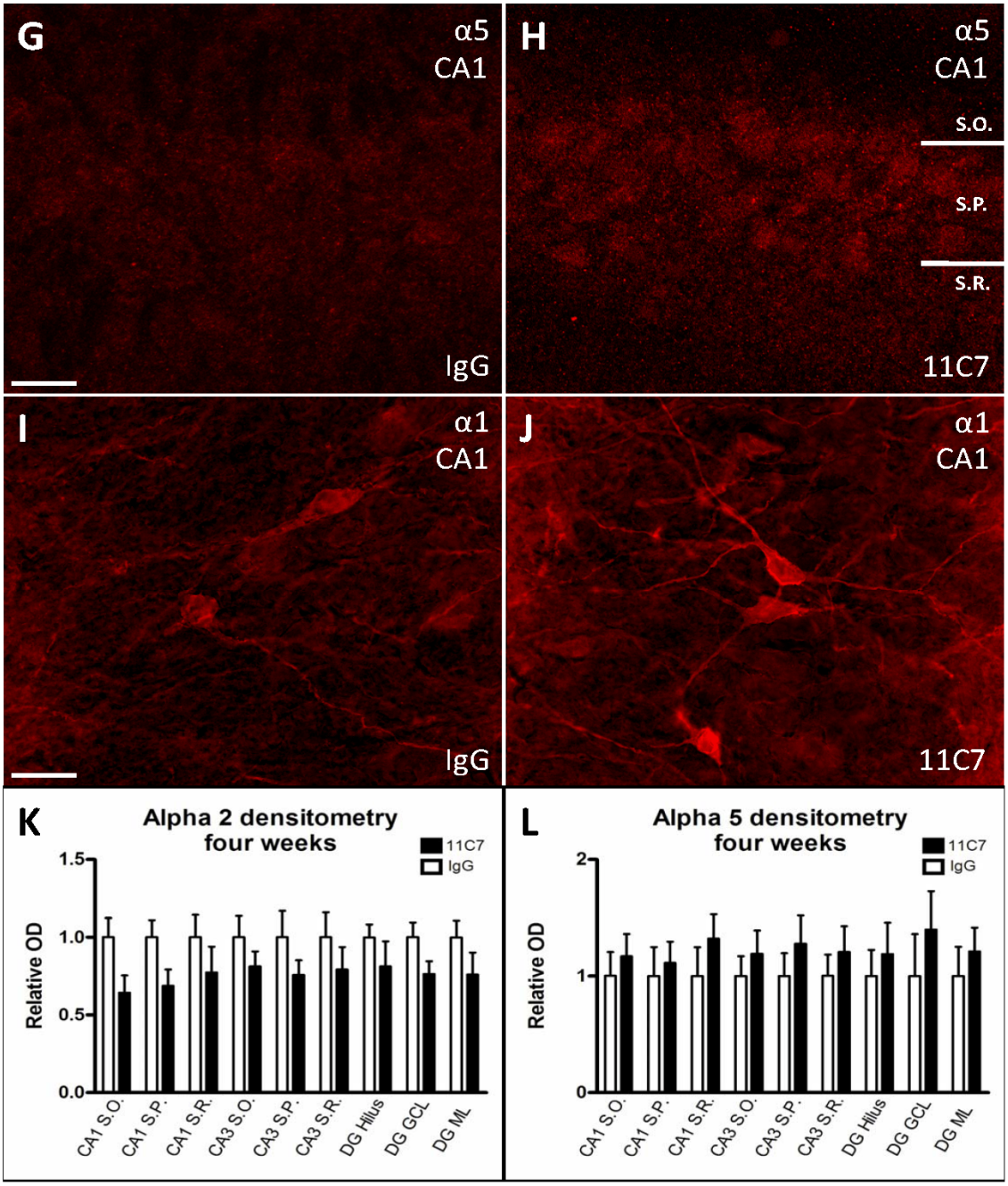
G
α5
CA1
IgG
H
α5
CA1
s.o.
S.P.
S.R.
11C7
I
α1
CA1
IgG
J
α1
CA1
11C7
K
Alpha 2 densitometry
four weeks
11C7
IgG
Relative OD
1.5
1.0
0.5
0.0
CA1 S.O.
CA1 S.P.
CA1 S.R.
CA3 S.O.
CA3 S.P.
CA3 S.R.
DG Hilus
DG GCL
DG ML
L
Alpha 5 densitometry
four weeks
11C7
IgG
Relative OD
2
1
0
CA1 S.O.
CA1 S.P.
CA1 S.R.
CA3 S.O.
CA3 S.P.
CA3 S.R.
DG Hilus
DG GCL
DG ML

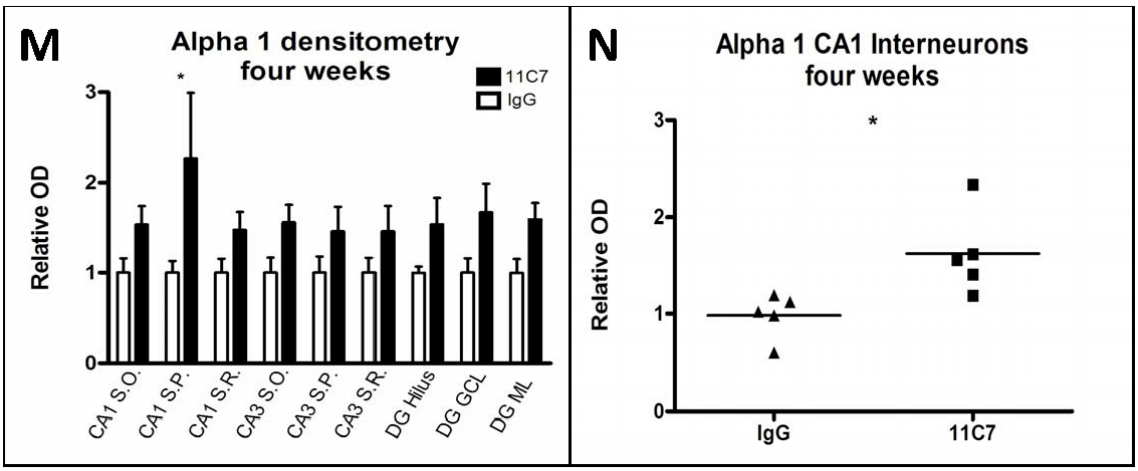


**Fig 10. $GABA_A$ receptor subunit subcellular localization.** A: $GABA_A$ receptor alpha 1 subunit localized along the membrane of an interneuron. B: Gephyrin localization around the same interneuron. C: Overlay of alpha 1 and gephyrin indicate the proper location of alpha 1 subunit at the postsynaptic site of inhibitory symapses and confirm the proper IHC protocol. D: $GABA_A$ receptor alpha 2 subunit localized at the axon initial segment (AIS) of a CA3 pyramidal neuron, indicating proper localization. E, F: Decreased labelling of alpha 2 at the AIS (indicated by the arrows) after Nogo-A neutralization (F) compared to IgG control (E) in the CA3 region. G, H: Alpha 5 increase labelling after Nogo-A neutralization (H) compared to IgG control (G) in the *stratum pyramidale* of the CA1 region. I, J: Increased labelling of alpha 1 subunit in interneurons after Nogo-A neutralization (J) compared to IgG control (I) in CA1 region. K: Graphical representation of the relative optic densities of alpha 2 in several regions of the hippocampus. L: Graphical representation of the relative densities of alpha 5 in several regions of the hippocampus. M: Graphical representation of the relative optic densities of alpha 1 in several regions of the hippocampus. N: Graphical representation of the relative optic densities of CA1 interneurons. N = 6 animals for 11C7 and control IgG treatment group for all quantifications except for the CA1 interneurons where N = 5. Errors bars are standard error of means (SEM) and the p-values are shown over the corresponding bars. White bars refer to IgG treatment and black bars to 11C7 treatment. S.O – *Stratum Oriens*; S.P – *Stratum Pyramidale*; S.R – *Stratum Radiatum*; DG H – Hilus; DG CGL – granule cell layer; DG ML – molecular layer. Scale bar A-D = 10 μm; Scale bar E-F = 100 μm. Scale bar G-J = 50 μm. 0.1 ≥ P-value ≥ 0.05 = * analyzed using the Mann-Whitney test.

## Behavioral Changes after Nogo-A neutralization in adult rats

In order to understand the effect of Nogo-A neutralization in adult rats an extensive set of behavioral tasks was performed.

The open field task assesses the general locomotor activity of the animals. ANOVA by SPSS did not reveal statistical differences between the anti-Nogo-A antibody and IgG treated groups in terms of locomotor activity, measured by the averaged total distance the animals traveled in the maze, which was similar between the animals of the two groups (P = 0.474) (**Fig. 11A; Table 7**). These results show that anti-Nogo-A antibody treatment for 10 days did not induce aberrant activity levels in adult intact rats.

Elevated plus maze is a test designed to assess animal anxiety. Anxious behavior is indexed by the percent of time spent in the open arms of the maze; high anxiety is indicated by a low percent of time in open arms and vice-versa. ANOVA of the percent of time spent in the open arms did not reveal significance differences between the 11C7 and control treated groups (P = 0.615) (**Fig. 11B, Table 7**).

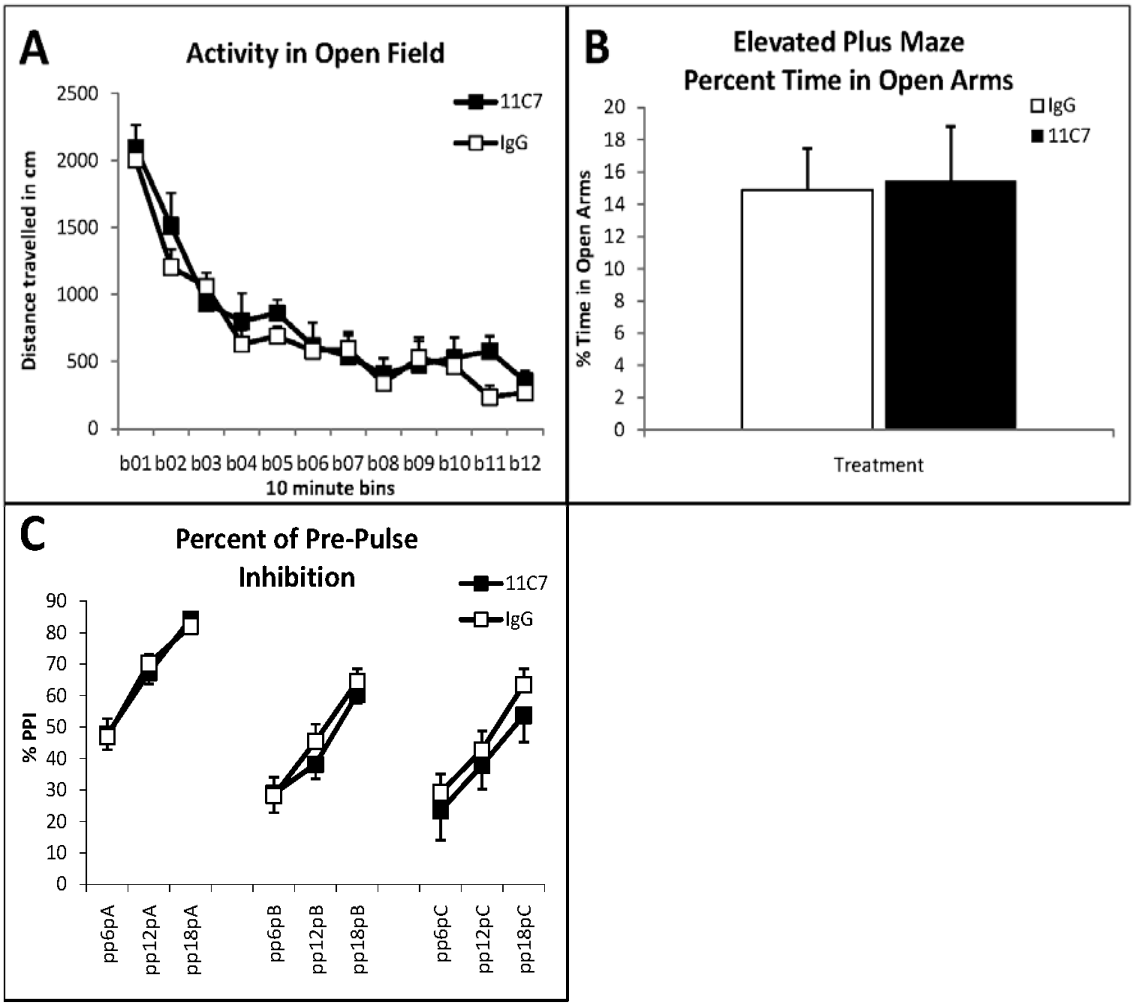


**Fig 11. Acitivty, anxiety and schizotypal behavior assessment.** A: Open Field. Activity performance in open field measured by locomotor activity. No differences were detected in animal performance between anti-Nogo-A treated and control treated groups. Average values for total distance in the field are expressed in centimeters. X-axis is subdivided in 10 minute bins. Error bras are presented as standard error of means (SEM). B: Elevated Plus Maze. Anxiety levels measured by the percent of time spent in the open arms. No differences were detected in animal performance between anti-Nogo-A treated and control treated groups indicating that Nogo-A neutralization does not induce increased anxiety levels. Error bars are presented as standard error of means (SEM). C: Prepulse Inhibition. Percent Prepulse Inhibition as a measure of Schizophrenic-like behaviour. No differences were detected between the two groups. Anti-Nogo-A treatment does not induce schizophrenia-like behaviour. Error bars are presented as standard error of means (SEM).

Prepulse Inhibition (PPI) refers to the reduction in startle reaction to a startle-eliciting "pulse" when it is shortly preceded by a weak "prepulse" stimulus (Hoffman and Searle, 1965). PPI deficits have been reported in schizophrenia patients and schizotypal personality disorders (Braff et al., 2001). Its deficiency in animals has been used as a model of the sensory motor gating deficits in schizophrenic patients (Geyer et al., 2001). Analysis of prepulse inhibition, used as a schizophrenia-like behavior test, did not show any differences between anti-Nogo-A and IgG control treated animals **(Fig. 11C**). No other significant interaction was observed, rendering the two groups indistinguishable. The average startle response showed increased reactivity as a

function of pulse intensity but no significant difference was observed between the two treatments and pulse intensity reactivity (data not shown). Increasing prepulse intensity led to increased magnitude of percent PPI. On the other hand, increasing pulse intensity decreased percent PPI magnitude. As illustrated in **Fig. 11C**, the increase in percentage PPI as a function of prepulse intensity was uniform across the three pulse intensities, thus PPI performance did not differ between the two treatment groups (**Table 7**). The rate of reduction was higher with increasing prepulse intensity. The rate of reduction was comparable between the two groups and across all three pulse intensities, suggesting that PPI is not affected by the different treatments and supporting the conclusion based on the percent PPI results.

In the water maze task, visual platform training did not reveal any differences between anti-Nogo-A or control IgG antibody treated groups with both groups showing a consistent reduction in escape path lengths with consecutive trials (data not shown).

During the reference memory acquisition phase, both groups of animals learned the spatial location of the platform. This was reflected in decreased escape latencies and path-lengths with continued training (**Fig. 12A**). A 2 x 4 (treatment x days) ANOVA of escape latency or path-length showed a significant effect of day ($P = 0.000$). No effect of treatment on escape latency or path-length was detected. This data was supported by the analysis of the path-length (data not shown) and another replicate has yielded the same conclusion (data not shown). In order to assess the memory performance of the animals, a probe test is made at the end of the acquisition phase. In this probe test the platform was removed and the percent of time spent by the animal in the quadrant the platform was located was analyzed. ANOVA did not reveal any differences between the two groups in percent of time spent or in percent of distance traveled in the quadrant where the platform was located (**Fig. 12B, Table 7**).

Another test using the Morris Water Maze apparatus was the assessment of working memory performance. In this task, every day the animals were confronted with a new platform location. During the first trial, the animals did not know the location of the platform so their performance was low. The animals' task for the second trial was to recall the location of platform, which they had learned during the first trial. The performance of the anti-Nogo-A antibody and control IgG treated groups was not statistically different. From a 15-second delay up to 180-minute delay, the animals were able to find the platform location with similar latencies (**Fig. 12C, Table 7**).

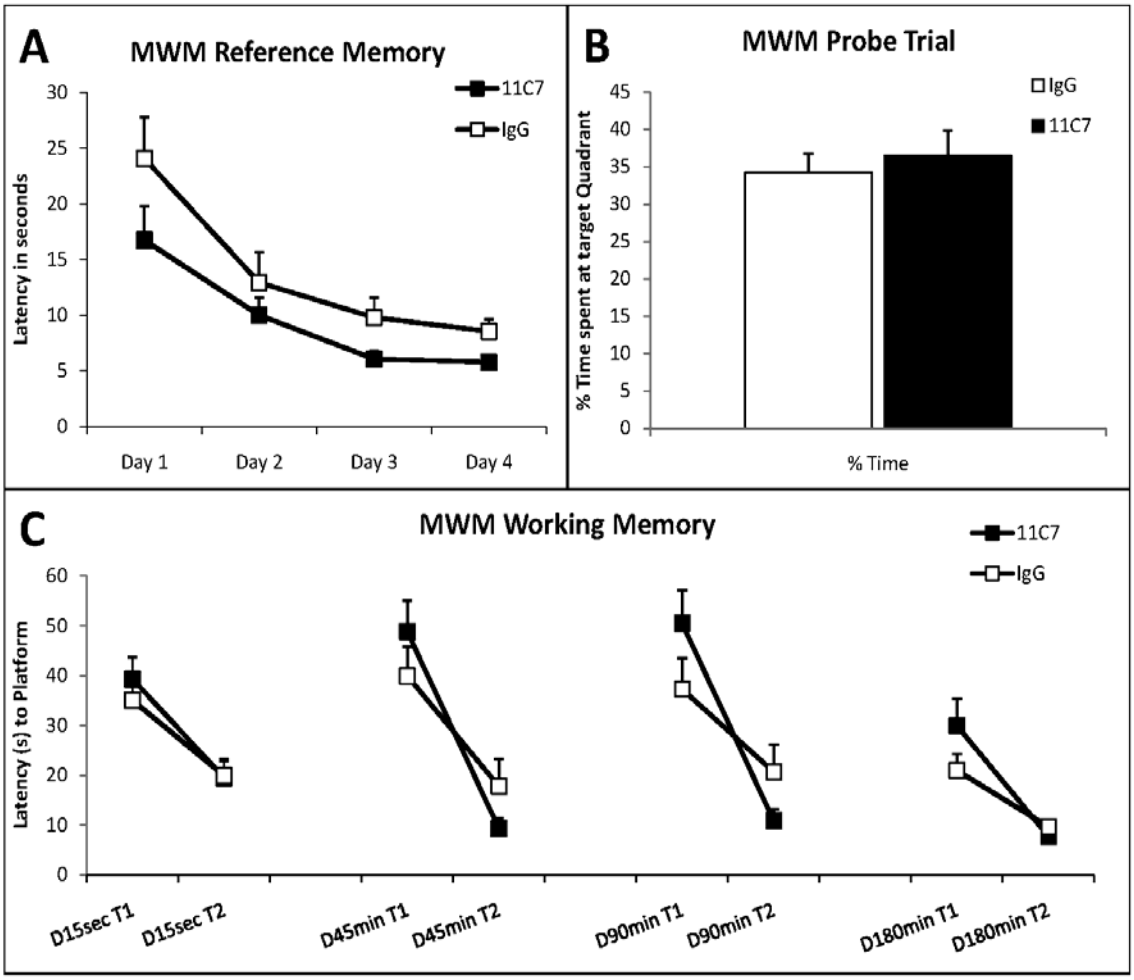


**Fig 12. Morris Water Maze.** A: Reference Memory. Learning curve during reference memory task with latency to reach the hidden platform in seconds. Bar graphs represent the percent of distance traveled and time spent in the quadrant where the platform was placed during reversal and during reference learning. No differences in performance were detected between the anti-Nogo-A treated and IgG control groups in learning and in probe trial performance. Error bars are presented as standard error of means (SEM).

In conclusion, the behavioral assessment of animals treated acutely with anti-Nogo-A antibodies revealed that there was generally no difference in behavioral responses in comparison to the IgG control groups in the tasks analyzed. All p-values from the analysis of variance (ANOVA) are summarized in **Table 7**.

These results indicate that there are no deleterious effects for animals' behavior in the tasks performed after Nogo-A neutralization, despite the molecular changes observed at the hippocampal level.

**Table 7. Summary of the statistical analysis of the behavioral experiments**

| Behavior Task | Variables | | P-values |
|---|---|---|---|
| **Open Field** | **Total Distance** | Bins | .000 |
| | | Bins*Treatment | .607 |
| | | Treatment | .474 |
| **Elevated Plus Maze** | **Percent Time in Open Arms** | Treatment | .615 |
| **Prepulse Inhibition** | **Percent PPI 100dB** | Prepulse | .000 |
| | | Prepulse*Treatment | .815 |
| | | Treatment | .998 |
| | **Percent PPI 110 dB** | Prepulse | .000 |
| | | Prepulse*Treatment | .598 |
| | | Treatment | .581 |
| | **Percent PPI 120dB** | Prepulse | .000 |
| | | Prepulse*Treatment | .769 |
| | | Treatment | .459 |
| **Morris Water Maze** | **Pathlength** | Day | .000 |
| **Reference Memory** | | Day*Treatment | .914 |
| | | Trial | .000 |
| | | Trial*Treatment | .685 |
| | | Day*Trial | .000 |
| | | Day*Trial*Treatment | .770 |
| | | Treatment | .067 |
| | **Latency** | Day | .000 |
| | | Day*Treatment | .747 |
| | | Trial | .000 |
| | | Trial*Treatment | .632 |
| | | Day*Trial | .000 |
| | | Day*Trial*Treatment | .841 |
| | | Treatment | .070 |
| **Morris Water Maze** | **Percent of time in Quadrant** | Treatment | .604 |
| **Reference Memory Probe** | **Percent of distance in Quadrant** | Treatment | .569 |
| **Trial** | **Velocity** | Treatment | .859 |
| **Morris Water Maze** | | Delay | .000 |
| **Working Memory** | | Delay*Treatment | .718 |
| | | Trial | .000 |
| | | Trial*Treatment | .076 |
| | | Delay*Trial | .030 |
| | | Treatment | .877 |
| | **15 second Delay** | Treatment | .650 |
| | **45 minute Delay** | Treatment | .955 |
| | **90 minute Delay** | Treatment | .757 |
| | **180 minute Delay** | Treatment | .330 |

## 3.5 Discussion

In this study, we investigated the effects of Nogo-A neutralization in adult intact Long-Evans rats. Several novel findings emerged from our study. Firstly, a transient growth response was observed in the hippocampus, being the highest at the two-week time point of anti-Nogo-A antibody treatment and diminishing with time to low levels at the four-week time-point. Secondly, we demonstrated that several components of both the excitatory and the inhibitory micro-circuitry of the hippocampus were up-regulated after Nogo-A neutralization. Excitatory synaptic markers increased at the four-week treatment time-point but not at two weeks. The inhibitory components also showed increased expression from the two-week to the four-week time-point, except for parvalbumin, which had already an increased expression after two weeks of antibody infusion. Parvalbumin expression was further increased at the four-week time-point. Thirdly, Post-synaptic $GABA_A$ receptor components showed differential regulation at the four-week time-point after Nogo-A neutralization. Fourthly, behavioral analysis did not reveal significant changes in the anxiety tests and open field locomotor activity was also indistinguishable between the anti-Nogo-A and IgG antibody treated groups. Memory performance in both reference and working memory tasks and PPI were not statistically different between the anti-Nogo-A and IgG control treatment groups.

Our results from the genomic and proteomic approaches indicated a possible growth response after Nogo-A neutralization, which was confirmed by the immunofluorescence and immunobloting studies. Down-regulation of Rras (a gene found to be up-regulated after Nogo-A neutralization) has been shown to be crucial for growth cone collapse (Ito et al., 2006; Negishi et al., 2005; Oinuma et al., 2004; Oinuma et al., 2007). We found Cdc42 slightly up-regulated, which has been shown to be of crucial importance for the formation of filopodia (Hall, 1998). It acts as a signaling switch to actin cytoskeleton reorganization (Hall, 1998) and its precise local activation is required at sites of growth (Cerione, 2004; Etienne-Manneville, 2004; Irazoqui et al., 2004). The regulation of key members of the small family of Rho GTPases in the direction of increased growth is coupled with the regulation of several cytoskeletal proteins, all pointing in the same direction: increased growth. The functional category “Cytoskeletal” was the category with highest number of proteins identified. The up-regulated proteins include two members of the well known collapsin response mediator protein (CRMP) family. CRMP-1 is involved in mediating semaphorin and neurotrophin controlled neuritic extension and plasticity (Bretin et al., 2005; Cohen-Salmon et al., 1997; Quach et al., 2004; Wang and Strittmatter, 1996; Yamashita et al., 2006). CRMP-2 up-regulation has been shown to be of utmost importance for axonal growth and its over-expression *in*

*vivo* was able to induce accelerated re-projection after peripheral injury (Fukata et al., 2002; Katano et al., 2006; Kimura et al., 2005; Suzuki et al., 2003; Yoshimura et al., 2006). Of this family, only CRMP-5 gene, involved in axon guidance, was found down-regulated. The evidence from the proteomic screen for cytoskeletal changes, which include the up-regulation of tubulin, actin, spectrin, cofilin, and NF68 clearly point in the direction of an increased neuritic growth response in the hippocampus of anti-Nogo-A antibody treated rats. These data were supported by the immunofluorescence and immunoblotting data and by our work done with organotypic hippocampal slice cultures, where we demonstrated an increase expression of NF68 after anti-Nogo-A antibody treatment for five days. Transitory growth of fibers in intact adult rats has been observed before after Nogo-A neutralization *in vivo* in Purkinje axons and in the corticospinal tract (Bareyre et al., 2002; Buffo et al., 2000; Gianola et al., 2003). The decrease of expression of the growth marker Gap43 and low expression of alpha-internexin from the two-week to the four-week treatment time-point indicates that this growth response is transient.

Genomic and proteomic analyses of the anti-Nogo-A treated adult rat hippocampus revealed the involvement of the small family of Rho GTPases. Interestingly, both techniques identified Rab3 as being down-regulated. Rab3a isoform is mostly expressed in the brain and is a key player in synaptic vesicle fusion that serves to regulate synaptic vesicle release at the synapse (Geppert and Sudhof, 1998). It is not essential for synaptic transmission exerting a regulatory role at the level of $Ca^{2+}$ triggered fusion step (Geppert et al., 1997). Its over-expression has been associated with an increased constitutive activation of exocytosis of secretory vesicles (Sudhof, 2004) and it has been reported to be required for CA3 hippocampal long term potentiation (Castillo et al., 1997). The down-regulation shown here would therefore suggest that there could be a decreased neurotransmission, however other evidence points in a different direction, suggesting that this might be a response to counterbalance an increased transmission, as seen by the up-regulation of the vesicular GABA transporter, the vesicular glutamate transporter and the general synaptic marker synaptophysin. PP1 is also a prominent regulator of synaptic plasticity. It controls the phosphorylation and activity several effectors governing synaptic plasticity (Greengard et al., 1999). Partial inhibition of PP1 by the inhibitor I-1* in young adult and aged mice improved learning and memory in an object recognition task. This effect correlated with increased phosphorylation of CamK II, GluR1 and CREB (Genoux et al., 2002). It was shown that PP1 inhibition decreases LTP in a frequency dependent manner, favoring potentiation over depression at intermediate frequencies

(5Hz) and increasing LTP at high frequencies (1 second at 100Hz), also impairing depotentiation (Jouvenceau et al., 2006).

One of the major changes we observed was the up-regulation of parvalbumin. It is not clear whether the increased expression of this calcium binding protein, present in a subset of GABA interneurons, could be due to a direct influence of Nogo-A or could be a consequence of a change in the excitatory/inhibitory balance. Nogo-A is expressed in sub-populations of interneurons of the hippocampus, although no direct evidence exists to whether Nogo-A and parvalbumin co-expressed. If both Nogo-A and parvalbumin are co-expressed, then a change in its expression or its neutralization could directly regulate parvalbumin expression. It is also plausible that a growth response would increase the number of synapses onto these interneurons leading to an increased activation of these cells and therefore an increase in parvalbumin expression. The observations from our ICAT experiment and from our immunofluorescence analyses showed an increase in the expression of the vesicular glutamate transporter. An increase in the excitation input onto interneurons would cause a rise in intracellular calcium and parvalbumin is known to be regulated by activity (probably to prevent $Ca^{2+}$ overload). One way to address this issue would be to analyze the number of excitatory synapses onto the parvalbumin positive interneurons by electron microscopy.

Besides the wide spread inhibitory function in the CNS, $GABA_A$ receptor function is involved in the modulation of several physiological states like anxiety, mood, memory or epileptogenic activity. Several components of the inhibitory synaptic system were regulated after Nogo-A neutralization. A general down-regulation of the alpha-2 subunit was observed throughout the entire hippocampus simultaneously to a clear loss of alpha-2 labeling of the axon initial segment of hippocampal CA3 pyramidal cells after Nogo-A neutralization. Alpha-1 and alpha-5 subunits were both up-regulated throughout the entire hippocampus, although, only alpha-1 had a statistically significant effect in CA1 *stratum pyramidale*. A sub-population of interneurons of the CA1 hippocampal region expressing the alpha-1 subunit had also a clear increase alpha-1 expression. The increased expression of certain $GABA_A$ receptor subunits could be a response to an increased excitation and hence a response to maintain the natural balance, or on the other hand, could also an increase of inhibition directly regulated by Nogo-A neutralization.

Along with the understanding of the circuitry changes, there is the change in electrophysiological properties of the hippocampal cells. The increased expression of certain $GABA_A$ receptor subunits suggests an increased inhibition. Electrophysiological measurements of hippocampal cells would indicate the amount and possibly the impact at the neuronal network level of some of the observed changes. Although the network

activity of the organotypic hippocampal slice cultures did not show an increased activity (potentially a decrease), a better characterization of the electrophysiological properties of the hippocampal cells can be achieved with acute slices and patch clamp techniques. The slices could be easily taken after the anti-Nogo-A treatment of the adult rats.

The work presented here demonstrates the capacity for growth induction after Nogo-A neutralization, whether *in vitro* (our unpublished results) or *in vivo*, in the intact CNS tissue. These results support the concept of Nogo-A function in the intact CNS as a tonic growth suppressor/stabilizer of the CNS network in the adult. Our work also extends this concept further.

Growth induction due to epileptic seizures in the hippocampus, particularly in the dentate gyrus, has been well documented. Considering this fact, it could be expected that the growth response observed after Nogo-A neutralization could lead to seizure induction. This phenomenon was not observed in our animals. One explanation relies on the observation that both excitatory and inhibitory components of the hippocampal network are up-regulated, which could result in the neutralization of either excessive excitation or excessive inhibition. Such phenomenon could be entirely independent of Nogo-A regulation and a consequence of the observed increased growth. On the other hand, there was a differential regulation of $GABA_A$ receptor subunits particularly the alpha-1 subunits. Interestingly, during the normal course of epilepsy development there is a loss of alpha-1 containing interneurons (Fritschy et al., 1999) and several reports have shown the up-regulation of Nogo-A in epilepsy (Bandtlow et al., 2004; Meier et al., 2003; Takeda et al., 2007). The role of Nogo-A in epilepsy is not clear but nonetheless it is intriguing to note the neuronal loss and down-regulation of alpha-1 and up-regulation of Nogo-A in epilepsy, as well as the opposite regulation by the neutralization and down-regulation of Nogo-A and the consequent up-regulation of alpha-1 shown in this study.

ALS is another disease where Nogo-A and alpha-1 have reversed expression. An increase in alpha-2 and a decrease in alpha-1 subunits of $GABA_A$ receptors has been shown in ALS-vulnerable motorneurons (Lorenzo et al., 2006). Our data show that the neutralization of Nogo-A leads to the down-regulation of alpha-2 and the up-regulation of alpha-1 subunits, at least in the hippocampus. It remains to be analyzed whether these changes also occur in the motor neurons of the spinal cord and brainstem. Although these are mere observations, a role of Nogo-A in the regulation of alpha-1 and alpha-2 expression cannot be excluded.

The changes in synaptic proteins and $GABA_A$ receptor subunits indicate that Nogo-A may have additional roles other than growth inhibition. The neutralization of Nogo-A

induces a growth response, which could eventually lead to axon arborization and/or spine density increases. Consequently, new synapses could be formed explaining the increased expression of synapse related proteins. In view of new evidence that Nogo-A is endogenously expressed in the dendritic tree of Purkinje cells and at the membrane of their spines near synapses (Aloy et al., 2006) other roles should be considered.

Elevated plus maze was developed to assess anxiety. Rats find it aversive to venture into the open arms of this maze since there is the lack of a safe environment. Conversely, the closed arms of this maze are safe places where the animal can move close to the walls. Anxiolytic drugs enable animals to venture more into the aversive open arms, spending more time exploring them. Anxiogenic drugs have the reverse effect. Knock-in point mutation of $GABA_A$ receptor subunit alpha-2 renders the animals insensitive to the anxiolytic effects of diazepam, demonstrating the crucial role of this $GABA_A$ receptor subunit in anxiety behavior mediation (Mohler, 2007). Considering the decreased expression of alpha-2 in the hippocampus after Nogo-A neutralization we could envisage, if anything, an anxiogenic effect and consequently, a decrease of the percent of time spent in the open arms of the maze by the animals with anti-Nogo-A antibody administration. Hence, we analyzed the performance of anti-Nogo-A acutely treated rats and compared it to control IgG treated rats. We found no detectable differences between anti-Nogo-A and control IgG treatments.

Open field is a task design to assess motor activity. Also in this task, there was no difference between the two treatment groups. From these sets of experiments, we conclude that the animals treated with anti-Nogo-A antibodies did not show increased anxiety and exhibit normal activity levels.

Several studies have shown the involvement of the GABAergic system in learning and memory (Gafford et al., 2005; Krebs-Kraft et al., 2007; Mohler, 2007; Stone et al., 2005). Molecules such as PP1 (discussed above) are involved in memory formation and their regulation could alter normal performance (Genoux et al., 2002; Jouvenceau et al., 2006). We used the Morris Water Maze apparatus to address the question of reference and working memory performance. Despite the molecular differences detected, there were no statistical differences during the acquisition phase of reference memory and the probe trials of reference learning indicated that both groups of animals learned similarly the location of the platform. In conclusion, these experiments indicate that reference memory was not affected by anti-Nogo-A antibody treatment but they left open the possibility of working memory changes. An improvement in working memory by the anti-Nogo-A antibody treated animals would be visible by a faster performance in reaching the platform or by the anti-Nogo-A antibody treated group remembering the platform over a significantly longer time than the IgG control group. Working memory

performance in this paradigm was not altered. There was no improvement or decline of performance detected in the anti-Nogo-A antibody compared to the IgG control treated group. Even by increasing the trial delay to 3 hours, the animals were able to rapidly find the platform location. These results clearly demonstrate that Nogo-A neutralization is not deleterious for either reference or working memory performance.

Our ongoing and unpublished results using Nogo-A knockout animals indicate that there are alterations in several behavioral tasks related with schizotypal behavior. Therefore, another set of behavioral tasks aimed at the identification of schizophrenia related symptoms. Although prepulse inhibition deficits are not unique to schizophrenia, prepulse inhibition is a commonly used test that is related to similar mechanisms of schizophrenia positive symptomatology in animal models and humans (Braff et al., 2001). Analysis of PPI responses did not show statistically significant differences between the two treatment groups, their performance was indistinguishable. Therefore, we conclude that acute Nogo-A neutralization does not induce schizophrenia type behavior. More importantly, these results are in contrast with our observations with Nogo-A knockout animals. They point to a difference in the chronic absence of Nogo-A, as is the case with Nogo-A knockout animals, and Nogo-A acute neutralization. The chronic absence of Nogo-A seems to cause behavioral changes related with schizotypal disorders possibly due to changes in circuitry or guidance during early development. On the other hand, acute neutralization of Nogo-A does not seem to have the same behavioral consquences, possibly due to the fact that the normal function and levels of Nogo-A were not affected during development and there is only a down-regulation of its expression.

In conclusion, the localization of Nogo-A in myelin has been proposed as the mechanism by which CNS axons fail to regenerate after injury. In the injured CNS, Nogo-A acts as a barrier and blocks growing axons from continuing growth after initial sprouting attempts. In the adult intact CNS, Nogo-A could serve as a regulatory molecule, ensuring stability of the established network by controlling both growth and synaptic events. Nogo-A treatment in intact CNS tissue induces a transient growth response in the hippocampus and it induces significant changes in the hippocampal micro-circuitry. Our observations are of importance, since they indicate that despite the molecular and cellular changes discussed above, no functional impairments or neurological disease conditions arise from acute Nogo-A neutralization. This is highly relevant for the application of Nogo-A treatment to injury models and of ongoing clinical trials.

**Acknowledgements:**

We thank Prof. Jean-Mark Fritschy for kindly lending the various $GABA_A$ receptor alpha subunit antibodies used in this work. This work has been supported by the Swiss National Foundation, the Swiss National Centre of Competence in Research, the Portuguese Fundação para a Ciência e Tecnologia and the GABBA PhD program in Porto, Portugal.

# Chapter 4: Conclusions and Outlook

# 4 Conclusions and Outlook

The goal of our study was to answer the question whether Nogo-A neutralization induced a growth response in the intact adult CNS and whether such a response could induce hippocampal dependent behavioral changes. We also wanted to understand which were the mechanisms involved in the growth response and/or behavioral changes. We expected a mild growth response, with increased plasticity, which could induce cognitive behavioral changes in the adult rat. We did not, however, expected gross cognitive behavioral changes.

We first used a cellular biology approach. Mature organotypic hippocampal slice cultures were used and treated with antibodies against Nogo-A or control antibodies for a five-day period. The outcome of this approach was the detection of a regenerative response in lesioned cultures by increased Gap43 expression and electrophysiological data demonstrating a recovery of CA1 evoked field potentials in response to CA3 stimulation. In intact cultures, we observed a growth response seen by an increase in NF68 positive fibers. Furthermore, genomic and proteomic techniques indicated the regulation of several molecules involved in different growth and synaptic events, including neurotransmission or transport activity. These changes strongly suggest the occurrence of a growth response and synaptogenesis after acute Nogo-A neutralization in organotypic hippocampal slice cultures.

We then extended our studies to the animal level. We analyzed several growth markers and synaptic markers after anti-Nogo-A antibody treatment of adult rats after a period of two or four weeks of antibody infusion. We also analyzed several different behaviors, which relate to hippocampal function. We observed a transient growth response, higher at the two-week time point and lower, although still detectable, at the four-week time-point using Gap43 as growth marker. The regulation of synaptic markers followed a different time course. Both the pre-synaptic excitatory vesicular glutamate transporter 1 and the pre-synaptic vesicular GABA transporter were down-regulated at the two-week time point but at the four-week time-point, they were significantly higher. On the other hand, the expression of parvalbumin, a calcium binding protein expressed in sub-populations of interneurons, was already elevated after two weeks of anti-Nogo-A antibody infusion and significantly higher after four weeks. We also observed a differential regulation of the $GABA_A$ receptor subunits alpha-1, alpha-5 and alpha-2 at the four-week time-point. On the behavioral level, no changes were detectable between animals with anti-Nogo-A and control IgG antibody treatment. The activity levels were normal, as well as anxiety levels. No signs of schizophrenia like behavior were

detected. Cognitively, the animals did not differ in their ability to perform on reference or working memory tasks.

In conclusion, Nogo-A neutralization in intact CNS tissue induces a transient growth response in the hippocampus and it induces significant changes in the hippocampal microcircuitry, although these were not expressed behaviorally. This is of major importance for application of Nogo-A treatment to injury models and clinical trials.

Nogo-A localization in myelin has been proposed as an important mechanism by which CNS axons fail to regenerate after injury. In the injured CNS, Nogo-A acts as a barrier and blocks growing axons from continuing growth after initial sprouting attempts. In the adult intact CNS, Nogo-A could serve as a regulatory molecule, ensuring stability of the established network. Its presence in myelin would ensure that well established networks would not suffer undesirable cross-connections due to possible aberrant growth. At the end of development, Nogo-A would also serve as a signal indicating that the network had been established.

On the other hand, in highly plastic areas of the adult brain, such as the hippocampus, Nogo-A is expressed in neurons. The neuronal Nogo-A function remains elusive but recent evidence of its expression peri-synaptically in the cerebellum and our evidence of pre- and post-synaptic changes after acute Nogo-A neutralization or over-expression suggest a possible role at the level of synapses. A putative mechanism for a regulatory function at synapses, considering Nogo-A as a repulsive molecule, could be to ensure that certain synapses do not form, maintaining the potential of a network to expand. Such function would be extremely important in networks such as the hippocampus, where its role in learning and memory would require the plasticity of new synapse formation.

As introduced previously, links between certain human diseases and Nogo-A expression have been made. Anxiety, memory, mood, epileptogenic activity in the hippocampus can be regulated by a modulation of $GABA_A$ receptor function. Interestingly, in some of the diseases introduced earlier, such as ALS and epilepsy, it was not only observed that an increase of Nogo-A expression occurred, but there was also a decrease in the expression levels of $GABA_A$ receptor subunit alpha-1 and an increase in alpha-2 (in epilepsy). Although the later change has been suggested as a compensatory reaction to the over-excitation characteristic of epilepsy, it cannot pass unnoticed that the neutralization of Nogo-A produced an up-regulation of alpha-1 and a down-regulation of alpha-2. Thus, the relationship between Nogo-A and the GABA system can prove of extreme relevance in the understanding of specific neurological diseases, such as ALS (Dupuis et al., 2002; Jokic et al., 2005; Pradat et al., 2007) and epilepsy (Bandtlow et al., 2004; Meier et al., 2003; Takeda et al., 2007).

No direct evidence for a direct interaction exists between Nogo-A and $GABA_A$ receptors. It is interesting to observe the increased Nogo-A expression and the increased expression of alpha-2 and decreased expression of alpha-1 in vulnerable motor neurons in ALS, and the increased Nogo-A expression, parvalbumin and alpha-1 decreased and alpha-5 increased expression in some Epilepsy models (Bouilleret et al., 2000; Fritschy et al., 1999). The general opposite regulation of all these molecules poses the question of their relationship. Except for the increased alpha-5 up-regulation in the epilepsy models, which is proposed to be a compensation due to the massive alpha-1 positive interneuron cell death (Bouilleret et al., 2000; Fritschy et al., 1999), the regulation of these molecules fits our present observations: Nogo-A neutralization leads to increased expression of parvalbumin, alpha-5, alpha-1, and decreased expression of alpha-2. In order to test the hypothetical relationship of these molecules, a study focusing on the localization of Nogo-A in relationship to the localization of the $GABA_A$ receptor subunits would be needed. The clarification of the physiological significance of GABAA-receptor subtypes, in combination with their cellular localization, will make it possible to identify neuronal circuits regulating the respective CNS states.

It has been shown that Nogo-A KO mice crossed with SOD1 mutant mice (ALS model) had an increased life expectancy, although the animals still progress through the disease and eventually die (Jokic et al., 2006). In that study, the localization or regulation of $GABA_A$ receptors was not analyzed. If $GABA_A$ receptor subunit composition would indeed change in these mice as is the case after Nogo-A neutralization this would strengthen the hypothesis of a link between Nogo-A and $GABA_A$ receptor subunit composition. A consequence of growth induction does not seem likely since Nogo-A KO do not have any obvious anatomical differences and although motor neurons die and there is peripheral denervation (which could induce some growth response), no lesion proper exists to induce a major growth response. A careful analysis of ALS sensitive motorneurons with regard to Nogo-A and $GABA_A$ receptor composition, as well as a growth response analysis, would clarify their relationship. The question whether Nogo-A and $GABA_A$ receptors co-localize or are in close vicinity would remain unanswered though. To address it, an electron microscopy analysis of intact animals, Nogo-A KO and SOD1/Nogo-A KO animals would be needed.

The mechanism of such possible interaction would remain elusive. Even in the case of no direct relationship confirmed, a regulation of $GABA_A$ receptor subunits could still be influenced by Nogo-A. Cdc42 is a molecule involved in the clustering and anchoring to the cytoskeletal scaffold of the $GABA_A$ receptors and is possibly downstream of Nogo-A signaling, since its activation state can be regulated by RhoA activity. Evidence

exists for regulatory relationships between $GABA_A$ receptor and Cdc42 but how a change in the activation of Cdc42 could influence the expression and composition of the former is not clear. $GABA_A$ receptors are clustered by binding to gephyrin (Grosskreutz et al., 2001; Kirsch et al., 1996), which in turn binds collybistin, a Cdc42 specific activator (Reid et al., 1999). The collybistin-gephyrin complex renders its membrane localization. It is possible that collybistin controls the gephyrin scaffold by regulating the proximal components of the cytoskeleton by activation of Cdc42 (Xiang et al., 2006). Interestingly, loss of gephyrin expression prevents the formation of $GABA_A$ receptors containing the alpha-2 and/or gamma-2 subunit, while the alpha-5 and alpha-1 subunits remain fully localized in gephyrin knockout animals, hence giving evidence for a subunit specific regulation of clustering (Kneussel et al., 2001).

The future identification of factors regulating the $GABA_A$ receptor gene expression, linked to Nogo-A pathway (Rac 1 and possibly Cdc42), may be of relevance also for disease states, such as after spinal cord injury as well as stroke, mood disorders or epilepsy. This knowledge could provide pharmacological strategies for the development of specific drugs for selective therapies in the field of neuronal plasticity.

# Chapter 5: Abbreviations

# 5 Abbreviations

3' UTR – 3' Untranslated Region
3D – Three dimensional
ACN – Acetonitrile
AD – Alzheimer's Disease
ALS – Amyotrophic Lateral Sclerosis
ANOVA – Analysis of Variance
CamKII – Calcium/Calmodulin-dependent Protein Kinase 2
cAMP – Cyclic Adenosine Monophosphate
Cdc42 – Cell Division Control Protein 42
cDNA – Complementary Deoxyribonucleic Acid
CNS – Central Nervous System
CREB – cAMP Responsive Element Binding Protein
CRMP – Collapsin Response Mediator Protein
cRNA – Complementary Ribonucleic Acid
CSF – Cerebro-spinal Fluid
CSPG – Chondroitin Sulfate Proteoglycans
CST – Corticospinal Tract
dB – Decibel
DIV – Days In Vitro
DNA – Deoxyribonucleic Acid
DTT – Dithiothreitol
EAE – Experimental Autoimmune Encephalomyelitis
ECM – Extracellular Matrix
EPM – Elevated Plus Maze
ER – Endoplasmatic Reticulum
Fab – Fragment Antigen Binding
FGF – Fibroblast Growth Factor
GA – Gluteraldehyde
GABA – Gama-aminobutyric Acid
Gap43 – Growth Associated Protein 43
GAPDH – Glyceraldehyde-3-phosphate dehydrogenase
GluR1 – Glutamate receptor 1
HPLC – High Performance Liquid Chromatography
Hz –Hertz
ICAT – quantitative proteomic Isotope-Coded Affinity Tag
IgG – Immunoglobulin G
IL1 – Interleukin 1
kDa – Kilodalton
KO – Knockout
LC-MS/MS – Liquid Chromatography-Mass Spectrometry/ Mass Spectrometry
LMNS – Lower Motor Neuron Syndrome
LRR domain – Leucine Rich Repeat
LTP – Long Term Potentiation
LTQ-FTICR – Linear Trap Quadrupole Fourier Transform Ion Cyclotron Resonance Mass Spectrometry
MAG – Myelin Associated Glycoprotein
MAP2a/b – Microtubule Associated Protein 2a/b
MEA – Multi-Electrode Array
mM – Millimolar
MOG – Myelin-Oligodendrocyte Glycloprotein

mRNA – Messenger Ribonucleic Acid

MS – Multuple Sclerosis

MWM – Morris Water Maze

NF68 – Neurofilament 68

OF – Open Field

OMgp – Oligodendrocyte Myelin Glycoprotein

P7 – Post-natal day 7

PBS – Phosphate Buffer Solution

PCI – Photothrombotic Cortical Injury

PFA – Paraformaldehyde

PLP – Proteolipid Protein

PNS – Peripheral Nervous System

PP1 – Serine/Threonine-protein Phosphatase

PPI – Prepulse Inhibition

RNA – Ribonucleic Acid

ROCK – Rho kinase Inhibitor

RTN – Reticulon

SCI – Spinal Cord Injury

Sema – Semaphorin

SLPI – Secretory Leukocite Protease Inhibitor

SOD – Superoxide Dismutase

SPSS – Statistical Package for Social Sciences

SUDEP – Sudden Unexpected Death from Epilepsy

T10 – Spinal Column Thoraxic Level 10

TBI – Traumatic Brain Injury

TBST – Tris Buffer Solution Tween-20

TCEP – *tris*(2-carboxyethyl)phosphine

TFA – Trifluoroacetic Acid

TIMP – Tissue Inhibitor of Metalloproteinase

TLE – Temporal Lobe Epilepsy

US – United States of America

vGAT – vesicular GABA Transporter

vGlut1 – vesicular Glutamate Transporter 1

# Chapter 6: References

# 6 References

Alabed, Y.Z., Grados-Munro, E., Ferraro, G.B., Hsieh, S.H., and Fournier, A.E. (2006). Neuronal responses to myelin are mediated by rho kinase. J Neurochem *96*, 1616-1625.

Aloy, E.M., Weinmann, O., Pot, C., Kasper, H., Dodd, D.A., Rulicke, T., Rossi, F., and Schwab, M.E. (2006). Synaptic destabilization by neuronal Nogo-A. Brain Cell Biol *35*, 137-156.

Amberger, V.R., Hensel, T., Ogata, N., and Schwab, M.E. (1998). Spreading and migration of human glioma and rat C6 cells on central nervous system myelin in vitro is correlated with tumor malignancy and involves a metalloproteolytic activity. Cancer Res *58*, 149-158.

Atalay, B., Bavbek, M., Cekinmez, M., Ozen, O., Nacar, A., Karabay, G., and Gulsen, S. (2007). Antibodies neutralizing Nogo-A increase pan-cadherin expression and motor recovery following spinal cord injury in rats. Spinal Cord.

Bahr, B.A. (1995). Long-term hippocampal slices: a model system for investigating synaptic mechanisms and pathologic processes. J Neurosci Res *42*, 294-305.

Bandtlow, C.E., Dlaska, M., Pirker, S., Czech, T., Baumgartner, C., and Sperk, G. (2004). Increased expression of Nogo-A in hippocampal neurons of patients with temporal lobe epilepsy. Eur J Neurosci *20*, 195-206.

Bareyre, F.M., Haudenschild, B., and Schwab, M.E. (2002). Long-lasting sprouting and gene expression changes induced by the monoclonal antibody IN-1 in the adult spinal cord. J Neurosci *22*, 7097-7110.

Barritt, A.W., Davies, M., Marchand, F., Hartley, R., Grist, J., Yip, P., McMahon, S.B., and Bradbury, E.J. (2006). Chondroitinase ABC promotes sprouting of intact and injured spinal systems after spinal cord injury. J Neurosci *26*, 10856-10867.

Bartolomei, J.C., and Greer, C.A. (2000). Olfactory ensheathing cells: bridging the gap in spinal cord injury. Neurosurgery *47*, 1057-1069.

Bartsch, U., Bandtlow, C.E., Schnell, L., Bartsch, S., Spillmann, A.A., Rubin, B.P., Hillenbrand, R., Montag, D., Schwab, M.E., and Schachner, M. (1995). Lack of evidence that myelin-associated glycoprotein is a major inhibitor of axonal regeneration in the CNS. Neuron *15*, 1375-1381.

Becker, T., Anliker, B., Becker, C.G., Taylor, J., Schachner, M., Meyer, R.L., and Bartsch, U. (2000). Tenascin-R inhibits regrowth of optic fibers in vitro and persists in the optic nerve of mice after injury. Glia *29*, 330-346.

Benowitz, L.I., and Yin, Y. (2007). Combinatorial treatments for promoting axon regeneration in the CNS: Strategies for overcoming inhibitory signals and activating neurons' intrinsic growth state. Dev Neurobiol *67*, 1148-1165.

Benson, M.D., Romero, M.I., Lush, M.E., Lu, Q.R., Henkemeyer, M., and Parada, L.F. (2005). Ephrin-B3 is a myelin-based inhibitor of neurite outgrowth. Proc Natl Acad Sci U S A *102*, 10694-10699.

Berger, T., and Frotscher, M. (1994). Distribution and morphological characteristics of oligodendrocytes in the rat hippocampus in situ and in vitro: an immunocytochemical study with the monoclonal Rip antibody. J Neurocytol *23*, 61-74.

Bieber, A.J., Warrington, A., Pease, L.R., and Rodriguez, M. (2001). Humoral autoimmunity as a mediator of CNS repair. Trends Neurosci *24*, S39-44.

Bonhoeffer, T., and Yuste, R. (2002). Spine motility. Phenomenology, mechanisms, and function. Neuron *35*, 1019-1027.

Bouilleret, V., Loup, F., Kiener, T., Marescaux, C., and Fritschy, J.M. (2000). Early loss of interneurons and delayed subunit-specific changes in GABA(A)-receptor expression in a mouse model of mesial temporal lobe epilepsy. Hippocampus *10*, 305-324.
Bradbury, E.J., Moon, L.D., Popat, R.J., King, V.R., Bennett, G.S., Patel, P.N., Fawcett, J.W., and McMahon, S.B. (2002). Chondroitinase ABC promotes functional recovery after spinal cord injury. Nature *416*, 636-640.
Braff, D.L., Geyer, M.A., and Swerdlow, N.R. (2001). Human studies of prepulse inhibition of startle: normal subjects, patient groups, and pharmacological studies. Psychopharmacology (Berl) *156*, 234-258.
Bramham, C.R., and Wells, D.G. (2007). Dendritic mRNA: transport, translation and function. Nat Rev Neurosci *8*, 776-789.
Bretin, S., Reibel, S., Charrier, E., Maus-Moatti, M., Auvergnon, N., Thevenoux, A., Glowinski, J., Rogemond, V., Premont, J., Honnorat, J., and Gauchy, C. (2005). Differential expression of CRMP1, CRMP2A, CRMP2B, and CRMP5 in axons or dendrites of distinct neurons in the mouse brain. J Comp Neurol *486*, 1-17.
Brosamle, C., Huber, A.B., Fiedler, M., Skerra, A., and Schwab, M.E. (2000). Regeneration of lesioned corticospinal tract fibers in the adult rat induced by a recombinant, humanized IN-1 antibody fragment. J Neurosci *20*, 8061-8068.
Buchli, A.D., and Schwab, M.E. (2005). Inhibition of Nogo: a key strategy to increase regeneration, plasticity and functional recovery of the lesioned central nervous system. Ann Med *37*, 556-567.
Buffo, A., Zagrebelsky, M., Huber, A.B., Skerra, A., Schwab, M.E., Strata, P., and Rossi, F. (2000). Application of neutralizing antibodies against NI-35/250 myelin-associated neurite growth inhibitory proteins to the adult rat cerebellum induces sprouting of uninjured purkinje cell axons. J Neurosci *20*, 2275-2286.
Burgess, J.W., Villablanca, J.R., and Levine, M.S. (1986). Recovery of functions after neonatal or adult hemispherectomy in cats. III. Complex functions: open field exploration, social interactions, maze and holeboard performances. Behav Brain Res *20*, 217-230.
Cafferty, W.B., Kim, J.E., Lee, J.K., and Strittmatter, S.M. (2007). Response to correspondence: Kim et al., "axon regeneration in young adult mice lacking Nogo-A/B." Neuron 38, 187-199. Neuron *54*, 195-199.
Caggiano, A.O., Zimber, M.P., Ganguly, A., Blight, A.R., and Gruskin, E.A. (2005). Chondroitinase ABCI improves locomotion and bladder function following contusion injury of the rat spinal cord. J Neurotrauma *22*, 226-239.
Cai, D., Deng, K., Mellado, W., Lee, J., Ratan, R.R., and Filbin, M.T. (2002). Arginase I and polyamines act downstream from cyclic AMP in overcoming inhibition of axonal growth MAG and myelin in vitro. Neuron *35*, 711-719.
Cai, D., Shen, Y., De Bellard, M., Tang, S., and Filbin, M.T. (1999). Prior exposure to neurotrophins blocks inhibition of axonal regeneration by MAG and myelin via a cAMP-dependent mechanism. Neuron *22*, 89-101.
Caltharp, S.A., Pira, C.U., Mishima, N., Youngdale, E.N., McNeill, D.S., Liwnicz, B.H., and Oberg, K.C. (2007). NOGO-A induction and localization during chick brain development indicate a role disparate from neurite outgrowth inhibition. BMC Dev Biol *7*, 32.
Caroni, P., Savio, T., and Schwab, M.E. (1988). Central nervous system regeneration: oligodendrocytes and myelin as non-permissive substrates for neurite growth. Prog Brain Res *78*, 363-370.

Caroni, P., and Schwab, M.E. (1988a). Antibody against myelin-associated inhibitor of neurite growth neutralizes nonpermissive substrate properties of CNS white matter. Neuron *1*, 85-96.
Caroni, P., and Schwab, M.E. (1988b). Two membrane protein fractions from rat central myelin with inhibitory properties for neurite growth and fibroblast spreading. J Cell Biol *106*, 1281-1288.
Castillo, P.E., Janz, R., Sudhof, T.C., Tzounopoulos, T., Malenka, R.C., and Nicoll, R.A. (1997). Rab3A is essential for mossy fibre long-term potentiation in the hippocampus. Nature *388*, 590-593.
Cerione, R.A. (2004). Cdc42: new roads to travel. Trends Cell Biol *14*, 127-132.
Chau, C.H., Shum, D.K., Li, H., Pei, J., Lui, Y.Y., Wirthlin, L., Chan, Y.S., and Xu, X.M. (2004). Chondroitinase ABC enhances axonal regrowth through Schwann cell-seeded guidance channels after spinal cord injury. Faseb J *18*, 194-196.
Chen, M.S., Huber, A.B., van der Haar, M.E., Frank, M., Schnell, L., Spillmann, A.A., Christ, F., and Schwab, M.E. (2000). Nogo-A is a myelin-associated neurite outgrowth inhibitor and an antigen for monoclonal antibody IN-1. Nature *403*, 434-439.
Chivatakarn, O., Kaneko, S., He, Z., Tessier-Lavigne, M., and Giger, R.J. (2007). The Nogo-66 receptor NgR1 is required only for the acute growth cone-collapsing but not the chronic growth-inhibitory actions of myelin inhibitors. J Neurosci *27*, 7117-7124.
Citri, A., and Malenka, R.C. (2007). Synaptic Plasticity: Multiple Forms, Functions, and Mechanisms. Neuropsychopharmacology.
Cohen-Salmon, M., Crozet, F., Rebillard, G., and Petit, C. (1997). Cloning and characterization of the mouse collapsin response mediator protein-1, Crmp1. Mamm Genome *8*, 349-351.
Coltman, B.W., Earley, E.M., Shahar, A., Dudek, F.E., and Ide, C.F. (1995). Factors influencing mossy fiber collateral sprouting in organotypic slice cultures of neonatal mouse hippocampus. J Comp Neurol *362*, 209-222.
Crossin, K.L., Hoffman, S., Tan, S.S., and Edelman, G.M. (1989). Cytotactin and its proteoglycan ligand mark structural and functional boundaries in somatosensory cortex of the early postnatal mouse. Dev Biol *136*, 381-392.
Crossin, K.L., Prieto, A.L., Hoffman, S., Jones, F.S., and Friedlander, D.R. (1990). Expression of adhesion molecules and the establishment of boundaries during embryonic and neural development. Exp Neurol *109*, 6-18.
David, S., and Lacroix, S. (2003). Molecular approaches to spinal cord repair. Annu Rev Neurosci *26*, 411-440.
Davies, S.J., Fitch, M.T., Memberg, S.P., Hall, A.K., Raisman, G., and Silver, J. (1997). Regeneration of adult axons in white matter tracts of the central nervous system. Nature *390*, 680-683.
DeBellard, M.E., Tang, S., Mukhopadhyay, G., Shen, Y.J., and Filbin, M.T. (1996). Myelin-associated glycoprotein inhibits axonal regeneration from a variety of neurons via interaction with a sialoglycoprotein. Mol Cell Neurosci *7*, 89-101.
Dengler, R., von Neuhoff, N., Bufler, J., Krampfl, K., Peschel, T., and Grosskreutz, J. (2005). Amyotrophic lateral sclerosis: new developments in diagnostic markers. Neurodegener Dis *2*, 177-184.
Di Scala, F., Dupuis, L., Gaiddon, C., De Tapia, M., Jokic, N., Gonzalez de Aguilar, J.L., Raul, J.S., Ludes, B., and Loeffler, J.P. (2005). Tissue specificity and regulation of the N-terminal diversity of reticulon 3. Biochem J *385*, 125-134.
Diekmann, H., Klinger, M., Oertle, T., Heinz, D., Pogoda, H.M., Schwab, M.E., and Stuermer, C.A. (2005). Analysis of the reticulon gene family demonstrates the absence of the neurite growth inhibitor Nogo-A in fish. Mol Biol Evol *22*, 1635-1648.

Dimou, L., Schnell, L., Montani, L., Duncan, C., Simonen, M., Schneider, R., Liebscher, T., Gullo, M., and Schwab, M.E. (2006). Nogo-A-deficient mice reveal strain-dependent differences in axonal regeneration. J Neurosci *26*, 5591-5603.
Dodd, D.A., Niederoest, B., Bloechlinger, S., Dupuis, L., Loeffler, J.P., and Schwab, M.E. (2005). Nogo-A, -B, and -C are found on the cell surface and interact together in many different cell types. J Biol Chem *280*, 12494-12502.
Domeniconi, M., Cao, Z., Spencer, T., Sivasankaran, R., Wang, K., Nikulina, E., Kimura, N., Cai, H., Deng, K., Gao, Y., *et al.* (2002). Myelin-associated glycoprotein interacts with the Nogo66 receptor to inhibit neurite outgrowth. Neuron *35*, 283-290.
Dou, C.L., and Levine, J.M. (1994). Inhibition of neurite growth by the NG2 chondroitin sulfate proteoglycan. J Neurosci *14*, 7616-7628.
Dubois, T., and Chavrier, P. (2005). [ARHGAP10, a novel RhoGAP at the cross-road between ARF1 and Cdc42 pathways, regulates Arp2/3 complex and actin dynamics on Golgi membranes]. Med Sci (Paris) *21*, 692-694.
Dupuis, L., Gonzalez de Aguilar, J.L., di Scala, F., Rene, F., de Tapia, M., Pradat, P.F., Lacomblez, L., Seihlan, D., Prinjha, R., Walsh, F.S., *et al.* (2002). Nogo provides a molecular marker for diagnosis of amyotrophic lateral sclerosis. Neurobiol Dis *10*, 358-365.
Emerick, A.J., Neafsey, E.J., Schwab, M.E., and Kartje, G.L. (2003). Functional reorganization of the motor cortex in adult rats after cortical lesion and treatment with monoclonal antibody IN-1. J Neurosci *23*, 4826-4830.
Enzmann, G.U., Benton, R.L., Talbott, J.F., Cao, Q., and Whittemore, S.R. (2006). Functional considerations of stem cell transplantation therapy for spinal cord repair. J Neurotrauma *23*, 479-495.
Eslamboli, A., Grundy, R.I., and Irving, E.A. (2006). Time-dependent increase in Nogo-A expression after focal cerebral ischemia in marmoset monkeys. Neurosci Lett *408*, 89-93.
Etienne-Manneville, S. (2004). Cdc42--the centre of polarity. J Cell Sci *117*, 1291-1300.
Etienne-Manneville, S., and Hall, A. (2002). Rho GTPases in cell biology. Nature *420*, 629-635.
Faissner, A., and Kruse, J. (1990). J1/tenascin is a repulsive substrate for central nervous system neurons. Neuron *5*, 627-637.
Fawcett, J.W., Housden, E., Smith-Thomas, L., and Meyer, R.L. (1989). The growth of axons in three-dimensional astrocyte cultures. Dev Biol *135*, 449-458.
Feuerstein, G. (2006). Inflammation and stroke: therapeutic effects of adenoviral expression of secretory Leukocyte Protease Inhibitor. Front Biosci *11*, 1750-1757.
Filbin, M.T. (1995). Myelin-associated glycoprotein: a role in myelination and in the inhibition of axonal regeneration? Curr Opin Neurobiol *5*, 588-595.
Filbin, M.T. (2003). Myelin-associated inhibitors of axonal regeneration in the adult mammalian CNS. Nat Rev Neurosci *4*, 703-713.
Filbin, M.T. (2006). Recapitulate development to promote axonal regeneration: good or bad approach? Philos Trans R Soc Lond B Biol Sci *361*, 1565-1574.
Fischer, D., He, Z., and Benowitz, L.I. (2004). Counteracting the Nogo receptor enhances optic nerve regeneration if retinal ganglion cells are in an active growth state. J Neurosci *24*, 1646-1651.
Fontoura, P., Ho, P.P., DeVoss, J., Zheng, B., Lee, B.J., Kidd, B.A., Garren, H., Sobel, R.A., Robinson, W.H., Tessier-Lavigne, M., and Steinman, L. (2004). Immunity to the extracellular domain of Nogo-A modulates experimental autoimmune encephalomyelitis. J Immunol *173*, 6981-6992.

Fouad, K., Klusman, I., and Schwab, M.E. (2004). Regenerating corticospinal fibers in the Marmoset (Callitrix jacchus) after spinal cord lesion and treatment with the anti-Nogo-A antibody IN-1. Eur J Neurosci *20*, 2479-2482.
Fouad, K., Schnell, L., Bunge, M.B., Schwab, M.E., Liebscher, T., and Pearse, D.D. (2005). Combining Schwann cell bridges and olfactory-ensheathing glia grafts with chondroitinase promotes locomotor recovery after complete transection of the spinal cord. J Neurosci *25*, 1169-1178.
Fournier, A.E., GrandPre, T., and Strittmatter, S.M. (2001). Identification of a receptor mediating Nogo-66 inhibition of axonal regeneration. Nature *409*, 341-346.
Fournier, A.E., Takizawa, B.T., and Strittmatter, S.M. (2003). Rho kinase inhibition enhances axonal regeneration in the injured CNS. J Neurosci *23*, 1416-1423.
Freund, P., Schmidlin, E., Wannier, T., Bloch, J., Mir, A., Schwab, M.E., and Rouiller, E.M. (2006). Nogo-A-specific antibody treatment enhances sprouting and functional recovery after cervical lesion in adult primates. Nat Med *12*, 790-792.
Freund, P., Wannier, T., Schmidlin, E., Bloch, J., Mir, A., Schwab, M.E., and Rouiller, E.M. (2007). Anti-Nogo-A antibody treatment enhances sprouting of corticospinal axons rostral to a unilateral cervical spinal cord lesion in adult macaque monkey. J Comp Neurol *502*, 644-659.
Fritschy, J.M., Kiener, T., Bouilleret, V., and Loup, F. (1999). GABAergic neurons and GABA(A)-receptors in temporal lobe epilepsy. Neurochem Int *34*, 435-445.
Fritschy, J.M., Weinmann, O., Wenzel, A., and Benke, D. (1998). Synapse-specific localization of NMDA and GABA(A) receptor subunits revealed by antigen-retrieval immunohistochemistry. J Comp Neurol *390*, 194-210.
Fukata, Y., Itoh, T.J., Kimura, T., Menager, C., Nishimura, T., Shiromizu, T., Watanabe, H., Inagaki, N., Iwamatsu, A., Hotani, H., and Kaibuchi, K. (2002). CRMP-2 binds to tubulin heterodimers to promote microtubule assembly. Nat Cell Biol *4*, 583-591.
Gafford, G.M., Parsons, R.G., and Helmstetter, F.J. (2005). Effects of post-training hippocampal injections of midazolam on fear conditioning. Learn Mem *12*, 573-578.
Gahwiler, B.H. (1981a). Morphological differentiation of nerve cells in thin organotypic cultures derived from rat hippocampus and cerebellum. Proc R Soc Lond B Biol Sci *211*, 287-290.
Gahwiler, B.H. (1981b). Nerve cells in organotypic cultures. Jama *245*, 1858-1859.
Gahwiler, B.H. (1981c). Organotypic monolayer cultures of nervous tissue. J Neurosci Methods *4*, 329-342.
Gahwiler, B.H., Capogna, M., Debanne, D., McKinney, R.A., and Thompson, S.M. (1997). Organotypic slice cultures: a technique has come of age. Trends Neurosci *20*, 471-477.
Gao, Y., Nikulina, E., Mellado, W., and Filbin, M.T. (2003). Neurotrophins elevate cAMP to reach a threshold required to overcome inhibition by MAG through extracellular signal-regulated kinase-dependent inhibition of phosphodiesterase. J Neurosci *23*, 11770-11777.
Gardner, J., and Ghorpade, A. (2003). Tissue inhibitor of metalloproteinase (TIMP)-1: the TIMPed balance of matrix metalloproteinases in the central nervous system. J Neurosci Res *74*, 801-806.
Genoux, D., Haditsch, U., Knobloch, M., Michalon, A., Storm, D., and Mansuy, I.M. (2002). Protein phosphatase 1 is a molecular constraint on learning and memory. Nature *418*, 970-975.
Geppert, M., Goda, Y., Stevens, C.F., and Sudhof, T.C. (1997). The small GTP-binding protein Rab3A regulates a late step in synaptic vesicle fusion. Nature *387*, 810-814.

Geppert, M., and Sudhof, T.C. (1998). RAB3 and synaptotagmin: the yin and yang of synaptic membrane fusion. Annu Rev Neurosci *21*, 75-95.
Geyer, M.A., Krebs-Thomson, K., Braff, D.L., and Swerdlow, N.R. (2001). Pharmacological studies of prepulse inhibition models of sensorimotor gating deficits in schizophrenia: a decade in review. Psychopharmacology (Berl) *156*, 117-154.
Gianola, S., Savio, T., Schwab, M.E., and Rossi, F. (2003). Cell-autonomous mechanisms and myelin-associated factors contribute to the development of Purkinje axon intracortical plexus in the rat cerebellum. J Neurosci *23*, 4613-4624.
Gil, V., Nicolas, O., Mingorance, A., Urena, J.M., Tang, B.L., Hirata, T., Saez-Valero, J., Ferrer, I., Soriano, E., and del Rio, J.A. (2006). Nogo-A expression in the human hippocampus in normal aging and in Alzheimer disease. J Neuropathol Exp Neurol *65*, 433-444.
Goldberg, J.L., Vargas, M.E., Wang, J.T., Mandemakers, W., Oster, S.F., Sretavan, D.W., and Barres, B.A. (2004). An oligodendrocyte lineage-specific semaphorin, Sema5A, inhibits axon growth by retinal ganglion cells. J Neurosci *24*, 4989-4999.
Goldshmit, Y., McLenachan, S., and Turnley, A. (2006). Roles of Eph receptors and ephrins in the normal and damaged adult CNS. Brain Res Rev *52*, 327-345.
Govek, E.E., Newey, S.E., and Van Aelst, L. (2005). The role of the Rho GTPases in neuronal development. Genes Dev *19*, 1-49.
Gramsbergen, A. (2001). Normal and abnormal development of motor behavior: lessons from experiments in rats. Neural Plast *8*, 17-29.
GrandPre, T., Li, S., and Strittmatter, S.M. (2002). Nogo-66 receptor antagonist peptide promotes axonal regeneration. Nature *417*, 547-551.
GrandPre, T., Nakamura, F., Vartanian, T., and Strittmatter, S.M. (2000). Identification of the Nogo inhibitor of axon regeneration as a Reticulon protein. Nature *403*, 439-444.
Greengard, P., Allen, P.B., and Nairn, A.C. (1999). Beyond the dopamine receptor: the DARPP-32/protein phosphatase-1 cascade. Neuron *23*, 435-447.
Gross, R.E., Mei, Q., Gutekunst, C.A., and Torre, E. (2007). The pivotal role of RhoA GTPase in the molecular signaling of axon growth inhibition after CNS injury and targeted therapeutic strategies. Cell Transplant *16*, 245-262.
Grosskreutz, Y., Hermann, A., Kins, S., Fuhrmann, J.C., Betz, H., and Kneussel, M. (2001). Identification of a gephyrin-binding motif in the GDP/GTP exchange factor collybistin. Biol Chem *382*, 1455-1462.
Grumet, M., Hoffman, S., Crossin, K.L., and Edelman, G.M. (1985). Cytotactin, an extracellular matrix protein of neural and non-neural tissues that mediates glia-neuron interaction. Proc Natl Acad Sci U S A *82*, 8075-8079.
Hakkoum, D., Stoppini, L., and Muller, D. (2006). Interleukin-6 promotes sprouting and functional recovery in lesioned organotypic hippocampal slice cultures. J Neurochem.
Hall, A. (1998). Rho GTPases and the actin cytoskeleton. Science *279*, 509-514.
Hansen, M.J., Dallal, G.E., and Flanagan, J.G. (2004). Retinal axon response to ephrin-as shows a graded, concentration-dependent transition from growth promotion to inhibition. Neuron *42*, 717-730.
Hauben, E., Ibarra, A., Mizrahi, T., Barouch, R., Agranov, E., and Schwartz, M. (2001). Vaccination with a Nogo-A-derived peptide after incomplete spinal-cord injury promotes recovery via a T-cell-mediated neuroprotective response: comparison with other myelin antigens. Proc Natl Acad Sci U S A *98*, 15173-15178.
He, W., Hu, X., Shi, Q., Zhou, X., Lu, Y., Fisher, C., and Yan, R. (2006). Mapping of interaction domains mediating binding between BACE1 and RTN/Nogo proteins. J Mol Biol *363*, 625-634.

He, Z., and Koprivica, V. (2004). The Nogo signaling pathway for regeneration block. Annu Rev Neurosci *27*, 341-368.
Hensel, T., Amberger, V.R., and Schwab, M.E. (1998). A metalloprotease activity from C6 glioma cells inactivates the myelin-associated neurite growth inhibitors and can be neutralized by antibodies. Br J Cancer *78*, 1564-1572.
Hering, H., and Sheng, M. (2001). Dendritic spines: structure, dynamics and regulation. Nat Rev Neurosci *2*, 880-888.
Hicks, R.R., Smith, D.H., Lowenstein, D.H., Saint Marie, R., and McIntosh, T.K. (1993). Mild experimental brain injury in the rat induces cognitive deficits associated with regional neuronal loss in the hippocampus. J Neurotrauma *10*, 405-414.
Hoffman, H.S., and Searle, J.L. (1965). Acoustic Variables in the Modification of Startle Reaction in the Rat. J Comp Physiol Psychol *60*, 53-58.
Hoffman, S., Crossin, K.L., and Edelman, G.M. (1988). Molecular forms, binding functions, and developmental expression patterns of cytotactin and cytotactin-binding proteoglycan, an interactive pair of extracellular matrix molecules. J Cell Biol *106*, 519-532.
Holopainen, I.E. (2005). Organotypic hippocampal slice cultures: a model system to study basic cellular and molecular mechanisms of neuronal cell death, neuroprotection, and synaptic plasticity. Neurochem Res *30*, 1521-1528.
Horie, H., Kadoya, T., Sango, K., and Hasegawa, M. (2005). Oxidized galectin-1 is an essential factor for peripheral nerve regeneration. Curr Drug Targets *6*, 385-394.
Hsieh, S.H., Ferraro, G.B., and Fournier, A.E. (2006). Myelin-associated inhibitors regulate cofilin phosphorylation and neuronal inhibition through LIM kinase and Slingshot phosphatase. J Neurosci *26*, 1006-1015.
Huang, J.K., Phillips, G.R., Roth, A.D., Pedraza, L., Shan, W., Belkaid, W., Mi, S., Fex-Svenningsen, A., Florens, L., Yates, J.R., 3rd, and Colman, D.R. (2005). Glial membranes at the node of Ranvier prevent neurite outgrowth. Science *310*, 1813-1817.
Huang, W.C., Kuo, W.C., Cherng, J.H., Hsu, S.H., Chen, P.R., Huang, S.H., Huang, M.C., Liu, J.C., and Cheng, H. (2006). Chondroitinase ABC promotes axonal re-growth and behavior recovery in spinal cord injury. Biochem Biophys Res Commun *349*, 963-968.
Huber, A.B., Weinmann, O., Brosamle, C., Oertle, T., and Schwab, M.E. (2002). Patterns of Nogo mRNA and protein expression in the developing and adult rat and after CNS lesions. J Neurosci *22*, 3553-3567.
Huot, J. (2004). Ephrin signaling in axon guidance. Prog Neuropsychopharmacol Biol Psychiatry *28*, 813-818.
Irazoqui, J.E., Gladfelter, A.S., and Lew, D.J. (2004). Cdc42p, GTP hydrolysis, and the cell's sense of direction. Cell Cycle *3*, 861-864.
Ito, Y., Oinuma, I., Katoh, H., Kaibuchi, K., and Negishi, M. (2006). Sema4D/plexin-B1 activates GSK-3beta through R-Ras GAP activity, inducing growth cone collapse. EMBO Rep *7*, 704-709.
Jain, A., Brady-Kalnay, S.M., and Bellamkonda, R.V. (2004). Modulation of Rho GTPase activity alleviates chondroitin sulfate proteoglycan-dependent inhibition of neurite extension. J Neurosci Res *77*, 299-307.
Jokic, N., Gonzalez de Aguilar, J.L., Dimou, L., Lin, S., Fergani, A., Ruegg, M.A., Schwab, M.E., Dupuis, L., and Loeffler, J.P. (2006). The neurite outgrowth inhibitor Nogo-A promotes denervation in an amyotrophic lateral sclerosis model. EMBO Rep *7*, 1162-1167.
Jokic, N., Gonzalez de Aguilar, J.L., Pradat, P.F., Dupuis, L., Echaniz-Laguna, A., Muller, A., Dubourg, O., Seilhean, D., Hauw, J.J., Loeffler, J.P., and Meininger, V.

(2005). Nogo expression in muscle correlates with amyotrophic lateral sclerosis severity. Ann Neurol *57*, 553-556.
Josephson, A., Widenfalk, J., Widmer, H.W., Olson, L., and Spenger, C. (2001). NOGO mRNA expression in adult and fetal human and rat nervous tissue and in weight drop injury. Exp Neurol *169*, 319-328.
Jouvenceau, A., Hedou, G., Potier, B., Kollen, M., Dutar, P., and Mansuy, I.M. (2006). Partial inhibition of PP1 alters bidirectional synaptic plasticity in the hippocampus. Eur J Neurosci *24*, 564-572.
Jurewicz, A., Matysiak, M., Raine, C.S., and Selmaj, K. (2007). Soluble Nogo-A, an inhibitor of axonal regeneration, as a biomarker for multiple sclerosis. Neurology *68*, 283-287.
Kadoya, T., and Horie, H. (2005). Structural and functional studies of galectin-1: a novel axonal regeneration-promoting activity for oxidized galectin-1. Curr Drug Targets *6*, 375-383.
Kaneko, S., Iwanami, A., Nakamura, M., Kishino, A., Kikuchi, K., Shibata, S., Okano, H.J., Ikegami, T., Moriya, A., Konishi, O., *et al.* (2006). A selective Sema3A inhibitor enhances regenerative responses and functional recovery of the injured spinal cord. Nat Med *12*, 1380-1389.
Karnezis, T., Mandemakers, W., McQualter, J.L., Zheng, B., Ho, P.P., Jordan, K.A., Murray, B.M., Barres, B., Tessier-Lavigne, M., and Bernard, C.C. (2004). The neurite outgrowth inhibitor Nogo A is involved in autoimmune-mediated demyelination. Nat Neurosci *7*, 736-744.
Katano, T., Mabuchi, T., Okuda-Ashitaka, E., Inagaki, N., Kinumi, T., and Ito, S. (2006). Proteomic identification of a novel isoform of collapsin response mediator protein-2 in spinal nerves peripheral to dorsal root ganglia. Proteomics *6*, 6085-6094.
Kerlero de Rosbo, N., Honegger, P., Lassmann, H., and Matthieu, J.M. (1990). Demyelination induced in aggregating brain cell cultures by a monoclonal antibody against myelin/oligodendrocyte glycoprotein. J Neurochem *55*, 583-587.
Kim, J.E., Li, S., GrandPre, T., Qiu, D., and Strittmatter, S.M. (2003). Axon regeneration in young adult mice lacking Nogo-A/B. Neuron *38*, 187-199.
Kim, J.E., Liu, B.P., Park, J.H., and Strittmatter, S.M. (2004). Nogo-66 receptor prevents raphespinal and rubrospinal axon regeneration and limits functional recovery from spinal cord injury. Neuron *44*, 439-451.
Kimura, T., Watanabe, H., Iwamatsu, A., and Kaibuchi, K. (2005). Tubulin and CRMP-2 complex is transported via Kinesin-1. J Neurochem *93*, 1371-1382.
Kirsch, J., Meyer, G., and Betz, H. (1996). Synaptic Targeting of Ionotropic Neurotransmitter Receptors. Mol Cell Neurosci *8*, 93-98.
Klapka, N., Hermanns, S., Straten, G., Masanneck, C., Duis, S., Hamers, F.P., Muller, D., Zuschratter, W., and Muller, H.W. (2005). Suppression of fibrous scarring in spinal cord injury of rat promotes long-distance regeneration of corticospinal tract axons, rescue of primary motoneurons in somatosensory cortex and significant functional recovery. Eur J Neurosci *22*, 3047-3058.
Kleiman, R., Banker, G., and Steward, O. (1990). Differential subcellular localization of particular mRNAs in hippocampal neurons in culture. Neuron *5*, 821-830.
Kline, A.E., Massucci, J.L., Marion, D.W., and Dixon, C.E. (2002). Attenuation of working memory and spatial acquisition deficits after a delayed and chronic bromocriptine treatment regimen in rats subjected to traumatic brain injury by controlled cortical impact. J Neurotrauma *19*, 415-425.

Kneussel, M., Brandstatter, J.H., Gasnier, B., Feng, G., Sanes, J.R., and Betz, H. (2001). Gephyrin-independent clustering of postsynaptic GABA(A) receptor subtypes. Mol Cell Neurosci *17*, 973-982.
Kolb, B., and Holmes, C. (1983). Neonatal motor cortex lesions in the rat: absence of sparing of motor behaviors and impaired spatial learning concurrent with abnormal cerebral morphogenesis. Behav Neurosci *97*, 697-709.
Kolb, B., Sutherland, R.J., and Whisaw, I.Q. (1983). Neonatal hemidecortication or frontal cortex ablation produces similar behavioral sparing but opposite effects on morphogenesis of remaining cortex. Behav Neurosci *97*, 154-158.
Kolb, B., and Whishaw, I.Q. (1998). Brain plasticity and behavior. Annu Rev Psychol *49*, 43-64.
Kotapka, M.J., Graham, D.I., Adams, J.H., and Gennarelli, T.A. (1994). Hippocampal pathology in fatal human head injury without high intracranial pressure. J Neurotrauma *11*, 317-324.
Kottis, V., Thibault, P., Mikol, D., Xiao, Z.C., Zhang, R., Dergham, P., and Braun, P.E. (2002). Oligodendrocyte-myelin glycoprotein (OMgp) is an inhibitor of neurite outgrowth. J Neurochem *82*, 1566-1569.
Krebs-Kraft, D.L., Wheeler, M.G., and Parent, M.B. (2007). The memory-impairing effects of septal GABA receptor activation involve GABAergic septo-hippocampal projection neurons. Learn Mem *14*, 833-841.
Kruse, J., Keilhauer, G., Faissner, A., Timpl, R., and Schachner, M. (1985). The J1 glycoprotein--a novel nervous system cell adhesion molecule of the L2/HNK-1 family. Nature *316*, 146-148.
Lee, J.K., Kim, J.E., Sivula, M., and Strittmatter, S.M. (2004). Nogo receptor antagonism promotes stroke recovery by enhancing axonal plasticity. J Neurosci *24*, 6209-6217.
Lemons, M.L., Howland, D.R., and Anderson, D.K. (1999). Chondroitin sulfate proteoglycan immunoreactivity increases following spinal cord injury and transplantation. Exp Neurol *160*, 51-65.
Lensch, M., Lohr, M., Russwurm, R., Vidal, M., Kaltner, H., Andre, S., and Gabius, H.J. (2006). Unique sequence and expression profiles of rat galectins-5 and -9 as a result of species-specific gene divergence. Int J Biochem Cell Biol *38*, 1741-1758.
Lenzlinger, P.M., Shimizu, S., Marklund, N., Thompson, H.J., Schwab, M.E., Saatman, K.E., Hoover, R.C., Bareyre, F.M., Motta, M., Luginbuhl, A., *et al.* (2005). Delayed inhibition of Nogo-A does not alter injury-induced axonal sprouting but enhances recovery of cognitive function following experimental traumatic brain injury in rats. Neuroscience *134*, 1047-1056.
Li, M., Shibata, A., Li, C., Braun, P.E., McKerracher, L., Roder, J., Kater, S.B., and David, S. (1996). Myelin-associated glycoprotein inhibits neurite/axon growth and causes growth cone collapse. J Neurosci Res *46*, 404-414.
Li, Q., Qi, B., Oka, K., Shimakage, M., Yoshioka, N., Inoue, H., Hakura, A., Kodama, K., Stanbridge, E.J., and Yutsudo, M. (2001). Link of a new type of apoptosis-inducing gene ASY/Nogo-B to human cancer. Oncogene *20*, 3929-3936.
Li, S., Liu, B.P., Budel, S., Li, M., Ji, B., Walus, L., Li, W., Jirik, A., Rabacchi, S., Choi, E., *et al.* (2004). Blockade of Nogo-66, myelin-associated glycoprotein, and oligodendrocyte myelin glycoprotein by soluble Nogo-66 receptor promotes axonal sprouting and recovery after spinal injury. J Neurosci *24*, 10511-10520.
Liao, H., Duka, T., Teng, F.Y., Sun, L., Bu, W.Y., Ahmed, S., Tang, B.L., and Xiao, Z.C. (2004). Nogo-66 and myelin-associated glycoprotein (MAG) inhibit the adhesion

and migration of Nogo-66 receptor expressing human glioma cells. J Neurochem *90*, 1156-1162.
Liebscher, T., Schnell, L., Schnell, D., Scholl, J., Schneider, R., Gullo, M., Fouad, K., Mir, A., Rausch, M., Kindler, D., *et al.* (2005). Nogo-A antibody improves regeneration and locomotion of spinal cord-injured rats. Ann Neurol *58*, 706-719.
Lindsay, S.J. (2004). Hand-held pneumatic impact handpiece for delicate, e.g. hand engraving operation, of jewelry, has variable fuel meter and work energy supply which regulate supply of pressurized fluid and of work energy based on pressure sensor output. In Derwent Innovations Index, U.S.P. Office, ed. (US, Lindsay, S J (LIND-Individual)), p. 13.
Liu, B.P., Fournier, A., GrandPre, T., and Strittmatter, S.M. (2002). Myelin-associated glycoprotein as a functional ligand for the Nogo-66 receptor. Science *297*, 1190-1193.
Logan, A., Baird, A., and Berry, M. (1999a). Decorin attenuates gliotic scar formation in the rat cerebral hemisphere. Exp Neurol *159*, 504-510.
Logan, A., Green, J., Hunter, A., Jackson, R., and Berry, M. (1999b). Inhibition of glial scarring in the injured rat brain by a recombinant human monoclonal antibody to transforming growth factor-beta2. Eur J Neurosci *11*, 2367-2374.
Lorenzo, L.E., Barbe, A., Portalier, P., Fritschy, J.M., and Bras, H. (2006). Differential expression of GABAA and glycine receptors in ALS-resistant vs. ALS-vulnerable motoneurons: possible implications for selective vulnerability of motoneurons. Eur J Neurosci *23*, 3161-3170.
Lyeth, B.G., Jenkins, L.W., Hamm, R.J., Dixon, C.E., Phillips, L.L., Clifton, G.L., Young, H.F., and Hayes, R.L. (1990). Prolonged memory impairment in the absence of hippocampal cell death following traumatic brain injury in the rat. Brain Res *526*, 249-258.
Maher, E.A., Furnari, F.B., Bachoo, R.M., Rowitch, D.H., Louis, D.N., Cavenee, W.K., and DePinho, R.A. (2001). Malignant glioma: genetics and biology of a grave matter. Genes Dev *15*, 1311-1333.
Manitt, C., Colicos, M.A., Thompson, K.M., Rousselle, E., Peterson, A.C., and Kennedy, T.E. (2001). Widespread expression of netrin-1 by neurons and oligodendrocytes in the adult mammalian spinal cord. J Neurosci *21*, 3911-3922.
Manitt, C., and Kennedy, T.E. (2002). Where the rubber meets the road: netrin expression and function in developing and adult nervous systems. Prog Brain Res *137*, 425-442.
Manitt, C., Wang, D., Kennedy, T.E., and Howland, D.R. (2006). Positioned to inhibit: netrin-1 and netrin receptor expression after spinal cord injury. J Neurosci Res *84*, 1808-1820.
Mann, F., and Rougon, G. (2007). Mechanisms of axon guidance: membrane dynamics and axonal transport in semaphorin signalling. J Neurochem.
Marklund, N., Fulp, C.T., Shimizu, S., Puri, R., McMillan, A., Strittmatter, S.M., and McIntosh, T.K. (2006). Selective temporal and regional alterations of Nogo-A and small proline-rich repeat protein 1A (SPRR1A) but not Nogo-66 receptor (NgR) occur following traumatic brain injury in the rat. Exp Neurol *197*, 70-83.
Markus, T.M., Tsai, S.Y., Bollnow, M.R., Farrer, R.G., O'Brien, T.E., Kindler-Baumann, D.R., Rausch, M., Rudin, M., Wiessner, C., Mir, A.K., *et al.* (2005). Recovery and brain reorganization after stroke in adult and aged rats. Ann Neurol *58*, 950-953.
Massey, J.M., Amps, J., Viapiano, M.S., Matthews, R.T., Wagoner, M.R., Whitaker, C.M., Alilain, W., Yonkof, A.L., Khalyfa, A., Cooper, N.G., *et al.* (2007). Increased chondroitin sulfate proteoglycan expression in denervated brainstem targets following

spinal cord injury creates a barrier to axonal regeneration overcome by chondroitinase ABC and neurotrophin-3. Exp Neurol.
Massey, J.M., Hubscher, C.H., Wagoner, M.R., Decker, J.A., Amps, J., Silver, J., and Onifer, S.M. (2006). Chondroitinase ABC digestion of the perineuronal net promotes functional collateral sprouting in the cuneate nucleus after cervical spinal cord injury. J Neurosci *26*, 4406-4414.
McBain, C.J., Boden, P., and Hill, R.G. (1989). Rat hippocampal slices 'in vitro' display spontaneous epileptiform activity following long-term organotypic culture. J Neurosci Methods *27*, 35-49.
McKeon, R.J., Schreiber, R.C., Rudge, J.S., and Silver, J. (1991). Reduction of neurite outgrowth in a model of glial scarring following CNS injury is correlated with the expression of inhibitory molecules on reactive astrocytes. J Neurosci *11*, 3398-3411.
McKerracher, L., David, S., Jackson, D.L., Kottis, V., Dunn, R.J., and Braun, P.E. (1994). Identification of myelin-associated glycoprotein as a major myelin-derived inhibitor of neurite growth. Neuron *13*, 805-811.
McKerracher, L., and Higuchi, H. (2006). Targeting Rho to stimulate repair after spinal cord injury. J Neurotrauma *23*, 309-317.
McKerracher, L., and Winton, M.J. (2002). Nogo on the go. Neuron *36*, 345-348.
McKinney, R.A., Debanne, D., Gahwiler, B.H., and Thompson, S.M. (1997). Lesion-induced axonal sprouting and hyperexcitability in the hippocampus in vitro: implications for the genesis of posttraumatic epilepsy. Nat Med *3*, 990-996.
McKinney, R.A., Luthi, A., Bandtlow, C.E., Gahwiler, B.H., and Thompson, S.M. (1999). Selective glutamate receptor antagonists can induce or prevent axonal sprouting in rat hippocampal slice cultures. Proc Natl Acad Sci U S A *96*, 11631-11636.
Mehta, N.R., Lopez, P.H., Vyas, A.A., and Schnaar, R.L. (2007). Gangliosides and Nogo receptors independently mediate myelin-associated glycoprotein inhibition of neurite outgrowth in different nerve cells. J Biol Chem.
Meier, S., Brauer, A.U., Heimrich, B., Schwab, M.E., Nitsch, R., and Savaskan, N.E. (2003). Molecular analysis of Nogo expression in the hippocampus during development and following lesion and seizure. Faseb J *17*, 1153-1155.
Menetrey, J., Perderiset, M., Cicolari, J., Dubois, T., Elkhatib, N., Khadali, F.E., Franco, M., Chavrier, P., and Houdusse, A. (2007). Structural basis for ARF1-mediated recruitment of ARHGAP21 to Golgi membranes. Embo J *26*, 1953-1962.
Merkler, D., Metz, G.A., Raineteau, O., Dietz, V., Schwab, M.E., and Fouad, K. (2001). Locomotor recovery in spinal cord-injured rats treated with an antibody neutralizing the myelin-associated neurite growth inhibitor Nogo-A. J Neurosci *21*, 3665-3673.
Merkler, D., Oertle, T., Buss, A., Pinschewer, D.D., Schnell, L., Bareyre, F.M., Kerschensteiner, M., Buddeberg, B.S., and Schwab, M.E. (2003). Rapid induction of autoantibodies against Nogo-A and MOG in the absence of an encephalitogenic T cell response: implication for immunotherapeutic approaches in neurological diseases. Faseb J *17*, 2275-2277.
Mi, S., Lee, X., Shao, Z., Thill, G., Ji, B., Relton, J., Levesque, M., Allaire, N., Perrin, S., Sands, B., *et al.* (2004). LINGO-1 is a component of the Nogo-66 receptor/p75 signaling complex. Nat Neurosci *7*, 221-228.
Mielke, J.G., Comas, T., Woulfe, J., Monette, R., Chakravarthy, B., and Mealing, G.A. (2005). Cytoskeletal, synaptic, and nuclear protein changes associated with rat interface organotypic hippocampal slice culture development. Brain Res Dev Brain Res *160*, 275-286.

Mikol, D.D., Gulcher, J.R., and Stefansson, K. (1990). The oligodendrocyte-myelin glycoprotein belongs to a distinct family of proteins and contains the HNK-1 carbohydrate. J Cell Biol *110*, 471-479.
Mingorance-Le Meur, A., Zheng, B., Soriano, E., and Del Rio, J.A. (2007). Involvement of the Myelin-Associated Inhibitor Nogo-A in Early Cortical Development and Neuronal Maturation. Cereb Cortex.
Mingorance, A., Fontana, X., Sole, M., Burgaya, F., Urena, J.M., Teng, F.Y., Tang, B.L., Hunt, D., Anderson, P.N., Bethea, J.R., *et al.* (2004). Regulation of Nogo and Nogo receptor during the development of the entorhino-hippocampal pathway and after adult hippocampal lesions. Mol Cell Neurosci *26*, 34-49.
Mingorance, A., Sole, M., Muneton, V., Martinez, A., Nieto-Sampedro, M., Soriano, E., and del Rio, J.A. (2006). Regeneration of lesioned entorhino-hippocampal axons in vitro by combined degradation of inhibitory proteoglycans and blockade of Nogo-66/NgR signaling. Faseb J *20*, 491-493.
Mohler, H. (2007). Molecular regulation of cognitive functions and developmental plasticity: impact of GABAA receptors. J Neurochem *102*, 1-12.
Monnier, P.P., Sierra, A., Schwab, J.M., Henke-Fahle, S., and Mueller, B.K. (2003). The Rho/ROCK pathway mediates neurite growth-inhibitory activity associated with the chondroitin sulfate proteoglycans of the CNS glial scar. Mol Cell Neurosci *22*, 319-330.
Moon, L.D., Asher, R.A., Rhodes, K.E., and Fawcett, J.W. (2001). Regeneration of CNS axons back to their target following treatment of adult rat brain with chondroitinase ABC. Nat Neurosci *4*, 465-466.
Mora, F., Segovia, G., and Del Arco, A. (2007). Aging, plasticity and environmental enrichment: Structural changes and neurotransmitter dynamics in several areas of the brain. Brain Res Rev *55*, 78-88.
Moreau-Fauvarque, C., Kumanogoh, A., Camand, E., Jaillard, C., Barbin, G., Boquet, I., Love, C., Jones, E.Y., Kikutani, H., Lubetzki, C., *et al.* (2003). The transmembrane semaphorin Sema4D/CD100, an inhibitor of axonal growth, is expressed on oligodendrocytes and upregulated after CNS lesion. J Neurosci *23*, 9229-9239.
Moreira, E.F., Jaworski, C.J., and Rodriguez, I.R. (1999). Cloning of a novel member of the reticulon gene family (RTN3): gene structure and chromosomal localization to 11q13. Genomics *58*, 73-81.
Morgenstern, D.A., Asher, R.A., and Fawcett, J.W. (2002). Chondroitin sulphate proteoglycans in the CNS injury response. Prog Brain Res *137*, 313-332.
Mukhopadhyay, G., Doherty, P., Walsh, F.S., Crocker, P.R., and Filbin, M.T. (1994). A novel role for myelin-associated glycoprotein as an inhibitor of axonal regeneration. Neuron *13*, 757-767.
Muller, D., Buchs, P.A., and Stoppini, L. (1993). Time course of synaptic development in hippocampal organotypic cultures. Brain Res Dev Brain Res *71*, 93-100.
Negishi, M., Oinuma, I., and Katoh, H. (2005). R-ras as a key player for signaling pathway of plexins. Mol Neurobiol *32*, 217-222.
Niclou, S.P., Franssen, E.H., Ehlert, E.M., Taniguchi, M., and Verhaagen, J. (2003). Meningeal cell-derived semaphorin 3A inhibits neurite outgrowth. Mol Cell Neurosci *24*, 902-912.
Nie, D.Y., Zhou, Z.H., Ang, B.T., Teng, F.Y., Xu, G., Xiang, T., Wang, C.Y., Zeng, L., Takeda, Y., Xu, T.L., *et al.* (2003). Nogo-A at CNS paranodes is a ligand of Caspr: possible regulation of K(+) channel localization. Embo J *22*, 5666-5678.

Niederost, B., Oertle, T., Fritsche, J., McKinney, R.A., and Bandtlow, C.E. (2002). Nogo-A and myelin-associated glycoprotein mediate neurite growth inhibition by antagonistic regulation of RhoA and Rac1. J Neurosci *22*, 10368-10376.
Nikonenko, I., Jourdain, P., Alberi, S., Toni, N., and Muller, D. (2002). Activity-induced changes of spine morphology. Hippocampus *12*, 585-591.
Nimchinsky, E.A., Sabatini, B.L., and Svoboda, K. (2002). Structure and function of dendritic spines. Annu Rev Physiol *64*, 313-353.
Noraberg, J., Poulsen, F.R., Blaabjerg, M., Kristensen, B.W., Bonde, C., Montero, M., Meyer, M., Gramsbergen, J.B., and Zimmer, J. (2005). Organotypic hippocampal slice cultures for studies of brain damage, neuroprotection and neurorepair. Curr Drug Targets CNS Neurol Disord *4*, 435-452.
Novak, G., Kim, D., Seeman, P., and Tallerico, T. (2002). Schizophrenia and Nogo: elevated mRNA in cortex, and high prevalence of a homozygous CAA insert. Brain Res Mol Brain Res *107*, 183-189.
Novak, G., and Tallerico, T. (2006). Nogo A, B and C expression in schizophrenia, depression and bipolar frontal cortex, and correlation of Nogo expression with CAA/TATC polymorphism in 3'-UTR. Brain Res *1120*, 161-171.
O'Neill, P., Whalley, K., and Ferretti, P. (2004). Nogo and Nogo-66 receptor in human and chick: implications for development and regeneration. Dev Dyn *231*, 109-121.
Oertle, T., Huber, C., van der Putten, H., and Schwab, M.E. (2003a). Genomic structure and functional characterisation of the promoters of human and mouse nogo/rtn4. J Mol Biol *325*, 299-323.
Oertle, T., Klinger, M., Stuermer, C.A., and Schwab, M.E. (2003b). A reticular rhapsody: phylogenic evolution and nomenclature of the RTN/Nogo gene family. Faseb J *17*, 1238-1247.
Oertle, T., Merkler, D., and Schwab, M.E. (2003c). Do cancer cells die because of Nogo-B? Oncogene *22*, 1390-1399.
Oertle, T., and Schwab, M.E. (2003). Nogo and its paRTNers. Trends Cell Biol *13*, 187-194.
Oertle, T., van der Haar, M.E., Bandtlow, C.E., Robeva, A., Burfeind, P., Buss, A., Huber, A.B., Simonen, M., Schnell, L., Brosamle, C., *et al.* (2003d). Nogo-A inhibits neurite outgrowth and cell spreading with three discrete regions. J Neurosci *23*, 5393-5406.
Oinuma, I., Ishikawa, Y., Katoh, H., and Negishi, M. (2004). The Semaphorin 4D receptor Plexin-B1 is a GTPase activating protein for R-Ras. Science *305*, 862-865.
Oinuma, I., Katoh, H., and Negishi, M. (2007). R-Ras controls axon specification upstream of glycogen synthase kinase-3beta through integrin-linked kinase. J Biol Chem *282*, 303-318.
Onoue, H., Satoh, J.I., Ogawa, M., Tabunoki, H., and Yamamura, T. (2007). Detection of anti-Nogo receptor autoantibody in the serum of multiple sclerosis and controls. Acta Neurol Scand *115*, 153-160.
Oohira, A., Matsui, F., and Katoh-Semba, R. (1991). Inhibitory effects of brain chondroitin sulfate proteoglycans on neurite outgrowth from PC12D cells. J Neurosci *11*, 822-827.
Oudega, M., and Xu, X.M. (2006). Schwann cell transplantation for repair of the adult spinal cord. J Neurotrauma *23*, 453-467.
Paganetti, P.A., Caroni, P., and Schwab, M.E. (1988). Glioblastoma infiltration into central nervous system tissue in vitro: involvement of a metalloprotease. J Cell Biol *107*, 2281-2291.

Papadopoulos, C.M., Tsai, S.Y., Alsbiei, T., O'Brien, T.E., Schwab, M.E., and Kartje, G.L. (2002). Functional recovery and neuroanatomical plasticity following middle cerebral artery occlusion and IN-1 antibody treatment in the adult rat. Ann Neurol *51*, 433-441.

Papadopoulos, C.M., Tsai, S.Y., Cheatwood, J.L., Bollnow, M.R., Kolb, B.E., Schwab, M.E., and Kartje, G.L. (2005). Dendritic Plasticity in the Adult Rat Following Middle Cerebral Artery Occlusion and Nogo-A Neutralization. Cereb Cortex.

Papadopoulos, C.M., Tsai, S.Y., Cheatwood, J.L., Bollnow, M.R., Kolb, B.E., Schwab, M.E., and Kartje, G.L. (2006). Dendritic plasticity in the adult rat following middle cerebral artery occlusion and nogo-a neutralization. Cereb Cortex *16*, 529-536.

Park, J.B., Yiu, G., Kaneko, S., Wang, J., Chang, J., He, X.L., Garcia, K.C., and He, Z. (2005). A TNF receptor family member, TROY, is a coreceptor with Nogo receptor in mediating the inhibitory activity of myelin inhibitors. Neuron *45*, 345-351.

Pearse, D.D., and Bunge, M.B. (2006). Designing cell- and gene-based regeneration strategies to repair the injured spinal cord. J Neurotrauma *23*, 438-452.

Pesheva, P., Spiess, E., and Schachner, M. (1989). J1-160 and J1-180 are oligodendrocyte-secreted nonpermissive substrates for cell adhesion. J Cell Biol *109*, 1765-1778.

Pradat, P.F., Bruneteau, G., Gonzalez De Aguilar, J.L., Dupuis, L., Jokic, N., Salachas, F., Le Forestier, N., Echaniz-Laguna, A., Dubourg, O., Hauw, J.J., *et al.* (2007). Muscle nogo-a expression is a prognostic marker in lower motor neuron syndromes. Ann Neurol.

Prieto, A.L., Jones, F.S., Cunningham, B.A., Crossin, K.L., and Edelman, G.M. (1990). Localization during development of alternatively spliced forms of cytotactin mRNA by in situ hybridization. J Cell Biol *111*, 685-698.

Prinjha, R., Moore, S.E., Vinson, M., Blake, S., Morrow, R., Christie, G., Michalovich, D., Simmons, D.L., and Walsh, F.S. (2000). Inhibitor of neurite outgrowth in humans. Nature *403*, 383-384.

Probstmeier, R., Stichel, C.C., Muller, H.W., Asou, H., and Pesheva, P. (2000). Chondroitin sulfates expressed on oligodendrocyte-derived tenascin-R are involved in neural cell recognition. Functional implications during CNS development and regeneration. J Neurosci Res *60*, 21-36.

Qi, B., Qi, Y., Watari, A., Yoshioka, N., Inoue, H., Minemoto, Y., Yamashita, K., Sasagawa, T., and Yutsudo, M. (2003). Pro-apoptotic ASY/Nogo-B protein associates with ASYIP. J Cell Physiol *196*, 312-318.

Qiu, J., Cai, D., Dai, H., McAtee, M., Hoffman, P.N., Bregman, B.S., and Filbin, M.T. (2002). Spinal axon regeneration induced by elevation of cyclic AMP. Neuron *34*, 895-903.

Quach, T.T., Duchemin, A.M., Rogemond, V., Aguera, M., Honnorat, J., Belin, M.F., and Kolattukudy, P.E. (2004). Involvement of collapsin response mediator proteins in the neurite extension induced by neurotrophins in dorsal root ganglion neurons. Mol Cell Neurosci *25*, 433-443.

Quarles, R.H., Everly, J.L., and Brady, R.O. (1973). Evidence for the close association of a glycoprotein with myelin in rat brain. J Neurochem *21*, 1177-1191.

Quarles, R.H., and Trapp, B.D. (1984). Localization of myelin-associated glycoprotein. J Neurochem *43*, 1773-1777.

Raineteau, O., Fouad, K., Bareyre, F.M., and Schwab, M.E. (2002). Reorganization of descending motor tracts in the rat spinal cord. Eur J Neurosci *16*, 1761-1771.

Raineteau, O., and Schwab, M.E. (2001). Plasticity of motor systems after incomplete spinal cord injury. Nat Rev Neurosci *2*, 263-273.

Reid, T., Bathoorn, A., Ahmadian, M.R., and Collard, J.G. (1999). Identification and characterization of hPEM-2, a guanine nucleotide exchange factor specific for Cdc42. J Biol Chem *274*, 33587-33593.
Reindl, M., Khantane, S., Ehling, R., Schanda, K., Lutterotti, A., Brinkhoff, C., Oertle, T., Schwab, M.E., Deisenhammer, F., Berger, T., and Bandtlow, C.E. (2003). Serum and cerebrospinal fluid antibodies to Nogo-A in patients with multiple sclerosis and acute neurological disorders. J Neuroimmunol *145*, 139-147.
Reines, A., Cereseto, M., Ferrero, A., Bonavita, C., and Wikinski, S. (2004). Neuronal cytoskeletal alterations in an experimental model of depression. Neuroscience *129*, 529-538.
Richard, M., Giannetti, N., Saucier, D., Sacquet, J., Jourdan, F., and Pellier-Monnin, V. (2005). Neuronal expression of Nogo-A mRNA and protein during neurite outgrowth in the developing rat olfactory system. Eur J Neurosci *22*, 2145-2158.
Robinson, W.H., Utz, P.J., and Steinman, L. (2003). Genomic and proteomic analysis of multiple sclerosis. Opinion. Curr Opin Immunol *15*, 660-667.
Roebroek, A.J., Ayoubi, T.A., Van de Velde, H.J., Schoenmakers, E.F., Pauli, I.G., and Van de Ven, W.J. (1996). Genomic organization of the human NSP gene, prototype of a novel gene family encoding reticulons. Genomics *32*, 191-199.
Rossi, F., Gianola, S., and Corvetti, L. (2007). Regulation of intrinsic neuronal properties for axon growth and regeneration. Prog Neurobiol *81*, 1-28.
Rothwell, N.J., and Hopkins, S.J. (1995). Cytokines and the nervous system II: Actions and mechanisms of action. Trends Neurosci *18*, 130-136.
Rothwell, N.J., and Strijbos, P.J. (1995). Cytokines in neurodegeneration and repair. Int J Dev Neurosci *13*, 179-185.
Rubin, B.P., Dusart, I., and Schwab, M.E. (1994). A monoclonal antibody (IN-1) which neutralizes neurite growth inhibitory proteins in the rat CNS recognizes antigens localized in CNS myelin. J Neurocytol *23*, 209-217.
Rudge, J.S., and Silver, J. (1990). Inhibition of neurite outgrowth on astroglial scars in vitro. J Neurosci *10*, 3594-3603.
Sakaguchi, T., Okada, M., and Kawasaki, K. (1994). Sprouting of CA3 pyramidal neurons to the dentate gyrus in rat hippocampal organotypic cultures. Neurosci Res *20*, 157-164.
Satoh, J., Onoue, H., Arima, K., and Yamamura, T. (2005). Nogo-A and nogo receptor expression in demyelinating lesions of multiple sclerosis. J Neuropathol Exp Neurol *64*, 129-138.
Schnell, L., and Schwab, M.E. (1990). Axonal regeneration in the rat spinal cord produced by an antibody against myelin-associated neurite growth inhibitors. Nature *343*, 269-272.
Schwab, M.E. (2004). Nogo and axon regeneration. Curr Opin Neurobiol *14*, 118-124.
Schwab, M.E., and Caroni, P. (1988). Oligodendrocytes and CNS myelin are nonpermissive substrates for neurite growth and fibroblast spreading in vitro. J Neurosci *8*, 2381-2393.
Schweigreiter, R., Walmsley, A.R., Niederost, B., Zimmermann, D.R., Oertle, T., Casademunt, E., Frentzel, S., Dechant, G., Mir, A., and Bandtlow, C.E. (2004). Versican V2 and the central inhibitory domain of Nogo-A inhibit neurite growth via p75NTR/NgR-independent pathways that converge at RhoA. Mol Cell Neurosci *27*, 163-174.
Seymour, A.B., Andrews, E.M., Tsai, S.Y., Markus, T.M., Bollnow, M.R., Brenneman, M.M., O'Brien, T.E., Castro, A.J., Schwab, M.E., and Kartje, G.L. (2005). Delayed treatment with monoclonal antibody IN-1 1 week after stroke results in recovery of

function and corticorubral plasticity in adult rats. J Cereb Blood Flow Metab *25*, 1366-1375.
Shaw, G., Banker, G.A., and Weber, K. (1985). An immunofluorescence study of neurofilament protein expression by developing hippocampal neurons in tissue culture. Eur J Cell Biol *39*, 205-216.
Shaw, G., and Weber, K. (1981). The distribution of the neurofilament triplet proteins within individual neurones. Exp Cell Res *136*, 119-125.
Shen, Y.J., DeBellard, M.E., Salzer, J.L., Roder, J., and Filbin, M.T. (1998). Myelin-associated glycoprotein in myelin and expressed by Schwann cells inhibits axonal regeneration and branching. Mol Cell Neurosci *12*, 79-91.
Sicotte, M., Tsatas, O., Jeong, S.Y., Cai, C.Q., He, Z., and David, S. (2003). Immunization with myelin or recombinant Nogo-66/MAG in alum promotes axon regeneration and sprouting after corticospinal tract lesions in the spinal cord. Mol Cell Neurosci *23*, 251-263.
Simonen, M., Pedersen, V., Weinmann, O., Schnell, L., Buss, A., Ledermann, B., Christ, F., Sansig, G., van der Putten, H., and Schwab, M.E. (2003). Systemic deletion of the myelin-associated outgrowth inhibitor Nogo-A improves regenerative and plastic responses after spinal cord injury. Neuron *38*, 201-211.
Smith, A., and Sugar, O. (1975). Development of above normal language and intelligence 21 years after left hemispherectomy. Neurology *25*, 813-818.
Snow, D.M., Lemmon, V., Carrino, D.A., Caplan, A.I., and Silver, J. (1990a). Sulfated proteoglycans in astroglial barriers inhibit neurite outgrowth in vitro. Exp Neurol *109*, 111-130.
Snow, D.M., Steindler, D.A., and Silver, J. (1990b). Molecular and cellular characterization of the glial roof plate of the spinal cord and optic tectum: a possible role for a proteoglycan in the development of an axon barrier. Dev Biol *138*, 359-376.
Sousa, S., Cabanes, D., Archambaud, C., Colland, F., Lemichez, E., Popoff, M., Boisson-Dupuis, S., Gouin, E., Lecuit, M., Legrain, P., and Cossart, P. (2005). ARHGAP10 is necessary for alpha-catenin recruitment at adherens junctions and for Listeria invasion. Nat Cell Biol *7*, 954-960.
Spillmann, A.A., Bandtlow, C.E., Lottspeich, F., Keller, F., and Schwab, M.E. (1998). Identification and characterization of a bovine neurite growth inhibitor (bNI-220). J Biol Chem *273*, 19283-19293.
Steindler, D.A., Cooper, N.G., Faissner, A., and Schachner, M. (1989). Boundaries defined by adhesion molecules during development of the cerebral cortex: the J1/tenascin glycoprotein in the mouse somatosensory cortical barrel field. Dev Biol *131*, 243-260.
Steward, O., Zheng, B., Banos, K., and Yee, K.M. (2007). Response to: Kim et al., "axon regeneration in young adult mice lacking Nogo-A/B." Neuron 38, 187-199. Neuron *54*, 191-195.
Stone, M.E., Grimes, B.S., and Katz, D.B. (2005). Hippocampal inactivation enhances taste learning. Learn Mem *12*, 579-586.
Stoppini, L., Buchs, P.A., and Muller, D. (1991). A simple method for organotypic cultures of nervous tissue. J Neurosci Methods *37*, 173-182.
Stoppini, L., Buchs, P.A., and Muller, D. (1993). Lesion-induced neurite sprouting and synapse formation in hippocampal organotypic cultures. Neuroscience *57*, 985-994.
Stoppini, L., Parisi, L., Oropesa, C., and Muller, D. (1997). Sprouting and functional recovery in co-cultures between old and young hippocampal organotypic slices. Neuroscience *80*, 1127-1136.

Streit, P., Thompson, S.M., and Gahwiler, B.H. (1989). Anatomical and Physiological Properties of GABAergic Neurotransmission in Organotypic Slice Cultures of Rat Hippocampus. Eur J Neurosci *1*, 603-615.
Strittmatter, S.M. (2002). Modulation of axonal regeneration in neurodegenerative disease: focus on Nogo. J Mol Neurosci *19*, 117-121.
Sudhof, T.C. (2004). The synaptic vesicle cycle. Annu Rev Neurosci *27*, 509-547.
Suzuki, Y., Nakagomi, S., Namikawa, K., Kiryu-Seo, S., Inagaki, N., Kaibuchi, K., Aizawa, H., Kikuchi, K., and Kiyama, H. (2003). Collapsin response mediator protein-2 accelerates axon regeneration of nerve-injured motor neurons of rat. J Neurochem *86*, 1042-1050.
Tagami, S., Eguchi, Y., Kinoshita, M., Takeda, M., and Tsujimoto, Y. (2000). A novel protein, RTN-XS, interacts with both Bcl-XL and Bcl-2 on endoplasmic reticulum and reduces their anti-apoptotic activity. Oncogene *19*, 5736-5746.
Tagerud, S., Libelius, R., and Magnusson, C. (2007). Muscle Nogo-A: a marker for amyotrophic lateral sclerosis or for denervation? Ann Neurol.
Takeda, Y., Kamida, T., Fujiki, M., and Kobayashi, H. (2007). Hippocampal Nogo-A and neo-Timm's staining in amygdala kindling rats. Neurol Res *29*, 199-203.
Tang, S., Qiu, J., Nikulina, E., and Filbin, M.T. (2001). Soluble myelin-associated glycoprotein released from damaged white matter inhibits axonal regeneration. Mol Cell Neurosci *18*, 259-269.
Tang, S., Woodhall, R.W., Shen, Y.J., deBellard, M.E., Saffell, J.L., Doherty, P., Walsh, F.S., and Filbin, M.T. (1997). Soluble myelin-associated glycoprotein (MAG) found in vivo inhibits axonal regeneration. Mol Cell Neurosci *9*, 333-346.
Tate, D.F., and Bigler, E.D. (2000). Fornix and hippocampal atrophy in traumatic brain injury. Learn Mem *7*, 442-446.
Teng, F.Y., and Tang, B.L. (2005). Why do Nogo/Nogo-66 receptor gene knockouts result in inferior regeneration compared to treatment with neutralizing agents? J Neurochem *94*, 865-874.
Thom, T., Haase, N., Rosamond, W., Howard, V.J., Rumsfeld, J., Manolio, T., Zheng, Z.J., Flegal, K., O'Donnell, C., Kittner, S., *et al.* (2006). Heart disease and stroke statistics--2006 update: a report from the American Heart Association Statistics Committee and Stroke Statistics Subcommittee. Circulation *113*, e85-151.
Torigoe, K., and Lundborg, G. (1998). Selective inhibition of early axonal regeneration by myelin-associated glycoprotein. Exp Neurol *150*, 254-262.
Toscano, M.A., Ilarregui, J.M., Bianco, G.A., Campagna, L., Croci, D.O., Salatino, M., and Rabinovich, G.A. (2007). Dissecting the pathophysiologic role of endogenous lectins: glycan-binding proteins with cytokine-like activity? Cytokine Growth Factor Rev *18*, 57-71.
Trapp, B.D., and Quarles, R.H. (1984). Immunocytochemical localization of the myelin-associated glycoprotein. Fact or artifact? J Neuroimmunol *6*, 231-249.
Trifunovski, A., Josephson, A., Bickford, P.C., Olson, L., and Brene, S. (2006). Selective decline of Nogo mRNA in the aging brain. Neuroreport *17*, 913-916.
Tsai, S.Y., Markus, T.M., Andrews, E.M., Cheatwood, J.L., Emerick, A.J., Mir, A.K., Schwab, M.E., and Kartje, G.L. (2007). Intrathecal treatment with anti-Nogo-A antibody improves functional recovery in adult rats after stroke. Exp Brain Res *182*, 261-266.
van de Velde, H.J., Roebroek, A.J., Senden, N.H., Ramaekers, F.C., and Van de Ven, W.J. (1994). NSP-encoded reticulons, neuroendocrine proteins of a novel gene family associated with membranes of the endoplasmic reticulum. J Cell Sci *107 ( Pt 9)*, 2403-2416.

Vastrik, I., Eickholt, B.J., Walsh, F.S., Ridley, A., and Doherty, P. (1999). Sema3A-induced growth-cone collapse is mediated by Rac1 amino acids 17-32. Curr Biol *9*, 991-998.
Velarde, M.C., Parisek, S.I., Eason, R.R., Simmen, F.A., and Simmen, R.C. (2005). The secretory leukocyte protease inhibitor gene is a target of epidermal growth factor receptor action in endometrial epithelial cells. J Endocrinol *184*, 141-151.
Venkatesh, K., Chivatakarn, O., Lee, H., Joshi, P.S., Kantor, D.B., Newman, B.A., Mage, R., Rader, C., and Giger, R.J. (2005). The Nogo-66 receptor homolog NgR2 is a sialic acid-dependent receptor selective for myelin-associated glycoprotein. J Neurosci *25*, 808-822.
Vourc'h, P., Moreau, T., Arbion, F., Marouillat-Vedrine, S., Muh, J.P., and Andres, C. (2003). Oligodendrocyte myelin glycoprotein growth inhibition function requires its conserved leucine-rich repeat domain, not its glycosylphosphatidyl-inositol anchor. J Neurochem *85*, 889-897.
Wang, F., Liang, Z., Hou, Q., Xing, S., Ling, L., He, M., Pei, Z., and Zeng, J. (2007a). Nogo-A is involved in secondary axonal degeneration of thalamus in hypertensive rats with focal cortical infarction. Neurosci Lett *417*, 255-260.
Wang, H., Yao, Y., Jiang, X., Chen, D., Xiong, Y., and Mu, D. (2006a). Expression of Nogo-A and NgR in the developing rat brain after hypoxia-ischemia. Brain Res *1114*, 212-220.
Wang, K.C., Kim, J.A., Sivasankaran, R., Segal, R., and He, Z. (2002a). P75 interacts with the Nogo receptor as a co-receptor for Nogo, MAG and OMgp. Nature *420*, 74-78.
Wang, K.C., Koprivica, V., Kim, J.A., Sivasankaran, R., Guo, Y., Neve, R.L., and He, Z. (2002b). Oligodendrocyte-myelin glycoprotein is a Nogo receptor ligand that inhibits neurite outgrowth. Nature *417*, 941-944.
Wang, L.H., and Strittmatter, S.M. (1996). A family of rat CRMP genes is differentially expressed in the nervous system. J Neurosci *16*, 6197-6207.
Wang, N., Thuraisingam, T., Fallavollita, L., Ding, A., Radzioch, D., and Brodt, P. (2006b). The secretory leukocyte protease inhibitor is a type 1 insulin-like growth factor receptor-regulated protein that protects against liver metastasis by attenuating the host proinflammatory response. Cancer Res *66*, 3062-3070.
Wang, S., Watanabe, T., Noritake, J., Fukata, M., Yoshimura, T., Itoh, N., Harada, T., Nakagawa, M., Matsuura, Y., Arimura, N., and Kaibuchi, K. (2007b). IQGAP3, a novel effector of Rac1 and Cdc42, regulates neurite outgrowth. J Cell Sci *120*, 567-577.
Wang, X., Li, X., Xu, L., Zhan, Y., Yaish-Ohad, S., Erhardt, J.A., Barone, F.C., and Feuerstein, G.Z. (2003). Up-regulation of secretory leukocyte protease inhibitor (SLPI) in the brain after ischemic stroke: adenoviral expression of SLPI protects brain from ischemic injury. Mol Pharmacol *64*, 833-840.
Weinmann, O., Schnell, L., Ghosh, A., Montani, L., Wiessner, C., Wannier, T., Rouiller, E., Mir, A., and Schwab, M.E. (2006). Intrathecally infused antibodies against Nogo-A penetrate the CNS and downregulate the endogenous neurite growth inhibitor Nogo-A. Mol Cell Neurosci *32*, 161-173.
Wiessner, C., Bareyre, F.M., Allegrini, P.R., Mir, A.K., Frentzel, S., Zurini, M., Schnell, L., Oertle, T., and Schwab, M.E. (2003). Anti-Nogo-A antibody infusion 24 hours after experimental stroke improved behavioral outcome and corticospinal plasticity in normotensive and spontaneously hypertensive rats. J Cereb Blood Flow Metab *23*, 154-165.
Wittmann, T., and Waterman-Storer, C.M. (2001). Cell motility: can Rho GTPases and microtubules point the way? J Cell Sci *114*, 3795-3803.

Wojcik, S., Engel, W.K., and Askanas, V. (2006). Increased expression of Noga-A in ALS muscle biopsies is not unique for this disease. Acta Myol *25*, 116-118.
Wong, E.V., David, S., Jacob, M.H., and Jay, D.G. (2003). Inactivation of myelin-associated glycoprotein enhances optic nerve regeneration. J Neurosci *23*, 3112-3117.
Wong, S.T., Henley, J.R., Kanning, K.C., Huang, K.H., Bothwell, M., and Poo, M.M. (2002). A p75(NTR) and Nogo receptor complex mediates repulsive signaling by myelin-associated glycoprotein. Nat Neurosci *5*, 1302-1308.
Woolf, C.J. (2003). No Nogo: now where to go? Neuron *38*, 153-156.
Xiang, S., Kim, E.Y., Connelly, J.J., Nassar, N., Kirsch, J., Winking, J., Schwarz, G., and Schindelin, H. (2006). The crystal structure of Cdc42 in complex with collybistin II, a gephyrin-interacting guanine nucleotide exchange factor. J Mol Biol *359*, 35-46.
Xiao, Z.C., Bartsch, U., Margolis, R.K., Rougon, G., Montag, D., and Schachner, M. (1997). Isolation of a tenascin-R binding protein from mouse brain membranes. A phosphacan-related chondroitin sulfate proteoglycan. J Biol Chem *272*, 32092-32101.
Xiong, L., Rouleau, G.A., Delisi, L.E., St-Onge, J., Najafee, R., Riviere, J.B., Benkelfat, C., Tabbane, K., Fathalli, F., Danics, Z., *et al.* (2005). CAA insertion polymorphism in the 3'UTR of Nogo gene on 2p14 is not associated with schizophrenia. Brain Res Mol Brain Res *133*, 153-156.
Xiong, N.X., Zhao, H.Y., Zhang, F.C., and He, Z.Q. (2007). Negative correlation of Nogo-A with the malignancy of oligodendroglial tumor. Neurosci Bull *23*, 41-45.
Xu, G., Nie, D.Y., Chen, J.T., Wang, C.Y., Yu, F.G., Sun, L., Luo, X.G., Ahmed, S., David, S., and Xiao, Z.C. (2004). Recombinant DNA vaccine encoding multiple domains related to inhibition of neurite outgrowth: a potential strategy for axonal regeneration. J Neurochem *91*, 1018-1023.
Yamashita, N., Uchida, Y., Ohshima, T., Hirai, S., Nakamura, F., Taniguchi, M., Mikoshiba, K., Honnorat, J., Kolattukudy, P., Thomasset, N., *et al.* (2006). Collapsin response mediator protein 1 mediates reelin signaling in cortical neuronal migration. J Neurosci *26*, 13357-13362.
Yan, R., Shi, Q., Hu, X., and Zhou, X. (2006). Reticulon proteins: emerging players in neurodegenerative diseases. Cell Mol Life Sci.
Yick, L.W., Wu, W., So, K.F., Yip, H.K., and Shum, D.K. (2000). Chondroitinase ABC promotes axonal regeneration of Clarke's neurons after spinal cord injury. Neuroreport *11*, 1063-1067.
Yiu, G., and He, Z. (2003). Signaling mechanisms of the myelin inhibitors of axon regeneration. Curr Opin Neurobiol *13*, 545-551.
Yoshimura, T., Arimura, N., Kawano, Y., Kawabata, S., Wang, S., and Kaibuchi, K. (2006). Ras regulates neuronal polarity via the PI3-kinase/Akt/GSK-3beta/CRMP-2 pathway. Biochem Biophys Res Commun *340*, 62-68.
Zagrebelsky, M., Buffo, A., Skerra, A., Schwab, M.E., Strata, P., and Rossi, F. (1998). Retrograde regulation of growth-associated gene expression in adult rat Purkinje cells by myelin-associated neurite growth inhibitory proteins. J Neurosci *18*, 7912-7929.
Zhao, X.H., Jin, W.L., and Ju, G. (2007). An in vitro study on the involvement of LINGO-1 and Rho GTPases in Nogo-A regulated differentiation of oligodendrocyte precursor cells. Mol Cell Neurosci.
Zheng, B., Atwal, J., Ho, C., Case, L., He, X.L., Garcia, K.C., Steward, O., and Tessier-Lavigne, M. (2005). Genetic deletion of the Nogo receptor does not reduce neurite inhibition in vitro or promote corticospinal tract regeneration in vivo. Proc Natl Acad Sci U S A *102*, 1205-1210.
Zheng, B., Ho, C., Li, S., Keirstead, H., Steward, O., and Tessier-Lavigne, M. (2003). Lack of enhanced spinal regeneration in Nogo-deficient mice. Neuron *38*, 213-224.

Zuo, J., Neubauer, D., Dyess, K., Ferguson, T.A., and Muir, D. (1998). Degradation of chondroitin sulfate proteoglycan enhances the neurite-promoting potential of spinal cord tissue. Exp Neurol *154*, 654-662.
Zuo, J., Neubauer, D., Graham, J., Krekoski, C.A., Ferguson, T.A., and Muir, D. (2002). Regeneration of axons after nerve transection repair is enhanced by degradation of chondroitin sulfate proteoglycan. Exp Neurol *176*, 221-228.